PNWD-3586
WTP-RPT-128 Rev 0

Hybrid Mixing System Test Results for Prototype Ultrafiltration Feed Process and High-Level Waste Lag Storage Vessels

MD Johnson
MA Gerber
JR Bontha
AP Poloski
RT Hallen
SK Sundaram
DE Wallace

April 2005

Prepared for Bechtel National Inc.
by Battelle – Pacific Northwest Division
under Contract 24590-101-TSA-W000-00004

LEGAL NOTICE

This report was prepared by Battelle Memorial Institute (Battelle) as an account of sponsored research activities. Neither Client nor Battelle nor any person acting on behalf of either:

MAKES ANY WARRANTY OR REPRESENTATION, EXPRESS OR IMPLIED, with respect to the accuracy, completeness, or usefulness of the information contained in this report, or that the use of any information, apparatus, process, or composition disclosed in this report may not infringe privately owned rights; or

Assumes any liabilities with respect to the use of, or for damages resulting from the use of, any information, apparatus, process, or composition disclosed in this report.

Reference herein to any specific commercial product, process, or service by trade name, trademark, manufacturer, or otherwise, does not necessarily constitute or imply its endorsement, recommendation, or favoring by Battelle. The views and opinions of authors expressed herein do not necessarily state or reflect those of Battelle.

This document was printed on recycled paper.
(8/00)

WTP-RPT-128 Rev 0

Hybrid Mixing System Test Results for Prototype Ultrafiltration Feed Process and High-Level Waste Lag Storage Vessels

MD Johnson
MA Gerber
JR Bontha
AP Poloski
RT Hallen
SK Sundaram
DE Wallace

4/21/05

for W. Tamosaitis

April 2005

ACCEPTED FOR

WTP PROJECT USE

Prepared for Bechtel National, Inc.
under Contract 24590-101-TSA-W000-00004

Test specification:	24590-WTP-TSP-RT-03-008 Rev. 0
Test plan:	TP-RPP-WTP-296
Test exceptions:	24590-WTP-TEF-RT-03-060, -081, -090; 24950-WTP-TEF-RT-04-002, -00004, -00029
R&T focus area:	Pretreatment
Test Scoping Statement(s):	B-100

Battelle - Pacific Northwest Division
Richland, Washington 99352

Completeness of Testing

This report describes the results of work and testing specified by Test Specification 24590-WTP-TSP-RT-03-008 Rev. 0 and Test Plan TP-RPP-WTP-296. The work and any associated testing followed the quality assurance requirements outlined in the Test Specification/Plan. The descriptions provided in this test report are an accurate account of both the conduct of the work and the data collected. Test plan results are reported. Also reported are any unusual or anomalous occurrences that are different from expected results. The test results and this report have been reviewed and verified.

Approved:

Gordon H. Beeman, Manager
WTP R&T Support Project

4/12/05
Date

Summary

Battelle – Pacific Northwest Division (PNWD) was contracted to provide Bechtel National Inc. (BNI) with results of simulant tests using the scaled prototypic ultrafiltration process (UFP) and lag storage (LS) vessels and associated pulse jet mixer (PJM) equipment for the Waste Treatment Plant (WTP) Project. The UFP and LS vessels are to be used in the WTP for mixing radioactive waste from the underground Hanford storage tanks. BNI, through its subcontract with PNWD, has tested PJM/hybrid-fitted mixing vessels at multiple scales to experimentally verify dimensional scaling effects in PJM systems. (The scaling methodologies of the mixing system for a generic 4-PJM vessel were validated by tests conducted at multiple scales earlier in the PJM testing program).

The process stream significant to this report is identified as "HLW pretreated sludge." Several vessels through which the HLW pretreated sludge stream will be processed will be mixed using PJM technology, air sparging, and steady jets generated by recirculation pumps. These technologies have been selected for use in so-called "black cell" regions of the WTP. Within these regions, maintenance capability will not be available for the operating life of the WTP. Thus, these technologies were selected for use because they lack moving mechanical parts that would require maintenance. The recirculation pumps will be located in an accessible area outside of the black cells.

Many of the waste slurries to be received and processed in the WTP exhibit non-Newtonian behavior. In particular, when stationary, they can develop gel-like properties and behave like very weak solids. When an applied force exceeds their shear strength, they act like a fluid and begin to flow. The majority of available knowledge for mixing non-Newtonian fluids is associated with the use of mechanical agitators. The subject of jet mixing and air sparging in non-Newtonian fluids is a relatively new and developing field. Some theoretical analysis and applied research are being pursued in industry and academia, but the field of non-steady jet mixing and air sparging in non-Newtonian fluids is essentially in its infancy.

In June 2003, the PJM Task Team consisting of BNI, PNWD, and mixing consultants addressed the non-Newtonian slurry mixing issues and developed an integrated strategy for scaled testing to demonstrate PJM mixing in WTP vessels containing non-Newtonian fluids. The purpose of the scaled PJM mixing tests was to provide information on the operating parameters critical for the uniform movement (total mobilization) of these non-Newtonian slurries. Initial (physical) scaled testing demonstrated in October 2003 that the baseline pulse jet designs in these vessels did not mix the non-Newtonian slurries to the extent necessary to meet WTP requirements. In November 2003, Phase I of the PJM program developed an alternative "PJM-only" configuration that mixed the vessels containing non-Newtonian slurries in accordance with WTP requirements (Bates et al. 2004). While the alternative PJM configuration provided acceptable mixing performance, implementation of the PJM-only mixing systems severely impacted the WTP facility designs due to increased numbers of PJMs, additional piping, and the significantly increased air consumption needed to operate these systems. To minimize the impact to overall project cost and schedule, the PJM Task Team was directed to develop PJM/hybrid mixing systems to reduce these effects on the WTP. This report documents the Phase II prototype scaled testing carried out in the LS and UFP scaled prototypes in the high-bay area of the Applied Process Engineering Laboratory (APEL).

Objectives

The overall objective of this work was to provide mixing performance information on the operating parameters critical for uniform movement (total mobilization) of the tank contents. The specific objective of the testing was to provide data on the mobilization of non-Newtonian simulants for assessing PJM mixing configurations for the UFP and LS vessels. PJM configurations include baseline designs provided by BNI and enhanced configurations and/or operational parameters that have been demonstrated to provide acceptable mobilization/mixing performance. The non-Newtonian simulant possessed target rheological characteristics similar to those predicted for WTP waste streams.

The final results of this testing effort will eventually be used to generate the engineering and bounding parametric correlations that will help ensure that the WTP Project has functional fluidic mixing systems for the UFP and LS non-Newtonian vessels. The objectives in the applicable test specifications were met. Table S.1 summarizes the testing objectives.

Table S.1. Test Objectives

Test Objective	Objective Met (Y/N)	Discussion
1. Provide design information on operating parameters	Y	Multiple PJM operational and geometric parameters exercised
2. Conduct tests in 1/4 scale vessel	Y	UFP vessel was scale factor of 1/4.94, LS was 1/4.29

Test Exceptions

Table S.2 describes the test exceptions for this work.

Table S.2. Test Exceptions

List Test Exceptions	Describe Test Exceptions
1. 24590-WTP-TEF-RT-03-060	Revised test matrix (constant drive volume test using 30 and 70 Pa yield strength Laponite). This test exception does not apply to the contents of this report.
2. 24590-WTP-TEF-RT-03-081	Revised test matrix for final “best” mixing configurations (describes use of “ram’s head” PJM nozzles). This test exception does not apply to the contents of this report.
3. 24950-WTP-TEF-RT-03-090	Revised test matrix to include addition of spargers to LS and the use of dye tracer, RF tags, and polycarbonate beads (as needed) to determine mixing volume and uniformity.
4. 24950-WTP-TEF-RT-04-002	Revised test matrix to include both spargers and recirculation pumps and the use of full-scale-diameter nozzles for some tests.
5. 24950-WTP-TEF-RT-04-00004	Revised test matrix/direction to reconfigure and test in LS and UFP test platforms to understand hybrid mixing designs.
6. 24950-WTP-TEF-RT-04-00029	Test matrix for velocity mapping.

Results and Performance Against Success Criteria

Each test was conducted by first configuring the PJMs in the desired geometric array and then placing them within the acrylic test tank with the nozzles at a specified offset from the ellipsoidal tank bottom. The geometric array included adjustments to the desired circular PJM/sparger/recirculation nozzle array radius and offset relative to one another as well as changes in nozzle diameter, subjacent height and impingement angle. Tests were conducted to determine the effectiveness of various array configurations and operating parameters; the full complement of LS and UFP tests with conclusive results are presented in the report. Table S.3 presents the success criteria established for these tests.

Table S.3. Success Criteria

List Success Criteria	How the Tests Did or Did Not Meet the Success Criteria
Demonstrate a combination of PJM operating conditions and physical arrangements that provide full mobilization of the UFP and LS vessels.	PJM geometrical and operational conditions meeting WTP criteria were identified for the LS and UFP vessels that provided complete tank mobilization (see Section 7). Mobilization of the simulant was assessed by use of dye and chloride tracers. Visual observation of the clear tank walls and the simulant surface indicated the dye was distributed throughout the simulant. Samples were obtained periodically during the test and core samples were taken at the completion of the tests. These samples were analyzed for dye and chloride concentrations to determine the fraction mixed and the mixing ratio. The results indicate that the simulant was mobilized and in several cases was homogeneous within experimental error.

Quality Requirements

PNWD implements the RPP-WTP quality requirements by performing work in accordance with the PNWD Waste Treatment Plant Support Project quality assurance project plan (QAPjP) approved by the RPP-WTP Quality Assurance (QA) organization. This work was performed to the quality requirements of NQA-1-1989 Part I, Basic and Supplementary Requirements, NQA-2a-1990, Part 2.7 and DOE/RW-0333P, Rev 13, Quality Assurance Requirements and Descriptions (QARD). These quality requirements are implemented through PNWD's *Waste Treatment Plant Support Project (WTPSP) Quality Assurance Requirements and Description Manual*. The analytical requirements are implemented through WTPSP’s Statement of Work (WTPSP-SOW-005) with the Radiochemical Processing Laboratory (RPL) Analytical Service Operations (ASO).

Experiments that were not method-specific were performed in accordance with PNWD’s procedures QA-RPP-WTP-1101, “Scientific Investigations,” and QA-RPP-WTP-1201, “Calibration Control System,” ensuring that sufficient data were taken with properly calibrated measuring and test equipment (M&TE) to obtain quality results.

PNWD addresses internal verification and validation activities by conducting an independent technical review of the final data report in accordance with PNWD's procedure QA-RPP-WTP-604. This review verifies that the reported results are traceable, that inferences and conclusions are soundly based, and the reported work satisfies the Test Plan objectives. This review procedure is part of PNWD's *WTPSP Quality Assurance Requirements and Description Manual*.

Research and Technology (R&T) Test Conditions

This report summarizes the test configurations and individual test parameters and results. As-built dimensions of test configurations are reported at a level consistent with the usefulness of the results. Test conditions are listed in Table S.4. Screening or scoping tests do not apply an equivalent level of rigor to the as-built configurations as those that were deemed most important or successful by the WTP Steering Committee. All testing reported was performed at approximately one-quarter scale. Proof of scaling relationships and correlations for pulse jet mixing are presented in Bamberger et al. (2005). Results supporting the performance of the sparging system are also reported in Poloski et al. (2005). Test equipment and materials provided prior to the start of testing included:

- scaled acrylic tanks
- scaled spun-steel dished tank bottom
- data acquisition and control system including computer and input/output hardware and software
- level measurement devices for the interior of each PJM and for simulant level in tank
- control manifold for compressed air, vacuum, and vent including pressure measurement for the manifold
- steel PJMs for candidate testing
- kaolin-bentonite clay mixture prepared with 80% kaolin and 20% bentonite clay with a specified yield strength.

Table S.4. Test Conditions

Test Conditions	Were Test Conditions Followed?
Prepare test plan to implement the test specification	Test plan prepared and approved by WTP R&T
Test units to be provided by BNI	UFP and LS test vessels and initial PJM units supplied by BNI
Test conditions specified in test matrix supplied in the test specification	Test matrix supplied (and superseded by subsequent updates via test exceptions)

Simulant Use

The rheological characteristics of the simulants are compared with actual waste rheology in Poloski et al. (2004). Mixing tests with actual waste are neither planned nor within the scope of the current efforts due to the difficulty of obtaining and working with actual waste samples. Should new or extended insight into actual waste properties become available, careful comparison with the properties of the simulants used in the current tests is recommended, and the potential impacts on hybrid mixing system performance should be investigated. The simulant used for all testing in this report was an aqueous kaolin/bentonite clay mixture (approximately 27 wt% clay constituted of approximately 80 wt% kaolin and 20 wt% bentonite) exhibiting a Bingham plastic rheology closely representing that of actual waste slurries.

Discrepancies and Follow-on Tests

No design or operations issues were associated with the testing and/or the results presented in this report. However, care must be exercised in using the data presented in this report in drawing broad conclusions about PJM performance in vessels with significantly larger dimensions than the test vessels. PJM scaling issues are addressed specifically in a separate report. The reader is encouraged to thoroughly understand the contents of the scaling technical basis report before applying or extrapolating the results presented here, as well as the background for simulant selection and sparger design (Poloski et al. 2005). Casual extrapolation of these results to actual waste behavior is not recommended. Should actual waste properties be found to differ significantly from those used to develop the simulant materials used in the current testing, additional PJM performance testing is strongly suggested.

Summary References

Bates JM, JW Brothers, JM Alzheimer, DE Wallace, and PA Meyer. 2004. T*est Results for Pulse Jet Mixers in Prototypic Ultrafiltration Feed Process and High-Level Waste Lag Storage Vessels*. WTP-RPT-110 Rev. A, Battelle – Pacific Northwest Division, Richland, Washington.

Poloski AP, PA Meyer, LK Jagoda, and PR Hrma. August 2004. *Non-Newtonian Slurry Simulant Development and Selection for Pulse Jet Mixer Testing.* PNWD-3495, Battelle – Pacific Northwest Division, Richland, Washington.

Poloski AP, ST Arm, JA Bamberger, B Barnett, R Brown, BJ Cook, CW Enderlin, MS Fountain, M Friedrich, BG Fritz, RP Mueller, F Nigl, Y Onishi, LA Schienbein, LA Snow, S Tzemos, M White, and JA Vucelik. 2005. *Technical Basis for Scaling of Air Sparging Systems for Mixing in non-Newtonian Slurries*. WTP-RPT-129 Rev 0, Battelle – Pacific Northwest Division, Richland, Washington.

Bamberger JA, PA Meyer, JR Bontha, CW Enderlin, DA Wilson, AP Poloski, JA Fort, ST Yokuda, HD Smith, F Nigl, M Friedrich, DE Kurath, GL Smith, JM Bates, and MA Gerber. 2005. *Technical Basis for Testing Scaled Pulse Jet Mixing Systems for non-Newtonian Slurries.* WTP-RPT-113 Rev 0, Battelle – Pacific Northwest Division, Richland, Washington.

Acknowledgments

The authors would like to thank Brent Barnett for his exhaustive technical review, Sheila Bennett for her outstanding editing skills in putting together this report, and David Lanigan for his drafting expertise in fixing the author's figures.

The scaled prototype testing often involved long hours, arduous conditions, and weekend work. Those who participated in the work documented in this report carried out these tests with alacrity and good spirits as well as technical excellence, and, when required, stoic determination. The authors would like to recognize all those who made the prototype testing program a success:

PJM Operations & Tracer Sampling: Stuart Arm, Judith Bamberger, Brent Barnett, Dave Blanchard, Bill Buchmiller, Abby Capatillo-Isenberg, Bill Combs, Jarrod Crum, Kate Deters, Michele Friedrich, Bob Fulton, Consuelo Guzman-Long, Mike Hall, Don Hartshorn, Chris Johnson, Ron Myers, Jackie Newell, Franz Nigl, Lawrence Schienbein, Sergei Sinkov, Harry Smith, Spyro Tzemos, Mike White, Wayne Wilcox, and Mac Zumhoff.

Rheology Analysis/Tracer Sampling: Bryan Cook, Lynette Jagoda, Renee Russell, and Bob Swoboda.

Drive Function Analysis: Jim Fort, Wassana Yantasee, and Satoru Yokuda.

Velocity Mapping Operations: Brent Barnett, Bill Buchmiller, Mike Hall, Don Hartshorn, Lawrence Schienbein, and Wayne Wilcox.

PJM Operations Admin & Logistics Support: Teri Claphan and Theresa Schott.

Core Sampling Operations: Evan Arntzen, Brad Barfuss, Rich Brown, Kate Deters, Bob Fulton, Jackie Newell, John Stephenson, Dan Tano, Susan Thorsten, and Jessica Vucelik.

Core Sampling Operations Admin & Logistics Support: Gayle Dirkes.

Facilities: Bill Buchmiller and Evan Jones.

Craft Support: Jerry Allen, Rod Bechtel, Greg Brodaczynski, Don Cravens, Rick Ehlers, Jim Harter, Tom Loftus, Randy Odd, Steve Panther, Heinz Schulz, and Steve Steer.

Quality Assurance: Kirsten Meier, Barry Sachs, and Tom Walker.

Contracts & Purchasing Support: Jamie Allessio, Lilly Burns, Kim Collins, Diane Leitch, Laurie Martin, Janie Vickerman, Diane Wallace, and Kathy Whelan.

Project Office Admin: Chrissy Charron.

Abbreviations and Acronyms

acfm	actual cubic feet per minute
APEL	Applied Process Engineering Laboratory
ASO	Analytical Service Operations
BHRG	British Hydromechanical Research Group
BNI	Bechtel National Inc.
DOE	U.S. Department of Energy
FMP	Fluid Mixing Processes
gpm	gallons per minute
H/D	ratio of slurry height to vessel diameter
HLP	HLW Lag Storage and Feed Blending Process System
HLW	high-level waste
IC	ion chromatography
ID	inner diameter
LAW	low-activity waste
LRB	laboratory record book
LS	lag storage
M&TE	measuring and test equipment
OD	outer diameter
PCD	Pitch circle diameter
PJM	pulse jet mixer
PNWD	Battelle—Pacific Northwest Division
PVC	polyvinyl chloride
QA	quality assurance
QAPjP	quality assurance project plan
QARD	Quality Assurance Requirements and Descriptions
R&T	research and technology
RF	radio frequency
ROB	region of bubbles
RPL	Radiochemical Processing Laboratory
scfm	standard cubic feet per minute
UFP	ultrafiltration feed process
UV-VIS	ultraviolet visible
VFD	variable frequency drive
WTP	Waste Treatment Plant
WTPSP	Waste Treatment Plant Support Project
ZOI	zone of influence

Contents

Figures

Tables

1.0 Introduction

1.1 Background

The Hanford Site has 177 single- and double-shell underground storage tanks containing radioactive waste. The U.S. Department of Energy (DOE) Office of River Protection's Waste Treatment Plant (WTP) is being designed and built to pretreat and then vitrify a large portion of this waste. The WTP will consist of three primary facilities: a pretreatment facility, a low-activity waste (LAW) vitrification facility, and a high-level waste (HLW) vitrification facility. The pretreatment facility will receive waste feed from the Hanford tank farms and separate it into 1) a high-volume, low-activity, liquid process stream stripped of most solids and radioisotopes and 2) a much smaller-volume HLW slurry containing the solids and most of the radioactivity. In the pretreatment facility, solids and radioisotopes will be removed from the waste by precipitation, filtration, and ion exchange processes to produce the LAW stream. The slurry of filtered solids will be blended with two ion exchange eluent streams containing soluble radioisotopes to produce the HLW stream. The HLW and LAW vitrification facilities will convert these process streams into glass, which will be poured directly into stainless steel canisters.

The process stream significant to this report is identified as "HLW pretreated sludge." Several vessels through which the HLW pretreated sludge stream will be processed will be mixed using pulse jet mixer (PJM) technology, air sparging, and steady jets generated by recirculation pumps. These technologies have been selected for use in so-called "black cell" regions of the WTP. Within these regions of the WTP, maintenance capability will not be available for the operating life of the WTP. Thus, these technologies were selected for use in these regions because they lack moving mechanical parts that would require maintenance. The recirculation pumps will be located in an accessible area outside of the black cells.

Many of the waste slurries to be received and processed in the WTP exhibit non-Newtonian behavior. In particular, when stationary, they can develop gel-like properties and behave like very weak solids. When an applied force exceeds their shear strength, they act like a fluid and begin to flow. The majority of available knowledge for mixing non-Newtonian fluids is associated with the use of mechanical agitators. The subject of jet mixing and air sparging in non-Newtonian fluids is a relatively new and developing field, with some theoretical analysis and applied research being pursued in industry and academia. The field of non-steady jet mixing and air sparging in non-Newtonian fluids is essentially in its infancy.

To address the non-Newtonian slurry mixing issues, the PJM Task Team consisting of Bechtel National, Inc. (BNI); Battelle – Pacific Northwest Division (PNWD); and mixing consultants developed an integrated strategy for scaled testing to demonstrate PJM mixing in WTP vessels containing non-Newtonian fluids in June 2003. The scaled PJM mixing tests were to provide information on the operating parameters critical for the uniform movement (total mobilization) of these non-Newtonian slurries. Initial (physical) scaled testing demonstrated in October 2003 that the baseline pulse jet designs in these vessels did not mix the non-Newtonian slurries to the extent necessary to meet WTP requirements. In November 2003, Phase I of the PJM program developed an alternative "PJM-only" configuration that mixed the vessels containing non-Newtonian slurries in accordance with WTP requirements (Bates et al. 2004). While the alternative PJM configuration provided acceptable mixing performance, implementation of the PJM-only mixing systems severely impacted the WTP facility designs due to increased numbers of PJMs, additional piping, and the significantly increased air consumption needed to operate these systems. To minimize the impact to overall project cost and schedule, the PJM Task Team was directed to develop PJM/hybrid mixing systems to reduce these effects on the WTP. This report summarizes the Phase II results of scaled prototypic testing.

1.2 Report Scope

Phase II of the PJM program investigated further alternative configurations to assess the effects of slurry rheology changes, reduced tank volume, PJM jet velocity and nozzle size, sparging, and recirculation pump operation. Phase II PJM/hybrid mixing systems completed additional testing to demonstrate that the modified configurations mixed non-Newtonian slurries within WTP requirements. This document describes the mixing processes and presents an overview of the PJM/hybrid design and scaling approach. It also describes an experimental approach and presents PJM/hybrid system optimization and final configuration results. This report and testing data support the ultrafiltration feed process (UFP) (UFP-VSL-00002A/2B) and HLW lag storage (LS) (HLP-VSL-00027A/B) design efforts by documenting the results of the phase II PJM scaled test platform testing.

1.3 Experimental Objectives

The testing configurations provided by the WTP project were selected to minimize the impact on the current plant design. The main objectives of testing were to:

- Provide testing results to optimize the PJM/hybrid mixing system operating parameters (PJM nozzle velocity, cycle frequency, etc.) and position (x, y, and z coordinates, nozzle angle, etc.) that will result in a well-mixed condition in UFP and LS test stands.
- Demonstrate complete mixing (i.e., no stagnant regions) with turbulent conditions in the majority of the slurry volume for the final UFP and LS configurations. Turbulent mixing conditions enhance heat transfer within the vessel and facilitate the suspension of waste particles.

1.4 Overview of the PJM-Hybrid Design Approach

The hybrid mixing systems considered in this work involved the combined use of PJMs, steady mixing jets created by recirculation pumps, and air sparging. The mixing technologies were combined to take advantage of their respective strengths. PJMs are used for mixing the lower region of the vessel and facilitating off-bottom suspension of solids. PJMs are ideally suited for these tasks because they discharge downward with nozzles near the vessel floor. The ideal PJM configuration for hybrid systems is one that creates a well-defined, highly turbulent cavern. The material in the upper region of the vessel is then transported by the other systems to the turbulent cavern, where it is mixed (with spargers and/or steady jets) as illustrated in Figure 1.1.

A high degree of turbulence is important to encourage both adequate mixing and gas removal as well as to minimize scaling issues for the scaled test platform results that will be applied at full scale (the technical basis for scaled-up testing is discussed in Bamberger et al. (2005). Additionally, having an obstruction-free interface between the mixed and unmixed regions simplifies the specification of spargers and jet nozzles.

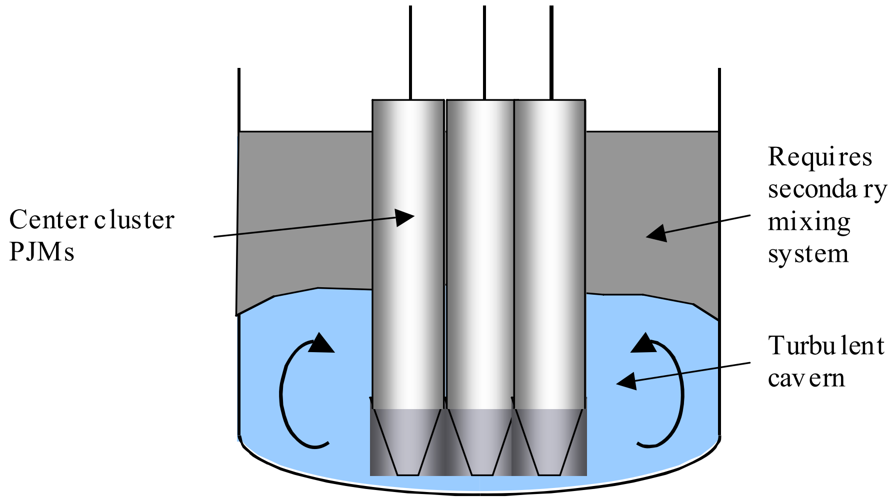

Figure 1.1. PJM-Hybrid Mixing Design Approach. Central cluster PJMs mix the lower region of the vessel, and secondary systems mix the upper region.

For a given PJM arrangement, mixing performance can be improved by increasing the discharge velocity or nozzle diameter. However, there is a limit to the improvement due to the fixed volume of fluid being discharged during a drive cycle. As the velocity or nozzle diameter increases, the drive time is reduced. For a given PJM nozzle diameter and discharge velocity, mixing performance can be improved only by increasing the discharge volume. The test program used the largest PJMs feasible to maximize drive time and thus mixing performance.

A centralized cluster of PJMs (operated simultaneously) with nozzles angled toward the tank wall was found to be most effective at creating a uniform mixing cavern. Tests were also conducted with varied arrays of PJMs and found to provide good overall mixing (determined by the dye method). However, the uniformity of the cavern was found to be highly sensitive to PJM nozzle angle alignment.

Steady turbulent jets from recirculation pumps are known to be effective in mobilizing and mixing applications. In general, mixing effectiveness is improved by increasing nozzle diameter or jet velocity. If the flow rate is fixed, mixing performance is improved only by increasing nozzle velocity, which implies a reduction in nozzle diameter. Mixing performance can also be improved by increasing the number of mixing jets. Jets are a source of linear momentum and tend to be highly directional with relatively small spread angles (about 15 degrees for a free Newtonian jet). Once they impinge on solid surfaces, they tend to follow the contour of that surface. Further, cavern formation (or similar channeling) can occur in non-Newtonian slurries. Single jets can be used to mix entire vessels if the flow rates are high enough; however, a single jet will often break through the fluid surface and dissipate its energy before complete mobilization occurs, particularly in non-Newtonian slurries. Ideally, the jet nozzles are angled upward just below the PJM cavern interface and aimed between the PJMs and the vessel wall. Material from the lower mixing zone is entrained and mixed into the upper region, a configuration well suited for operation at reduced operating volumes. Hence, by distributing the total available flow through multiple jets, more regions of the vessel can be mobilized and overall mixing improved. Air sparge tubes provide mixing an alternative mechanism. Rising air bubbles produce drag on surrounding fluid, creating an upward pumping effect. Once at the surface, fluid must recirculate downward. The net result is an upward bubble zone of mixing referred to as the region of bubbles (ROB) surrounded by a larger, downward zone referred to as the zone of influence (ZOI). Sparge ZOIs will interact in beneficial ways if neighboring sparge points are spaced closely enough. However, these interactions for non-Newtonian fluids are not fully understood and are not addressed in this document. Locating the outlet of the sparge tube near the bottom of the tank and well inside the PJM cavern provides increased transfer between the sparged regions and the PJM cavern, which enhances mixing outside the cavern.

1.5 Overview of the Scaling Approach

The scaling approach involved testing in several scaled vessels with representative non-Newtonian simulants. Five test stands were tested with PJMs; three were used to investigate scaling laws and two were scaled versions of the full-scale tanks. Scale-up and application of the mixing technologies were based on a mix of well-known theory and developments by the PJM mixing program.

Several different approaches were taken for the scale-up and design rating of the mixing systems. Scale-up of steady jet performance (i.e., recirculation pump mixing) was based on well-established turbulent jet theory. Scale-up of PJM mixing performance was based on modifications to steady jet theory to account for the intermittent nature of the PJMs and non-Newtonian rheology. Dimensional analysis was used to identify the important physical properties and system parameters as well as to guide the scaled test operations. In addition to theoretical considerations, mixing tests were performed at three physical scales with different simulants to demonstrate that the scaled approach was valid. A summary of both the scaling theory and the scaling test results is presented in Bamberger et al. (2005). The sparging system configurations are based on nearly full-scale tests with single- and multisparge-tube test stands (Poloski et al. 2005). The scaling approach involves keeping a constant number of sparge tubes per unit area.

Scaled models of WTP vessels were used to evaluate the various mixing configurations. This report focuses on the results of LS and UFP vessels. Both the UFP and LS vessels (described in Sections 2.1 and 2.2, respectively) had scale factors in the range of 4 to 5. Approximately 150 separate runs were conducted with these units containing various configurations of PJMs, recirculation pumps, and spargers. Section 7 presents the results obtained with the final configurations.

Section 3 describes the experimental approach and Section 4 the effectiveness of solids suspension. Section 5 describes velocity mapping results, and Section 6 details the optimization of the PJM/hybrid system. Conclusions are presented in Section 8 and cited references in Section 9. Supporting documentation is provided in the appendixes.

1.6 Quality Requirements

PNWD implements the RPP-WTP quality requirements by performing work in accordance with the PNWD Waste Treatment Plant Support Project quality assurance project plan (QAPjP) approved by the RPP-WTP Quality Assurance (QA) organization. This work was performed to the quality requirements of NQA-1-1989 Part I, Basic and Supplementary Requirements, NQA-2a-1990, Part 2.7 and DOE/RW-0333P, Rev 13, Quality Assurance Requirements and Descriptions (QARD). These quality requirements are implemented through PNWD's *Waste Treatment Plant Support Project (WTPSP) Quality Assurance Requirements and Description Manual*. The analytical requirements are implemented through WTPSP's

Statement of Work (WTPSP-SOW-005) with the Radiochemical Processing Laboratory (RPL) Analytical Service Operations (ASO).

Experiments that were not method-specific were performed in accordance with PNWD's procedures QA-RPP-WTP-1101, "Scientific Investigations," and QA-RPP-WTP-1201, "Calibration Control System," ensuring that sufficient data were taken with properly calibrated measuring and test equipment (M&TE) to obtain quality results.

PNWD addresses internal verification and validation activities by conducting an independent technical review of the final data report in accordance with PNWD's procedure QA-RPP-WTP-604. This review verifies that the reported results are traceable, that inferences and conclusions are soundly based, and the reported work satisfies the Test Plan objectives. This review procedure is part of PNWD's *WTPSP Quality Assurance Requirements and Description Manual*.

2.0 Scaled Test Stands

This section describes the geometrically scaled test stands used to represent the full-scale UFP and LS vessels in testing the mixing effectiveness of various PJM/hybrid mixer designs. The dimensional information presented in this section is divided into three categories based on 1) standard component size, 2) measurements taken before or during or recreated after testing, and 3) nominal or approximate measurements based on target values or ranges.

The first category pertains to the internal or external diameters of the stainless steel or polyvinyl chloride (PVC) tubing/piping materials used in construction of the pulse tubes, nozzles, recirculation lines, and sparger lines. Although the actual diameters vary from manufacturer to manufacturer, these values are generally within ±5%. In the text, tables, and figures, only the nominal sizes are listed for the diameters of pulse tubes, nozzles, recirculation lines, and sparger lines unless otherwise noted.

The second category of dimensional measurements is quantified based on measurements made with a tape measure, protractor, or caliper and are presented as such in the discussion with the appropriate uncertainties. This category typically applies to direct measurements of nonstandard tubing and piping materials and assemblies used in the tests.

The third category of measurements mainly corresponds to dimensional information that was impossible to obtain exactly or measure directly, such as spatial locations and elevations of the vessel internals relative to its bottom (e.g., distance of nozzles from bottom). Although significant efforts were made to achieve the target values specified in the testing sequences, no direct as-built measurements were made in most cases because of space limitations within the tank (i.e., manned entry was not possible). In other cases, direct measurements were made using less precise measuring devices (carpenter's rule or objects such as a tube with a measured mark) that were placed beside the items being measured but could only be read from outside the tank. In addition, this category also includes measurements that were not recorded at the time of testing and could only be estimated based on information obtained during testing or construction/installation. This category of measurements is indicated as nominal or approximate in the text, tables, and figures and should be treated as such, irrespective of the precision implied by the reported measurement. The test stand configurations and operating conditions for the test sequences in this document are subject to the dimensional constraints presented in this section.

2.1 UFP Scaled Test Stand

The UFP scaled test stand consisted of an ellipsoidal-bottom, open-top tank containing four or six PJMs in a fixed configuration, with or without sparger tubes in a fixed configuration, and in some sequences a recirculation system with recirculation pump discharge and suction lines at various locations within the tank. A Plexiglas shroud enclosed the PJM assembly in test sequences 15 and 16. Test sequence numbers not presented in this document area those for which no conclusive mixing result was obtained, or sequences used to derive drive functions or check system performance.

The 168-inch-diameter, full-scale UFP tank was represented by a 34 ± 1-inch-ID clear acrylic vessel. The geometric scale factor was approximately 4.94. The scaled UFP test vessel was 90½ ± ½ inches tall with the bottom an approximately 2:1 elliptical dish head of stainless steel. All PJMs used for the tests in the UFP scaled platform were provided by BNI.

Figure 2.1 is a simplified diagram of a PJM. The dimensions reported in this figure are approximate. The PJMs consisted of a 6-inch-diameter schedule 40 stainless-steel pipe with a domed stainless steel cap attached at the top. The dome was approximately 5 inches high with approximately 2 inches nearly parallel with the 6-inch pipe. The domed cap was connected to a 2-inch-diameter stainless steel coupling, attached in turn to a 2-inch-diameter schedule 40 stainless-steel pipe. The 2-inch-diameter pipe was approximately 13¼ inches long and connected to a ¾-inch-diameter schedule 40 stainless-steel pipe via a stainless-steel reducer coupling. This pipe supplied air pressure, vent, and vacuum inputs to the PJM.

The bottom of the 6-inch-diameter pipe was welded to a 6-inch-diameter stainless-steel coupling, where a stainless-steel conical section was attached. The conical section had a 60° taper that was truncated at its lower end and welded to a 2-inch-diameter schedule 40 threaded pipe section, where a nozzle assembly was attached via a 2-inch-diameter coupling or reducer coupling. The upper end of the cone was welded to a section of 6-inch-diameter schedule 40 stainless steel pipe that threaded into the 6-inch-diameter coupling welded onto its lower end. The overall length of the straight section of pipe, including the threaded section attached to the cone and the straight section of the dome cap, was approximately 37 inches (± 1 inch). This corresponds to a PJM height scale factor of approximately 4.32. The difference between the UFP tank dimension scale factor and the pulse tube dimension scale factor was dictated by the need to use standard pipe sizes for procurement expediency. However, the volume expelled from the PJMs was consistent with the UFP vessel scale factor of approximately 4.94.

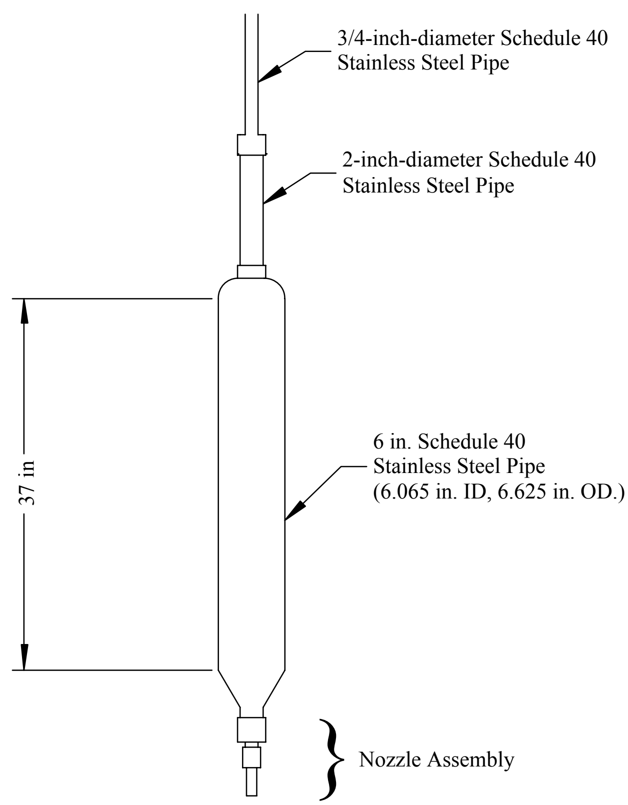

Figure 2.1. Schematic Diagram of PJM Used in UFP Scaled Test Stand

A nozzle assembly was attached to the bottom of each PJM tube. Except where noted, the center and perimeter PJM nozzle assemblies were constructed so that the lowest points on the nozzle assemblies were raised the same distance off the tank bottom directly below them.

A summary of the UFP test sequences and corresponding PJM/hybrid mixer configurations is presented in Table 2.1. In this table the sequence and run numbers are test identifiers, and "test type" refers to whether the test parameter observed was mixing, solids lift, or cloud height. The mixing tests used tracers to assess the extent of mixing; the technique is described in Section 3.1.2. The solids lift and cloud-height tests used glass beads to assess the ability of the PJMs to mobilize solids off the bottom of the tank. That technique is described in Section 3.1.3. The test mode entry indicates the operational modes of PJM/hybrid systems during the testing sequence (e.g., PJMs, spargers, and recirculation pumps/nozzles). Details of the PJMs, sparger tube assembly, and recirculation system configurations used in the tests are included in Sections 2.1.1 through 2.2.

2.1.1 UFP Scaled Test Stand Configurations

Different physical arrangements and varying combinations of PJMs, spargers, and recirculation nozzles were used for the mixing, solids-lift, and cloud-height testing in the UFP scaled test stand. Table 2.2 summarizes the three PJM/sparger configurations used during the tests. Plan and elevation views of the vessel and internals for the three PJM/sparger configurations with nominal dimensions are shown in Figures 2.2 through 2.7. The PJM and sparger tube positions reported in these figures are considered approximate and are based on templates used to position the PJMs and procedures used to set the target elevations of the PJM nozzle tips.

The PJM arrays consisted of either four or six PJMs, one in the center and either three or five equally spaced around the center. The four-PJM configuration was generally referred to as the "trifoil" (3+1), and the two six-PJM configurations were generally referred to as the "cluster" (5+1) and "cluster" (5+1) configurations. Both the trifoil and cluster configurations included sparger tubes that were made from ½-inch OD (0.37-inch ID) stainless steel tubing.

Figures 2.2 and 2.3 are plan and elevation views, respectively, of the trifoil configuration that was used to study the PJM and sparger hybrid configurations without obstruction of the spargers by additional PJMs in test sequences 1, 2, and 3B. Because the PJMs were to generate a mixed region at the bottom of the vessel, and the spargers were to extend the mixed region to the simulant surface, four PJMs were deemed suitable for testing. The trifoil configuration consisted of one PJM in the center and three spaced at 120º intervals around it on a pitch circle diameter (PCD) of approximately 14¼ inches. Four spargers were used in this configuration; the center sparger was approximately midway between adjacent perimeter PJMs at a radial position of approximately 5 inches from the tank centerline. The perimeter spargers were placed about midway between adjacent perimeter PJMs at a PCD of 20⅜ inches, based on measurements of a template used to position the PJMs and spargers. The lower ends of the sparger tubes were approximately 3 to 4 inches from the tank floor, based on procedures used to set them at target elevations.

Table 2.1. UFP Test Sequences Presented in this Report and Corresponding PJM, Sparger, and Recirculation Pump Configurations[a,b]

				PJM Configuration				Sparger Configuration			Recirculation Pump Discharge Configuration			
Seq. No.	**Run**	**Test Type**	**Test Mode**	**PJM Arrangement**	**Nozzle Type**	**Noz. Dia. (in.)**	**Elevation (in.)[c]**	**No. of Spargers**	**Radial Pos.**	**Elevation (in.)[c]**	**Noz. Dia (in.)**	**PCD (in.)**	**Elevation (in.)[c]**	**Angle**
1	1	Mixing	PJM Only	Trifoil (3+1)	45º (3); Vertical (1)	0.82	2	--	--	--	--	--	--	--
1	2	Mixing	PJM Only	Trifoil (3+1)	45º (3); Vertical (1)	0.82	2	--	--	--	--	--	--	--
1	3	Mixing	PJM + Sparging	Trifoil (3+1)	45º (3); Vertical (1)	0.82	2	1 (near center)	Figure 2.2	4	--	--	--	--
1	4	Mixing	PJM + Sparging	Trifoil (3+1)	45º (3); Vertical (1)	0.82	2	3 (outer)	Figure 2.2	4	--	--	--	--
2	1	Mixing	PJM Only	Trifoil (3+1)	45º (3); Vertical (1)	0.82	2	--	--	--	--	--	--	--
2	2	Mixing	PJM Only	Trifoil (3+1)	45º (3); Vertical (1)	0.82	2	--	--	--	--	--	--	--
2	3	Mixing	PJM + Sparging	Trifoil (3+1)	45º (3); Vertical (1)	0.82	2	1 (near center)	Figure 2.2	4	--	--	--	--
2	4	Mixing	PJM + Sparging	Trifoil (3+1)	45º (3); Vertical (1)	0.82	2	3 (outer)	Figure 2.2	4	--	--	--	--
3B	0	Mixing	PJMs Only	Trifoil (3+1)	45º (3); Vertical (1)	0.82	2	--	--	--	--	--	--	--
3B	1	Mixing	PJM + Pump	Trifoil (3+1)	45º (3); Vertical (1)	0.82	2	--	--	--	0.957	11	23 ¾	0º, down
3B	2	Mixing	PJM + Pump	Trifoil (3+1)	45º (3); Vertical (1)	0.82	2	--	--	--	0.957	11	23 ¾	0º, down
3B	3	Mixing	PJM + Pump + Sparging	Trifoil (3+1)	45º (3); Vertical (1)	0.82	2	1 (near center)	Figure 2.2	4	0.957	11	24	0º, down
7	1-4	Solids Lift	PJMs only	Cluster (5+1)	45º (5); Vertical (1)	0.82	2	--	--	--	--	--	--	--
7	5	Solids Lift	Center PJM only	Cluster (5+1)	Vertical (1)	0.82	2	--	--	--	--	--	--	--
7A	1	Cloud Test	PJMs Only	Cluster (5+1)	45º (5); Vertical (1)	0.82	2	--	--	--	--	--	--	--
7A	2	Cloud Test	PJMs Only	Cluster (5+1)	45º (5); Vertical (1)	0.82	2	--	--	--	--	--	--	--
8	1-7	Solids Lift	PJMs Only	Cluster (5+1)	60º (5); Vertical (1)	0.82	2	--	--	--	--	--	--	--
9	1-4	Solids Lift	PJMs Only	Expanded Cluster (5+1)	45º (5); Vertical (1)	0.82	2	--	-	--	--	--	--	--
9A	1a	Cloud Test	PJMs Only	Expanded Cluster (5+1)	45º (5); Vertical (1)	0.82	2	--	--	--	--	--	--	--
9A	2a	Cloud Test	PJMs Only	Expanded Cluster (5+1)	45º (5); Vertical (1)	0.82	2	--	--	--	--	--	--	--
10	1–3	Solids Lift	PJMs Only	Expanded Cluster (5+1)	30º (5); Vertical (1)	0.82	2	--	--	--	--	--	--	--
10A	1a	Cloud Test	PJMs Only	Expanded Cluster (5+1)	30º (5); Vertical (1)	0.82	2	--	--	--	--	--	--	--
10A	2a	Cloud Test	PJMs Only	Expanded Cluster (5+1)	30º (5); Vertical (1)	0.82	2	--	--	--	--	--	--	--

Table 2.1 (contd)

				PJM Configuration				Sparger Configuration			Recirculation Pump Discharge Configuration			
Seq. No.	**Run**	**Test Type**	**Test Mode**	**PJM Arrangement**	**Nozzle Type**	**Noz. Dia. (in.)**	**Elevation (in.)[(c)]**	**No. of Spargers**	**Radial Pos.**	**Elevation (in.)[(c)]**	**Noz. Dia (in.)**	**PCD (in.)**	**Elevation (in.)[(c)]**	**Angle**
11	1	Mixing	PJMs Only	Expanded Cluster (5+1)	30º (5); Vertical (1)	0.82	2	--	--	--	--	--	--	--
11	2	Mixing	PJMs Only	Expanded Cluster (5+1)	30º (5); Vertical (1)	0.82	2	--	--	--	--	--	--	--
12	1	Mixing	PJMs Only	Expanded Cluster (5+1)	30º (5); Vertical (1)	0.82	2	--	--	--	--	--	--	--
12	2	Mixing	PJM + Pump	Expanded Cluster (5+1)	30º (5); Vertical (1)	0.82	2	--	--	--	0.64	25.5	8	45°[(d)]
13	1	Mixing	PJM Only	Cluster (5+1)	45º (5); Vertical (1)	0.82	1¼	--	--	--	--	--	--	--
13	2	Mixing	PJM Only	Cluster (5+1)	45º (5); Vertical (1)	0.82	1¼	--	--	--	--	--	--	--
13	3	Mixing	PJM + Pump	Cluster (5+1)	45º (5); Vertical (1)	0.82	1¼	--	--	--	1.107	25	17⅛	0° down
15[(e)]	1	Mixing	PJM Only	Cluster (5+1)	45º (5); Vertical (1)	0.82	1¼	--	--	--	--	--	--	--
15[(e)]	2	Mixing	PJM + Pump + Sparging	Cluster (5+1)	45º (5); Vertical (1)	0.82	1¼	3 around perimeter	Figure 2.4	4	1.107	25	17⅛	0º, down
16[(e)]	1	Mixing	PJM + Sparging	Cluster (5+1)	45º (5); Vertical (1)	0.82	1¼	3 around perimeter	Figure 2.4	4	--	--	--	--

(a) Test results discussed in Sections 6 and 7.
(b) Configuration spatial and dimensional distances values in table do not reflect the type of measurement or accuracy. See text for details.
(c) Approximate distance from the bottom of the tank under the nozzle-distance is slightly less for peripheral spargers.
(d) Angle above horizontal (see Figure 2.18)
(e) Configuration selected.

Table 2.2. Summary Description of UFP Scaled Test Stand PJM and Sparger Configurations

Configuration Name	General Description	Nominal PCD of Perimeter PJMs	Nominal PCD of Spargers	Applicable Sequences
Trifoil (3+1)	Three equally spaced perimeter PJMs surround a center PJM. Three perimeter air spargers are equally spaced between perimeter PJMs and midway between the perimeter PJM tube wall and the tank wall. A single center air sparge is placed between one of the perimeter spargers and the center PJM tube wall (Figures 2.2 and 2.3).	14¼ inch	10-inch center sparger *or* 20⅜ inch perimeter spargers	1, 2, 3B
Cluster (5+1)	Five equally spaced perimeter PJMs surround a center PJM. Three spargers, installed for sequences 15 and 16, are approximately equally spaced around tank (Figures 2.4 and 2.5).	14¾ inch	24 inch	7, 7A, 8, 13, 15, 16
Expanded Cluster (5 + 1)	Five equally spaced perimeter PJMs surround a center PJM; the perimeter PJMs are about 2 inches farther outward than those in the cluster (5+1) configuration. No spargers (Figures 2.6 and 2.7).	18⅜ inch	NA	9, 9A, 10, 10A, 11, 12

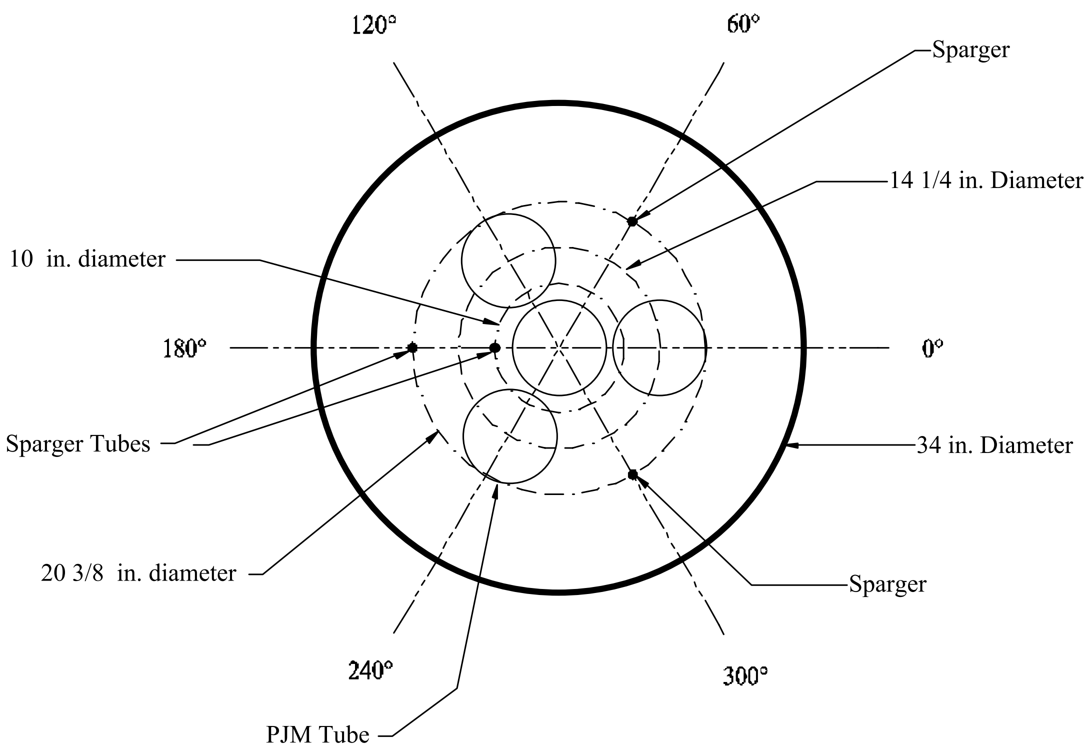

Figure 2.2. Plan View of Trifoil Configuration in UFP Scaled Test Stand Showing Nominal Locations of PJMs and Spargers Used in Sequences 1, 2, and 3B

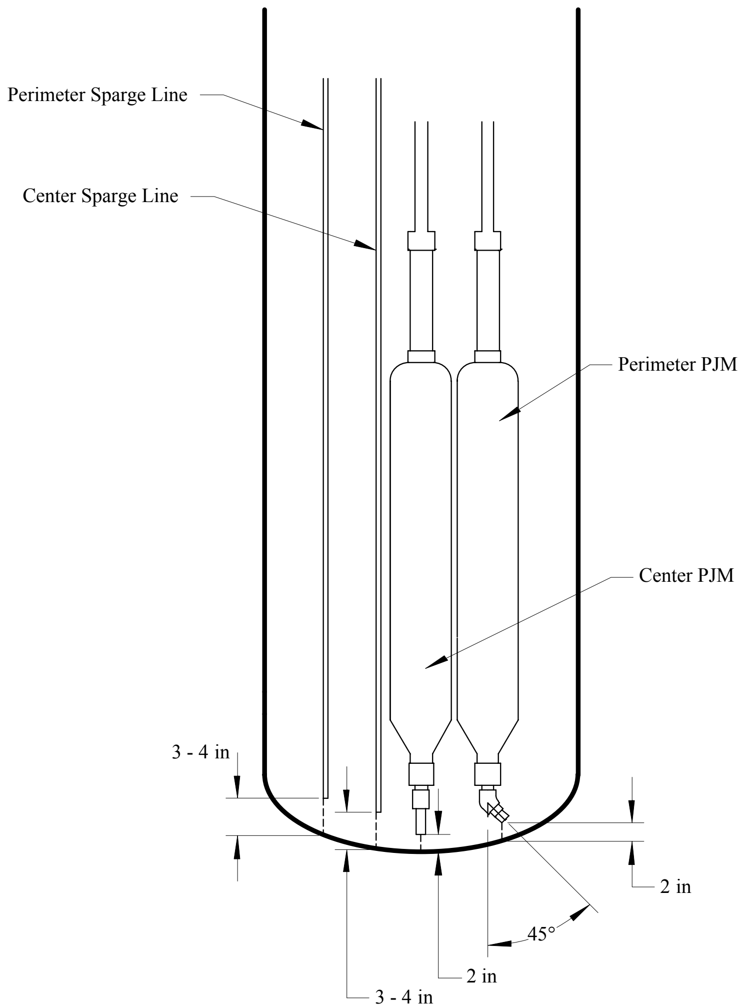

Figure 2.3. Elevation View of Trifoil Configuration in UFP Scaled Test Stand Showing Nominal Locations of PJMs (with center and 45° nozzle assemblies) and Spargers Used in Sequences 1, 2, and 3B.

Figures 2.4 and 2.5 are top and plan views, respectively, of the cluster (5+1) configuration that was used in sequences 7, 7A, 8, 13, 15, and 16. The actual vessel will have six PJMs arranged in a configuration similar to that evaluated in the test stand.

Figures 2.6 and 2.7 are top and plan views of the expanded cluster configuration. This configuration was used in sequences 9, 9A, 10, 10A, 11, and 12 and underwent limited evaluation as a variation of the cluster configuration. The expanded cluster configuration consisted of six PJMs, one in the center and five perimeter PJMs at 72º intervals around the center. The perimeter PJMs in the expanded cluster configuration were positioned on a PCD of approximately 18⅜ inches about the tank centerline. This configuration did not include any sparger tubes.

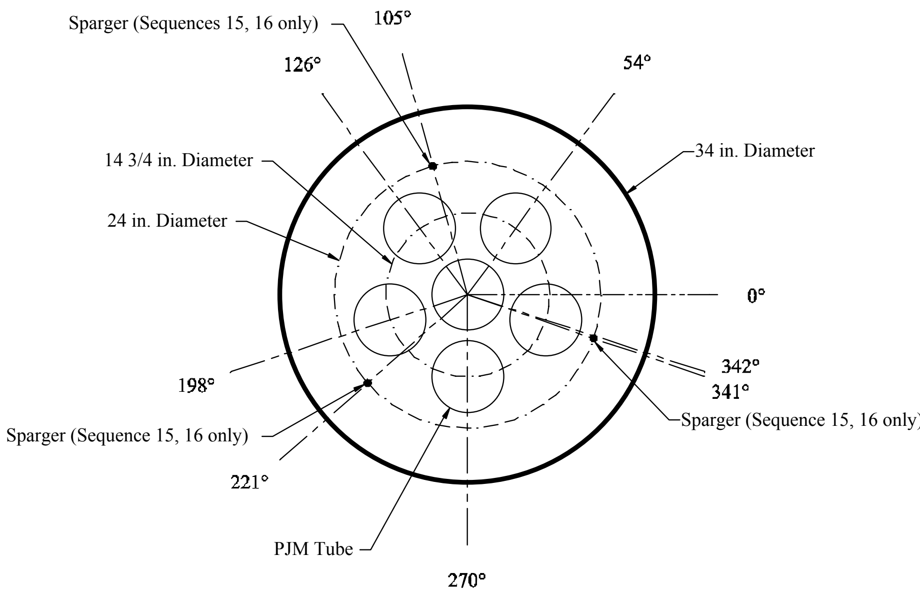

Figure 2.4. Plan View of Cluster Configuration in UFP Scaled Test Stand Showing Nominal Locations of PJMs and Spargers Used in Sequences 7, 7A, 8, 13, 15, and 16

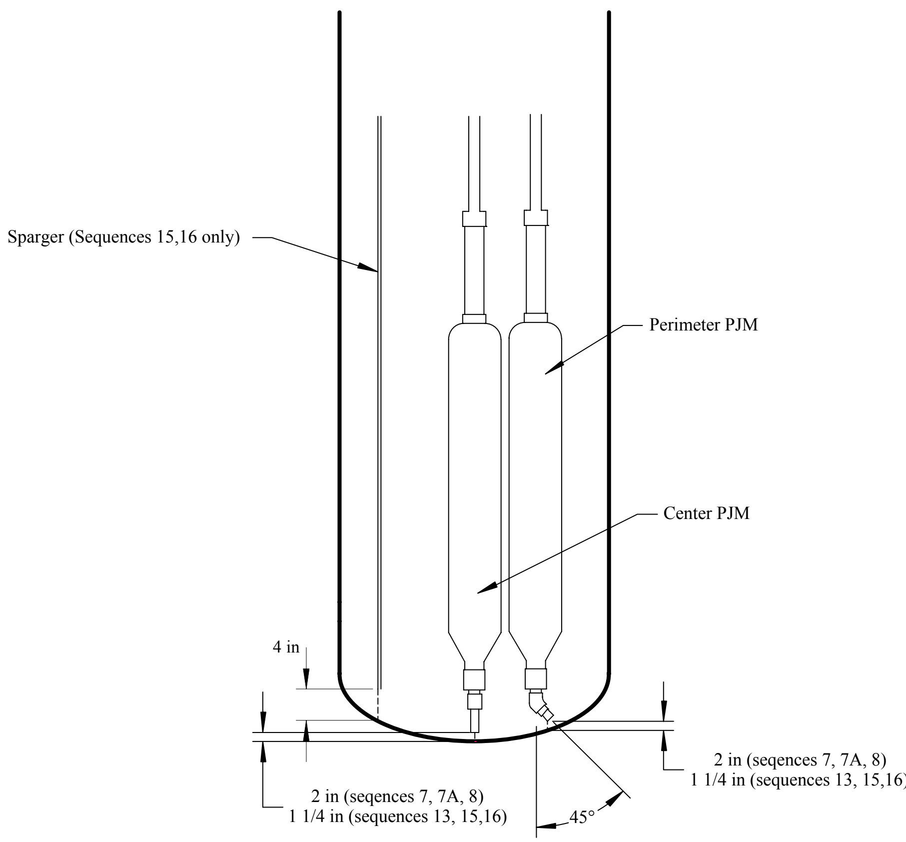

Figure 2.5. Elevation View of Cluster Configuration in UFP Scaled Test Stand Showing Nominal Locations of PJMs (with center and 45° nozzle assemblies) and Spargers Used in Sequences 7, 7A, 8, 13, 15, and 16

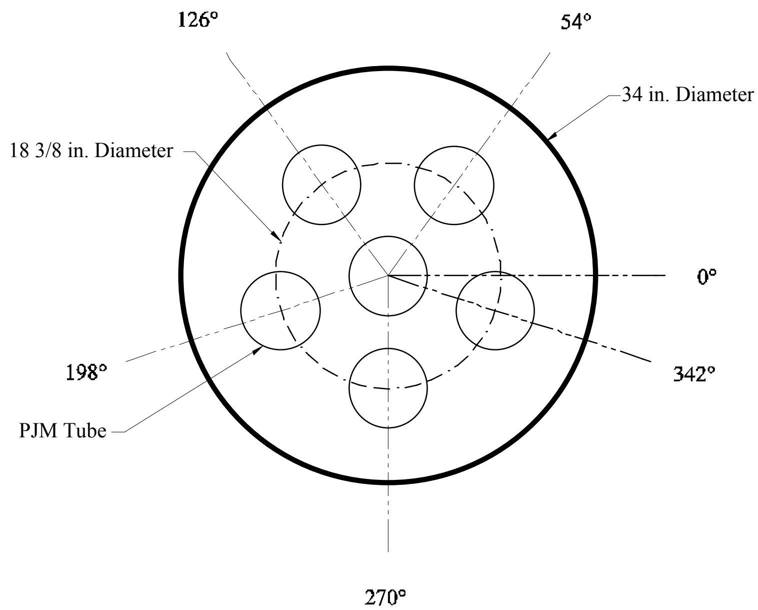

Figure 2.6. Plan View of Expanded Cluster Configuration in UFP Scaled Test Stand Showing Nominal Locations of PJMs and Spargers Used in Sequences 9, 9A, 10, 10A, 11, and 12

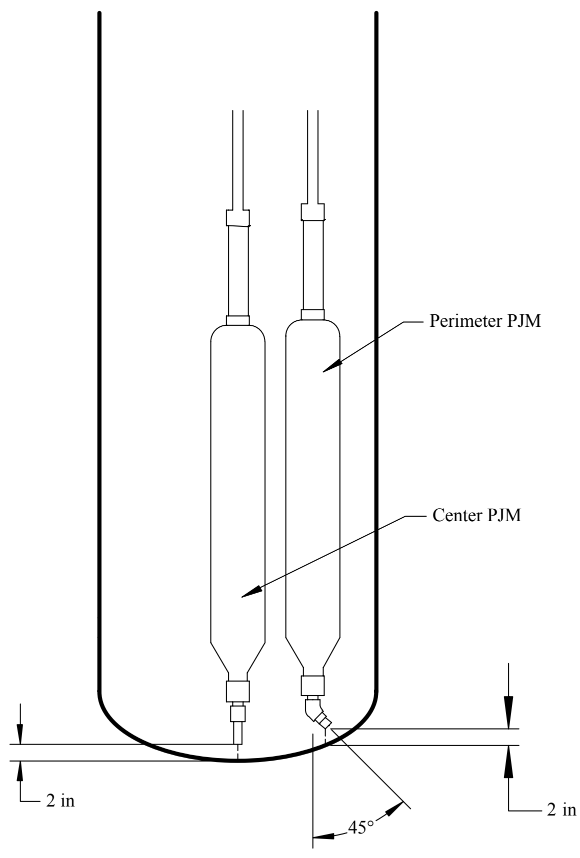

Figure 2.7. Elevation View of Expanded Cluster Configuration in UFP Scaled Test Stand Showing Nominal Locations of PJMs (with center and 45° nozzle assemblies) and Spargers Used in Sequences 9, 9A, 10, 10A, 11 and 12

The cluster configuration consisted of six PJMs, one in the center and five around the perimeter at 72º intervals. The perimeter PJMs in this configuration were positioned on a PCD of approximately 14¾ inches about the tank centerline. Only sequences 15 and 16 had spargers installed in the cluster PJM configuration; three spargers were equally spaced around the tank centerline and approximately 12 inches from it, based on measurements of the distance between the center PJM nozzle and the sparger tubes. The approximate angular location of each sparger tube was determined by measuring its location with respect to the positions of three or more of the ¾-inch pipelines supplying air to the PJMs. The orientation was chosen to place one of the sparge tubes on the opposite side of the tank from the recirculation pump discharge line used in these sequences. The sparger tubes were made of ½-inch-OD stainless steel tubing, and the lower ends of the tubes were 4 inches above the bottom of the tank, measured from the tank floor beneath the sparge tube either by placing the tube on the tank bottom and raising it 4 inches or by placing a tube (marked 4 inches from its end) next to the sparge tube and adjusting the sparger tube outlet level to this mark. All measurements were made with a tape measure. A Plexiglas shroud was placed around the PJM cluster for sequences 15 and 16. The shroud is discussed in detail in Section 2.1.4.

2.1.2 PJM Nozzle Assemblies

The nozzle assemblies used in the UFP test stand were configured to direct the slurry at specific orientations relative to the tank bottom. The center PJM nozzle assemblies always directed the flow vertically downward (0º) at the tank centerline. The perimeter PJM nozzles for most tests directed the flow at a 45º angle from vertical in a radial direction away from the tank centerline. This orientation directed the flow at an incident angle approximately normal to the tank bottom. Angles of 30º and 60º were also employed with alternative perimeter PJM nozzle assemblies to investigate the effects of nozzle angle. The target nozzle elevation (distance above tank bottom) for the PJM assemblies was established by lowering the PJM assembly into the tank so that the lowest point on the perimeter and center PJM nozzles touched the tank bottom at the same time and then raising the entire PJM assembly to achieve the target distance from the nozzle to the tank bottom.

The lowest point on the PJM assemblies was raised to a target elevation of approximately 2 inches for sequences 1, 2, 3B, 7, 7A, 8, 9, 9A, 10, 11, and 12 and approximately 1¼ inches for sequences 13, 15, and 16. Figures 2.3, 2.5, and 2.7 show the elevations for the center and 45º perimeter nozzle assemblies in these sequences. In sequences 8, 10, 10A, 11, and 12 the 45º nozzle assemblies were replaced with nozzle angles of 30º or 60º on the perimeter PJMs without adjusting the vertical length of the center PJM nozzle assembly. In these sequences the PJM assembly was lowered until the center and/or perimeter PJM nozzle assemblies touched the tank bottom and then raised to the target elevation. Slight differences in vertical height and lateral displacement of the lowest points of these alternative nozzle assemblies could have resulted in actual elevations being slightly different than the target level of 2 inches.

The center PJM nozzle assembly for both trifoil (3+1) and cluster (5+1) PJM configurations (Figure 2.8) consisted of (in order of assembly) a 5½-inch-long, ¾-inch-diameter schedule 40 stainless steel pipe connected to a 1 × ¾-inch-diameter stainless steel bushing inserted into a 2 × 1-inch-diameter stainless steel reducer coupling. The pipe forming the nozzle tip extended 4 15/16 inches out of the bushing, as shown in the figure, and pointed straight down toward the center of the tank bottom. The dimensions shown for the center PJM nozzle in Figure 2.8 are based on direct measurements of the nozzle assembly used in sequence 13 with a tape measure.

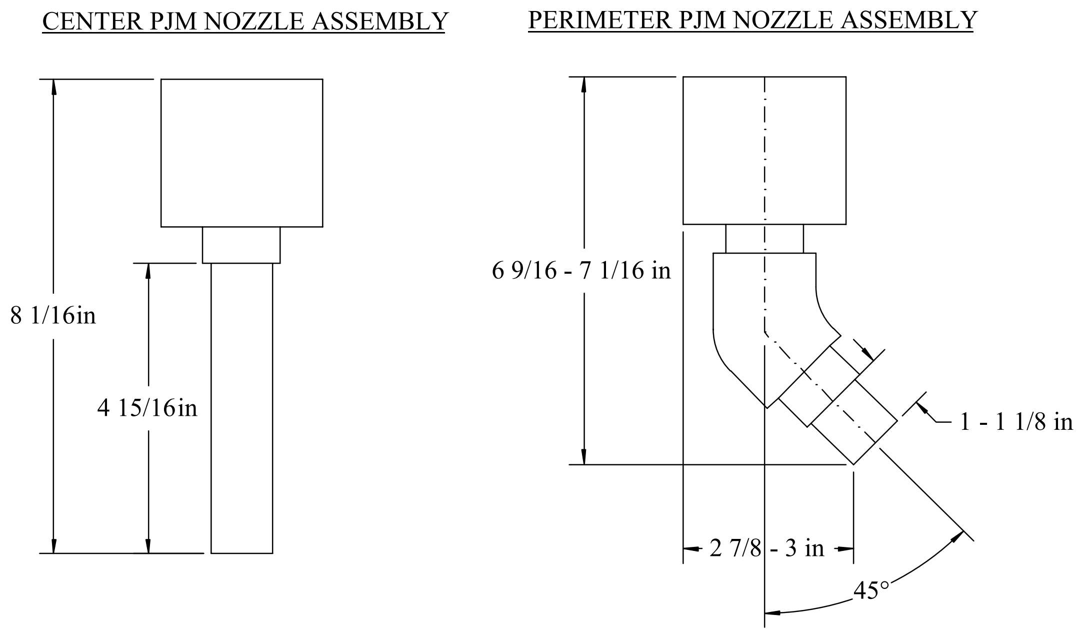

Figure 2.8. Schematic of Center and 45° Perimeter Nozzle Assemblies Used in UFP Scaled Test Stand and Range of Dimensions

The center nozzle assembly for the expanded cluster PJM configuration was similar to that used in the other two configurations except that the pipe forming the nozzle tip was calculated to be approximately 1⅜ inches longer to account for the larger PCD of the perimeter PJM tubes and the curvature of the tank bottom.

All of the perimeter PJM nozzle assemblies except those used in sequences 8, 10, 10A, 11, and 12 used standard schedule 40 stainless-steel pipe and fittings consisting of (in order of assembly) a nominal 1½-inch-long, ½-inch-diameter pipe, a 1 × ¾-inch-diameter bushing, a 1-inch-diameter 45° elbow, a 1-inch-diameter nipple, and a 2 × 1-inch-diameter threaded reducer coupling (see Figure 2.8). The pipe forming the nozzle tip extended approximately 1 to 1⅛ inches out of the bushing and pointed radially from the tank centerline at a 45° angle (based on the 45° elbow fitting). The lowest point on the nozzle tip was raised approximately 2 inches off the bottom for sequences 1, 2, 3B, 7, 7A, 9, and 9A and 1¼ inches off the bottom for sequences 13, 15, and 16. The dimensions shown in Figure 2.8 for the 45° perimeter PJM nozzles are direct measurements with a tape measure of the five nozzle assemblies used in sequence 13, three of which were also used in the trifoil configuration. The perimeter PJM nozzle assemblies used in sequences 8, 10, 10A, 11, and 12 were applied to investigate the effects of alternative perimeter nozzle angles on solids lift, cavern formation, and mixing. Schematic diagrams of these nozzle assemblies are shown in Figure 2.9.

The 60° nozzle assemblies (used in sequence 8) consisted of, in order of assembly, a nominal 1½-inch-long, ¾-inch-diameter schedule 40 stainless steel pipe, a 1 × ¾-inch-diameter stainless steel bushing, a 90º stainless steel elbow (elevation elbow), a 1-inch-diameter schedule 40 stainless steel nipple, a second 90º stainless steel elbow (lateral arm elbow), a second nipple, and a 2 × 1-inch-diameter stainless steel coupling. Measurements were carried out on two complete nozzle assemblies and two partial assemblies, each consisting of the two elbows and a connecting nipple. The lateral arms were

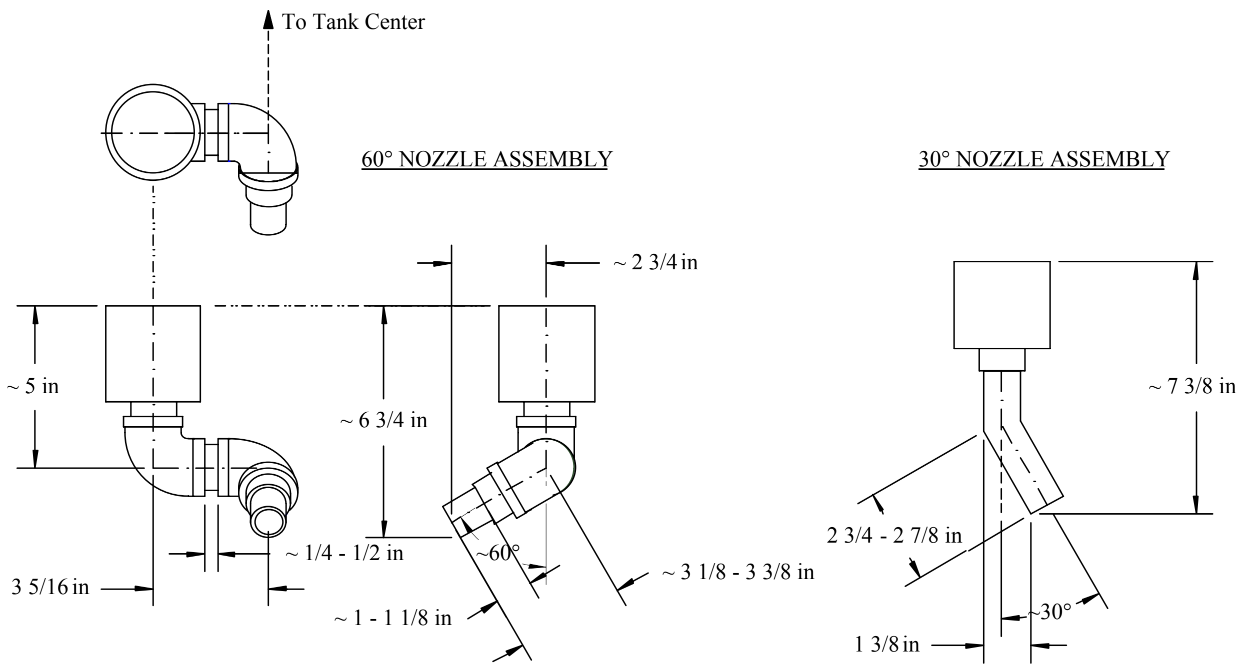

Figure 2.9. Schematic of 60° and 30° Perimeter PJM Nozzle Assemblies Used in UFP Scaled Test Stand and Range of Dimensions Measured

oriented so that the nozzles were aimed radially away from the center PJM nozzle, as shown in Figure 2.9. This resulted in placing the nozzle tip midway between adjacent PJMs instead of pointing radially outward from the perimeter PJM centerline.

The 30º nozzle assemblies, which were used in sequences 10, 10A, 11, and 12, consisted of nominal 5-inch-long, ¾-inch-diameter, schedule 40 stainless steel pipe cut approximately 2¾ inches from the nozzle outlet, both pieces beveled at 15º and welded together again to produce an approximately 2⅝-inch-long straight section at the nozzle tip (measured at centerline) welded at 30º to an approximate 1¾-inch-long pipe section (measured at pipe centerline). Each nozzle tip was inserted into a 1 × ¾-inch-diameter stainless steel bushing that, in turn, was inserted into a 2 × 1-inch-diameter stainless steel reducer coupling. The dimensions are based on direct measurements of the nozzle tips before and after reassembly with the bushings.

2.1.3 Recirculation System Configuration

Several different recirculation system configurations were used in sequences 3B, 12, 13, and 15. The recirculation system shown in Figure 2.10 consisted of two centrifugal pumps placed in parallel and then connected in series with a diaphragm pump that served to eliminate cavitation. The centrifugal pumps fed a manifold that supplied flow to up to four separate discharge lines. The recirculation pump system was configured to supply flow to a single discharge line in sequences 3B, 13, and 15 and was operated at a target flow rate of 90 ± 5 gpm. The discharge line nozzle was sized so the linear velocity exiting the nozzle was approximately 40 ft/sec for sequence 3B and approximately 30 ft/sec for sequences 13 and

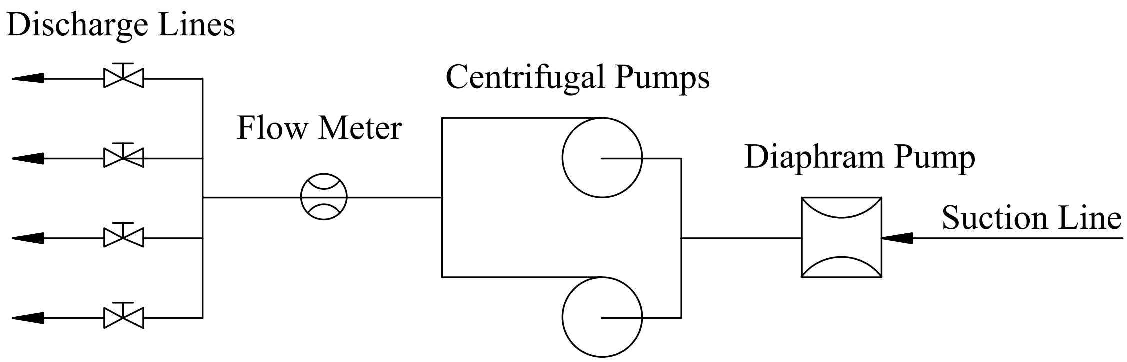

Figure 2.10. Configuration of Major Recirculation System Components

15. Sequence 12 used three discharge lines (see Figure 2.16) with a combined flow rate of 90 ± 5 gpm and nozzles sized to produce a linear velocity of approximately 32 ft/sec. Table 2.3 summarizes the recirculation system configurations evaluated in the UFP scaled test stand.

Two recirculation system configurations were used with the trifoil PJM configuration; both contained a single discharge line of 2-inch-diameter schedule 40 stainless steel pipe connected to a nozzle assembly with a 1-inch-diameter schedule 40 stainless steel nozzle tip pointing down and a single suction line consisting of 2-inch-diameter schedule 40 PVC pipe.

Figures 2.11 and 2.12 display the locations of the pump discharge and suction lines in the trifoil scaled UFP test stand for sequence 3B. The discharge-line nozzle for sequence 3B was situated approximately midway between two of the perimeter PJMs at a radial position approximately 5½ inches from the tank centerline and 23¾ inches above the tank bottom below the discharge nozzle tip. The nozzle assembly used in sequence 3B (Figure 2.13) consisted of a 4-inch-long, 1-inch-diameter schedule 80 PVC pipe extending 2¾ inches out of a 2 × 1-inch-diameter schedule 40 PVC slip-slip reducer bushing that was inserted into a 2-inch-diameter schedule 40 PVC coupling. The pump suction line in sequence 3B was at a radial position approximately 13 inches from the tank centerline at an angular position of 300º and an elevation of approximately 4 inches as measured from the edge of the inlet closest to the tank centerline to the tank floor. The suction line exited the tank through a port on the side of the tank about 14¾ inches above the bottom at the centerline.

A single recirculation pump discharge line was also used with the cluster PJM configuration in sequences 13 and 15. It was also placed in the scaled platform during sequence 16 but was not operated. Figures 2.14 and 2.15 show the locations of the pump discharge and suction lines used in this configuration. Also shown in Figure 2.14 is the location of a Plexiglas shroud that was used in sequences 15 and 16 (discussed in detail in Section 2.1.4). The discharge line was approximately 12½ inches away from the tank centerline and offset approximately 3⅛ inches from the PJM that was on the opposite side of the tank from the recirculation pump suction line, as shown in Figure 2.16. This placed it at an angular position of about 284°. The nozzle assembly shown in Figure 2.13 consisted of a 10 15/16-inch-long, 1-inch-diameter schedule 40 stainless-steel pipe bored to a 1.107-inch-ID and extending 10 1/16 inches out of a 2 × 1-inch-diameter stainless steel reducer coupling. The bottom of the nozzle tip was raised 17⅛ inches above the tank bottom, as shown in Figure 2.15.

Table 2.3. Summary Description of Recirculation System Configurations for UFP Scaled Test Stand

Description/PJM Configuration	Applicable Sequences	Discharge Line(s)				Suction Line	
		Number	Location[(a)]	Elevation of Nozzle	Nozzle Orientation	Location[(a)]	Elevation of Inlet
Single vertical pump discharge line/trifoil	3B	1	11-inch PCD from tank centerline at ~300°	23¾ inches above tank bottom	Straight down	26-inch PCD from tank centerline outboard of perimeter PJM at ~90°	4 inches above tank bottom
Single vertical pump discharge line/cluster	13,15	1	25-inch PCD from tank centerline at ~284°	17⅛ inches above tank bottom	Straight down	9-inch PCD from tank centerline exiting through tank wall side port at~90°	3⅞ inches above tank bottom
Three 45° angled pump discharge lines/expanded cluster	12	3	Nominal 25½-, 26-, and 27½-inch PCD from tank center-line at ~24°, ~146° and ~263°	8 inches above tank bottom below lateral arm of nozzle assembly	45° above horizontal pointed 90° with respect to tank centerline	4½ inches from tank centerline exiting through tank wall side port at ~90° location	3 inches above tank bottom
(a) Angular values are measured counterclockwise from the 0° reference, as indicated in Figure 2.2.							

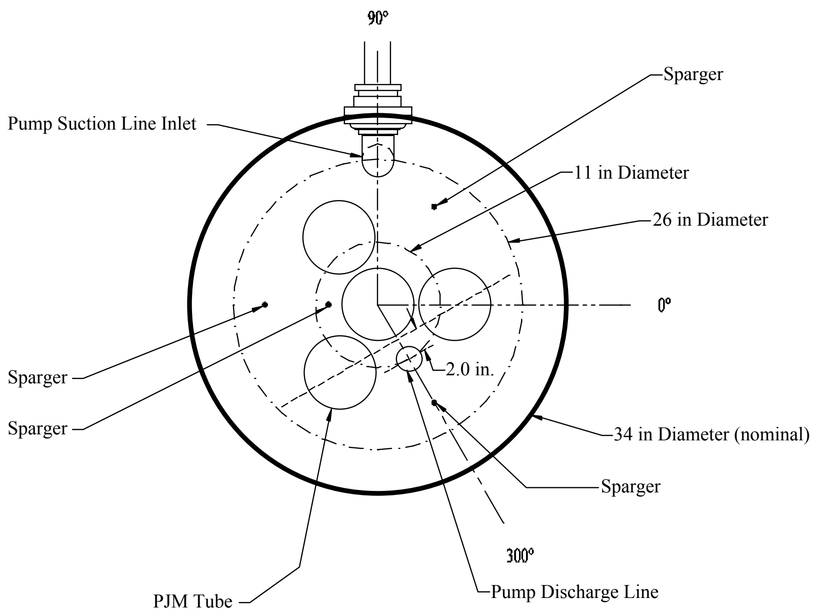

Figure 2.11. Plan View of Trifoil Configuration in UFP Scaled Test Stand Showing Nominal Location of Recirculation Components Used in Sequence 3B

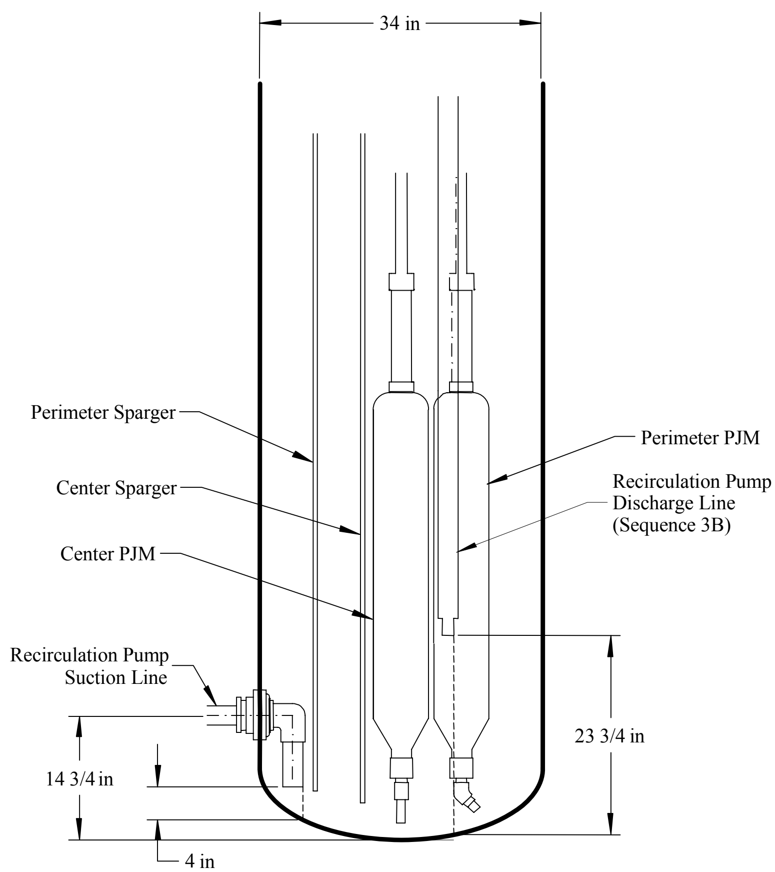

Figure 2.12. Elevation View of Trifoil Configuration in UFP Scaled Test Stand Showing Nominal Locations of Recirculation System Components Used in Sequence 3B

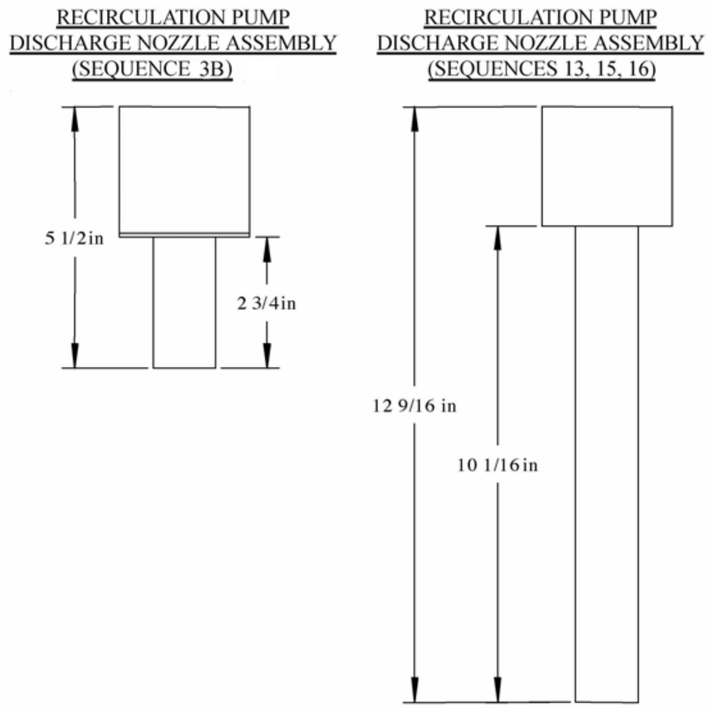

Figure 2.13. Elevation View of UFP Scaled Test Stand Recirculation Pump Discharge Line Nozzles Used in Sequences 3B (left), 13, and 15 (right)

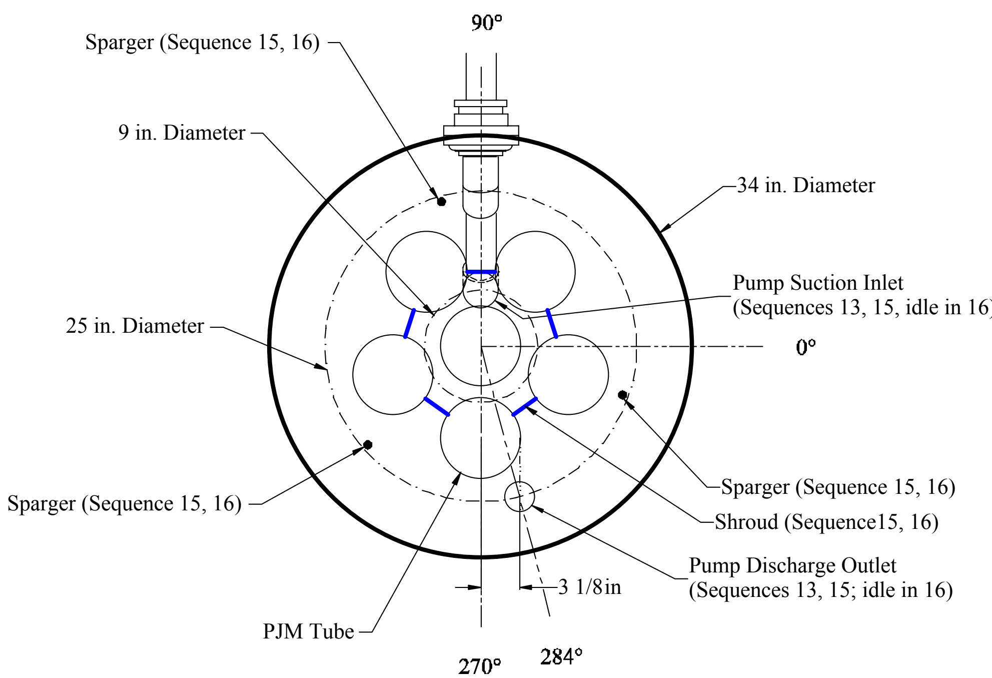

Figure 2.14. Plan View of UFP Cluster Configuration in UFP Scaled Test Stand Showing Nominal Locations of Recirculation System Components Used in Sequences 13, 15, and 16 and the PJM Shroud Used in Sequences 15 and 16

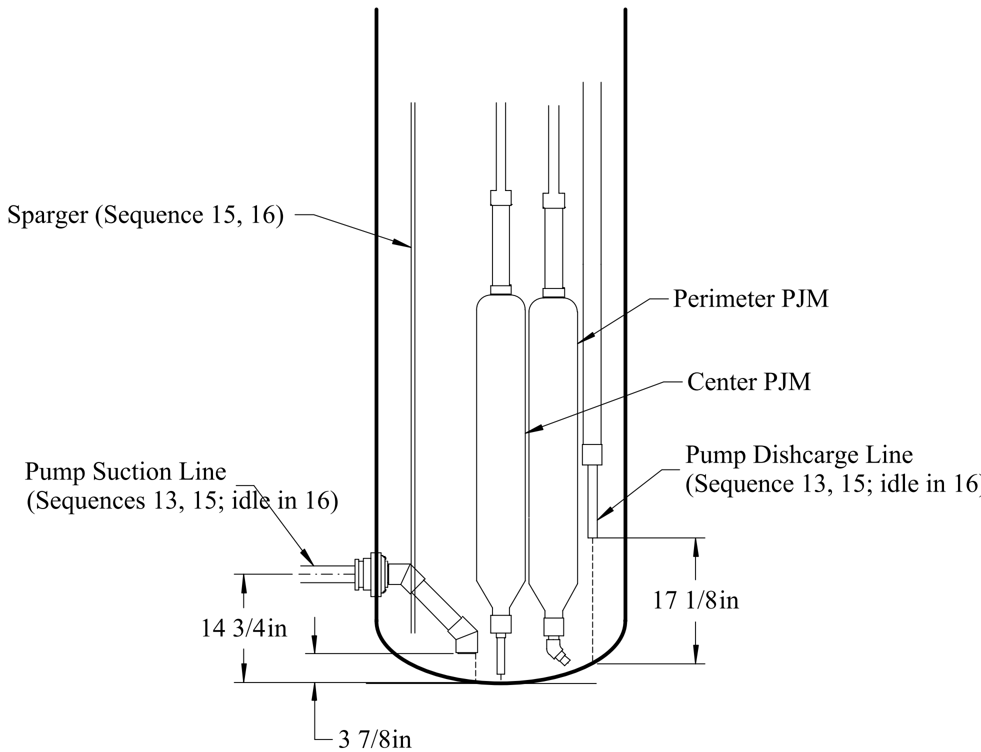

Figure 2.15. Elevation View of UFP Cluster Configuration in UFP Scaled Test Stand Showing Nominal Locations of Recirculation System Components Used in Sequences 13, 15, and 16

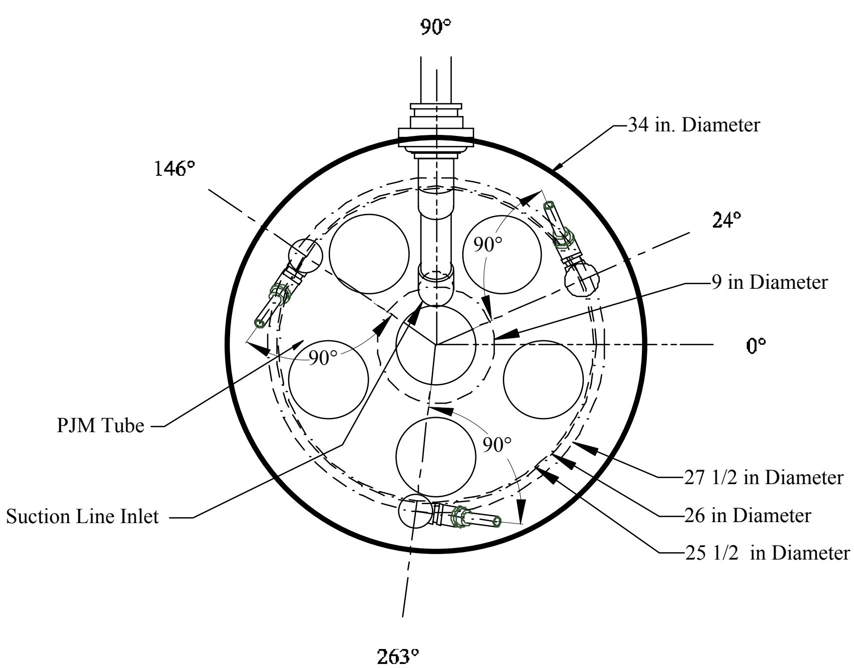

Figure 2.16. Plan View of Expanded Cluster Configuration in UFP Scaled Test Stand Showing Nominal Locations of Recirculation System Components Used in Sequence 12

The centerline of the recirculation pump suction line inlet was approximately 4½ inches from the tank centerline and approximately 3⅞ inches above the tank bottom measured from the edge of the suction inlet closest to the tank centerline. In both configurations, the suction line inlet was pointed down but exited the tank through a side port approximately 14¾ inches above the tank bottom centerline, as shown in Figure 2.15.

A recirculation system was also used with the expanded cluster configuration in the scaled test stand in sequence 12. The expanded cluster configuration in this sequence used 30° perimeter PJM nozzle assemblies and incorporated three 2-inch-diameter stainless steel pump discharge lines, as shown in Figures 2.16 and 2.17. The pump discharge-line nozzle assemblies shown in Figure 2.18 consisted of (in order of assembly) a 3 to 3½-inch-long, ½-inch-diameter schedule 40 stainless steel pipe, a 1 × ½-inch-diameter stainless steel bushing, a 45° stainless steel elevation elbow, a stainless steel nipple, a 90° stainless steel elbow, a second stainless steel nipple, and a 2 × 1-inch-diameter stainless steel reducer coupling that connected the assembly to the 2-inch-diameter discharge line. The elbows were aligned to aim the nozzle tip 45° above horizontal. The key dimensions of the nozzle assembly are based on measurements made with a tape measure on one complete nozzle assembly attached to a recirculation line and two partially built nozzle assemblies.

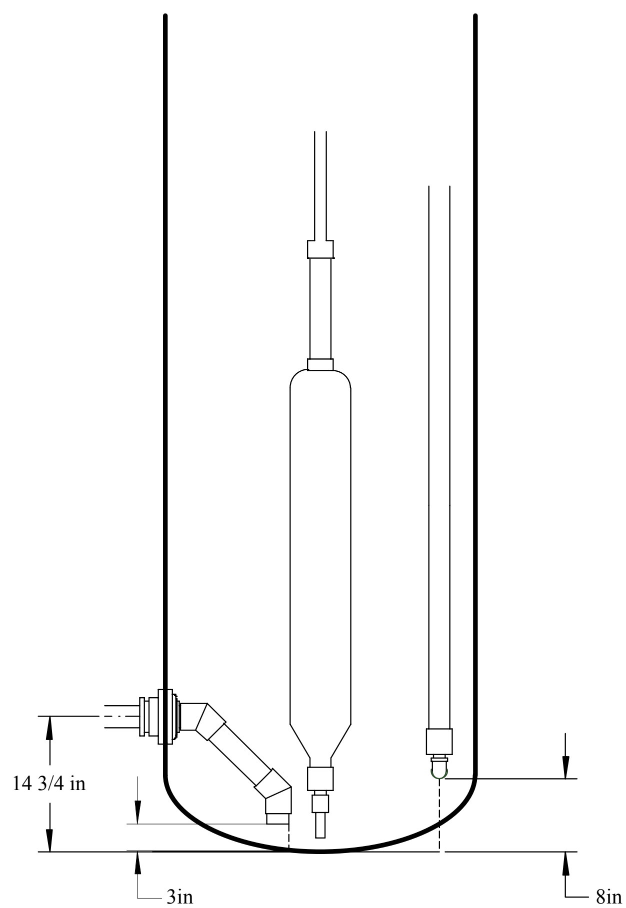

Figure 2.17. Elevation View of Expanded Cluster Configuration Used in UFP Scaled Test Stand Showing Nominal Locations of Recirculation System Components Used in Sequence 12

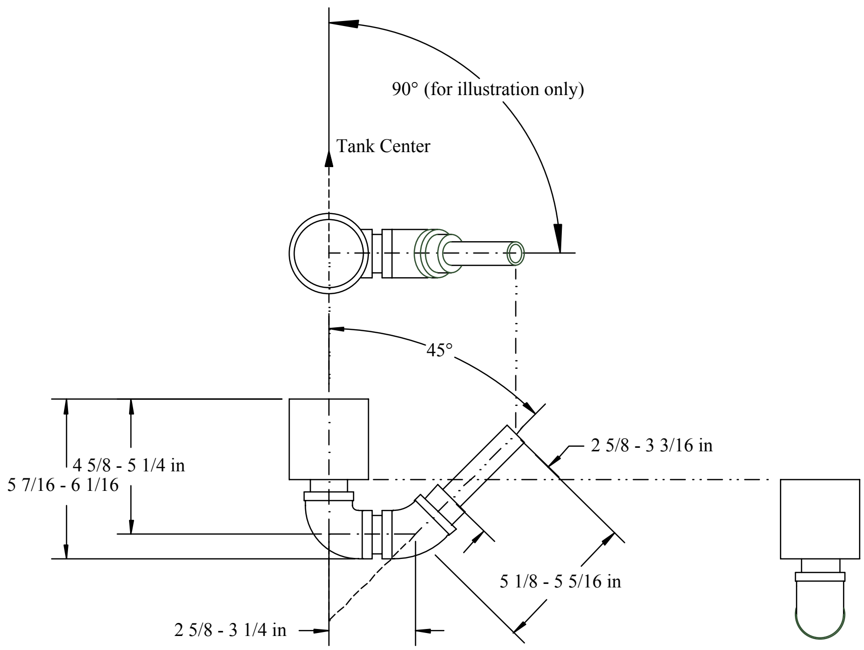

Figure 2.18. UFP Test Stand Recirculation Pump Discharge Nozzle Assembly Used in Sequence 12

The three discharge lines in sequence 12 were installed at approximate angular locations of 24º, 146º, and 263º around the center PJM at an estimated radius of 12¾ to 13¾ inches, based on careful observations of the recirculation line positions with respect to the nearest PJMs and discussions with the craftsmen. The lowest points on the nozzle assemblies were calculated to be approximately 8 inches above the bottom of the tank based on measurements of the positions of the brackets used to support two of the discharge lines that were still in place on the 2-inch discharge line pipes after they were removed from the test stand and the elevations of the PJM assembly support beams where the support brackets were attached. The nozzle assemblies were oriented so the discharge nozzle plumes would miss the PJMs. This placed the orientation of the nozzle assemblies slightly less than 90° with respect to the centerline. The plan view in Figure 2.16, however, shows the nominal orientation of the nozzle assemblies at 90°.

The suction line for sequence 12, also shown in Figures 2.16 and 2.17, was constructed of 2-inch-diameter schedule 40 PVC pipe and two 45° elbows. The centerline of the suction line inlet was approximately 4½ in. from the tank centerline and approximately 3 inches above the bottom of the tank directly below the inlet. The suction line exited the tank through the port 14¾ inches above the tank bottom at the centerline. The suction line location is based on both direct measurements of its position with respect to the center PJM nozzle and tank bottom and with respect to direct measurements of the inlet assembly components to determine the distance of the nozzle from the tank wall.

2.1.4 Scaled PJM Assembly Shroud Configuration for UFP Test Stand

A Plexiglas shroud was placed around the PJM assembly for sequences 15 and 16 to prevent slurry flow into the inner annulus formed between the perimeter and center PJMs. The sides of the shroud extended between the proximal sides of adjacent perimeter PJMs, as shown in Figure 2.14. The bottom of the shroud was at the bottom of the coupling connecting the conical section of the PJM to the cylindrical section, as shown in Figure 2.19. The bottom of the shroud was a flat Plexiglas plate with holes for the PJM conical sections to pass through (Figure 2.19). The top of the sides of the shroud extended up to the 2-inch-diameter couplings connecting the caps of the PJMs to the 2-inch air line, as shown in Figure 2.20. The top of the shroud consisted of five connected wedge-shaped sections of Plexiglas forming a five-sided pyramid with holes provided for the center PJM air line and for sample lines to the perimeter PJMs. The Plexiglas top formed an angle of approximately 130° with the Plexiglas sides (approximately 40° above horizontal) and the slope gradually decreased to approximately 125° with the center PJM air line (approximately 25° below horizontal). The joints where the Plexiglas pieces met the PJM surfaces, piping, or another Plexiglas sections were caulked with silicon sealant. The interior of the shrouded PJM assembly was filled with a rigid polyurethane foam sealant, injected as expandable, polyurethane intermediate and cured over several days to provide rigid support to the shroud.

Figure 2.19. Side View of UFP Scaled Shroud (left) and Bottom (right)

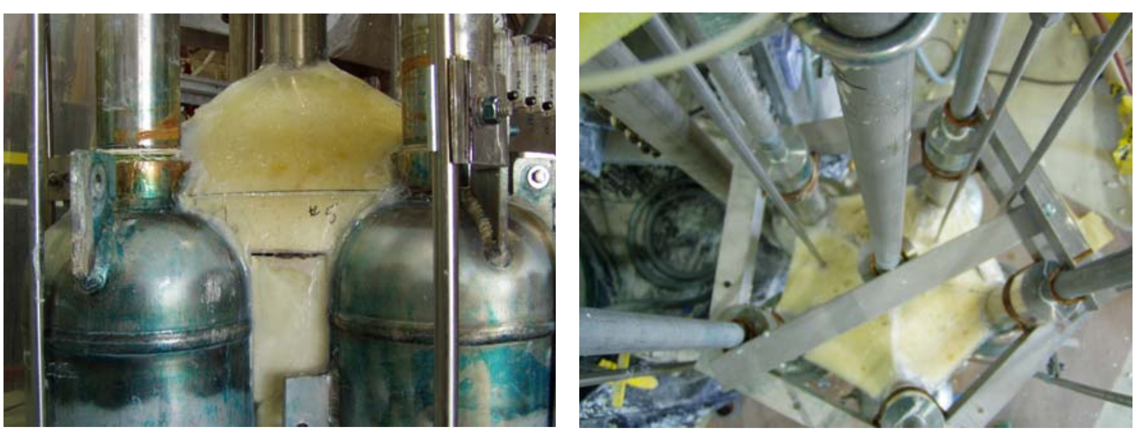

Figure 2.20. Top View of UFP Scaled Shroud Side (left) and Top (right)

2.2 Lag Storage Scaled Test Stand

The LS scaled test stand consisted of a round-bottom, open-top tank containing eight PJMs in a fixed configuration, with or without sparger tubes also in a fixed configuration, and in some sequences a recirculation system with recirculation pump discharge and suction lines at various locations within the tank. A Plexiglas shroud was used in test sequences 26 through 28 to enclose the PJM assembly. Test sequence numbers not presented in this document are those for which no conclusive mixing result was obtained or sequences used to derive drive functions or check system performance.

The 300-inch-diameter full-scale LS tank was represented by a 70 ± 1-inch-ID clear acrylic vessel. The scale factor was approximately 4.29. The scaled LS acrylic vessel was 90½ ± 1 inches tall with the bottom composed of a stainless steel 100-6% tank cap. All PJMs used in the LS scaled test stand were provided by BNI. Figure 2.21 shows a simplified diagram of a PJM. The dimensions reported are considered approximate.

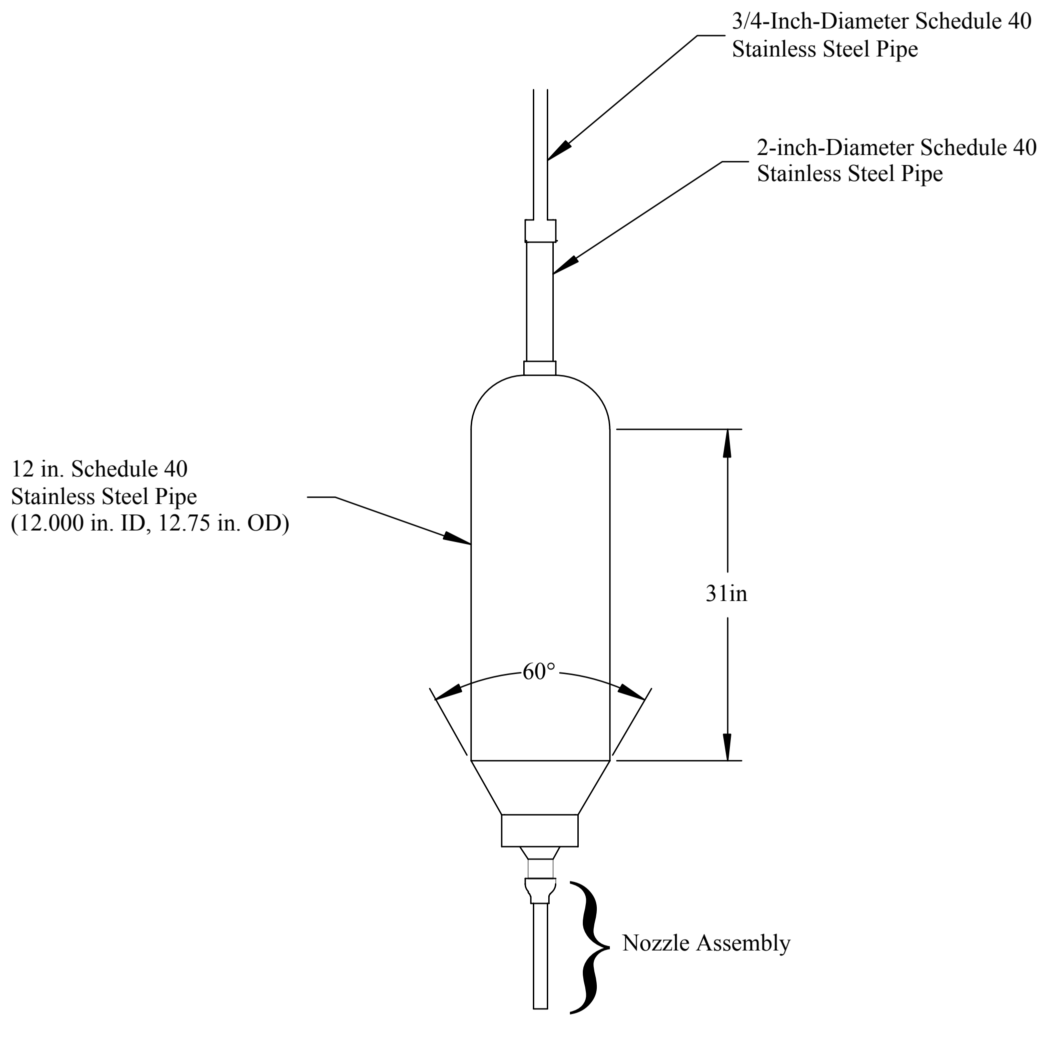

Figure 2.21. Schematic Diagram of PJM Used in LS Scaled Test Stand

The PJMs consisted of a nominal 28½-inch-long, 12-inch-diameter schedule 40 stainless steel pipe with a domed stainless steel cap welded to the top. The dome was nominally 7 inches long and approximately 2 inches of it were parallel with the 12-inch-diameter pipe. The domed cap was connected to a 2-inch-diameter stainless steel coupling that was, in turn, attached to a 2-inch-diameter schedule 40 stainless steel pipe. The 2-inch-diameter pipe was nominally 13¼ inches long and connected to a ¾-inch-diameter schedule 40 stainless steel pipe via a 2 × 1-inch-diameter stainless steel reducer coupling. The bottom of the 12-inch-diameter pipe was welded to a 60° tapered conical section that was truncated at its lower end where it was welded to a 6-inch-diameter schedule 40 stainless steel coupling (7⅜-inch-OD). A second 60° tapered cone was welded to a 6-inch-diameter schedule 40 stainless steel pipe section that was threaded into the 6-inch-diameter coupling. This cone was also truncated at its lower end and welded to a threaded section of 2-inch-diameter schedule 40 stainless steel pipe. A nozzle assembly was threaded onto the bottom of this section.

The cylindrical section of each PJM, including the straight section of the dome cap, was approximately 31 ±1 inches high, corresponding to a PJM height scale factor of approximately 4.93. The difference between the LS tank and pulse tube dimension scale factors was the need to use standard pipe sizes for procurement expediency. However, the volume expelled from the PJMs was consistent with the LS scale factor of approximately 4.29.

A nozzle assembly was attached to the bottom of each PJM tube. Except where noted, the center and perimeter PJM nozzle assemblies were constructed so that the lowest points on the perimeter and center PJM nozzle assemblies were the same distance from the tank bottom directly below their lowest points.

Table 2.4 is a summary of the LS test sequences and corresponding PJM/hybrid mixer configurations. In this table the sequence and run numbers are test identifiers, and "test type" refers to whether the test parameter observed was mixing, solids lift, or cloud height. The mixing tests used tracers to assess the extent of mixing; that technique is described in subsection 3.1.2.1. The solids lift and cloud-height tests used glass beads to assess the ability of the PJMs to mobilize solids off of the bottom of the tank, and that technique is described in Section 3.1.3. The test mode entry indicates the operational modes of PJM/hybrid systems during the testing sequence (e.g., PJMs, spargers, and recirculation pumps/nozzles). Details of the PJMs, sparger tube assembly, and recirculation system configurations used in the tests are given in Sections 2.2.1 through 2.2.4.

Table 2.4. LS Test Sequences Presented in this Report and the Corresponding PJM, Sparger, and Recirculation Pump Configurations[a, b]

Seq. No.	Run	Test Type	Test Mode	PJM Configuration				Sparger Configuration			Recirculation. Pump Discharge Config.				
				PJM Arrangement	**Nozzle Type**	**Noz. Dia. (in.)**	**Elevation (in.)[c]**	**No.**	**PCD (in.)**	**Elevation (in.)[c]**	**No. of Nozzles**	**Nozzle dia. (in.)**	**PCD (in.)**	**Elevation (in.)[c]**	**Angle[d]**
2A	1	Mixing	PJMs Only	Cluster (7+1)	45° (7) Vertical (1)	(7) 0.957 (1) 1.049	2	--	--	--	--	--	--	--	--
2A	2	Mixing	PJMs Only	Cluster (7+1)	45° (7) Vertical (1)	(7) 0.957 (1) 1.049	2	--	--	--	--	--	--	--	--
2A	3	Mixing	PJMs + Spargers	Cluster (7+1)	45° (7) Vertical (1)	(7) 0.957 (1) 1.049	2	4	61¾	1¾	--	--	--	--	--
2A	4	Mixing	PJMs + Spargers	Cluster (7+1)	45° (7) Vertical (1)	(7) 0.957 (1) 1.049	2	8	61¾	1¾	--	--	--	--	--
3	1	Mixing	PJMs Only	Cluster (7+1)	45° (7) Vertical (1)	(7) 0.957 (1) 1.049	2	--	--	--	--	--	--	--	--
3	2	Mixing	PJMs Only	Cluster (7+1)	45° (7) Vertical (1)	(7) 0.957 (1) 1.049	2	--	--	--	--	--	--	--	--
3	3	Mixing	PJMs + Spargers	Cluster (7+1)	45° (7) Vertical (1)	(7) 0.957 (1) 1.049	2	4	61¾	1¾	--	--	--	--	--
3	4	Mixing	PJMs + Spargers	Cluster (7+1)	45° (7) Vertical (1)	(7) 0.957 (1) 1.049	2	8	61¾	1¾	--	--	--	--	--
4	1	Mixing	PJMs Only	Cluster (7+1)	45° (7) Vertical (1)	(7) 0.957 (1) 1.049	2	--	--	--	--	--	--	--	--
4	2	Mixing	PJMs Only	Cluster (7+1)	45° (7) Vertical (1)	(7) 0.957 (1) 1.049	2	--	--	--	--	--	--	--	--
4	3	Mixing	PJMs + Spargers	Cluster (7+1)	45° (7) Vertical (1)	(7) 0.957 (1) 1.049	2	4	61¾	1¾	--	--	--	--	--
4	4	Mixing	PJMs + Spargers	Cluster (7+1)	45° (7) Vertical (1)	(7) 0.957 (1) 1.049	2	8	61¾	1¾	--	--	--	--	--
5	1	Mixing	PJMs + Pump	Cluster (7+1)	45° (7) Vertical (1)	(7) 0.957 (1) 1.049	2	--	--	--	4	0.622	59⅛	29	30° Up
5	2	Mixing	PJMs + Pump	Cluster (7+1)	45° (7) Vertical (1)	(7) 0.957 (1) 1.049	2	--	--	--	4	0.622	59⅛	29	30° Up
6	1	Mixing	PJMs Only	Cluster (7+1)	45° (7) Vertical (1)	1.380	2	--	--	--	--	--	--	--	--
6	2	Mixing	PJMs Only	Cluster (7+1)	45° (7) Vertical (1)	1.380	2	--	--	--	--	--	--	--	--
6	3	Mixing	PJMs + Spargers	Cluster (7+1)	45° (7) Vertical (1)	1.380	2	4	61¾	1¾	--	--	--	--	--
6	4	Mixing	PJMs + Spargers	Cluster (7+1)	45° (7) Vertical (1)	1.380	2	8	61¾	1¾	--	--	--	--	--
7	1	Mixing	PJMs Only	Cluster (7+1)	45° (7) Vertical (1)	(7) 0.957 (1) 1.049	2	--	--	--	--	--	--	--	--
7	2	Mixing	PJMs Only	Cluster (7+1)	45° (7) Vertical (1)	(7) 0.957 (1) 1.049	2	--	--	--	--	--	--	--	--

Table 2.4 (contd)

Seq. No.	Run	Test Type	Test Mode	PJM Configuration				Sparger Configuration			Recirculation. Pump Discharge Config.				
				PJM Arrangement	Nozzle Type	Noz. Dia. (in.)	Elevation (in.)[c]	No.	PCD (in.)	Elevation (in.)[c]	No. of Nozzles	Nozzle dia. (in.)	PCD (in.)	Elevation (in.)[c]	Angle[d]
7	3	Mixing	PJMs + Pump	Cluster (7+1)	45º (7) Vertical (1)	(7) 0.957 (1) 1.049	2	--	--	--	4	0.622	59⅛	29	30º Up
7	4	Mixing	PJMs + Pump	Cluster (7+1)	45º (7) Vertical (1)	(7) 0.957 (1) 1.049	2	--	--	--	4	0.622	59⅛	29	30º Up
7	5	Mixing	PJMs + Pump + Sparging	Cluster (7+1)	45º (7) Vertical (1)	(7) 0.957 (1) 1.049	2	4	61¾	1¾	4	0.622	59⅛	29	30º Up
7	6	Mixing	PJMs + Pump + Sparging	Cluster (7+1)	45º (7) Vertical (1)	(7) 0.957 (1) 1.049	2	8	61¾	1¾	4	0.622	59⅛	29	30º Up
8	1	Mixing	PJMs Only	Cluster (4+3+1)	45º (3) 135 (4) Vertical (1)	(7) 0.957 (1) 0.957	2	--	--	--	--	--	--	--	--
8	2	Mixing	PJMs Only	Cluster (4+3+1)	45º (3) 135 (4) Vertical (1)	(7) 0.957 (1) 0.957	2	--	--	--	--	--	--	--	--
9	1	Mixing	PJMs + Pump	Cluster (7+1)	45º (7) Vertical (1)	(7) 0.957 (1) 1.049	2	--	--		1	1.278	16½	4	Vertically down
9	2	Mixing	PJMs + Pump	Cluster (7+1)	45º (7) Vertical (1)	(7) 0.957 (1) 1.049	2	--	--		1	1.278	16½	4	Vertically down
9	3	Mixing	PJMs + Pump + Spargers	Cluster (7+1)	45º (7) Vertical (1)	(7) 0.957 (1) 1.049	2	4	61¾	1¾	1	1.278	16½	4	Vertically down
10	1	Mixing	PJMs + Pump	Cluster (7+1)	45º (7) Vertical (1)	(7) 0.957 (1) 1.049	2	--	--	--	1	1.278	59⅛	16	30º Up
10	2	Mixing	PJMs + Pump	Cluster (7+1)	45º (7) Vertical (1)	(7) 0.957 (1) 1.049	2	--	--	--	1	1.278	59⅛	16	30º Up
11	1	Mixing	PJMs + Pump	Cluster (7+1)	45º (7) Vertical (1)	(7) 0.957 (1) 1.049	2	--	--	--	2	0.91	59⅛	16	30º Up
11	2	Mixing	PJMs + Pump	Cluster (7+1)	45º (7) Vertical (1)	(7) 0.957 (1) 1.049	2	--	--	--	2	0.91	59⅛	16	30º Up
12	1	Mixing	PJMs Only	Cluster (4+3+1)	45º (4) 135 (3) Vertical (1)	(7) 0.957 (1) 0.957	2	--	--	--	--	--	--	--	--
12	2	Mixing	PJMs Only	Cluster (4+3+1)	45º (4) 135 (3) Vertical (1)	(7) 0.957 (1) 0.957	2	--	--	--	--	--	--	--	--
13	1	Mixing	PJMs + Spargers	Cluster (4+3+1)	45º (4) 135 (3) Vertical (1)	(7) 0.957 (1) 0.957	2	4	61¾	1¾	--	--	--	--	--
16	1 - 6	Solids Lift	PJMs Only	Cluster (7+1)	45º (7) Vertical (1)	(7) 0.957 (1) 1.049	2	--	--	--	--	--	--	--	--
16A	7	Cloud Test	PJMs Only	Cluster (7+1)	45º (7) Vertical (1)	(7) 0.957 (1) 1.049	2	--	--	--	--	--	--	--	--

Table 2.4 (contd)[a, b]

Seq. No.	Run	Test Type	Test Mode	PJM Configuration				Sparger Configuration			Recirculation. Pump Discharge Config.				
				PJM Arrangement	Nozzle Type	Noz. Dia. (in.)	Elevation (in.)[c]	No.	PCD (in.)	Elevation (in.)[c]	No. of Nozzles	Nozzle dia. (in.)	PCD (in.)	Elevation (in.)[c]	Angle[d]
16A	8	Cloud Test	PJMs Only	Cluster (7+1)	45º (7) Vertical (1)	(7) 0.957 (1) 1.049	2	--	--	--	--	--	--	--	--
16A	9	Cloud Test	PJMs Only	Cluster (7+1)	45º (7) Vertical (1)	(7) 0.957 (1) 1.049	2	--	--	--	--	--	--	--	--
17	1-4	Solids Lift	PJMs Only	Expanded Cluster (7+1)	23º (7) Vertical (1)	(7) 0.957 (1) 0.957	2	--	--	--	--	--	--	--	--
17A	1a	Cloud Test	PJMs Only	Expanded Cluster (7+1)	23º (7) Vertical (1)	(7) 0.957 (1) 0.957	2	--	--	--	--	--	--	--	--
17A	2a	Cloud Test	PJMs Only	Expanded Cluster (7+1)	23º (7) Vertical (1)	(7) 0.957 (1) 0.957	2	--	--	--	--	--	--	--	--
18A	1a	Cloud Test	PJMs Only	Expanded Cluster (7+1)	15º (7) Vertical (1)	(7) 0.935 (1) 0.957	2	--	--	--	--	--	--	--	--
18A	2a	Cloud Test	PJMs Only	Expanded Cluster (7+1)	15º (7) Vertical (1)	(7) 0.935 (1) 0.957	2	--	--	--	--	--	--	--	--
19	1	Mixing	PJMs Only	Expanded Cluster (7+1)	15º (7) Vertical (1)	(7) 0.935 (1) 0.957	2	--	--	--	--	--	--	--	--
19	2	Mixing	PJMs Only	Expanded Cluster (7+1)	15º (7) Vertical (1)	(7) 0.935 (1) 0.957	2	--	--	--	--	--	--	--	--
20	1	Mixing	PJMs Only	Cluster (7+1)	45º (7) Vertical (1)	(7) 0.957 (1) 0.957	2	--	--	--	--	--	--	--	--
20	2	Mixing	PJMs + Pump	Cluster (7+1)	45º (7) Vertical (1)	(7) 0.957 (1) 0.957	2	--	--	--	2	0.78	59⅛	17¾	25º Up
21	1	Mixing	PJMs Only	Cluster (7+1)	45º (7) Vertical (1)	(7) 0.957 (1) 0.957	1 1/2	--	--	--	--	--	--	--	--
21	2	Mixing	PJMs Only	Cluster (7+1)	45º (7) Vertical (1)	(7) 0.957 (1) 0.957	1 1/2	--	--	--	--	--	--	--	--
21	3	Mixing	PJMs + Pump	Cluster (7+1)	45º (7) Vertical (1)	(7) 0.957 (1) 0.957	1 1/2	--	--	--	2	0.78	59⅛	17¾	25º Up
26[e]	1	Mixing	PJMs Only	Cluster (7+1)	45º (7) Vertical (1)	(7) 0.957 (1) 0.957	1 1/2	--	--	--	--	--	--	--	--
26[e]	2	Mixing	PJMs + Pump + Spargers	Cluster (7+1)	45º (7) Vertical (1)	(7) 0.957 (1) 0.957	1 1/2	8	61¾	4	2	0.78	59⅛	17¾	25º Up
27[e]	1	Mixing	PJMs + Spargers	Cluster (7+1)	45º (7) Vertical (1)	(7) 0.957 (1) 0.957	1 1/2	8	61¾	4	--	--	--	--	--
28[e]	1	Mixing	PJMs + Pump + Spargers	Cluster (7+1)	45º (7) Vertical (1)	(7) 0.957 (1) 0.957	1 1/2	4	61¾	4	2	0.78	59⅛	17¾	25° Up

(a) Test results discussed in Sections 6 and 7.
(b) Configuration spatial and dimensional distances values in table do not reflect the type of measurement or accuracy. See text for details.
(c) Approximate distance from the bottom of the tank under the nozzle
(d) Angle from horizontal.
(e) Configuration selected.

2.2.1 LS PJM and Sparger Configurations

Three PJM/sparger configurations were used in the LS scaled test stand, the cluster (7+1), cluster (4+3+1) and expanded cluster (7+1). Table 2.5 summarizes the variations of these PJM/sparger configurations. Plan and elevation views of the vessel and internals for the three configurations and their variations are shown in Figures 2.22 through 2.27. The PJM and sparger tube positions reported in these figures are considered approximate and are based on templates used to position the PJMs and procedures used to set the target elevations of the PJM nozzle tips.

Both PJM configurations consisted of eight PJMs, one in the center and seven equally spaced around it. The perimeter PJMS in the cluster configuration were placed on an approximately 30-inch PCD so the tube walls of adjacent PJMS touched at the weld joints on the cylindrical sections of the PJM tubes. This configuration also had eight sparger tubes made of ½-inch-OD (0.37-inch-ID) stainless steel tubing used in sequences 2A, 3-13, 16, 16A, 26, 27, and 28 (the sparger tubes weren't used for some of these sequences). The sparger tubes were also spaced approximately equally around the tank centerline on a PCD of approximately 61¾ inches, as shown in Figure 2.22. The same PJM spacing was used in sequences 20 and 21, but spargers were not installed in the tank. The sparger tubes used in sequences 2A, 3, 4, 6, 7, 9, and 13 were raised to a target elevation of approximately 1¾ inches above the tank bottom immediately below the sparger tubes. The sparger tubes were raised 4 inches off the bottom for sequences 26, 27, and 28, based on measurements with a carpenters rule or a tube with a mark 4 inches above its lower end.

Table 2.5. Summary Description of LS Tank Prototype PJM and Sparger Configurations

Configuration	Configuration Variation	Nominal PCD of Perimeter PJMs	Sequences Used
Cluster (7+1)	Seven equally spaced perimeter PJMs surround a center PJM. All perimeter PJMs used 45° nozzles (sequence 6 used a larger diameter nozzle tip). Eight air spargers equally spaced around the tank at a PCD about 61¾ inches (except in sequences 20 and 21 when they were not installed).	30 in.	2A, 3, 4, 5, 6, 7, 9, 10, 11, 16, 16A, 20, 21, 26, 27, 28
Cluster (4+3+1)	Seven equally spaced perimeter PJMs surround a center PJM so the center and perimeter PJM tube walls touch. Three perimeter PJMs with 135° nozzles were alternated with four perimeter PJMs (numbers 1, 3, 5, 7) with 45° nozzles. Eight air spargers equally spaced around the tank at PCD of about 61¾ in.	30 in.	12, 13
	Seven equally spaced perimeter PJMs surround a center PJM so the center and perimeter PJM tube walls touch. Four perimeter PJMs with 135° nozzles (numbers 1, 3, 5, 7) were alternated with three perimeter PJMs with 45° nozzles. Eight air spargers equally spaced around the tank at PCD of about 61¾ in.	30 in.	8
Expanded Cluster (7+1)	Seven equally spaced perimeter PJMs surround a center PJM so the center and perimeter PJM tube walls do not touch. Either 15° or 23° nozzle assemblies were used with perimeter PJM assemblies in this configuration with no air spargers.	35 in.	17, 17A, 18A, 19

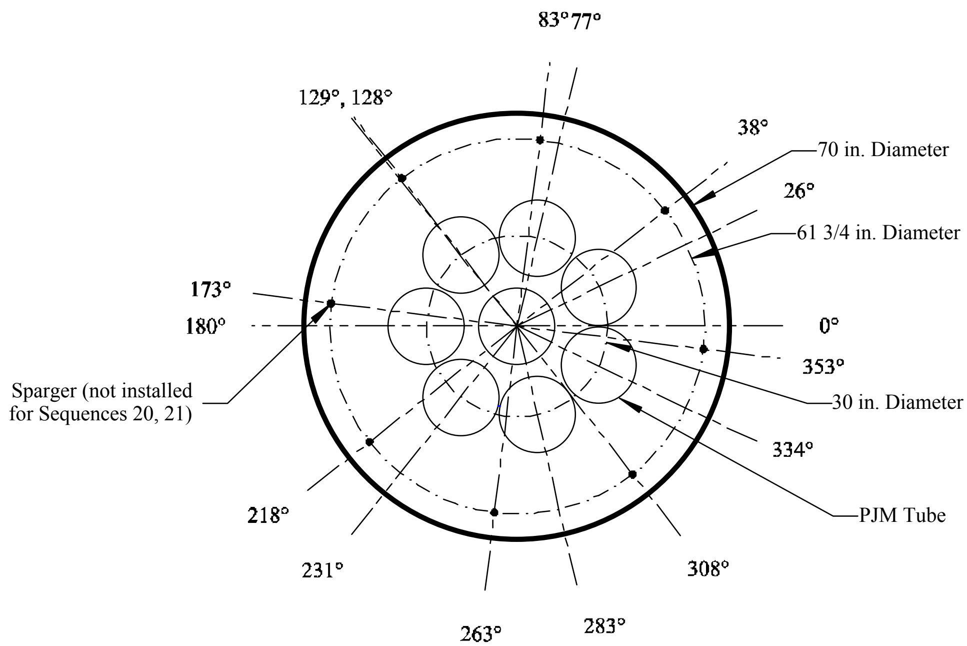

Figure 2.22. Plan View of Cluster (7+1) and (4+3+1) Configurations Used in LS Scaled Test Stand Showing Nominal Locations of PJMs and Spargers Used in Sequences 2A, 3–13, 16, 16A, 20, 21, and 26–28

The cluster configuration had three variations that differed in the type of nozzle assemblies used with the perimeter PJMs (nozzle assemblies are discussed in detail in Section 2.2.2). Most tests were conducted using all seven perimeter nozzle assemblies with nozzle tips pointed radially away from the tank centerline at 45° with respect to the vertical axis. The lowest points on all nozzle tips were raised to a target level of approximately 2 inches above the tank bottom as measured immediately beneath the nozzles in sequences 2A, 3, 4, 5, 6, 7, 9, 10, 11, 16, and 16A and to between 1¾ and 2 inches above the bottom for sequence 20. The nozzle tips were raised approximately 1½ inches above the tank bottom in sequences 21, 26, 27, and 28 based on measurements with a carpenter's rule. Figure 2.23 shows an elevation view of the LS scaled test stand, indicating where the measurements were made for nozzle tip elevation.

Perimeter PJM nozzle-angle configurations are shown in Figures 2.24 and 2.25. Three 45° nozzle assemblies were used in sequence 8, and four 45° nozzle assemblies were used in sequences 12 and 13. The lowest point on the 45° nozzles were approximately 2 inches above the subjacent tank bottom. Because of the upward angle (see Figure 2.32), the lowest point on the nozzle outlets was approximately 5⅝ inches higher for the 135° nozzle assemblies (approximately 7⅝ inches above the subjacent tank bottom).

The expanded cluster configuration used in sequences 17, 17A, 18A, and 19 was similar to the cluster configuration except that the perimeter PJMs in the expanded cluster were placed on a PCD of approximately 35 inches, as shown in Figure 2.26. For the 23° nozzle assemblies, the lowest points of the center and perimeter nozzles were approximately 2 inches and 1.8 inches, respectively, above the subjacent tank bottom (Figure 2.27). The distance from tank bottom and the horizontal positions of the 15° nozzles was slightly different than with the 23° nozzles because of the altered angle and nozzle length (see Figure 2.31). The expanded-cluster configuration did not include sparger tubes.

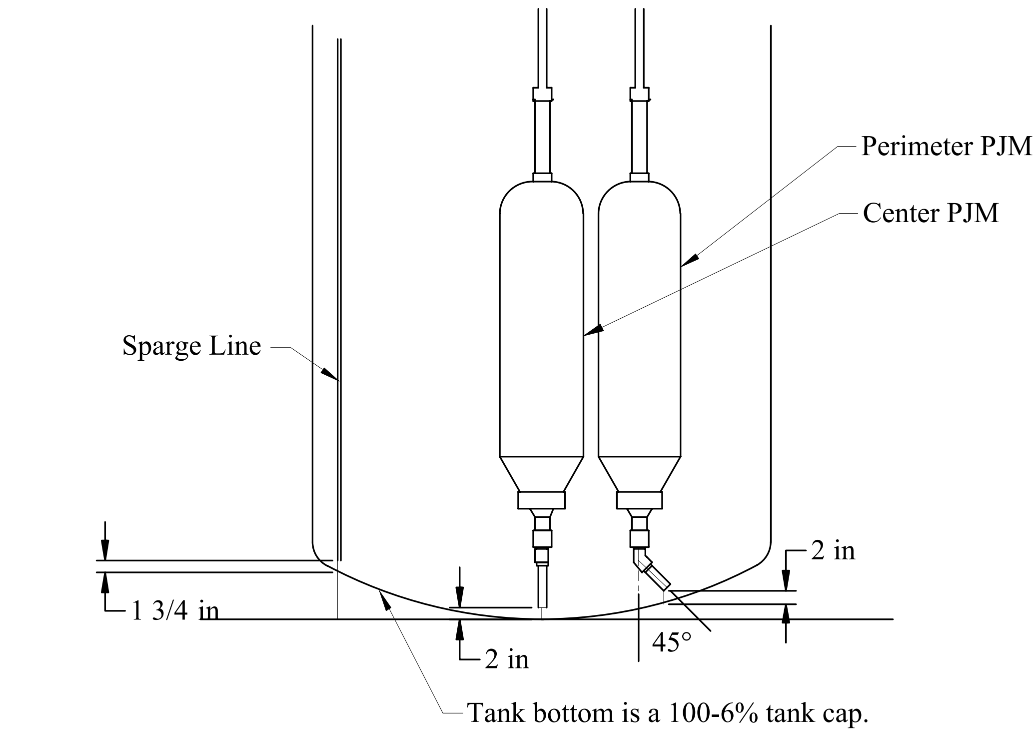

Figure 2.23. Elevation View of Cluster (7+1) Configuration in LS Scaled Test Stand Showing PJM Center and 45° Perimeter Nozzle and Sparger Elevations Used in Sequences 2A, 3–7, 9, 10, 11, 16, and 16A

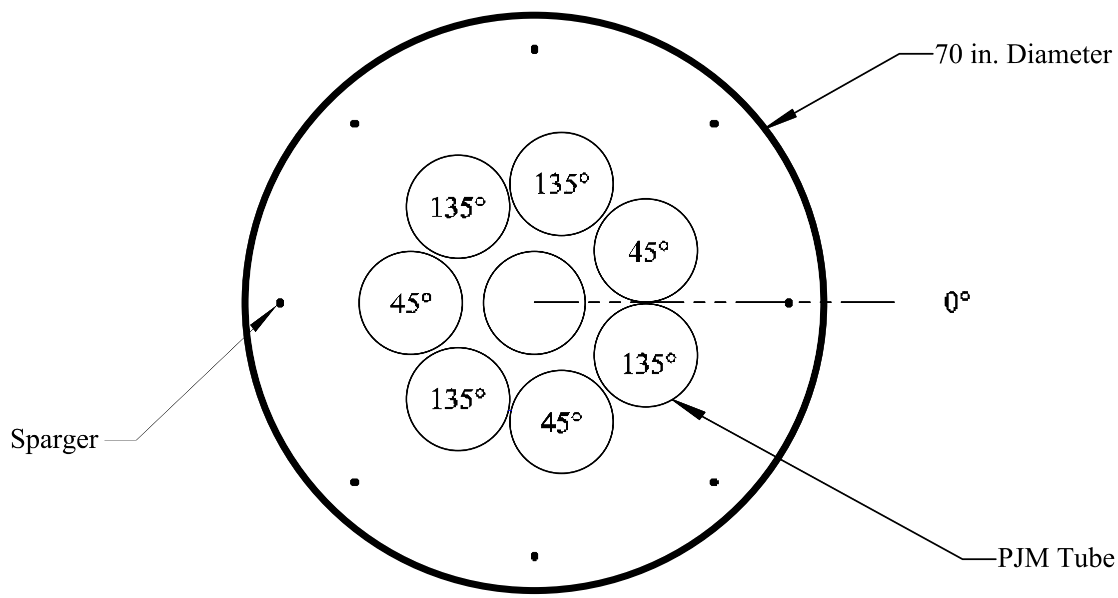

Figure 2.24. Plan View of Cluster (4+3+1) Configuration in LS Scaled Test Stand Showing Arrangement of 45° and 135° PJM Nozzle Assemblies Used in Sequence 8

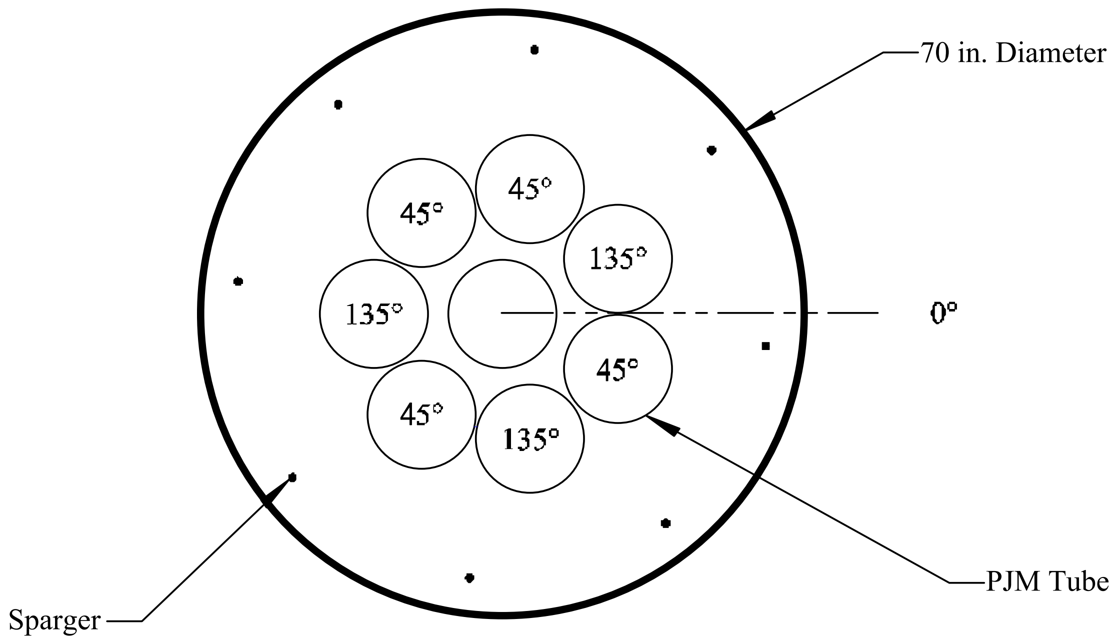

Figure 2.25. Plan View of Cluster (4+3+1) Configuration in LS Scaled Test Stand Showing Arrangement of 45° and 135° PJM Nozzle Assemblies Used in Sequences 12 and 13

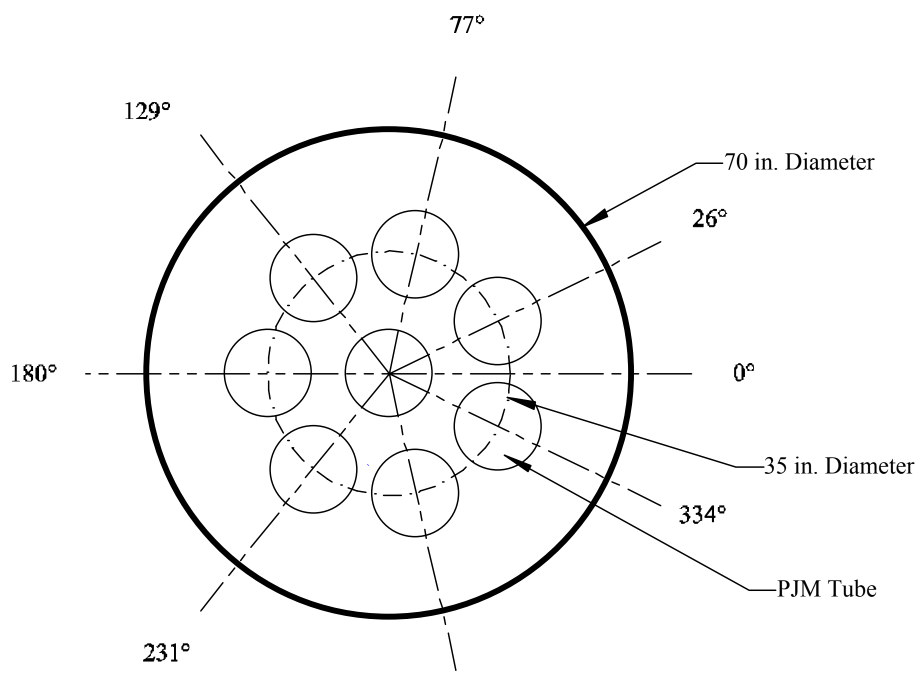

Figure 2.26. Plan View of Expanded Cluster (7+1) Configuration in LS Scaled Test Stand Showing Nominal Locations of Center and Perimeter PJM Tubes for Sequences 17, 17A, 18A, and 19

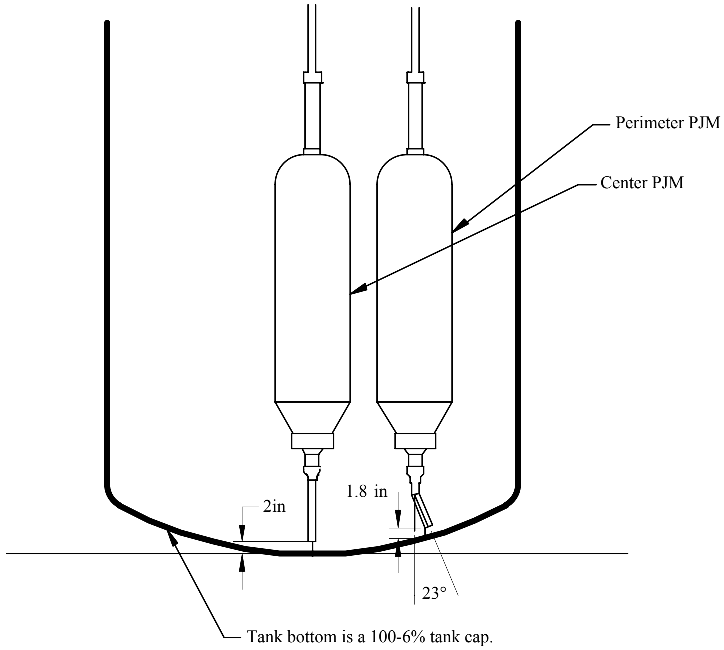

Figure 2.27. Elevation View of Expanded Cluster (7+1) Configuration in LS Scaled Test Stand Showing Nominal PJM Center and 23° Perimeter Nozzle Assembly Elevations Used in Sequences 17 and 17A

2.2.2 PJM Nozzle Assemblies

The nozzle assemblies used in the LS scaled test stand were configured to direct the PJM discharge at specific orientations relative to the tank bottom. These are summarized in Table 2.6. The center PJM nozzle assemblies always directed the flow vertically downward (0°) at the tank centerline. The perimeter PJM nozzles, for most tests, directed the flow at a 45° vertical angle in a direction radially away from the tank centerline. This orientation directed the flow at an incident angle approximately normal to the tank bottom. Angles of 15°, 23°, and 135° with respect to vertically downward were also applied to perimeter PJM nozzle assemblies in order to investigate the effects of the angle of incidence.

The center PJM nozzle assemblies with nozzle tips of four different diameters were used with the center PJM in the LS scaled test stand. The center PJM nozzle assembly shown in Figure 2.28 for sequences 2A, 3, 4, 5, 7, 8, 9, 10, 11, 16, and 16A consisted of a 10⅜-inch-long, 1-inch-diameter schedule 40 stainless steel pipe (nominal 1.049-inch ID) inserted into a 2 × 1-inch-diameter stainless steel reducer coupling and extending approximately 9⅞ inches out of it.

The center PJM nozzle assembly for sequence 6, also shown in Figure 2.28, consisted of a 10-inch-long, 1¼-inch-diameter schedule 40 stainless steel pipe (nominal 1.38-inch ID) inserted into a 2 × 1¼-inch-diameter stainless steel reducer coupling and extending approximately 9½ inches out of it.

The center PJM nozzle assembly shown in Figure 2.29 for sequences 8, 12, 13, 20, 21, 26, 27, and 28 consisted of a 9¾-inch-long, 1-inch-diameter schedule 80 stainless steel pipe (nominal 0.957-inch ID) inserted into a 2 × 1-inch-diameter stainless steel reducer coupling and extending approximately 9½ inches out of it. The center PJM nozzle assembly for sequences 17, 17A, 18A, and 19, also shown in

Table 2.6. Summary of Nozzle Assemblies Attached to PJM Lines for the LS Prototype

Nozzle Type	Standard Pipe Dimension (stainless steel except where noted)	Inner Diameter (in.)	Orientation above vertically downward	PJM Configurations Using Nozzle Assembly	Sequences Used
Center PJM	1 inch Schedule 40	1.049	0°	Cluster (7+1)	2A, 3, 4, 5, 7, 9, 10, 11, 16, 16A
	1-inch Schedule 80	0.957	0°	Cluster (7+1)	20, 21, 26, 27, 28
	1-inch Schedule 80	0.957	0°	Cluster (4+3+1)	8, 12, 13
	1-inch Schedule 80	0.957	0°	Expanded Cluster (7+1)	17, 17A, 18A, 19
Perimeter PJM	1¼-inch Schedule 40	1.380	0°	Cluster (7+1)	6
	1-inch Schedule 80 PVC	0.957	45°	Cluster (7+1)	2A, 3, 4, 5, 7, 9, 10, 11, 16, 16A, 20, 21, 26, 27, 28
	1-inch Schedule 80 PVC	0.957	45°	Cluster (4+3+1)	8, 12, 13
	1¼-inch Schedule 40 PVC	1.380	45°	Cluster (7+1)	6
	1-inch Schedule 80	0.957	23°	Expanded Cluster (7+1)	17, 17A

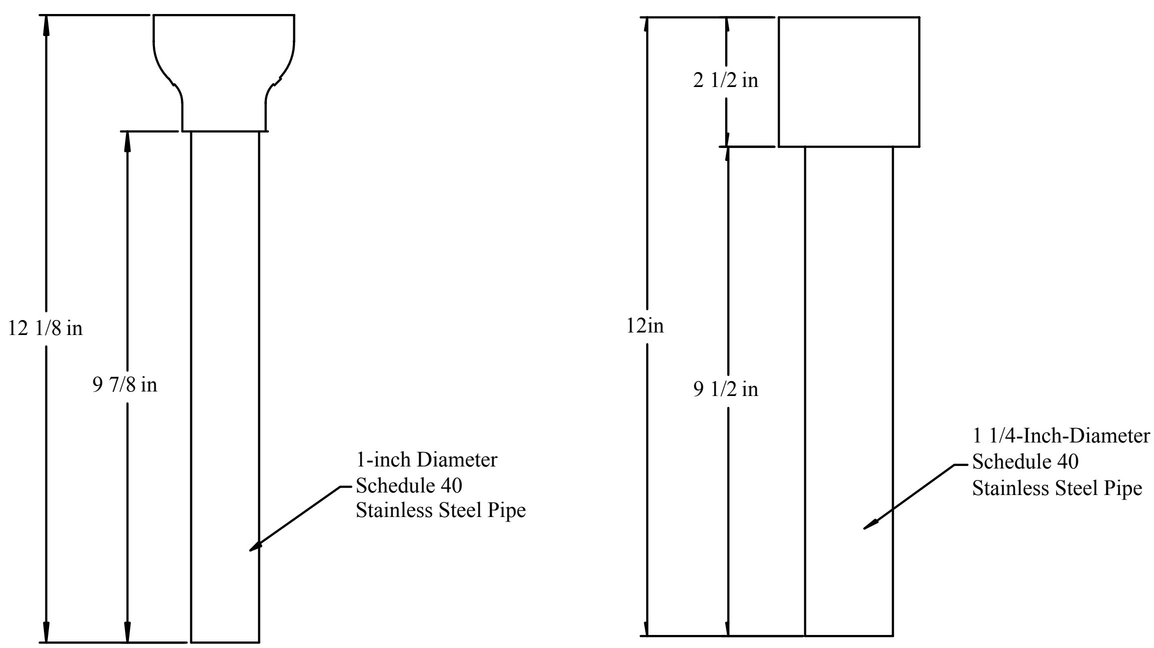

Figure 2.28. LS Scaled Test Stand PJM Center Nozzle Assemblies with Nozzle Tips Constructed from 1-inch- (left) and 1¼-inch-Diameter (right) Schedule 40 Stainless Steel Pipe, Showing Nominal Dimensions

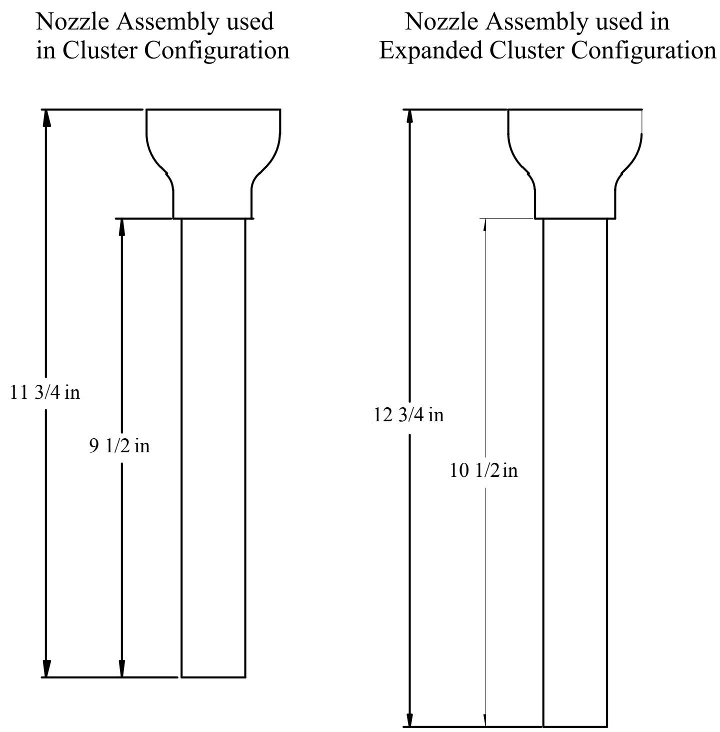

Figure 2.29. LS Scaled Test Stand Center 1-inch-Diameter Schedule 80 Stainless Steel Pipe Center PJM Nozzle Assemblies Used in Cluster (left) and Expanded Cluster Configurations Showing Nominal Dimensions

Figure 2.29, consisted of a 1-inch-diameter schedule 80 stainless steel pipe (nominal 0.957-inch ID) inserted into a 2 × 1-inch-diameter stainless steel reducer coupling. However, it was 11 inches long and extended 10½ inches out of the reducer coupling. This increased nozzle tip length was needed to accommodate a greater difference between the center and perimeter nozzle elevations imposed by the larger PCD for the perimeter PJMs in the expanded cluster configuration used for these sequences.

The most frequently used perimeter PJM nozzle assemblies consisted of (in order of assembly) a nominal 5-inch-long, 1-inch-diameter schedule 80 PVC pipe, a 1¼ × 1-inch-diameter PVC bushing, a 45° PVC elbow, a 2 × 1¼-inch diameter PVC bushing, and a 2-inch-diameter PVC coupling. The nozzle tips extended 3⅞ to 4⅛ inches out of the bushings (see Figure 2.30). Key measurements were made of the seven nozzle assemblies while they were attached to the PJMs. Sequences 2A, 3, 4, 5, 7, 9, 10, 11, 16, 16A, 20, 21, 26, 27, and 28 used this nozzle for all seven perimeter PJMs. Sequence 8 used this nozzle in three of the perimeter PJMs (alternating with 135° nozzle assemblies, as shown in Figure 2.24), while sequences 12 and 13 used it in four of the perimeter PJMs (alternating with 135° assemblies, as shown in Figure 2.25).

Sequence 6 also used a 45° nozzle assembly, but the nozzle tip had a larger diameter. This nozzle assembly, also shown in Figure 2.30, consisted of, in order of assembly, a nominal 5-inch-long, 1¼-inch-diameter schedule 40 PVC pipe, a 45° PVC elbow, a 2 × 1¼-inch-diameter PVC bushing, and a 2-inch-diameter PVC coupling. The nozzle tip extended approximately 3¾ inches out of the elbow. Key measurements were made of the seven nozzle assemblies with a tape measure.

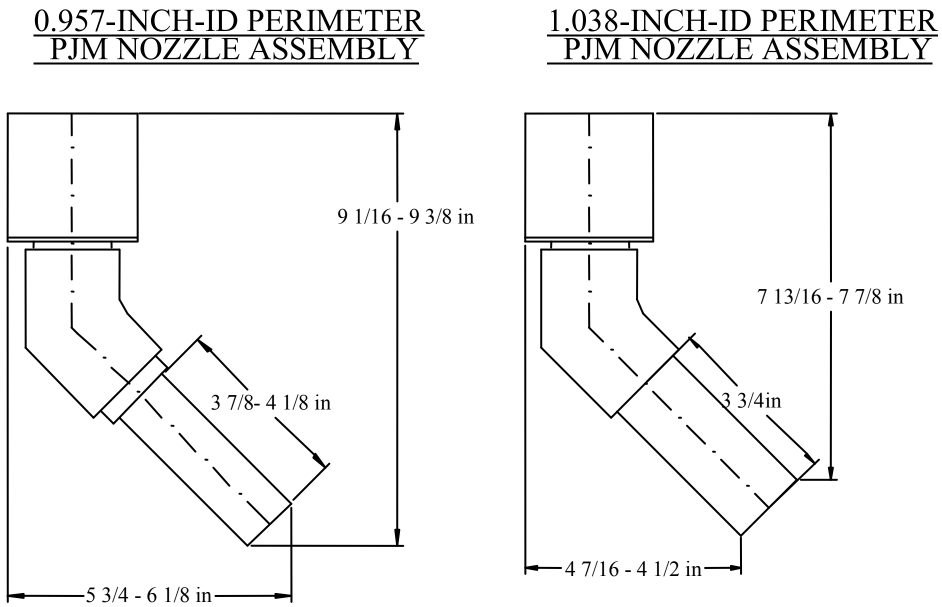

Figure 2.30. LS Scaled Test Stand Perimeter Nozzle Assemblies with Nozzle Tips Constructed from 1-inch-Diameter Schedule 80 PVC Pipe (left) and 1¼-inch-Diameter (right) Schedule 40 PVC Pipe, Showing Nominal Dimensions

The 15° and 23° perimeter PJM nozzle assemblies used in sequences 17, 17A, 18A, and 19 were used to investigate the effects of alternative perimeter nozzle angles on solids lift, cavern formation, and mixing. Schematic diagrams of these nozzle assemblies are shown in Figure 2.31. The nozzle tips for the 15° assemblies that were used in sequences 18A, and 19 consisted of a nominal 8¼–inch-long, 1-inch-diameter schedule 80 PVC pipe, heated and bent, starting 2¾ to 3¾ inches from the nozzle tip to form an approximate 15° angle with PJM axis. The nozzle tips were inserted approximately ½ inch into 2 × 1-inch-diameter stainless steel tapered reducer couplings. The diagram on the left in Figure 2.31 shows a typical nozzle assembly and nominal dimensions. Key measurements of the nozzle tips were made with a straight edge to find where the bends started from each end.

The nozzle tips for the 23° nozzle assemblies used in sequences 17 and 17A consisted of a nominal 8½-inch-long, 1-inch-diameter schedule 80 stainless steel pipe cut into two pieces approximately 6 inches from the nozzle tip. Both pieces were beveled at approximately 12.5° and welded together to produce an approximate 23° angle between a nominal 6-inch straight section of pipe at the nozzle tip outlet end (measured along its longest side) and a nominal 2½-inch straight section of pipe (measured along its longest side). The nozzle tips were inserted approximately ⅜ inch into 2 × 1-inch-diameter stainless steel tapered reducer couplings. The diagram on the right in Figure 2.31 is of a typical nozzle assembly with nominal dimensions. Key measurements of the nozzle tips were made using a straight edge to find where the bends started from each end.

The 135° perimeter PJM nozzle assemblies shown in Figure 2.32 and used in sequences 8, 12, and 13 consisted of, in order of assembly, a nominal 5⅛-inch-long, 1-inch-diameter schedule 80 PVC pipe, a 2 × 1-inch-diameter PVC bushing, a 2-inch-diameter 90° PVC elbow, a short section of 2-inch-diameter schedule 40 PVC pipe, a 45° PVC elbow, a second short section of 2-inch-diameter schedule 40 PVC pipe,

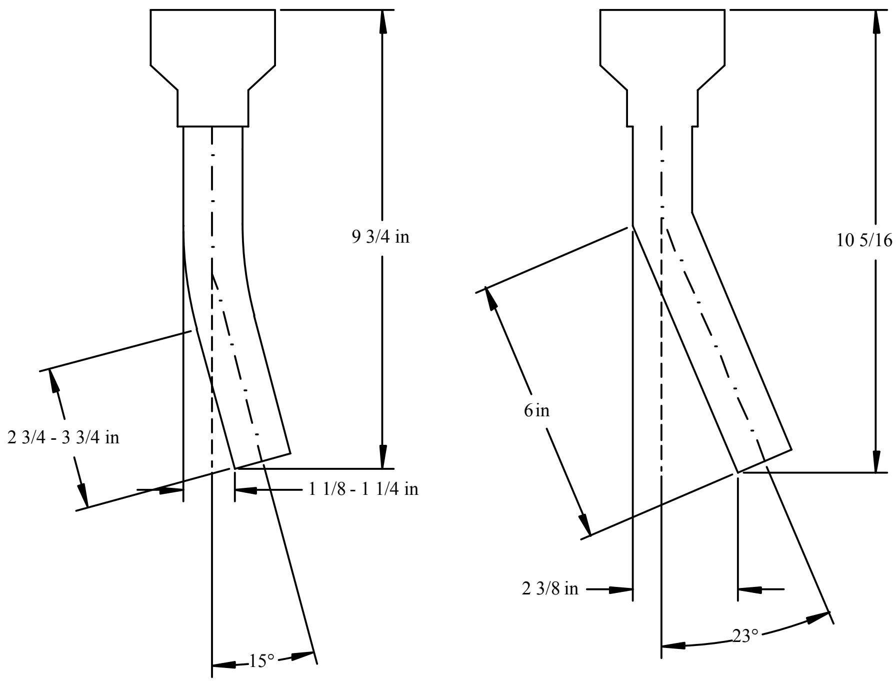

Figure 2.31. LS Scaled Test Stand 15° (left) and 23° (right) Perimeter PJM Nozzle Assemblies and Range of Dimensions

and a 2-inch-diameter PVC coupling. The short sections of pipe were sized to minimize the gap between the two elbows and between the 45° elbow and the coupling. Key measurements were made of three nozzle assemblies.

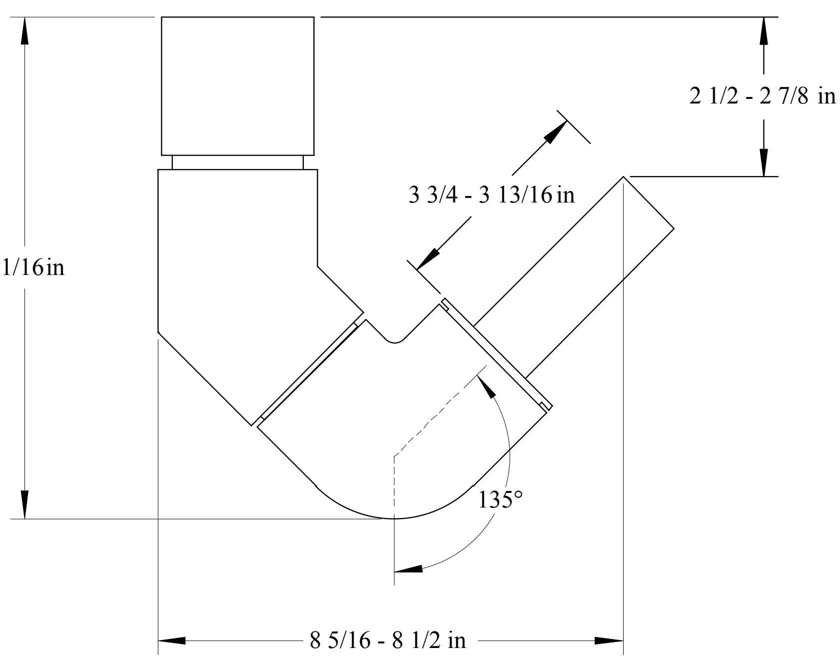

Figure 2.32. Schematic of 135° Perimeter PJM Nozzle Assemblies Used in LS Scaled Test Stand and Range of Dimensions

2.2.3 Recirculation System Configurations

Several different recirculation system configurations were used in sequences 5, 7, 9, 10, 11, 20, 21, 26, and 28. The recirculation system was in place for sequence 27 but was not used. The configuration for sequence 27 matched that of sequences 21, 26, and 28. The same recirculation system used in the UFP scaled test stand and shown in Figure 2.10 was used with the LS scaled test stand. It consisted of two centrifugal pumps placed in parallel and connected in series to a diaphragm pump that served to eliminate cavitation in the pumps. The centrifugal pumps fed a manifold that supplied flow to up to four separate discharge lines depending on the sequence. The recirculation pump system was configured to supply flow to one, two, or four discharge lines and was operated at a target flow rate of 120 ±5 gpm. The pump discharge lines inserted into the LS tank consisted of 2-inch-diameter schedule 40 stainless steel pipes with a nozzle assembly attached. The nozzle tips in the discharge line nozzle assemblies were sized so that the linear velocity exiting the nozzle was approximately 30 ft/sec for sequences 5, 7, 9, 10, and 11 and approximately 40 ft/sec for sequences 20, 21, 27, and 28. The pump suction line that was inserted into the LS tank consisted of 3-inch schedule 80 PVC pipe. The end of the suction line had two sets of four 1½-inch holes drilled within approximately 4¾ inches of the suction inlet to provide additional area for simulant flow. Table 2.7 summarizes the recirculation system configurations evaluated in the LS scaled test stand.

Sequences 5 and 7 used four discharge lines and a suction line, as shown in Figures 2.33 and 2.34. The suction line was in the space between the center PJM and two adjacent perimeter PJMs and was elevated 1 inch and 16 inches, respectively, above the tank bottom for sequences 5 and 7. The nozzle assemblies shown in Figure 2.35 were attached to the discharge lines at the four corners of a rectangle at an approximate PCD of 59⅛ inches. The assemblies consisted of (in order of assembly) a nominal 2 15/16-inch-long, ½-inch-diameter schedule 40 stainless steel pipe, a nested assembly of 1 × ½-inch-, 1½ × 1-inch-, and 2 × 1½-inch- diameter PVC bushings, a 2-inch-diameter, 90° PVC elbow, a 2-inch-diameter schedule 80 PVC nipple (with ¼-inch extension in length), and a second 90° elbow. The nozzle tips extended 2 5/16 to 2⅝ inches out of the 1 × ½-inch-diameter reducer bushings, as shown in the figure, based on measurements of three of the four nozzle tips. The nozzles assemblies were oriented inward so the nozzle tips were closer to the PJMs than the tank wall, and set at an angle so that the nozzle jet did not strike the PJM tube walls. The nozzle tips pointed approximately 30° above horizontal. The centerlines of the lateral arm of the nozzle assemblies were elevated approximately 28½ to 29 inches above the tank bottom measured at the tank centerline.

Sequence 9 used a single discharge line and a suction line, as shown in Figures 2.36 and 2.37. The pump discharge line was in the space between the center PJM and two adjacent perimeter PJMs at an approximate angular location of 103° and approximately 8¼ inch radially from the tank centerline (on a 16½-inch-PCD about the tank centerline) based on the location of the center point in the space between the PJMs. The discharge line nozzle assembly shown in Figure 2.38 was attached to the discharge line and consisted of, in order of assembly, a nominal 3 13/16-inch-long, 1¼-inch-diameter schedule 80 PVC pipe, a 1½ × 1¼-inch-diameter stainless steel bushing, and a 2 × 1½-inch-diameter stainless steel reducer coupling. The nozzle tip extended approximately 3 9/16 inches out of the bushing. The lowest point on the nozzle assembly was 4 inches above the bottom of the tank immediately below the discharge line. The pump suction line was approximately 28¾ inches radially from the tank centerline (57½ inch PCD about the tank centerline). The suction line was raised approximately 16 to 17 inches above the tank bottom immediately below the suction line.

Table 2.7. Summary Description of Recirculation System Configurations for LS Scaled Test Stand

Description	No. of Discharge Lines	Discharge Line Location	Nozzle Assembly Lowest Point Elevation	Nozzle Tip Orientation	Suction Line Location	Suction Line Inlet Elevation
Quad discharge lines (sequences 5 and 7).	4	Located on 59⅛-inch PCD around tank centerline at 51°, 129°, 231°, and 309° from 0° data point.	28½ to 29 inches above tank bottom	Lateral arm oriented generally toward tank centerline. Nozzle tip aimed ~30° above horizontal and oriented so nozzle jet misses PJM tube walls.	Located 8¼ inches from tank centerline (in space between center and two perimeter PJMs) at 309° from 0° data location	Raised 1 inch (seq. 5) and 16 inches (seq. 7) above tank bottom (measured below suction inlet)
Single vertical pump discharge line (sequence 9)	1	Located 8¼ inches from tank centerline (in space between center and perimeter PJMs) 103° from 0° data point	4 inches above tank bottom below nozzle tip	Straight down	Located 28¾ inches from tank centerline; 306° from 0° data point	Raised 16–17 inches above tank bottom below suction inlet
Single and dual 30° pump discharge line(s) (sequences 10, 11).	1 in seq. 10, 2 in seq. 11	Located on 59⅛-inch PCD around tank centerline. Dual nozzles 51° and 231° and single nozzle 129° from 0° data point.	13½ to 16 inches above tank bottom at tank centerline	Lateral arm oriented generally away from tank centerline. Nozzle tip aimed approximately ~30° above horizontal and oriented ~47° with respect to tank centerline	Located 28¾ inches from tank centerline; 306° from 0° data point	Raised 3½ inches above tank bottom below suction inlet
Dual pump discharge lines (sequences 20, 21, 26, 28)	2	Located on 59⅛-inch PCD around tank centerline. Dual nozzles 129° and 309° from 0° data point.	13½ to 14 inches above tank bottom below lateral arm of nozzle assembly	Lateral arm oriented generally away from tank centerline. Nozzle tip aimed ~ 25° above horizontal and oriented ~ 48° with respect to tank	Located 8¼ inches from tank centerline (in space between center and perimeter PJMs) at 257° from 0° data point	Raised 10 inches above tank bottom below suction inlet

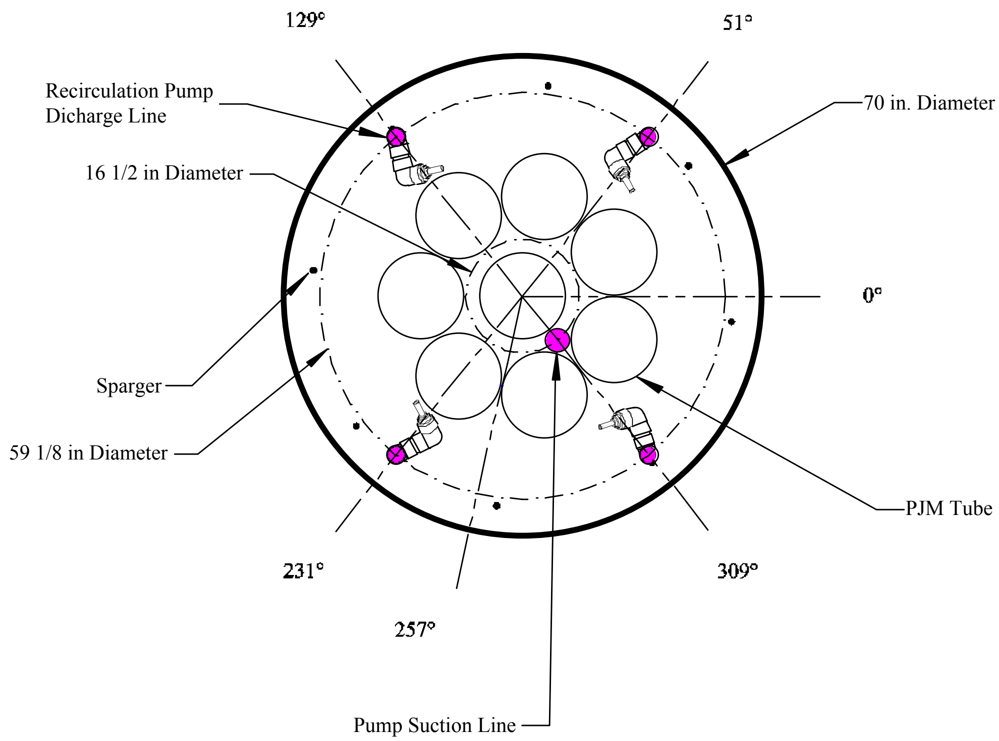

Figure 2.33. Plan View of Cluster (7+1) Configuration in the LS Scaled Test Stand Showing Nominal Locations of Recirculation Line Components for the Four Discharge Line Nozzle Configuration Used in Sequences 5 and 7

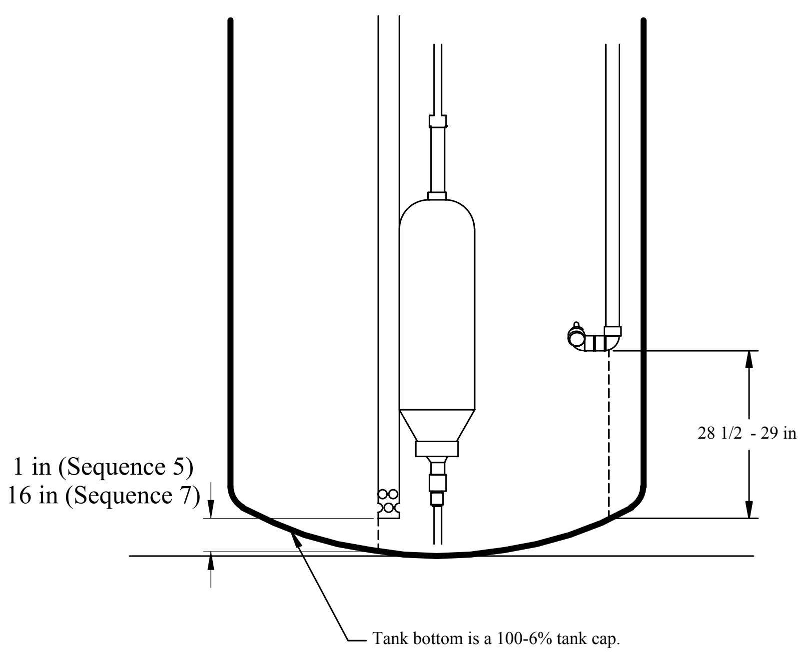

Figure 2.34. Elevation View of Cluster (7+1) in LS Scaled Test Stand Showing Nominal Elevations of Recirculation Line Components for Four Discharge Line Nozzle Configuration Used in Sequences 5 and 7

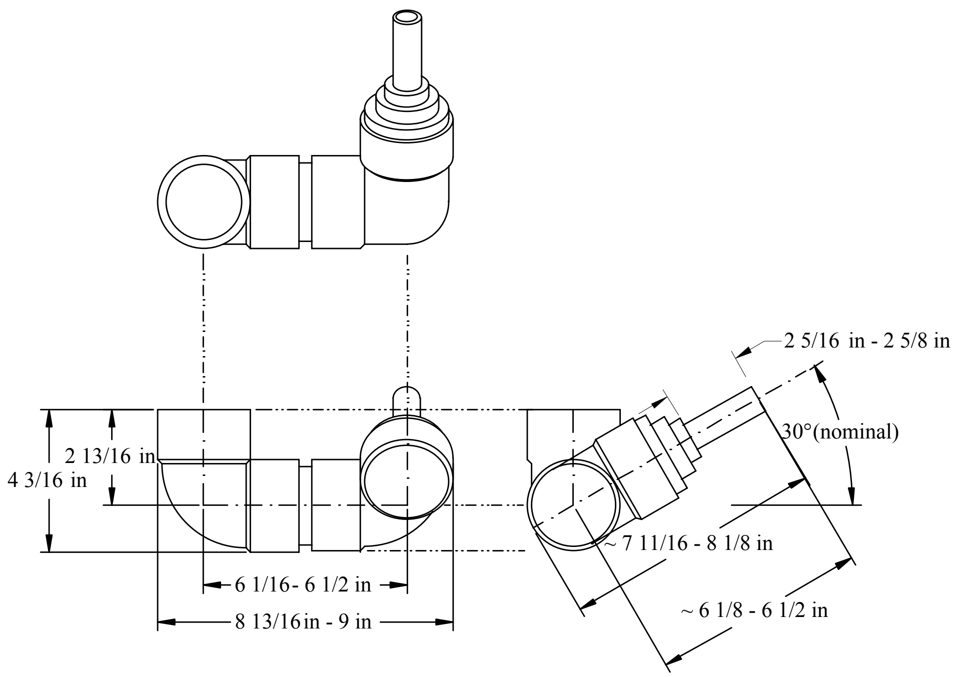

Figure 2.35. LS Scaled Test Stand Recirculation Pump Discharge Nozzle Assembly Used in Sequences 5 and 7

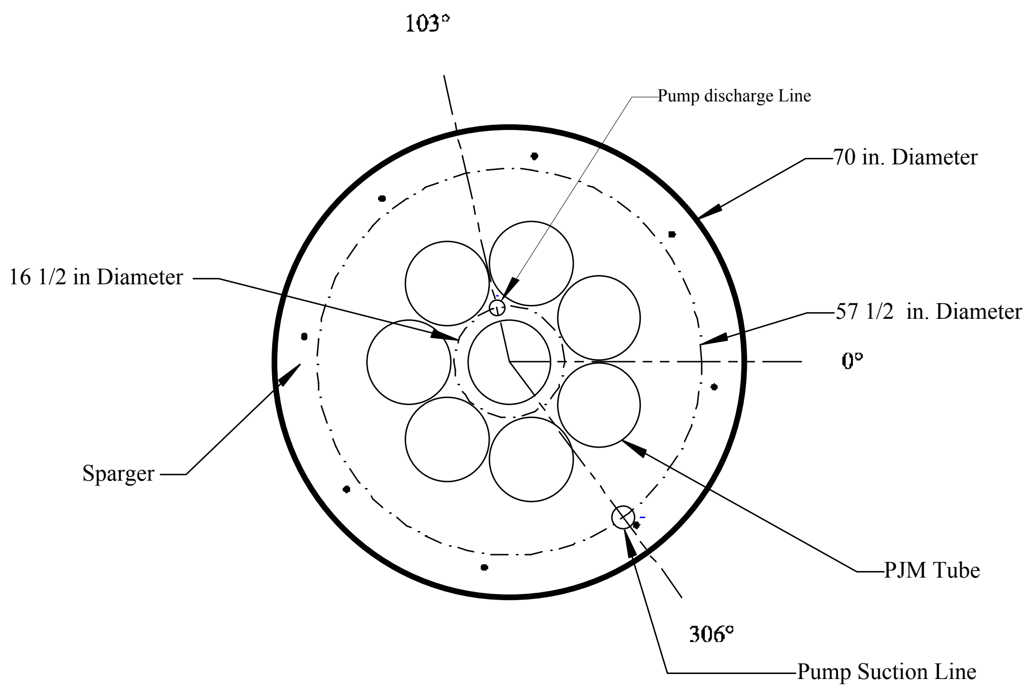

Figure 2.36. Plan View of Cluster (7+1) Configuration in LS Scaled Test Stand Showing Nominal Locations of Recirculation Line Components for Single Vertical Discharge Line Nozzle Configuration Used in Sequence 9

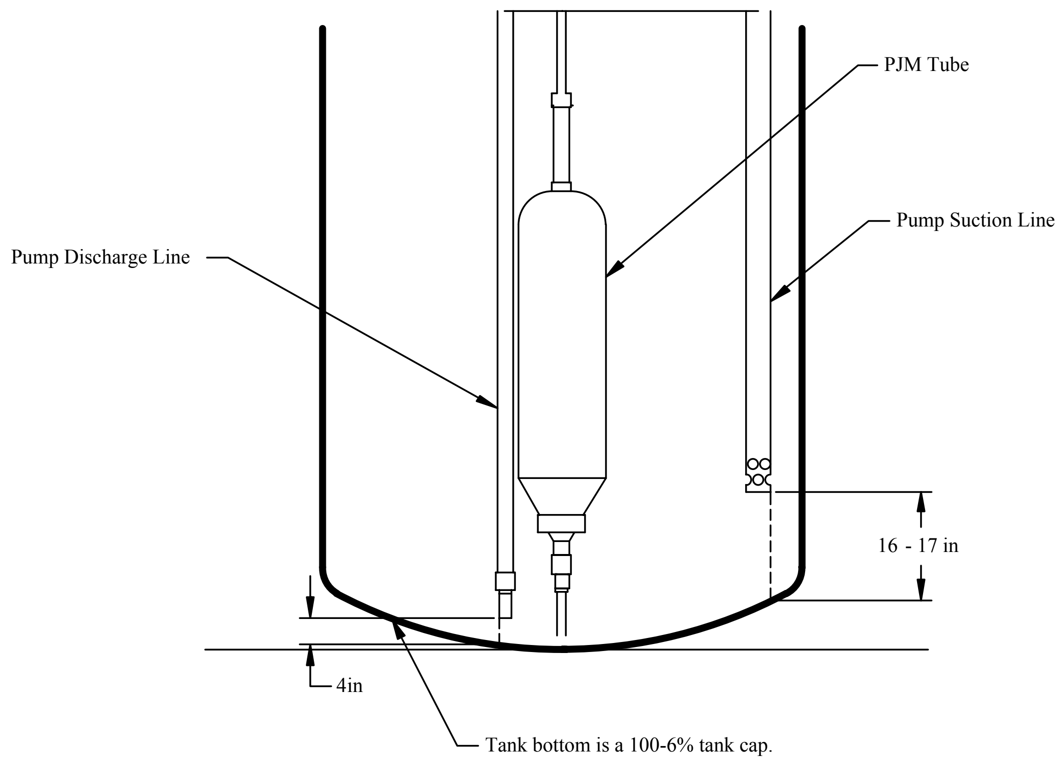

Figure 2.37. Elevation View of Cluster (7+1) Configuration in LS Scaled Test Stand Showing Nominal Elevations of Recirculation Line Components for Single Vertical Discharge Line Nozzle Configuration Used in Sequence 9

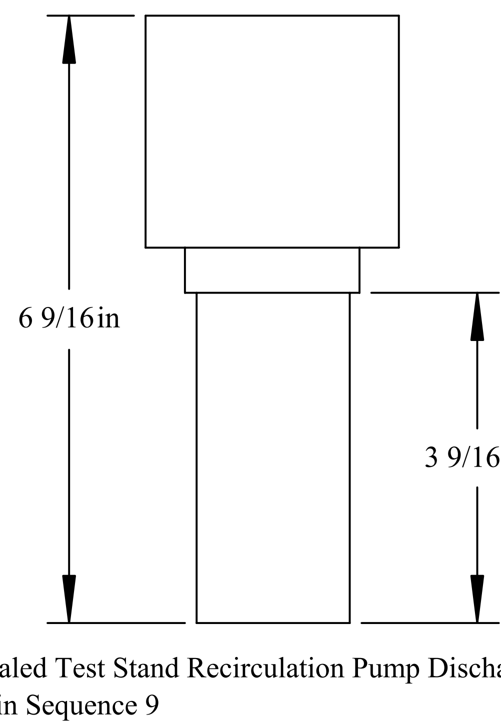

Figure 2.38. LS Scaled Test Stand Recirculation Pump Discharge Nozzle Assembly Used in Sequence 9

The recirculation pump discharge and suction lines for sequences 10 and 11 were installed in the LS scaled test stand as shown in Figures 2.39 and 2.41. Both configurations used the same suction line but different discharge lines according to the desired configuration. The single suction line and three discharge lines were at the corners of a quadrilateral. The suction line was near one corner, the single discharge line used in sequence 10 was at the opposite corner, and the discharge lines used in the dual-discharge nozzle configuration in sequence 11 were at the remaining two corners, opposite one another. All three discharge lines were approximately the same distance from the tank centerline on an approximate 59⅛-inch PCD. The centerlines of the lateral arms of the nozzle assemblies for all three discharge lines were elevated approximately 13½ to 16 inches above the tank bottom measured at the tank centerline, as shown in Figure 2.40. The suction line was at a radius of 28¾ inches (57½-inch PCD). The suction line inlet was approximately 3½ inches above the tank bottom immediately below the suction line, as shown.

The single discharge nozzle assembly used in sequence 10 and shown in Figure 2.41 consisted of (in order of assembly) a nominal 7-inch-long, 1¼-inch-diameter schedule 80 PVC pipe, a 1¼-inch-diameter 90° PVC elbow, a 1¼-inch-diameter schedule 80 carbon steel nipple, a second 90° PVC elbow, a short piece of 1 ¼ inch-diameter schedule 40 tubing, a 2 × 1¼ inch-diameter PVC reducer bushing, and a 2-inch-diameter PVC coupling. The nozzle tip extended 6 9/16 inches out of the 1¼-inch-diameter 90° PVC elbow, as shown. The lateral arm of the nozzle assembly (containing the two elbows) was oriented outward, forming an angle of approximately 41° with the tank centerline, as shown in Figure 2.39, so the nozzle tips were closer to the tank wall than the PJMs, and the nozzle jet did not strike the PJM tube walls. Because of this orientation, the elevation arm of the nozzle assemblies (containing the nozzle tips) formed an angle that was approximately 47° with the centerline, as shown in Figure 2.39. The nozzle tip was pointed approximately 30° above horizontal.

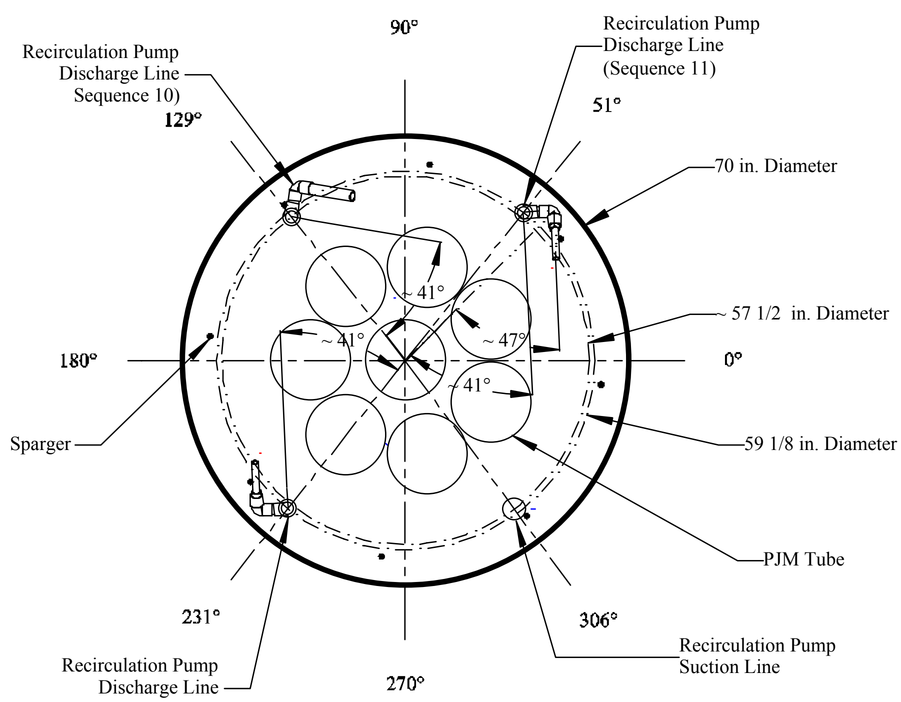

Figure 2.39. Plan View of Cluster (7+1) Configuration in LS Scaled Test Stand Showing Nominal Locations of Recirculation Line Components for Single- and Dual-Discharge Line Nozzle Configurations Used in Sequences 10 and 11

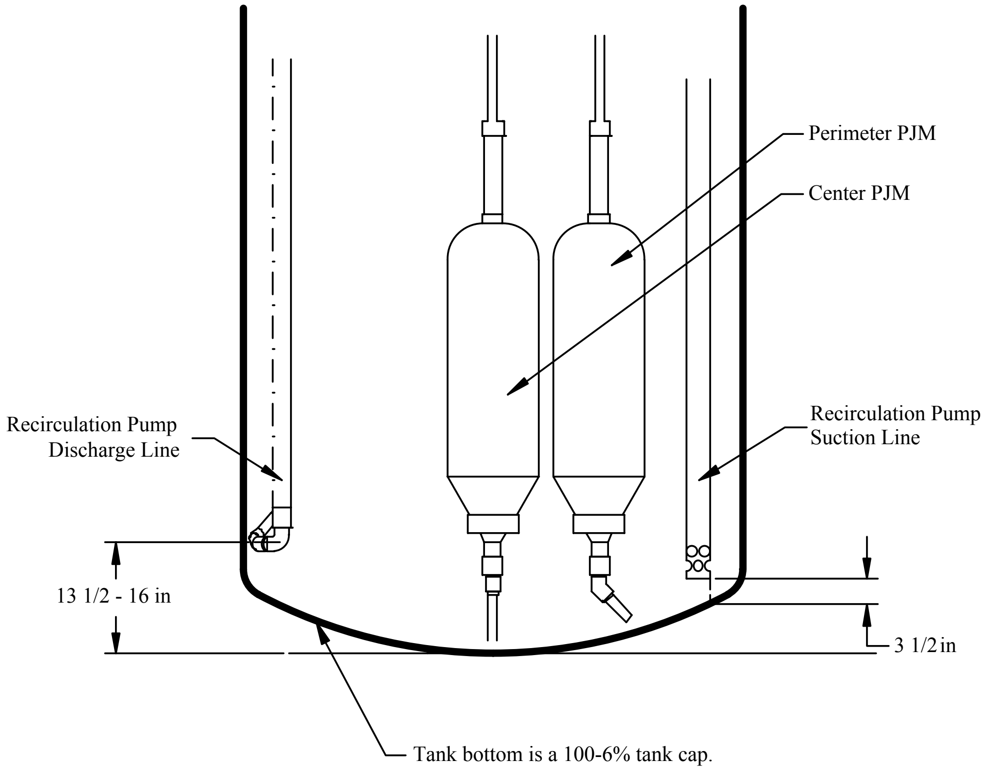

Figure 2.40. Elevation View of Cluster (7+1) Configuration in LS Scaled Test Stand Showing Nominal Elevations of Recirculation Line Components for Single- and Dual-Discharge Line Nozzle Configurations Used in Sequences 10 and 11

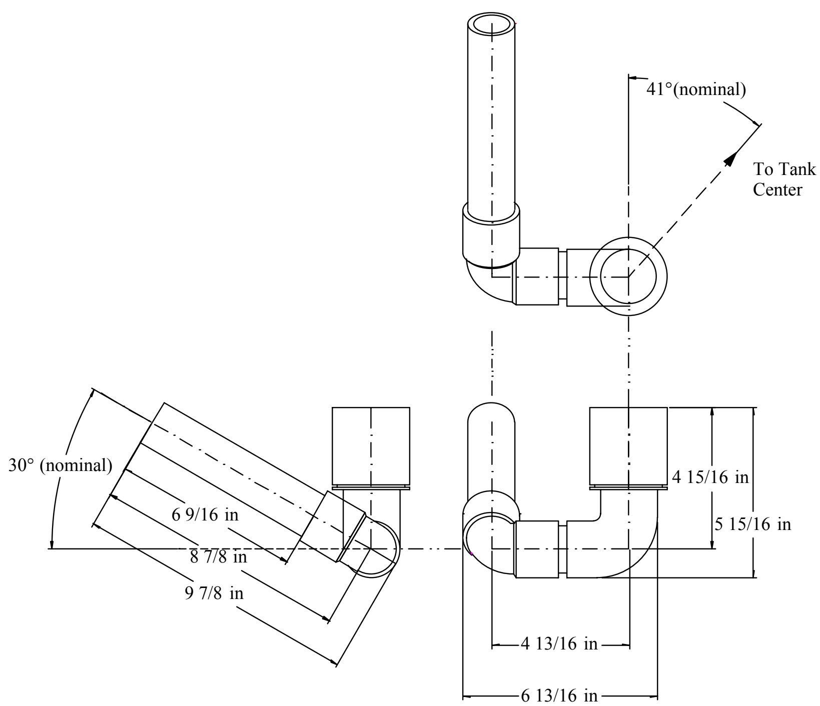

Figure 2.41. LS Scaled Test Stand Recirculation Pump Discharge Nozzle Assembly Used in Sequence 10

The two discharge nozzle assemblies used in sequence 11 and shown in Figure 2.42 consisted of (in order of assembly) a nominal 6-inch-long, ¾-inch-diameter schedule 40 stainless steel pipe bored to a 0.91-inch ID, a 1¼ × ¾-inch-diameter stainless steel bushing, a 1¼-inch-diameter 90° PVC elbow, a 1¼-inch-diameter schedule 80 carbon steel nipple, a second 90° PVC elbow, a short piece of 1¼ inch-diameter schedule 40 tubing, a 2 × 1¼-inch-diameter PVC reducer bushing, and a 2-inch-diameter PVC coupling. The nozzle tips extended 5⅜ and 5⁷⁄₁₆ inches from the 1¼ × ¾-inch-diameter reducer bushings, as shown in the figure. The lateral arms of the nozzle assemblies (containing the two elbows) were oriented outward, forming an angle of approximately 41° with the tank centerline, as shown in Figure 2.39, so the nozzle tips were closer to the tank wall than the PJMs, and the nozzle jet did not strike the PJM tube walls. Because of this orientation, the elevation arm of the nozzle assemblies (containing the nozzle tips) formed an angle of approximately 47° with the centerline, as shown in Figure 2.39 for one of the nozzles. The nozzle tips pointed approximately 30° above horizontal.

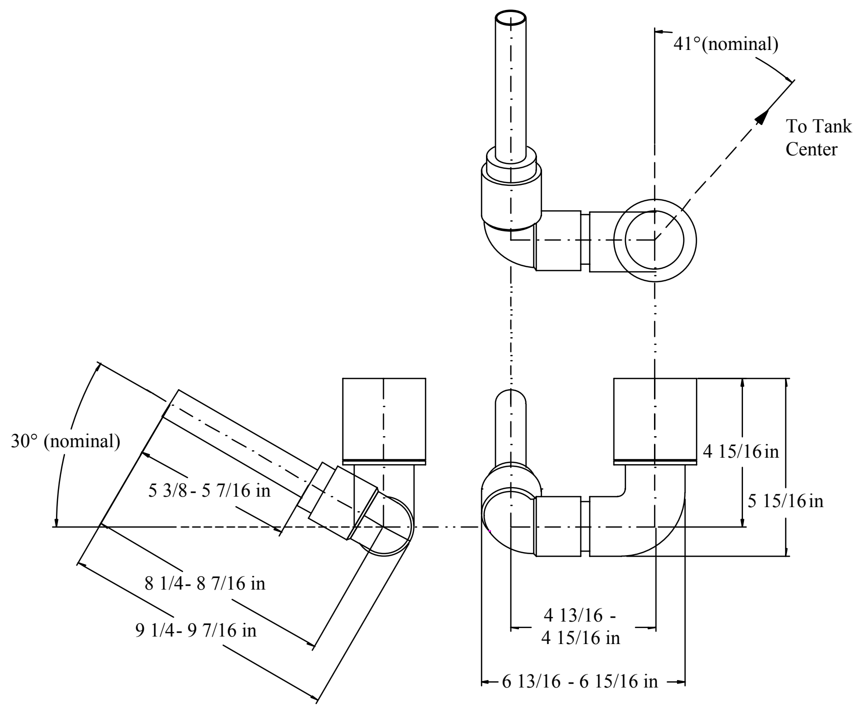

Figure 2.42. LS Scaled Test Stand Recirculation Pump Discharge Nozzle Assembly Used in Sequence 11

The recirculation system configuration in sequences 20, 21, 26, and 28 had two discharge lines and a suction line, as shown in Figures 2.43 and 2.44 (the discharge and suction lines were in place during sequence 27 but not used). The suction line was approximately 10 inches above tank bottom measured at the tank centerline. The nozzle assemblies used in sequence 20 that were attached to the discharge lines, as shown in Figure 2.43, contained nozzle tips consisting of 4½- and 4⁵⁄₁₆-inch-long, ¾-inch-diameter schedule 40 stainless steel pipes that were bored to 0.80 inches in diameter. The nozzle tips were threaded into two of the nozzle assemblies previously used for sequences 5 and 7 using 1 × ¾-inch-diameter reducer bushings instead of the 1 × ½-inch-diameter reducer bushings in the nozzle assemblies. The nozzle tips extended 3¹³⁄₁₆ and 4 inches out of the 1 × ¾-inch reducer bushings, as shown in Figure 2.45. The nozzle tip assemblies used in sequences 21, 26, and 28 were the same as those used in sequence 20 but they were

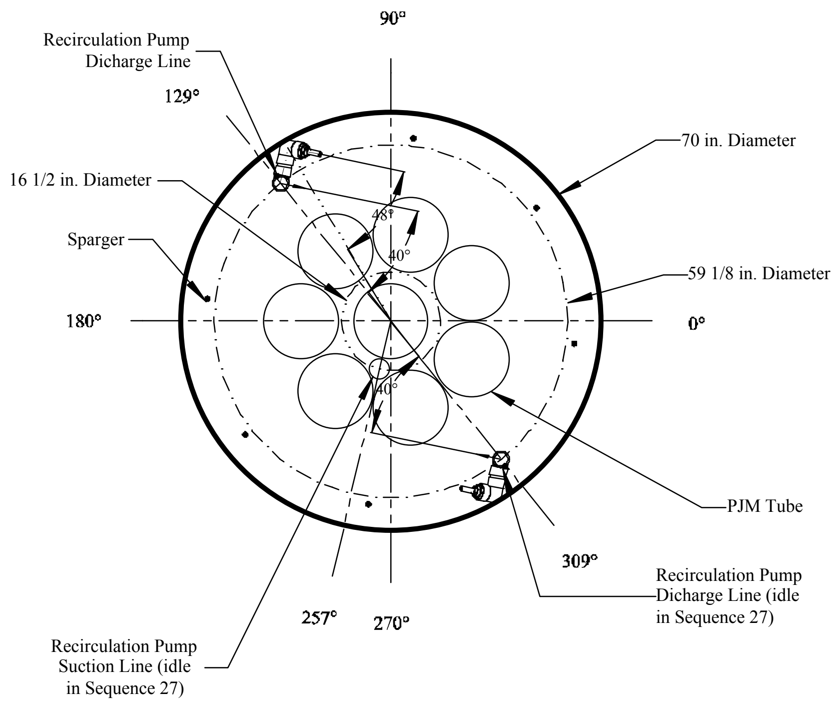

Figure 2.43. Plan View of Cluster (7+1) Configuration in LS Scaled Test Stand Showing Nominal Locations of Recirculation Line Components for Dual-Discharge Line Nozzle Configuration Used in Sequences 20, 21, 26, and 28

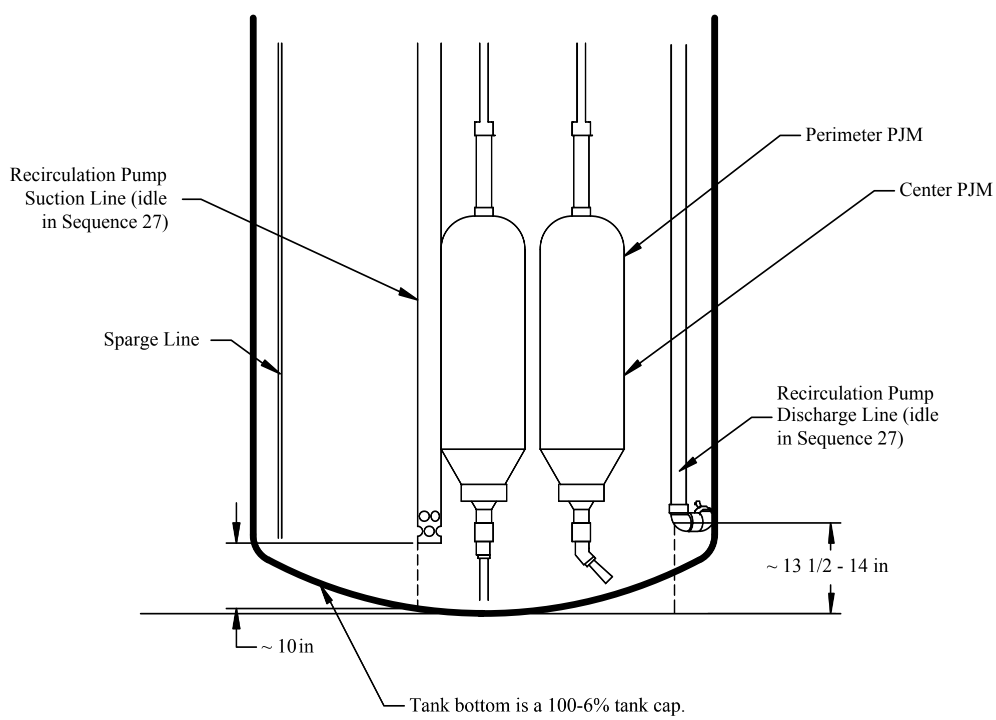

Figure 2.44. Elevation View of LS Cluster (7+1) Scaled Test Stand Showing Nominal Elevations of Recirculation Line Components for Dual-Discharge Line Nozzle Configurations Used in Sequences 20, 21, 26, and 28

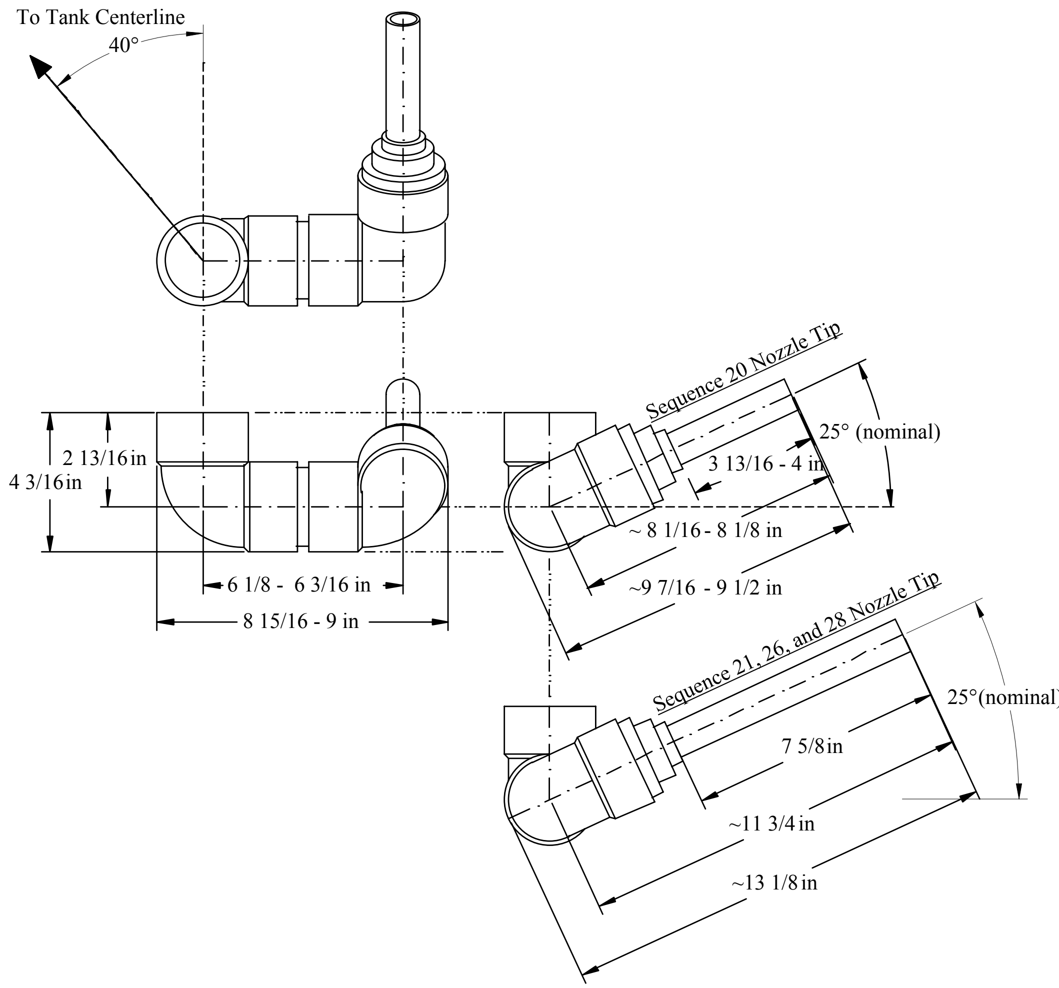

Figure 2.45. LS Scaled Test Stand Recirculation Pump Discharge Nozzle Assembly with Nozzle Tips Used in Sequence 20 and in Sequences 21, 26, and 28

fitted with 8-inch-long nozzle tips (extending 7⅝ inches from the reducer bushing) and bored to 0.78-inch ID. The lateral arms of the nozzle assemblies were oriented outward, forming an angle of approximately 40° with the tank centerline, as shown in Figure 2.43, so the nozzle tips were closer to the tank wall than the PJMs and the nozzle jets did not strike the PJM tube walls. The elevation arm of the assembly containing the nozzle tip formed an angle of approximately 48° with the centerline, as shown in Figure 2.43 for one of the nozzles. The nozzle tips pointed approximately 25° above horizontal. The centerlines of the lateral arms of the nozzle assemblies were elevated approximately 13½ to 14 inches above the tank bottom measured at the tank centerline.

2.2.4 PJM Assembly Shroud

A Plexiglas shroud was placed around the PJM assembly for sequences 26, 27, and 28 to prevent slurry flow into the inner annulus formed between the perimeter PJMs and the center PJM. The bottom of the shroud was a flat Plexiglas plate with holes for the PJM conical sections and the recirculation system pump suction line to pass through (Figure 2.46). The shroud was glued to the PJM support frame used to position

Figure 2.46. Close-up of LS Scaled Shroud Bottom Prior to Trimming and Caulking (left) and Foam Stripping Between Adjacent Perimeter PJMs (right)

the bottom of the PJM assembly. The support frame was at the bottom of the coupling connecting the lower conical section of the PJM to the upper, as shown in the figure. The sides of the shroud were formed by pressing insulation foam stripping in the space between adjacent perimeter PJMs, as shown in Figure 2.46, and covering them with silicon caulking. Plexiglas inserts were placed between the upper conical sections of adjacent PJMs where they were glued to the outsides of the PJM support frame, as shown in Figure 2.47. The top of the sides of the shroud between adjacent perimeter PJMs extended up to the bottom of the 2-inch-diameter couplings connected to the caps of the PJMs using Plexiglas inserts. The top of the shroud (Figure 2.47) consisted of seven wedge-shaped sections of Plexiglas plate connected to form a seven-sided pyramid, with holes provided for the center PJM air line, the recirculation system pump suction line, and sample lines to the perimeter PJMs. The Plexiglas top was angled so that the center of the top was approximately 4 inches higher than the perimeter of the top where it met the Plexiglas side inserts. The joints, where the Plexiglas pieces met the PJM surfaces, piping, or another Plexiglas sections, were caulked with silicon sealant. The interior of the shrouded PJM assembly was filled with a rigid polyurethane foam sealant, injected as expandable foam polyurethane intermediate and cured over several days, to provide rigid support to the shroud.

Figure 2.47. Plexiglas Insert Between PJMs near LS Scaled Shroud Bottom (left) and Top View Showing Shroud Top and Plexiglas Insert Between PJMs Near Shroud Top (right)

2.3 PJM/Hybrid System and Data Acquisition

2.3.1 PJM System Operation

Unlike conventional PJMs, whose operation is regulated by jet pump pairs driven by compressed air, the test systems used a series of solenoid valves and a combination of an air compressor and vacuum pump to simulate the drive and suction phases of PJM operation. These operations were controlled through a control logic program using DASYLab that turns the appropriate solenoid valves on and off at specified times. The duration of each phase, the applied pressure, and the vacuum can all be independently varied to simulate the operation of the PJMs. The PJMs were generally operated at a specific average nozzle velocity, $\bar{u}_{ave}$, which is defined as

$$\bar{u} = \frac{\Delta H}{\Delta t} * AR \tag{2.1}$$

where ΔH is the length of the PJM stroke, Δt is the time for achieving the stroke, and AR is the area ratio of the PJM to the nozzle. Actual PJM discharge is a transient phenomenon with initial velocity acceleration, followed by a nearly steady period of maximum or peak velocity, and ending with a deceleration.

Typically, Eq. (2.1) was used to prescribe a desired *nominal* operating velocity for the PJMs. A more meaningful velocity definition for scaled testing is the peak average velocity, which is defined as

$$\bar{u}_{peak} = \frac{1}{t_D - t_m} \int_{t_m}^{t_D} u(t)\, dt \tag{2.2}$$

where t_m is the time when the instantaneous velocity u is at a maximum and t_D is the time when the drive phase ends. This velocity is believed to more accurately characterize the useful jet mixing energy.

To calculate the peak average velocity given by Eq. (2.2), the instantaneous velocity u(t) must be known. This was attempted by differentiating real-time PJM fill level data obtained from capacitance level-probes inside the PJMs. This method was found to be somewhat inaccurate due to the limited transient response of the capacitance level probes. To overcome this, instantaneous PJM velocity was determined from transient PJM drive pressure. This method was validated against video analysis transient slurry surface level during PJM operation and found to be accurate. Examples of velocity drive functions derived from drive pressure for the final UFP and LS mixing configurations are shown in Appendix B.

In addition to the PJM operation, the recirculation pump flow rates were controlled using a variable frequency drive (VFD) on the centrifugal pumps and the air pressure to the diaphragm pump. Finally, the sparger air flow rates were controlled using rotameters.

During each mixing test, several variables such as PJM liquid levels and pressures, tank and ambient temperatures, recirculation pump flow rate, and density were monitored continuously and recorded digitally on a computer. The liquid/slurry level inside each PJM was measured using Drexelbrook capacitance level probes and transmitters. The functionality of the level probes was checked prior to the start of a sequence of tests, which typically ran from four to eight hours. Compressor and vacuum supply pressures and the pressures inside each PJM were monitored using Endress + Hauser ceramic pressure transducers. The tank and ambient temperatures were measured using Type K thermocouples. The flow rate and density of the slurry from the recirculation pump was measured using a 3-inch MicroMotion Coriolis mass flow meter. In addition to these variables, which were digitally monitored, the sparger air flow rates and pressures were recorded manually on the run data log sheets or in the project laboratory record books (LRBs).

3.0 Experimental Approach

The PJM cluster configuration concept, or one central pulse tube and the rest clustered around it, was chosen for both the UFP and LS vessels. These configurations were selected to minimize the impact on the current WTP design. The PJM cluster configuration provides a mixed turbulent cavern in the bottom of the vessel that suspends waste particles and is scalable. Supplemental mixing of the upper portion of the vessels relies on recirculation pumps or spargers. This section describes the experimental approach.

3.1 Overview of Experimental Approach

3.1.1 Simulant Rheology

The simulant used was an aqueous suspension of kaolin/bentonite clay; approximately 27 wt% clay mixture consisting of 80 wt% EPK kaolin and 20 wt% CH200 bentonite (Poloski et al. 2004a). This mixture exhibits a Bingham plastic rheology that closely represents that of actual waste slurries; the simulant was used to investigate the scale-up behavior of PJMs and to assess the performance of the scaled testing platforms presented in this report.

3.1.2 Mixing Effectiveness Determination

The primary measurement in the scaled test platforms was the size and extent of the mobilization cavern resulting from PJM operations and PJMs combined with recirculation (i.e., steady jet) and/or sparging. This was achieved using a chemical tracer method discussed in Poloski et al. (2004b). This section deals only with the method in which the tracer was injected into the tank and how the samples were collected.

The required amount of tracer (typically Brilliant Blue dye in an amount equal to approximately 5 g per 100 gal of clay simulant in the tank and/or NaCl in an amount equal to approximately 20 g per 100 gal of clay simulant in the tank) was mixed with approximately 2 L of the same clay simulant used in the testing. The concentrated tracer/clay mixture was injected before the start of a test at the lowest nozzle velocity of that test sequence. The concentrated tracer slurry was injected into the bottom third of the center PJM during the vacuum and vent phases of the PJM cycle over approximately 10 minutes. When tracer injection was completed, the injection line was purged with clean clay to ensure complete transfer of the tracer into the PJM. Once the line was purged, simulant samples from the tank were collected over at least 45 minutes of PJM operation. Samples were withdrawn at various times from five sample lines installed in the PJMs and the tank. Three of these samples were drawn from three PJMs and the remaining two from the annulus between the PJM and tank wall at elevations representing the lower and upper halves of the tank, respectively. After completion of the specified run conditions, the tank was completely homogenized, and final homogenized samples were collected. Comparison of the tracer concentration in the various samples with the final homogenized samples provides the percent mixed as a function of time and run conditions. Complete and successful mixing is defined as 100% as indicated by the chemical tracer method.

3.1.2.1 Dye and Tracer Techniques

Mixing performance in the PJM test vessels was assessed using tracer chemicals, as described in the previous section. A summary of the technique used is shown in Figure 3.1. The chemicals used were food dye color No. 1 (Brilliant Blue FCF) and sodium chloride (NaCl). Brilliant Blue FCF was used as the primary tracer for the first set of testing and is discussed in detail in this section and in Appendix A. Because the chloride ion does not interact with or absorb on the clay, the NaCl tracer was further developed and used as the primary tracer method for the second set of testing. Initially, a sample of simulant was drawn from the test vessel to baseline the tracer levels. Next, a stock solution of these materials was prepared by dissolving them in water. This stock solution was then blended with a sample of the test simulant to achieve rheological properties like those of the actual test simulant. This solution was introduced into the center PJM tube during operation by opening a valve on a sample injection line during the PJM suction phase. During the drive phase, the valve was closed and the injected dye driven from the PJM tube. This procedure allowed the tracer dye to be introduced gradually into the system over several drive/suction cycles and minimized the potential for a large amount of concentrated tracer to enter a stagnant region of the tank. This was observed when the concentrated tracer had significantly different physical properties from the bulk simulant. Such physical properties include density, entrained air due to surface tension, and rheological parameters.

After the dye was injected, the experimental clock started and samples were drawn from five locations in each test vessel. Samples 1, 2, and 3 were taken directly from three separate pulse tubes. These samples represent the contents of the well-mixed cavern. Sample locations 4 and 5 were between the pulse tubes and the tank wall. Location 4 was at a low elevation, and 5 was at a high elevation. Figures 3.2 and 3.3 are schematic diagrams of the tracer sampling locations in the LS vessel and UFP vessel, respectively.

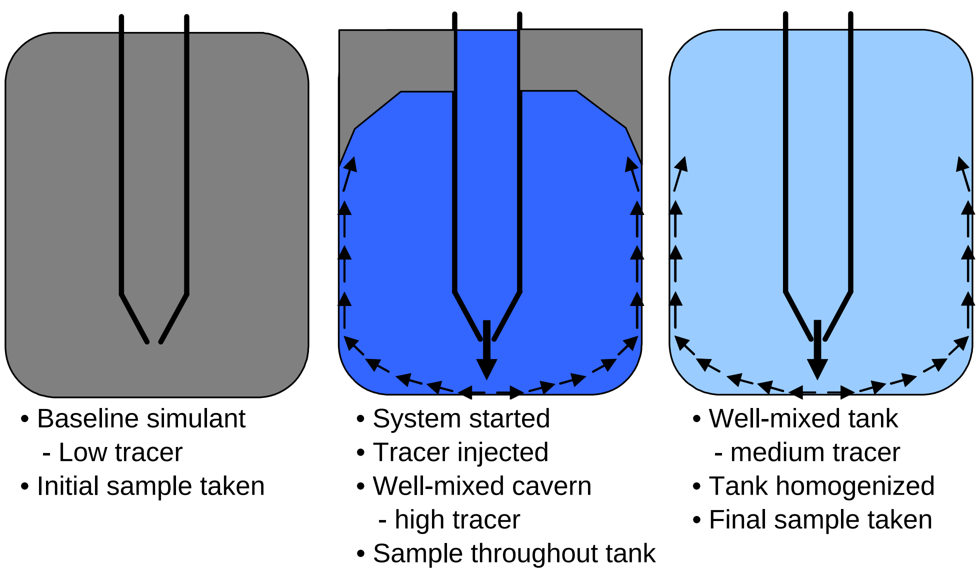

Figure 3.1. Summary of Tracer Dye Technique Steps

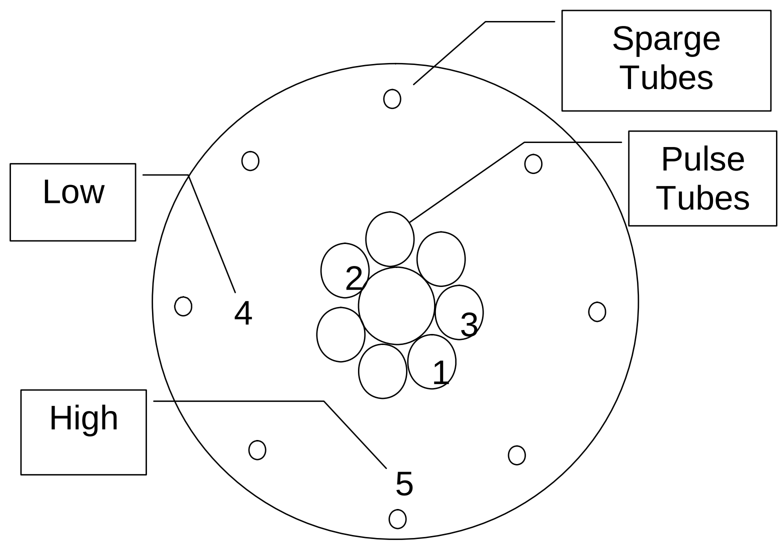

Figure 3.2. Schematic of LS Scaled Test Stand Vessel Tracer Sampling Locations

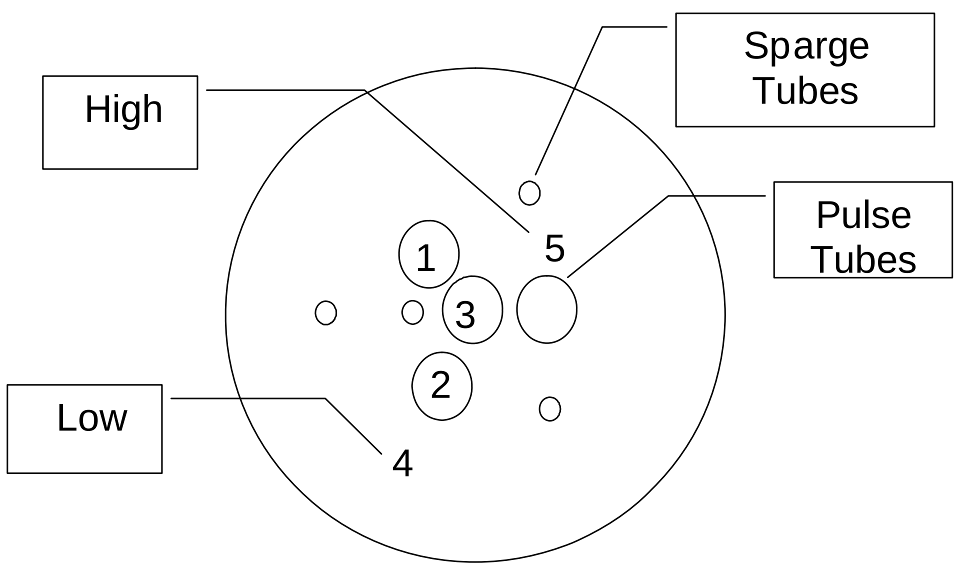

Figure 3.3. Schematic of UFP Vessel Scaled Test Stand Tracer Sampling Locations

Multiple run conditions were typically employed for each tracer injection. The tracer test started with the lowest energy condition to form the initial well-mixed cavern. Additional systems (e.g., recirculation pumps or sparging tubes) or increased pulse tube velocities were then used as subsequent run conditions to form larger mixing caverns.

During the initial run condition, samples were drawn from locations 1, 4, and 5 approximately every 10 minutes after the dye was injected. After 45–90 minutes of operation, samples were drawn from all locations and the next experimental condition used. During subsequent runs, samples from locations 1, 4, and 5 were taken every 15 minutes. After 45–90 minutes of operation, samples were drawn from all sample locations, and the next experimental condition was used. This procedure was used to quantify the transient behavior of the mixed regions within the tank. The first run condition was examined in more detail because the anticipated amount of energy required to reach steady state in that run was greater than subsequent runs, where a significant mixed region already existed.

Samples were drawn using a vacuum system. A vacuum was placed on the sample lines in the tank, and the simulant was drawn through the lines and collected in stoppered beakers using a trap. When sampling, the lines were initially purged of simulant into a separate beaker. This step loaded the sample line with simulant from the sample location at the appropriate time. A clean beaker was then attached and the newly loaded simulant collected. The simulant was then transferred into containers for tracer analysis. A sample extraction typically took 2 to 5 minutes to complete.

Tracer analysis consisted of two measurements, one for the dye and one for the NaCl. The concentration of dye was measured using an ultraviolet visible (UV-VIS) spectrometer, which requires a transparent sample. To overcome this limitation, the opaque kaolin:bentonite simulant was centrifuged and the analysis performed on the centrifuged liquid portion of the sample. The spectrometer measures the optical absorbance of the sample at multiple wavelengths of light. When the dye is present in the system, a peak absorbance is observed at approximately 630 nm. According to Beer's law, the magnitude of this absorbance peak is directly proportional to the concentration of dye in the system.

For the NaCl tracer, a either a chloride ion selective electrode (ISE) or ion chromatography (IC) was used to measure the concentration of chloride present in the samples. The ISE instrument measures the potential difference across an electrode that is surrounded by a membrane that allows chloride ions to pass from the sample material into the electrode cell. The IC method was used for LS sequences 21 and 26–28 and UFP sequences 13, 15 and 16. Equation (3.1) was used to calculate the fraction mixed:

$$X_j = \frac{C_f - C_0}{C_j - C_0} \tag{3.1}$$

where

X_j is the fraction mixed of the j-th tank sample
C_f is the tracer concentration of the final homogenized simulant
C_0 is the tracer concentration of the initial baseline simulant
C_j is the tracer concentration of the j-th tank sample.

When the aqueous phase tracer does not absorb onto the solid phase, the liquid phase concentration can be measured with the techniques described above, and Eq. (3.1) can be used to directly calculate the fraction of the tank mixed. The chloride ion did not appear to absorb onto the simulant particles, and this equation is used for the NaCl tracer. Because the spectrometer measures absorbance, which is proportional to concentration, Eq. (3.1) can be rewritten for the dye tracer as follows:

$$X_j = \frac{A_f - A_0}{A_j - A_0} \tag{3.2}$$

where

X_j is the fraction mixed of the j-th tank sample
A_f is the optical absorbance of the final homogenized simulant
A_0 is the optical absorbance of the initial baseline simulant
A_j is the optical absorbance of the j-th tank sample.

Unfortunately, the dye tracer absorbs onto the clay particles in significant quantity. In this situation Eq. (3.1) still applies, but the concentrations used in the equation must account for both the liquid and solid phases. This is accomplished using

$$C = Y_l C_l + Y_s C_S \tag{3.3}$$

where

C is the tracer concentration
C_l is the tracer concentration of the liquid phase
C_s is the tracer concentration of the solid phase
Y_l is the liquid phase mass fraction
Y_s is the solid phase mass fraction.

The distribution of tracer between the liquid and solid phases is typically described using a distribution coefficient:

$$C_s = K_d C_l \tag{3.4}$$

where K_d is the distribution coefficient.

To complicate matters further, the distribution coefficient is also a function of liquid phase dye concentration. When Eq. (3.3) and (3.4) are substituted into Eq. (3.1), the following results:

$$X_j = \frac{Y_l\left(A_f - A_o\right) + Y_s\left(K_{df} A_f - K_{do} A_o\right)}{Y_l\left(A_j - A_o\right) + Y_s\left(K_{dj} A_j - K_{do} A_o\right)} \tag{3.5}$$

where

K_{df} is the distribution coefficient at the homogenized tank tracer concentration
K_{do} is the distribution coefficient at the initial baseline tracer concentration
K_{dj} is the distribution coefficient at the j-th tank sample tracer concentration.

When K_d is null or constant, Eq. (3.5) reduces to Eq. (3.2). Over the small dye concentration ranges observed in the scaled platform testing, the assumption of a constant distribution coefficient holds, and Eq. (3.2) can be used. As A_j approaches A_f, K_{dj} approaches K_{df}, and the error associated in using Eq. (3.2) approaches zero. In addition, the distribution coefficient function varies from batch to batch of simulant, and other factors such as temperature and contact time will also affect the distribution coefficient function. Lastly, the solids loading of the simulant was often varied for rheological purposes. For these reasons, Eq. (3.2) is used to estimate the fraction mixed using the dye tracer. The error associated with this assumption is predicted using estimated values for the liquid and solid mass fractions and the distribution coefficient. Appendix A contains further details on these parameters.

Using the fraction mixed, Eq. (3.1) can produce results inconsistent with a realistic fraction mixed value. For instance, when the sample concentration, C_j, is less than the final sample concentration, C_f, the fraction mixed value is greater than unity, which is not realistic. This occurs when samples are withdrawn from regions in which the tracer has not yet arrived. For example, when the sample concentrations are equal to the initial test concentration, C_0, the fraction mixed approaches infinity. On a plot, these values are large enough that they cannot be observed with other samples with higher tracer concentrations. To simplify the data analysis in these situations, these data can be computed as a normalized concentration ratio referred to as the "mixing ratio." The equation for the mixing ratio, *MR*, is

$$MR_j = \frac{C_f - C_j}{C_f - C_0} \tag{3.6}$$

When the sample tracer concentration is equal to the initial test concentration, the mixing ratio is unity. When the sample tracer concentration is equal to the final test concentration, the mixing ratio is zero. Lastly, when the sample tracer concentration is above the final test concentration, the mixing ratio is negative. This corresponds to a situation where the sample location is within the mixing cavern, and the fraction mixed calculation may be performed. From this information, the data analysis of mixing-ratio data is summarized by Table 3.1.

Table 3.1. Mixing-Ratio Data Interpretation

Mixing Ratio Values	**Description**
~1	Tracer concentration near initial tracer test concentration; tracer has not reached sample location.
~0 to 1	Tracer concentration between initial and final tracer test concentration; tracer has begun to reach sample location or slow laminar mixing is occurring with large concentration gradients.
~0	Tracer concentration is near final tracer test concentration; vessel is nearly homogeneous.
< ~0	Tracer concentration is above final tracer test concentration; sample location is within the mixing cavern. Fraction mixed values can be calculated.
High degree of noise	Noisy results indicate that tracer concentrations are varying in a temporal manner. This occurs when simulant with a small amount of tracer is mixing with high tracer simulant. Such results indicate transient behavior where the mixing cavern is growing or the vessel is micro-mixing previously quiescent simulant.
Low degree of noise	As micro-mixing proceeds, local concentration gradients within the vessel disappear, and samples will reach stable values. This indicates that mixing has reached a steady-state value.

Because the mixing ratio contains the same variables and information as the fraction mixed value, a transformation function between fraction mixed space and mixing-ratio space exists. This transformation function is

$$MR = 1 - \frac{1}{X} \tag{3.7}$$

A transformation function of the propagated error between fraction mixed and mixing ratio is

$$\Delta MR = \frac{\Delta X}{X^2} \tag{3.8}$$

The equations for fraction mixed described earlier in this section can be applied to calculate mixing ratio and the corresponding errors from Eq. (3.7) and (3.8), respectively.

The objective of these tests was to find the PJM configuration and operating conditions that lead to a fully mobilized, homogenous vessel. Two steps are performed to evaluate a tank as homogenous. The first step is to see whether the results from each sample location for a run are consistent. This involves calculating the mixing ratio and corresponding uncertainty for the final sample set in a run. Test results are shown in Appendix A. The test results are termed "consistent" if the range of mixing ratios with the associated error for each location contains zero:

$$MR - 2\Delta MR \leq 0 \leq MR + 2\Delta MR \tag{3.9}$$

The consistency test can be applied to one or two standard deviations for different confidence levels. If the results are consistent within two standard deviations, the test is termed consistent. (Values for this evaluation for the UFP optimization and final configuration tests are included in Tables 6.1 and 7.1, respectively; values for the LS optimization and final configuration tests are listed in Tables 6.3 and 7.4.)

3.1.2.2 Core Sampling Techniques

Core samples were taken at the conclusion of LS sequences 26, 27, and 28, and UFP sequences 15 and 16. A 1-inch-diameter PVC pipe was used for core acquisition; this was placed inside a 2-inch-diameter PVC pipe (capped with a 1-inch reducer on the bottom) that was filled with shaved dry ice to freeze the sample before removing it from the tank. The sampling tube assembly was vibrated into position using a concrete vibrator; the assembly was top-capped with a plug and removed after a 60-minute freezing period had elapsed. The bottom of the core was capped with another plug after removal. Cores were transported vertically to a large walk-in freezer and stored vertically for later analysis (visual and tracer content).

3.1.2.3 Visual Observations of Dye Tracers

Visual observations of the tank surface and walls supplemented the understanding of the test results. Observations were made to characterize flow conditions on the tank surface, including easily observed upwelling of material due to PJM discharge, recirculation pump operation, or air sparging. Because in all experiments the chemical tracer was Brilliant Blue dye, observations of the slurry surface were made to ensure that dye did not prematurely break through the surface during tracer injection. The surface was also monitored during the run to assess whether dye broke through the surface due to upwelling of new slurry onto the surface. A video camera recorded the simulant surface during each test. The tank walls were monitored during tracer dye injection to confirm that the perimeter PJMs were discharging dyed slurry. After dye injection, the tank walls were observed for evidence of dyed slurry spreading upward and/or laterally along the wall. Dry erase markers were used to map dyed areas on the tank wall and for sketching a cylindrical projection map of the dyed areas on the acrylic tank wall. The markings on the wall were also recorded with a video recorder. Mapping tracer locations along the tank walls supplemented interpretation of tracer on the slurry surface for breakthrough due to cavern growth, flow due to spargers or pump recirculation, and interpretation of tracer sampling results. In some runs, direct evidence was observed of turbulence due to air spargers or PJM discharges, which were observed as a rippling effect extending up the tank wall at specific locations. This supplemented the tracer observations of cavern height at the tank wall. Observations of dark particulates entrained in the slurry at the tank wall were also made to follow flow lines during some of the recirculating pump operations, particularly of flow toward the pump return line.

3.1.3 Solids Suspension Effectiveness Determination

Under some conditions, the rheology was low and solids settled to the bottom of the tank. PJMs are well designed to pick up such solids because they direct a turbulent jet against the bottom of the tank. Solids suspension in mechanically stirred tanks is characterized by the "just suspended" criteria developed by Zwietering (1958; Atiemo-Obeng 2003), where no solids remain on the bottom of the tank for more than a few seconds (i.e., "lifting"). The British Hydromechanical Research Group-Fluid Mixing Processes (BHRG-FMP) consortium has shown that for steady downward-pointing jets an equation of functionality similar to that of Zwietering can be developed. The same form and functionalities would be expected to apply for multiple pulsed jets:

$$V_{js} = K * (\Delta\rho)^A \, (dp)^B \, X^C \tag{3.10}$$

where

V_{js} = minimum velocity to suspend solids
$\Delta\rho$ = density difference between solids and liquid
dp = maximum particle size
X = wt% of solids
A, B, C = constants with values less than 1.

To determine the solids-lift characteristics of several of the pulse jet-mixed tanks in the WTP facilities, we ran tests that were similar to those done by Zwietering and FMP. A small concentration of 4-mm glass beads was placed in the bottom of the tank (using water as the working fluid) and the PJM velocity increased in increments until the solids were observed to lift off the bottom and become suspended. Many have shown that visual and instrumentation methods for determining the just-suspended velocity give similar results (e.g., Brown et al. 2003). The Zwietering and FMP correlations show that the minimum velocity required to suspend solids is a weak function of solids fraction and particle size and mainly depends on density. Thus, using dense glass (2500 kg/m^3) and large particles gives a good estimate of the exact velocity required and eases observation.

Cloud height tests were also performed using a substantially greater quantity of the same 4-mm glass beads in water. Movement patterns and bead cloud heights were observed and measured by observers while the test stands were operated in various modes and drive velocities. Cloud tests were conducted in both LS and UFP vessels using PJMs (no spargers or recirculation pumps) with target nozzle velocities at 8 and 12 m/s. The tests used the same 4-mm beads as in the solids lifting tests, but a greater quantity was added; the total mass of beads used in cloud tests was 15 or 21 kg in the UFP and 30 or 60 kg in the LS, depending on the test sequence specifications. Exterior lighting was arranged so that the limits of the cloud could be visually estimated through the transparent tank wall. For each run (two to three runs per sequence, see Tables 3.2 and 3.3), observations of maximum cloud height above tank bottom were mapped around the perimeter of the tanks during the discharge stroke of the PJMs. Runs lasted approximately 20 to 60 minutes depending on test parameters specified and thus allowed several repetitions of cloud development for visual estimation. Results of the solids-lift tests are summarized in Section 4 (Tables 4.1 and 4.3), as are the results of the cloud tests (Tables 4.2 and 4.4).

3.2 UFP Scaled Prototype Test Sequences

Seventeen test sequences were performed using the UFP scaled prototype test stand (10 mixing test sequences and seven solids suspension sequences); the tests are summarized in Table 3.2. ("A" and "B" suffixes are treated as separate sequences.) Testing results for the UFP scaled prototype test stand are presented in Section 6.1 (UFP Design Optimization Results) and 7.1 (UFP Final Configuration Results); solids suspension effectiveness testing results are presented in Section 4.

Table 3.2. UFP Test Sequences Presented in this Report and Corresponding PJM, Sparger, and Recirculation Pump Target Operating Conditions[(a)]

Seq. No	Run	Test Type	Test Mode	Target PJM Nozzle Velocity (m/s)	No. of Spargers Operating	Target Sparger Flow Rate (scfm per sparge tube)	No. Pump Discharge Lines, Nozzle Angle	Pump Target Flow Rate (gpm)
1	1	Mixing	PJM Only	8	--	--	--	--
1	2	Mixing	PJM Only	12	--	--	--	--
1	3	Mixing	PJM + Sparging	12	1 center	3	--	--
1	4	Mixing	PJM + Sparging	12	3 perimeter	1	--	--
2	1	Mixing	PJM Only	8	--	--	--	--
2	2	Mixing	PJM Only	12	--	--	--	--
2	3	Mixing	PJM + Sparging	12	1 center	3	--	--
2	4	Mixing	PJM + Sparging	12	3 perimeter	1	--	--
3B	0	Mixing	PJMs Only	8	--	--	--	--
3B	1	Mixing	PJM + Pump	8	--	--	1 vertical	90
3B	2	Mixing	PJM + Pump	12	--	--	1 vertical	90
3B	3	Mixing	PJM + Pump + Sparging	12	1 center	3	1 vertical	90
7	1-4	Solids lift	PJMs Only	4, 6, 8, 6.7	--	--	--	--
7	5	Solids lift	Center PJM Only	6	--	--	--	--
7A	1	Cloud test	PJMs Only	8	--	--	--	--

Table 3.2 (contd)

Seq. No	Run	Test Type	Test Mode	Target PJM Nozzle Velocity (m/s)	No. of Spargers Operating	Target Sparger Flow Rate (scfm per sparge tube)	No. Pump Discharge Lines, Nozzle Angle	Pump Target Flow Rate (gpm)
7A	2	Cloud test	PJMs Only	12	--	--	--	--
8	1-7	Solids lift	PJMs Only	3.9, 4.5, 5.0, 5.5 6.0, 6.5, 7.0	--	--	--	--
9	1-4	Solids lift	PJMs Only	6.0, 5.4, 6.0, 7.0	--	--	--	--
9A	1	Cloud test	PJMs Only	8	--	--	--	--
9A	2	Cloud test	PJMs Only	12	--	--	--	--
10	1–3	Solids lift	PJMs Only	4.8, 5.7, 6.2	--	--	--	--
10A	1a	Cloud test	PJMs Only	8				
10A	2a	Cloud test	PJMs Only	12	--	--	--	--
11	1	Mixing	PJMs Only	8	--	--	--	--
11	2	Mixing	PJMs Only	12	--	--	--	--
12	1	Mixing	PJMs Only	12	--	--	--	--
12	2	Mixing	PJM + Pump	12	--	--	3 at 135°[(b)]	90
13	1	Mixing	PJM Only	8	--	--	--	--
13	2	Mixing	PJM Only	12	--	--	--	--
13	3	Mixing	PJM + Pump	12	--	--	1 vertical	90
15[(c)]	1	Mixing	PJM Only	12	--	--	--	--
15[(c)]	2	Mixing	PJM + Pump + Sparging	12	3 (perimeter)	0.1	1 vertical	90
16[(c)]	1	Mixing	PJM + Sparging	12	3 (perimeter)	2.3	1 vertical	No flow

(a) Test results discussed in Sections 4 through 7.2.
(b) 45º above horizontal
(c) Final configuration selected.

3.3 LS Scaled Prototype Test Sequences

Twenty-two test sequences were performed using the LS scaled prototype test stand (17 mixing test sequences and five solids suspension test sequences); these tests are summarized in Table 3.3. Mixing test results for the LS scaled prototype test stand are presented in Section 6.2 (LS Design Optimization Results) and in Section 7.2 (LS Final Configuration Results); solids suspension effectiveness testing results are presented in Section 4.

Table 3.3. LS Test Sequences Presented in this Report and the Corresponding PJM, Sparger, and Recirculation Pump Target Operating Conditions[(a)]

Seq. No.	Run	Test Type	Test Mode	PJM Target Nozzle Velocity (m/s)	No. of Spargers Operating	Target Sparger Flow Rate (per sparge tube) (scfm)	No. Pump Discharge Lines, Nozzle Elevation Angle	Pump Target Flow Rate (gpm).
2A	1	Mixing	PJMs Only	8	--	--	--	--
2A	2	Mixing	PJMs Only	12	--	--	--	--
2A	3	Mixing	PJMs + Spargers	12	4	3	--	--
2A	4	Mixing	PJMs + Spargers	12	8	3	--	--
3	1	Mixing	PJMs only	8	--	--	--	--
3	2	Mixing	PJMs only	12	--	--	--	--
3	3	Mixing	PJMs + spargers	12	4	3	--	--
3	4	Mixing	PJMs + spargers	12	8	3	--	--
4	1	Mixing	PJMs Only	8	--	--	--	--
4	2	Mixing	PJMs Only	12	--	--	--	--
4	3	Mixing	PJMs + Spargers	12	4	3	--	--
4	4	Mixing	PJMs + Spargers	12	8	3	--	--
5	1	Mixing	PJMs + Pump	8	--	--	4, 30°	120
5	2	Mixing	PJMs + Pump	12	--	--	4, 30°	120
6	1	Mixing	PJMs Only	8	--	--	--	--
6	2	Mixing	PJMs Only	12	--	--	--	--
6	3	Mixing	PJMs + Spargers	12	4	3	--	--
6	4	Mixing	PJMs + Spargers	12	8	3	--	--
7	1	Mixing	PJMs Only	6	--	--	--	--
7	2	Mixing	PJMs Only	8	--	--	--	--
7	3	Mixing	PJMs + Pump	8	--	--	4, 30°	120
7	4	Mixing	PJMs + Pump	12	--	--	4, 30°	120
7	5	Mixing	PJMs + Pump + Sparging	12	4	3	4, 30°	120
7	6	Mixing	PJMs + Pump + Sparging	12	8	3	4, 30°	120
8	1	Mixing	PJMs Only	8	--	--	--	--
8	2	Mixing	PJMs Only	12	--	--	--	--
9	1	Mixing	PJMs + Pump	8	--	--	1, vertical down	120
9	2	Mixing	PJMs + Pump	12	--	--	1, vertical down	120
9	3	Mixing	PJMs + pump + Spargers	12	4	3	1, vertical down	120
10	1	Mixing	PJMs + Pump	8	--	--	1, 30°	120
10	2	Mixing	PJMs + Pump	12	--	--	1, 30°	120
11	1	Mixing	PJMs + Pump	8	--	--	2, 30°	120
11	2	Mixing	PJMs + Pump	12	--	--	2, 30°	120
12	1	Mixing	PJMs Only	8	--	--	--	--

Table 3.3 (contd)

Seq. No.	Run	Test Type	Test Mode	PJM Target Nozzle Velocity (m/s)	No. of Spargers Operating	Target Sparger Flow Rate (per sparge tube) (scfm)	No. Pump Discharge Lines, Nozzle Elevation Angle	Pump Target Flow Rate (gpm).
12	2	Mixing	PJMs Only	12	--	--	--	--
13	1	Mixing	PJMs + Spargers	8	4	3	--	--
13	2	Mixing	PJMs + Spargers	12	4	3	--	--
16	1 - 6	Solids lift	PJMs Only	8, 9, 9.2, 7, 8, 8.5	--	--	--	--
16A	7	Cloud test	PJMs Only	8.5	--	--	--	--
16A	8	Cloud test	PJMs Only	10	--	--	--	--
16A	9	Cloud test	PJMs Only	12	--	--	--	--
17	1-4	Solids lift	PJMs Only	8.5, 9.4, 8.8, 8.5	--	--	--	--
17A	1	Cloud test	PJMs Only	12	--	--	--	--
17A	2	Cloud test	PJMs Only	8	--	--	--	--
18A	1	Cloud test	PJMs Only	12	--	--	--	-
18A	2	Cloud test	PJMs Only	8	--	--	--	--
19	1	Mixing	PJMs Only	8	--	--	--	--
19	2	Mixing	PJMs Only	12	--	--	--	--
20	1	Mixing	PJMs	12	--	--	--	--
20	2	Mixing	PJMs + Pump	12	--	--	2, 25°	120
21	1	Mixing	PJMs Only	8	--	--	--	--
21	2	Mixing	PJMs Only	12	--	--	--	--
21	3	Mixing	PJMs + Pump	12	--	--	2, 25°	120
26[b]	1	Mixing	PJMs only	12	--	--	-	-
26[b]	2	Mixing	PJMs + Pump + Spargers	12	8	1	2, 25°	120
27[b]	1	Mixing	PJMs + Spargers	12	8	3	--	--
28[b]	1	Mixing	PJMs + Pump + Spargers	12	4	0.2	2, 25°	120

(a) Test results discussed in Sections 4 through 7.2.
(b) Final configuration selected.

4.0 Solids Suspension Effectiveness

Seven solids suspension test sequences were carried out in the UFP scaled prototype test stand, and five solids suspension test sequences were performed in the LS scaled prototype ("A" suffixes are counted as separate sequences). The solids suspension tests were performed by placing a small concentration of 4-mm glass beads in the bottom of the tank and increasing PJM velocity in increments until the solids were observed to lift off the bottom. Solids lift was defined as observing lifting off the bottom of a vortex of glass beads whose axis is parallel to the tank bottom, such that if at any moment during the drive phase of the PJM cycle all the beads were lifted off the tank bottom, the solids lift test was declared positive ("yes"). (If the axis of the vortex was vertical, the beads at the bottom of the vortex did not act like they were resting on the tank bottom in a pile). One difficulty was the ability to see the bottom of the tank near the tank wall from outside the tank. A video camera placed in a clear Plexiglas tube was used to assist observations at these locations. A second problem was that the bead lift was not uniform around the tank (i.e., the velocities were asymmetric with respect to the tank centerline), possibly because the center PJM was not exactly coaxial with the tank centerline and because of slight variations in the symmetry of locations of perimeter PJM nozzles. This was more pronounced in the LS tank, in part because a bolt head extended out of the tank bottom at the tank centerline, creating a potential shadow. In the LS tank, if very good lift was occurring on one side of the tank but not the other, and marginal liftoff was occurring at intermediate locations, lift-off was declared.

The cloud test levels were measured at intervals around the tank either outboard from a perimeter PJM tube or approximately midway between PJM tubes. These levels are considered approximate because there was considerable variability in the cloud heights during several PJM discharge cycles observed in series. Also, the clouds often consisted of a series of sharply pointed plumes whose locations were not always adjacent to those where measurement tapes were fixed. The plumes changed elevation and lateral position during a discharge cycle and often overlapped other plumes, particularly near the end of the PJM discharge cycle. Adjacent plumes may or may not have similar maximum heights. When there was considerable fluctuation in the height of a plume, multiple observers were used to estimate the cloud height and provide descriptions of cloud topography.

The test conditions and results of the various solids lift and cloud tests performed in UFP scaled test stands are shown in Tables 4.1 and 4.2, and the PJM configurations for LS scaled test stands are presented in Tables 4.3 and 4.4. For the solids lift tests, the lowest velocity at which all beads were lifted off the bottom at some point during the drive phase for a given sequence are highlighted in bold in Tables 4.1 and 4.3. For all the solids suspension tests, a slurry of 4-mm glass beads (specific gravity 2.5 g/cm^3) in water was used. The concentration of the glass beads was approximately 0.4 and 0.5 wt%, respectively, for the UFP and LS scaled test stands. The peak average nozzle velocities were determined based on the measured level probe values.

Table 4.1. Summary of UFP Test Conditions and Status of Solids Lifting

Sequence	Run No.	Peak Average PJM Nozzle Velocity, m/s	Solids Lifting Status (Y/N)
7	1	4.8	No
7	2	6.4	No
7	**3**	**7.1**	**Yes**
7	4	7.7	Yes
7	5	6.2 (only center PJM operating)	No
8	1	4.1	No
8	2	4.9	No
8	3	5.4	No
8	4	5.9	No
8	5	6.9	No
8	**6**	**7.4**	**Yes**
8	7	8.1	Yes
9	**1**	**7.5**	**Yes**
9	2	6.0	No
9	3	6.7	No
9	4	8.4	Yes
10	1	5.0	No
10	2	6.3	No
10	**3**	**7.2**	**Yes**

Table 4.2. UFP Cloud Test Summary

Sequence	Run	PJM Config.	Perimeter nozzle angle	Peak avg nozzle velocity (m/s)	Lower range of cloud height above tank bottom	Upper range of cloud height above tank bottom	Comments
7A	1	Cluster (5+1)	45°	10.1	23½	27¼	Cloud concentrates between adjacent PJMs and between tank wall and point between perimeter PJM centerlines and outermost point on tubes; few beads move farther in.
7A	2	Cluster (5+1)	45°	17.9	25½	31½	Cloud shape similar to Run 1 but flatter, higher up wall; appears made up of multiple narrow plumes that spill into spaces between plumes at end of discharge, creating overall flat appearance of cloud
9A	1A	Expanded cluster (5+1)	45°	9.9	23½	27½	Cloud concentrates between adjacent PJMs and between perimeter PJM centerlines and tank wall; few beads move farther in.
9A	2A	Expanded cluster (5+1)	45°	18.8	30¾	37½	Cloud slopes downward about 14 in. from near tank wall to just inside perimeter PJM centerline; most beads don't move farther in except at very end of PJM discharge.
10A	1A	Expanded cluster (5+1)	30°	10.2	18	26	Majority of beads populate dense clouds between PJMs; cloud level drops 1 in. from wall to just inside perimeter PJM centerline, then slopes steeply downward.
10A	2A	Expanded cluster (5+1)	30°	18.3	13½	23¾	Cloud level slopes downward only about 1 in. between tank wall and tank centerline

Table 4.3. Summary of LS Test Conditions and Status of Solids Lifting

Sequence	Run No.	Peak Average PJM Nozzle Velocity (m/s)	Solids Lifting Status (Y/N)
16	1	8.2	No
16	2	9.4	Yes
16	3	10.4	Yes
16	4	7.4	No
16	5	8.3	No
16	**6**	**8.7**	**Yes**
17	1	8.8	Inconclusive
17	**2**	**10.4**	**Yes**
17	3	9.5	No
17	4	9.1	No

Table 4.4. LS Cloud Test Summary

Sequence	Run	PJM Config.	Perimeter Nozzle Angle	Peak Avg Nozzle velocity (m/s)	Lower Range of Cavern Height above tank bottom	Upper Range of Cavern Height above tank bottom	Comments
16A	7	Cluster (7+1)	45°	8.8	31¼	38	29.8 kg of glass beads used. Cloud visible near wall between adjacent perimeter PJMs; adding more beads may make cloud visible outboard of PJMs
16A	8	Cluster (7+1)	45°	11.0	32	39¾	59.8 kg of glass beads used in this and subsequent runs. Well-defined clouds of beads visible near tank wall between adjacent perimeter PJMs. Just enough beads outboard of PJMs to define cloud height. Clouds about 6 in. thick and next to tank wall.
16A	9	Cluster (7+1)	45°	15.3	31½	55¼	Cloud about 8 in. thick and near tank wall. Bead defined cavern erratic in shape, not following regular sine wave. In some places cloud height dropped 10 in. over several inches along tank wall. In other cases level remained constant between adjacent PJMs.
17A	1A	Expanded cluster (7+1)	23°	15.4	27¼	45	Cloud concentrated between adjacent PJMs and dropped downward and inward toward tank centerline.
17A	2A	Expanded cluster (7+1)	23°	8.3	19¾	30½	Clouds concentrated near wall between adjacent PJMs; not enough beads outboard of PJMs to define cloud. Clouds highest near wall, drop quickly away from wall to tank bottom at a radius approximately defined by innermost points on perimeter PJM tube walls.
18A	1A	Expanded cluster (7+1)	15°	15.1	27	41½	Cloud better distributed between tank centerline and wall, forming broad ring-shaped vortex with small hole near tank centerline. Cloud occupies entire volume above PJM nozzles under PJM assembly and extends to wall in spokes between adjacent PJMs. Outboard of perimeter PJMs cloud sweeps out, leaving zones of no beads.
18A	2A	Expanded cluster (7+1)	15°	8.3	16	20½	Not enough beads in cloud to define cloud height outboard of perimeter PJMs. Motion of beads toward center of tank more rolling than bead lifting, with a hole about the diameter of the center PJM tube at tank centerline and beads piling up several inches deep between center hole and perimeter PJM. Bead lifting only occurred in space between adjacent perimeter PJMs and tank wall.

5.0 Velocity Mapping

Velocity mapping was carried out in both prototype test stands equipped in their final configurations using a mast-mounted ultrasonic Doppler velocity probe (Imasonic) and a Met-Flow UVP-DUO MX signal processor. The velocity probe reads liquid movement along its longitudinal axis by correlating a detected Doppler shift of reflections from an outgoing 1 MHz ultrasonic pulse train. The probe measures fluid velocities along its longitudinal axis only (i.e., moving directly toward or away from the probe face). All testing was done at a pressure/drive-time-matched peak average velocity of 12 m/s; target simulant yield strength was 30–36 Pa with a target tank-fill aspect ratio (L/D) of 1.4 in the UFP test stand and 0.74 in the LS test stand. Spargers were not used in any velocity mapping activities. The test matrix for the UFP test stand included a recirculation pump (90 gpm target flow rate), but no pump was used during LS velocity mapping. The cavern height/velocity mapping criterion for both test stands was to obtain a maximum velocity for a majority (>50%) of PJM cycles in a sample that meets or exceeds a velocity of 80 mm/s. Due to PJM cycle variability and flow artifacts from submerged structural members, cavern heights often must be reported as a 2 to 3-inch range. All heights are measured in inches up from tank bottom center (datum).

5.1 UFP Velocity Mapping Results

Velocity mapping of the UFP vessel was performed according to the matrix of conditions given in Table 5.1. The positions mapped in the UFP test stand were numbered as in Figure 5.1. Cavern heights[(a)] obtained in the UFP test stand for conditions 1 and 2 are detailed in Table 5.2; velocities and detection heights obtained in the UFP test stand for conditions 3 and 4 are presented in Table 5.3.

Table 5.1. UFP Velocity Mapping Test Matrix

Test Condition and Probe Orientation[(a)]	Measurement Type	Operating Conditions[(b)]
Condition 1, horizontal probe orientation	Cavern height measurement	PJMs on, recirculation pump off
Condition 2, horizontal probe orientation	Cavern height measurement	PJMs and recirculation pump on
Condition 3, vertical probe orientation (wall); horizontal (center positions)	Wall/bottom velocity mapping	Recirculation pump only (PJMs off)
Condition 4, vertical probe orientation (wall); horizontal (center positions)	Wall/bottom velocity mapping	PJMs only (recirculation pump off)
(a) Horizontal orientation has probe pointed toward tank center in wall positions and toward tank wall in center positions unless otherwise noted. (b) Recirculation pump target flow rate 90 gpm.		

(a) The cavern height obtained by velocity mapping is not directly comparable with the fraction mixed results presented in Section 7 but is based on a velocity cutoff of 80 mm/s, implying that the simulant is mobilized at greater cavern heights where the velocity may be less than the cutoff. Any simulant motion that distributes the tracer will lead to an increase in the apparent cavern size based on the mixing results.

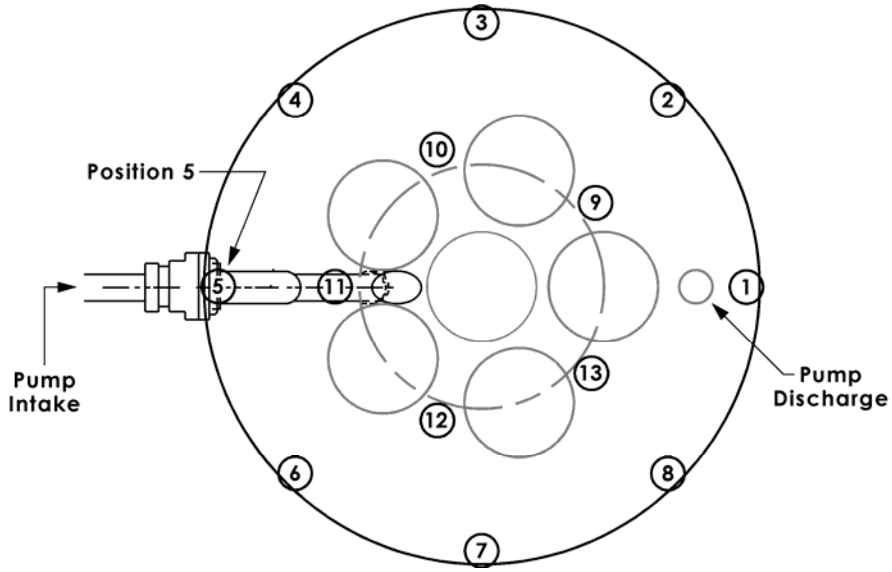

Figure 5.1. UFP Velocity Mapping Positions

Table 5.2. UFP Cavern Height Measurement Conditions 1 and 2 (height up from tank bottom center)[(a)]

Probe Position	Condition 1 Cavern Ht (in.)	Condition 2 Cavern Ht (in.)	Difference in Cavern Ht (in.). (Cond. 2 – Cond. 1)
1	20.5	Pump outlet interference- no measurement	N/A
2	24.5	18.5–19[(b)]	N/A (different probe orientations)
3	15.5	18.5	3
4	12.5	12.5	0
5	NM[(c)]	NM	NM
6	10.5	10.5	0
7	10.5	12.5	2
8	20.5–23.5	20.5–24.5	~0
9	17.5	22.5	5
10	12.5	20.5	8
11	NM	NM	NM
12	15.5–16.5	15.5	~0
13	18.5	25.5	7
Average[(d)]	16.4	18	1.6

(a) Target H/D = 1.4; nominal static simulant depth 47.6 inches.
(b) Vertical probe orientation for this measurement due to excessive noise in horizontal orientation.
(c) NM = No measurement possible due to recirculation pump intake pipe interference.
(d) Average cavern heights are based on all values and use the mean value for positions where a range of cavern height is shown. The average difference in cavern height in the last column is different than the difference between columns 2 and 3 because some positions (1, 2, 5, 11) do not have comparable readings.

Table 5.3. UFP Velocity Mapping Measurements Conditions 3 and 4 (height up from tank bottom center)[a]

Probe Position and Orientation	Condition 3 Detection Height (in.)	Wall/Bottom Velocity (mm/s)	Condition 4 Detection Height (in.)	Wall/Bottom Velocity (mm/s)
1 V	NM[b]	NM	15.5–16.5	600– <80[e]
2 V	10–10.5	< 80–450	18.5–19	200– <80[e]
3 V	4.5	200	15.5–17	<80–900
4 V	None	N/A(< 20)	14.5–16.5	<80–900
5 V	None	N/A (< 20)	15.5–16.5[c]	<80–500
6 V	None	N/A (< 20)	16–16.5	500–900
7 V	None	N/A (< 20)	15.5–16.5	<80–400
8 V	None	N/A (< 20)	16.5–17.5	<80–400
9 H	1.5	200[d]	3.5	200
10 H	3.5	200[d]	3.5	150
11 H	NM	N/A (< 20)	NM	N/A
12 H	3.5	200[d]	3.5	200
13 H	3.5	150[d]	3.5	200

(a) Target H/D = 1.4; nominal static simulant depth 47.6 inches.
(b) NM = No measurement possible due to recirculation pump intake pipe interference.
(c) Measurement taken east of recirculation intake line, approximately half way to position 4; no velocity visible for conditions 3 or 4 at position 5.
(d) Probe pointed toward recirculation outlet.
(e) Results correct as shown; see discussion below.

UFP average cavern heights for conditions 1 and 2 (PJMs only versus PJMs with recirculation pump) (see Table 5.2 and Figure 5.1) differed by an average of 1.6 inches (averaging excluded positions for which there are no directly comparable data). The greatest difference in cavern height was observed in positions 9, 10, and 13 (positions 10 and 13 are on opposite sides of the PJM array), with smaller effects noted at positions 3 and 7 (on tank walls 180° apart, each bearing 90° from the pump outlet). Little or no difference in cavern heights was noted at positions 4, 6, 8, and 12. The lack of change in cavern height at these positions is probably due to the recirculation intake pipe projecting from the wall at position 5 (the intake volume through the pipe necessarily engrossed much of the recirculation loops' outlet volume).

While position 8 showed no appreciable velocity (<20 mm/s) from pump-only measurements, position 12 showed similar pump-only and PJM-only velocities near the bottom (~200 mm/s). The anomalous results with respect to cavern height (little change between conditions 1 and 2) versus greatly different bottom velocities may be due to slight asymmetries in the tank construction/PJM array mounting observed during earlier testing with transparent simulants. The positions with the greatest difference in cavern height between PJMs-only and PJMs with recirculation pump conditions (positions 9, 10, and 13) all showed tank-bottom pump-only velocities from ~150 to ~200 mm/s, confirming the influence of the recirculation pump at these locations. It would appear that the pump output closely follows the curve of the tank bottom to the opposite side of the vessel, where much of this volume is engrossed by the recirculation intake port.

Tank-wall velocity measurements typically indicated a sharp boundary between flow and no flow with measurements varying by hundreds of mm/s over less than 1 inch of elevation. The two anomalous results here were at positions 1 and 2 during PJM-only operation (condition 4), where velocity decreased substantially over a short decrease in elevation. These positions are closest to the recirculation pump outlet pipe and were probably subject to wake effects.

5.2 LS Velocity Mapping Results

Velocity mapping was carried out in the LS test stand with only PJMs operational (without recirculation). Cavern height measurements were taken with horizontal probe orientation at all numbered locations (see Figure 5.2) and also with vertical probe orientation at all wall locations (1–8). Horizontal-orientation bottom velocity readings were also taken at inner ring locations (positions 9–15). LS cavern heights and velocity mapping results are presented in Table 5.4.

Velocity mapping results from the LS test stand were more consistent at different measurement positions and less sharply delineated vertically than the UFP results. The velocity spread for tank bottom measurements and the differences in cavern heights were also substantially less for the LS vessel than for the UFP.

Cavern heights (using horizontal probe orientation) varied from 20.5 to 25.5 inches at the wall positions (1–8) and from 22.5 to 25.5 inches at the center positions (9–15); average cavern height for all positions (horizontal probe orientation) was 23.5 inches. Cavern height at the wall (vertical probe orientation) varied from 21 inches at position 5 to 17.5 inches at position 7; this position also had the lowest cavern reading with the horizontal probe orientation. No vertical-orientation wall cavern height was

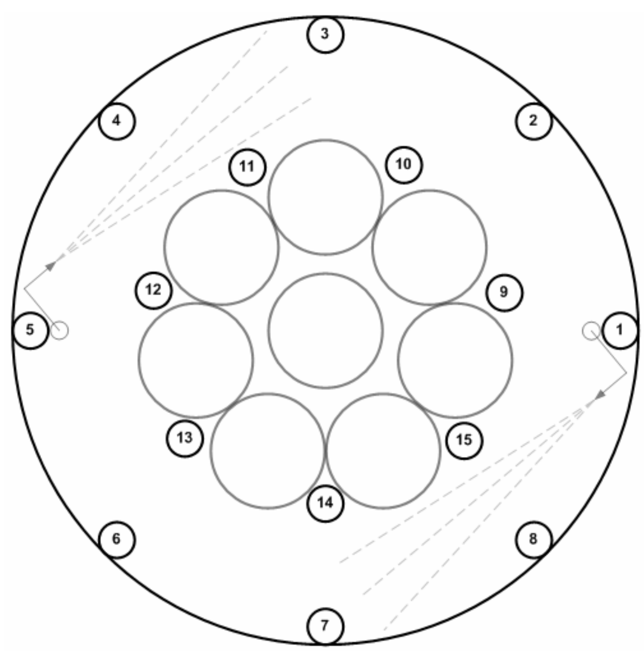

Figure 5.2. LS Velocity Mapping Positions (recirculation pump nozzles shown for orientation only; no recirculation used during mapping)

Table 5.4. LS Velocity Mapping Results (height up from tank bottom center)[(a)]

Position	Cavern Height (horizontal) (in.)	Wall Cavern Height (vertical) (in.)	Center Tank Bottom Velocity (horizontal) (mm/s)	Center Tank Bottom Measurement Height (in.)
1	25.5	18.5	N/A[(b)]	N/A
2	24.5	18.5	N/A	N/A
3	23	20.5	N/A	N/A
4	25.5	20.5	N/A	N/A
5	24.5	21	N/A	N/A
6	21	No reading along wall	N/A	N/A
7	20.5	17.5	N/A	N/A
8	23.5	19.5	N/A	N/A
9	22.5	N/A	800 (erratic)	4
10	23.5	N/A	900	3.5
11	24.5	N/A	1200	4.5 (2.5 inches north of position 11)
12	25.5	N/A	600	3.5
13	22.5	N/A	Signal saturated (>1250)	4
14	22.5	N/A	600	4
15	24	N/A	Signal saturated (>1250)	4.5
Average cavern ht	23.5	19.4 (excluding position 6)	N/A	N/A

(a) Target H/D = 0.74; nominal static simulant depth 51.8 in.
(b) NA = measurement positions are not applicable (see Figure 5.2).

obtained for position 6, which showed minimal velocity (<30 mm/s) at all elevations sampled along the wall; the proximity of a sparge-tube array mounting bracket may have contributed to this anomalous result by diverting flow away from the wall toward the center. The cavern height at this position (21 inches) was comparable to those at adjacent wall locations (24.5 inches at position 5 and 20.5 inches at position 7). Center tank bottom average velocities varied from approximately 600 mm/s at positions 12 and 14 to over 1250 mm/s (saturated detector) at positions 13 and 15. (Reported velocities are averages of the five highest cycle velocities in a sample train).

6.0 PJM/Hybrid System Optimization Results

The mixing tests performed and the percent mixed results for system optimization test sequences for the UFP and LS scaled test stands are summarized in Tables 6.1 and 6.3, respectively. The peak average nozzle velocities (Eq. 2.2) are calculated from the differential drive pressure (i.e., the difference of actual drive pressure and head at the PJM nozzle). The PJMs, spargers, and recirculation pump configurations and operating conditions for the various sequences are presented in Tables 2.1 through 2.4. All tests were performed with kaolin/bentonite clay simulant. The yield stress was determined from thoroughly mixed samples (mixed by PJM overblow and sparging) collected before and after a sequence of runs. The yield stress of the kaolin/bentonite clay simulant is the average of the results for these samples. The H/D is the ratio of the simulant fill height to tank diameter.

The actual nozzle velocities listed in Tables 6.1–6.4 were calculated based on the peak average velocity ($\bar{u}_{peak}$) (Eq. 2.2) defined in Bamberger et al. (2005). The peak average nozzle velocities are based on averages of all the PJMs (four or six for UFP and eight for LS) taken over 25 representative cycles of PJM operation during a run. Actual drive functions for final configuration test sequences (UFP test sequences 15 and 16 and LS test sequences 26, 27, and 28) are shown in Appendix B; results for these tests are given in the following section. The cycle times listed in Tables 6.1 and 6.3 for the two test stands were set based on scaling approximately equal to the inverse of the geometric scale factor, that is, 4.94 and 4.29 for the UFP and LS scaled test stands, respectively. Test sequence numbers not presented in this document are those for which no conclusive mixing result was obtained or sequences used to derive drive functions or check system performance.

For tests using a recirculation pump, the pump flow rates were scaled approximately by the inverse square of the geometric scale factor, that is, 4.94^2 (24.4) and 4.29^2 (18.0) for the UFP and LS scaled test stands, respectively. The recirculation flow rates listed in Tables 6.1 and 6.3 are based on the average flow rate measured over a run. In calculating recirculation pump averages, startup transients were ignored.

For tests that involved sparging, no scaling was applied in setting the operating air flow rates, and the flow rate through the sparger tubes was based on the readout of the rotameters included in-line with each sparger. The sparger air flow rates shown in Tables 6.1 and 6.2 are either target flow rates (scfm) or actual flow rates (acfm) at the bottom of the sparge tube outlet; a post-calibration of the flow meters indicated the sparger flow rates were within ±15%.

The "fraction mixed" and the mixing ratio results presented in Tables 6.1 and 6.3 are based on measurements obtained from the tracer (either dye or salt solution) injected into the simulant before the start of a test sequence. The approach is discussed in Section 3.1 and Poloski et al. (2004b). The error in the fraction mixed values is due to a linear isotherm assumption for dye absorption. This error goes to zero as the fraction mixed goes to 100%. Isotherm errors using the Cl^- ion tracer are insignificant. Experimental variability due to sampling and analysis is still present. The percent mixed versus yield Reynolds number for the various tests conducted with the UFP scaled test stand are shown in Figure 6.1 (the highest yield Reynolds number, PJM-only test shown is sequence 15, run1). Similar results for the LS scaled test stand are shown in Figure 6.2 (the data point for sequence 20, run 1 is midway between the two PJM/pump data points in the upper-left corner of the figure).

Table 6.1. Test Conditions and Fraction Mixed Results for Optimization Tests Performed in UFP Test Stand

Seq.	Run	Test Mode	H/D	Yield Stress (Pa)	Peak Avg Noz Vel. (m/s)	Cycle Time (sec)	Sparger Flow Rate (per sparge tube) (scfm)	Pump Flow Rate (gpm)	Fraction Mixed	Error[a] (±)	Mixing Ratio				Mixing Ratio Probability Score[b,c]	
											Dye	Error	Chloride	Error	Dye	Chloride
1	1	PJM Only	1.8	19	8[d]	27	--	--	Inc	--	Inc	--	N/M	--	Inc	N/M
1	2	PJM Only	1.8	19	12[d]	27	--	--	Inc	--	Inc	--	N/M	--	Inc	N/M
1	3	PJM + spargers	1.8	19	12[d]	27	3[e]	--	0.98	0.09	-0.02	0.1	N/M	--	66%	N/M
1	4	PJM + spargers	1.8	19	12[d]	27	1[e]	--	0.95	0.09	-0.05	0.1	N/M	--	95%	N/M
2	1	PJM Only	1.8	35	8.1	27	--	--	0.53	0.093	Inc	--	N/M	--	Inc	N/M
2	2	PJM Only	1.8	35	13.7	27	--	--	0.64	0.074	Inc	--	N/M	--	Inc	N/M
2	3	PJM + spargers	1.8	35	14.0	27	3[e]	--	1.1	0.013	Inc	--	N/M	--	Inc	N/M
2	4	PJM + spargers	1.8	35	13.9	27	1[e]	--	0.96	0.0088	Inc	--	N/M	--	Inc	N/M
3B	1	PJMs Only	1.4	37	8.7	27	--	--	0.65	0.12	Inc	--	Inc	--	Inc	Inc
3B	2	PJM + Pump	1.4	37	8.7	27	--	90	0.98	0.0074	-0.02	0.09	0.03	0.2	98%	58%
3B	3	PJM + Pump	1.4	37	15.8	27	--	87	1.0	0.0019	0.01	0.09	-0.02	0.2	97%	77%
3B	4	PJM + Pump + Sparging	1.4	37	15.9	27	3[e]	95	1.0	0.0038	0.01	0.09	-0.02	0.2	95%	69%
11	1	PJMs Only	1.4	34	8[d]	27	--	--	Inc	--	Inc	--	Inc	--	Inc	Inc
11	2	PJMs Only	1.4	34	12[d]	27	--	--	Inc	--	--	--	--	--	Inc	Inc
12	1	PJMs Only	1.8	20	12[d]	27	--	--	Inc	--	Inc	--	Inc	--	Inc	Inc
12	2	PJM + Pump	1.8	20	12[d]	27	--	90[e]	0.95	0.07	-0.05	0.07	-0.011	0.2	97%	55%
13	1	PJMs Only	1.4	34	8[d]	27	--	--	Inc	--	Inc	--	Inc	--	Inc	Inc
13	2	PJMs Only	1.4	34	12[d]	27	--	--	Inc	--	Inc	--	Inc	--	Inc	Inc
13	3	PJM + Pump	1.4	34	12[d]	27	--	90[e]	1.04	0.10	0.04	0.1	-0.4	0.2	42%	35%

(a) Estimated error due to assumption of linear isotherm for dye absorption. Experimental error is not included.
(b) Inc = inconsistent results; N/M = not measured.
(c) An average mixing ratio of zero with an error of 0.1 corresponds to a probability score of 68%. Probability scores greater than 68% are considered high confidence while values below 68% are considered lower confidence (see subsection 3.1.2.1); a high confidence (>68% probability score) infers that the system fully mixed the test vessels.
(d) Target velocity; actual velocities were not calculated for these tests.
(e) Target flow rate.
Note: Test sequences not presented here are those for which no conclusive mixing result was obtained or were used to derive drive functions or check system performance.

Table 6.2. Summary Dye Tracer Visual Observations for UFP Optimization Tests

Seq. No.	Run No.	Config test mode	Peak avg PJM nozzle velocity (m/s)	No. spargers, target flow rate per sparge tube (scfm)	No. pump discharge lines, nozzle angle, target flow rate	Summary visual observations
1	1	Trifoil (3+1), PJM only	8[a]	--	--	No dye breakthrough on surface. Dye observed on tank wall localized near perimeter PJM nozzles.
1	2	Trifoil (3+1), PJM only	12[a]	--	--	No dye breakthrough on surface. Solid dye observed on tank wall near perimeter PJM nozzles more spread out than run 1. Patches of dye extended as high as 10 inches above lower tank rim
1	3	Trifoil (3+1), PJM + sparging	12[a]	1 (center), 3	--	Soccer ball sized sparger bubbles quickly covered surface with dye. Dye on wall was almost completely uniform by end of run.
1	4	Trifoil (3+1), PJM + sparging	12[a]	3 (perimeter), 1	--	Sparger bubbles smaller than in run 3 (about 8-inch diameter). Dye on entire wall was mostly uniform in color. Areas without dye appeared stagnant, suggesting a coat of very viscous slurry on wall at these locations.
2	1	Trifoil (3+1), PJM only	8.1	--	--	No dye breakthrough on surface. Dye observed on tank wall localized near perimeter PJM nozzles. Some mottled patches of dye extended upward about 15 inches from lower rim.
2	2	Trifoil (3+1), PJM only	13.7	--	--	No dye breakthrough on surface. Dye observed on tank wall still localized near perimeter PJM nozzles spread upward to about 7 inches above lower rim. Mottled dye patches from run 1 disappeared.
2	3	Trifoil (3+1), PJM + sparging	14.0	1 (center), 3	--	Soccer ball sized sparger bubbles quickly covered surface with dye. Dye on wall was uniform on side closest to sparger and mottled with elongated patches of dye on the other side.
2	4	Trifoil (3+1), PJM + sparging	13.9	3 (perimeter), 1	--	Sparger bubbles smaller than in run 3 (about 8-inch diameter). Dye on entire wall was uniform in color.
3B	1	Trifoil (3+1), PJMs only	8.7	--	--	No dye breakthrough on surface. Dye observed on tank wall near perimeter PJM Nozzles about 3 inches above lower tank rim after injection. Dyed areas coincided with turbulence observed during PJM discharge and reached 24 inches above lower rim.
3B	2	Trifoil (3+1), PJM + pump	8.7	--	1 vertical, 90	Dye slowly reached surface; about ⅓ of surface covered with dye at end of run. About ⅔ of tank wall was uniformly dyed up to slurry surface.
3B	3	Trifoil (3+1), PJM + pump	15.8	--	1 vertical, 90	Dye slowly covered slurry surface over course of run. Similarly, tank walls slowly uniform in color over the course of the run.

Table 6.2 (contd)

Seq. No.	Run No.	Config test mode	Peak avg. PJM nozzle velocity (m/s)	No. spargers, target sparger flow rate per sparge tube (scfm)	No. pump discharge lines, nozzle angle, target flow rate	Summary visual observations
3B	4	Trifoil (3+1), PJM + pump + sparging	15.9	1 (center), 3	1 vertical, 90	Dye uniformly covered tank walls and slurry surface at start of run. Bubbles from the sparger produced bead-shaped splash zone about 5 x 12 inches around perimeter sparger closest to the center. A few small bubbles also erupted on the surface on the side of the center PJM opposite the center sparger.
11	1	Expanded Cluster (5+1), PJMs only	8[a]	--	--	No dye breakthrough on surface. Dye observed on tank wall localized near perimeter PJM nozzles about 2 to 4 in. above lower tank rim, and a few patches of dye that extend about 7 inches higher up the wall. Faint patches of dye formed between the solid patches, forming a nearly complete band of dye around the lower tank rim ranging as high as 6 inches above the rim.
11	2	Expanded Cluster (5+1), PJMs only	12[a]	--	--	Dye appeared on the surface of the slurry near the end of the run localized mostly between one perimeter PJM and the nearby tank wall. Dye was observed near the two adjacent perimeter PJMs. A little less than 25% of the slurry surface was dyed at the end of the test. Patches of dye observed in run 1 remained similar during this run except that three vertical patches of mottled dye outboard of three adjacent PJMs extended 21 to 30 inches above lower rim. Turbulence noted 4 to 7 inches above lower rim near perimeter PJMs.
12	1	Expanded Cluster (5+1), PJMs only	12[a]	--	--	Fresh slurry appeared to slowly upwell on surface during PJM discharge. After about 24 minutes dye appeared on support structures about 5 inches below surface and on surface about 4 minutes later. About 80% of the annulus between the perimeter and center PJMs was dyed at end of run. Dye extended halfway up tank wall near all but one perimeter PJM so about ⅓ of surface was dyed. Dye covered about ⅓ of tank wall from the top to about 33 inches by end of run.
12	2	Expanded Cluster (5+1), PJM + pump	12[a]	--	3 at 45°,[b] 90	Difficult to determine whether new slurry breaking surface during PJM discharge could be attributed to pump. No evidence of plumes from pump discharge lines during PJM suction. Took about 5 minutes to cover 80% of slurry surface after starting pump. Surface completely covered by end of run. Most of tank wall had a mottled dyed appearance by end of run; appeared that suction line was creating a flow shadow above it.
13	1	Cluster (5+1), PJM only	8[a]	--	--	Dye breakthrough on surface occurred about 20 minutes after dye injection near a perimeter PJM. The dye surfaced in a crease about midway between PJM and tank wall. Less than 10% of slurry surface dyed by end of run. Dye observed on tank wall near perimeter PJM nozzles about 3 inches above lower tank rim; a few patches of dye extend about 11 inches above rim except near the suction line, where a patch of dye extended about 24 inches above rim.

Table 6.2 (contd)

Seq. No.	Run No.	Config test mode	Peak avg. PJM nozzle velocity (m/s)	No. spargers, target sparger flow rate per sparge tube (scfm)	No. pump discharge lines, nozzle angle, target flow rate	Summary Visual Observations
13	2	Cluster (5+1), PJM only	12[a]	--	--	Dye that appeared on the slurry surface during run 1 slowly faded during this run. It appeared near the end of the run that dye was reaching the surface in a new seam almost on the opposite side of the tank. Dye covered about 20% of the slurry surface at end of run. Patches of dye on tank wall broadened and reaches as high as 32 inches above lower rim. Turbulence observed outboard of perimeter PJMs about 8 to 12 inches above lower rim.
13	3	Cluster (5+1), PJM + pump	12[a]	--	1 vertical, 90	Dye on surface at end of run 2 slowly moved toward pump discharge line and disappeared below surface. About 20 min into the run, dye surfaced in a seam between the PJM on the opposite side of the tank and the tank wall, and later at the wall in that location. The seam extended both directions around the tank during the rest of the run. Surface essentially completely dyed by end of run. Dye moved up tank wall fastest near PJMs on opposite side of tank from pump discharge line after pump started. The wall near the pump took about 30 minutes to become dyed. By end of run, wall dyed in a mixture of solid and marbled patches.

(a) Target velocities; actual velocities not calculated for this test.
(b) Angle above horizontal.

Table 6.3. Test Conditions, Fraction Mixed Results for Optimization Tests Performed in LS Test Stand

Seq.	Run	Test Mode	H/D	Yield Stress (Pa)	Peak Avg. Noz. Vel. (m/s)	Cycle Time (sec)	Sparger Flow Rate (per sparge tube)	Pump Flow Rate (gpm)	Fraction Mixed	Error[a] (±)	Mixing Ratio				Mixing Ratio Probability Score[b,c]	
											Dye	Error	Chloride	Error	Dye	Chloride
2A	1	PJMs only	0.74	20	8[d]	45	-	--	Inc	--	Inc	--	N/M	--	Inc	N/M
2A	2	PJMs only	0.74	20	12[d]	45	-	--	Inc	--	Inc	--	N/M	--	Inc	N/M
2A	3	PJMs + spargers	0.74	20	12[d]	45	3 scfm[e]	--	Inc	--	Inc	--	N/M	--	Inc	N/M
2A	4	PJMs + spargers	0.74	20	12[d]	45	3 scfm[e]	--	1.03	0.06	0.03	0.06	N/M	--	99%	N/M
3	1	PJMs only	0.74	11	8[d]	45	-	--	Inc	--	Inc	--	N/M	--	Inc	N/M
3	2	PJMs only	0.74	11	12[d]	45	-	--	Inc	--	Inc	--	N/M	--	Inc	N/M
3	3	PJMs + spargers	0.74	11	12[d]	45	3 scfm[e]	--	Inc	--	Inc	--	N/M	--	Inc	N/M
3	4	PJMs + spargers	0.74	11	12[d]	45	3 scfm[e]	--	0.99	0.08	-0.01	0.08	N/M	--	100%	N/M
4	1	PJMs only	0.74	38	7.9	45	-	--	0.54	0.15	Inc	--	N/M	--	Inc	N/M
4	2	PJMs only	0.74	38	13.4	45	-	--	0.65	0.13	Inc	--	N/M	--	Inc	N/M
4	3	PJMs + spargers	0.74	38	13.3	45	3 scfm[e]	--	0.87	0.052	Inc	--	N/M	--	97%	N/M
4	4	PJMs + spargers	0.74	38	13.2	45	3 scfm[e]	--	0.97	0.014	-0.01	0.08	N/M	--	0%	N/M
5	1	PJMs + pump	0.74	38	8[d]	45	--	120[e]	Inc	--	Inc	--	N/M	--	Inc	N/M
5	2	PJMs + pump	0.74	38	12[d]	45	--	120[e]	0.83	0.12	-0.21	0.12	N/M	--	2%	N/M
6	1	PJMs only	0.74	38	8[d]	45	--	--	N/M[f]	--	N/M	--	N/M	--	N/M[f]	N/M[f]
6	2	PJMs only	0.74	38	12[d]	45	--	--	Inc	--	Inc	--	N/M	--	Inc	N/M
6	3	PJMs + spargers	0.74	38	12[d]	45	3 scfm[e]	--	0.90	0.12	-0.11	0.12	N/M	--	45%	N/M
6	4	PJMs + spargers	0.74	38	12[d]	45	3 scfm[e]	--	0.94	0.11	-0.06	0.11	N/M	--	80%	N/M
7	1	PJMs only	1	36	4.9	55	--	--	0.24	0.11	Inc	--	N/M	--	Inc	N/M
7	2	PJMs only	1	36	7.3	45	--	--	0.42	0.085	Inc	--	N/M	--	Inc	N/M
7	3	PJMs + pump	1	36	7.3	45	--	121	0.55	0.06	Inc	--	N/M	--	Inc	N/M
7	4	PJMs + pump	1	36	11.4	45	--	119	1.1	0.01	Inc	--	N/M	--	Inc	N/M
7	5	PJMs + pump + spargers	1	36	11.4	45	3 scfm[e]	122	1.1	0.0058	Inc	--	N/M	--	Inc	N/M
7	6	PJMs + pump + spargers	1	36	11.4	45	3 scfm[e]	121	0.93	0.0067	-0.07	0.12	N/M	--	71%	N/M
11	1	PJMs + pump	0.74	37	7.9	45	--	121	0.66	0.033	Inc	--	N/M	--	Inc	N/M
11	2	PJMs + pump	0.74	37	14.0	45	--	115	0.95	0.0055	Inc	--	N/M	--	Inc	N/M
12	1	PJMs only	0.74	36	8[d]	45	--	--	0.99	0.27	Inc	--	-0.01	0.27	Inc	62%
12	2	PJMs only	0.74	36	12[d]	45	--	--	0.99	0.27	Inc	--	-0.01	0.27	Inc	60%

Table 6.3 (contd)

Seq.	Run	Test Mode	H/D	Yield Stress (Pa)	Peak Avg. Noz. Vel. (m/s)	Cycle Time (sec)	Sparger Flow Rate (per sparge tube)	Pump Flow Rate (gpm)	Fraction Mixed	Error(a) (±)	Mixing Ratio				Mixing Ratio Probability Score(b,c)	
											Dye	Error	Chloride	Error	Dye	Chloride
13	1	PJMs + spargers	0.74	36	8(d)	45	3 scfm(e)	--	0.70	0.31	Inc	--	-0.43	0.45	Inc	4%
13	2	PJMs + spargers	0.74	36	12(d)	45	3 scfm(e)	--	0.88	0.37	Inc	--	-0.14	0.37	Inc	35%
20	1	PJMs only	0.74	35	15.5	45	--	--	0.96	0.0097	-0.04	0.1	-0.43	0.4	91%	2%
20	2	PJMs + pump	0.74	35	15.5	45	--	122	1.0	0.00069	0	0.1	-0.31	0.4	98%	9%
21	1	PJMs only	0.74	36	8(d)	45	--	--	Inc	--	Inc	--	Inc	--	Inc	Inc
21	2	PJMs only	0.74	36	12(d)	45	--	--	0.96	0.13	-0.04	0.13	Inc	--	85%	Inc
21	3	PJMs + pump	0.74	36	12(d)	45	--	120(e)	1.09	0.12	0.08	0.12	-0.47	0.24	67%	0%

(a) Estimated error due to assumption of linear isotherm for dye absorption. Experimental error not included.
(b) Inc = inconsistent results; N/M = not measured.
(c) An average mixing ratio of zero with an error of 0.1 corresponds to a probability score of 68%. Probability scores greater than 68% are considered high confidence while values below 68% are considered lower confidence (see subsection 3.1.2.1); a high confidence (>68% probability score) infers that the system fully mixed the test vessels.
(d) Target velocity; actual velocities were not calculated for this test.
(e) Target flow rate.
(f) Run terminated due to sampling difficulty at given drive conditions.
Note: Test sequences not presented here are those for which no conclusive mixing result was obtained or were used to derive drive functions or check system performance.

Table 6.4. Summary Dye Tracer Visual Observations for LS Optimization Tests

Seq. No.	Run	Test Mode	Peak avg. PJM nozzle velocity (m/s)	No. of spargers, target sparger flow rate (scfm per sparge tube)	No. pump discharge lines, nozzle angle, target flow rate	Summary visual observations
2A	1	PJMs only	8[a]	--	--	No upwelling of dye on surface, but halfway through run dye observed opposite each perimeter PJM along tank wall near bottom.
2A	2	PJMs only	12[a]	--	--	No significant difference from run 1, but zones of dye at tank bottom were larger, ranging in height from 36.5 to 74 inches below tank rim.
2A	3	PJMs + spargers	12[a]	4,3	--	Entire annulus dyed within 1 minute; center zone largely unaffected except for overflow from annulus. Most of tank completely dyed by end of run, except regions with irregular zones of undyed slurry, correlating to areas with no PJMs or sparge tubes nearby. Splash zones of sparge tubes extend inward less than halfway to PJMs.
2A	4	PJMs + spargers	12[a]	8,3	--	Splash zones closer together, creating a continuous bubbling zone along the tank wall, reaching inward two-thirds of the distance to the PJMs
4	1	PJMs only	7.9	--	--	No breakthrough of dye on slurry surface during run. Solid patches of dye observed on tank walls near perimeter PJMs extending 10 to 12 inches above lower tank rim.
4	2	PJMs only	13.4	--	--	No breakthrough of dye on slurry surface. Solid patches of dye observed in run 1 on tank wall reduced in height during run 2 so extended 4 to 6 inches above lower tank rim.
4	3	PJMs + spargers	13.3	4, 3	--	Slurry surface in annulus between perimeter PJMs and tank wall completely dyed in less than a minute. Slurry surface between center and perimeter PJMs largely unaffected except for occasional flow from annulus. Most of tank wall dyed by end of run. A couple of patches of undyed slurry where there were no PJMs or spargers.
4	4	PJMs + spargers	13.2	8, 3	--	Tank surface and walls completely dyed during this run.
5	1	PJMs + pump	8[a]	--	4, 30°, 120 gpm	Dye observed at bottom rim near perimeter PJMs before recirculation pump started. When pump started, dye immediately observed on surface and many places on walls. It took 30 minutes to dye surface between center and perimeter PJMs. Tank walls completely dyed by end of run. Discharge lines produced upwelling plumes less pronounced as slurry filled tank.
5	2	PJMs + pump	12[a]	--	4, 30°, 120 gpm	No flow from two discharge lines opposite each other.
6	1	PJMs only	8[a]	--	--	Run terminated before dye injection; sampling system inoperative at low drive time/high simulant viscosity.
6	2	PJMs only	12[a]	--	--	Dye observed on tank wall up to slurry surface near three adjacent perimeter PJMs; also on surface near three PJMs extending from tank wall to just inside radius described by perimeter PJM centerlines. About 20% of surface covered with dye by end of run. Dye also observed near other PJMs ranging from 3 to 15 inches above lower rim.

Table 6.4 (contd)

Seq. No.	Run	Test mode	Peak avg. PJM nozzle velocity (m/s)	No. of spargers, target sparger flow rate (scfm per sparge tube)	No. pump discharge lines, nozzle angle, target flow rate	Summary Visual Observations
6	3	PJMs + spargers	12[(a)]	4, 3	--	Sparger bubbles appeared soccer ball-shape. Dye on tank walls extended as high as 36 in. above lower rim at several locations around the tank.
6	4	PJMs + spargers	12[(a)]	8, 3	--	No observations of note made.
7	1	PJMs only	4.9	--	--	No dye observed on slurry surface during the run. Patches of dye observed on tank wall near 3 of the 7 perimeter PJMs, extending from 15 to 26 inches above lower rim near two PJMs and almost to the surface near the third PJM.
7	2	PJMs only	7.3	--	--	No dye observed on slurry surface during this run. Patches of dye on tank walls grew in number and size extending from 9 to 47 inches above lower tank rim.
7	3	PJMs + pump	7.3	--	4, 30°, 120 gpm	Dye observed on slurry surface 8 minutes after run began where support beam touched slurry surface during PJM discharge. Dye slowly covered surface during run, about ⅓ covered at end of run. Surface coverage consisted of two large patches on opposite sides of tank. About 80% of tank wall covered with dyed slurry by end of run.
7	4	PJMs + pump	11.4	--	4, 30°, 120 gpm	Surface of slurry completely dyed by end of run. Tank walls uniformly dyed except for two narrow strips of undyed slurry.
7	5	PJMs + pump + sparging	11.4	4, 3	4, 30°, 120 gpm	The spargers produced bubbles the size of soccer balls.
7	6	PJMs + pump + sparging	11.4	8, 3	4, 30°, 120 gpm	With eight spargers the soccer ball sized bubbles were separated by 4- to 8-inch gaps.
8	1	PJMs only	8[(a)]	--	--	Dye appeared on slurry surface between two adjacent perimeter PJMs and tank wall before dye injection complete. It spread during the run so about half the surface was dyed about 40 minutes after completion of dye injection. Surface appeared fully dyed by end of run. Tank walls appeared completely dyed by end of run.
8	2	PJMs only	12[(a)]	--	--	No noteworthy observations made.
9	1	PJMs + pump	8[(a)]	--	1, vertical down, 120 gpm	No dye observed on slurry surface; surface gradually formed crust with 1-inch-high ridges. Broad patches of dye on tank walls 16 to 41 inches above lower rim; patches changed from dyed to undyed and back again in some areas.
9	2	PJMs + pump	12[(a)]	--	1, vertical down, 120 gpm	Dye appeared to break through to surface at end of run forming three patches covering about ¼ of surface; the trend of changing patterns of dyed and undyed areas continued in this run.
9	3	PJMs + pump + spargers	12[(a)]	4, 3	1, vertical down, 120 gpm	Slurry surface uniformly dyed by end of run; tank walls had uniform color. It was hypothesized that when the spargers were turned on a plug of thick slurry was forced against the wall in several places, creating stagnant patches of undyed slurry.

Table 6.4 (contd)

Seq. No.	Run	Test mode	Peak avg. PJM nozzle velocity (m/s)	No. of spargers, target sparger flow rate (scfm per sparge tube)	No. pump discharge lines, nozzle angle, target flow rate	Summary visual observations
10	1	PJMs + pump	8[(a)]	--	1, 30°, 120 gpm	Undyed slurry surfaced during PJM discharge above where pump discharge plume first struck tank wall about 1 min after recirculation pump turned on. More than 90% of slurry surface covered with dye after 9 minutes of pump operation. Surface almost completely dyed by end of run. Dye spread from where the pump discharge line plume struck the tank wall and spread upward and laterally in both directions. By end of run ¾ of tank wall uniformly dyed and the rest mottled with dye.
10	2	PJMs + pump	12[(a)]	--	1, 30°, 120 gpm	Slurry surface and tank wall uniformly dyed by end of run.
11	1	PJMs + pump	7.9	--	2, 30°, 120 gpm	Before starting pump, dye observed at lower rim near four perimeter PJMs. Two areas of upwelling above where pump discharge line plumes first struck tank wall. These plumes formed dyed patches that quickly grew upward and laterally. It was difficult to track dyed slurry on tank wall throughout the entire run and impossible to observe dyed slurry reaching the surface due to insufficient contrast between the dyed and undyed slurry.
11	2	PJMs + pump	14.0	--	2, 30°, 120 gpm	No noteworthy observations were made.
12	1	PJMs only	8[(a)]	--	--	Before dye injection, very slow upwelling occurred during PJM discharge between perimeter PJMs with 135° nozzles and tank wall. Insufficient contrast between dyed and undyed slurry to observe dye breakthrough during this run. It was possible to observe dye on tank wall initially during the run but interpretation questionable. Turbulence observed at tank wall outboard from PJMs with 135° nozzles that extended 25 to 27 inches above lower rim.
12	2	PJMs only	12[(a)]	--	--	Surface appeared less viscous during this run; highly active plumes of upwelling slurry observed above PJMs with 135° nozzles, plumes extending 1 ft from tank wall inward and laterally 3 ft or more each direction lasting 3–5 seconds during each discharge cycle. Turbulence patterns observed in run 1 extended to surface in run 2.
13	1	PJMs + spargers	8[(a)]	4, 3	--	No noteworthy observations made due to insufficient contrast between dyed and undyed slurry. Flow behavior of PJMs with 135° nozzles similar to run 1 in sequence 12. Spargers produced soccer-ball-sized bubbles.
13	2	PJMs + spargers	12[(a)]	4, 3	--	No noteworthy observations made due to insufficient contrast between dyed and undyed slurry. Flow behavior of PJMs with 135° nozzles similar to run 2 in sequence 12. Spargers produced soccer-ball-sized bubbles.
19	1	PJMs only	8[(a)]	--	--	No dye observed on slurry surface during run. After injection, solid patches of dye observed outboard of perimeter PJMs extending 9 to 11 inches above lower rim. Slurry surface between center and perimeter PJMs and between the latter and the tank wall moved up and down at approximately the same rate during PJM cycle.

Table 6.4 (contd)

Seq. No.	Run	Test mode	Peak avg. PJM nozzle velocity (m/s)	No. of spargers, target sparger flow rate (scfm per sparge tube)	No. pump discharge lines, nozzle angle, target flow rate	Summary visual observations
19	2	PJMs only	12[(a)]	--	--	Dye on slurry surface between center and perimeter PJMs about 30 minutes into run. By end of run this zone was dyed, and dye extended to outermost points on four adjacent perimeter PJMs. Approximately ¼ of surface was dyed. Nearly continuous band of dye on the tank wall extended from lower rim upward 9 to 11 inches.
20	1	PJMs + pump	15.5	--	2, 25°, 120 gpm	Dye on surface near perimeter PJM after about 20 min. Eventually, six perimeter PJMs and ⅔ of surface dyed, including half from center to wall and a lobe on opposite side not extending to wall. Solid patches of dye observed on wall near perimeter PJMs within several minutes of injection, extending 5 to 11 inches up. Patches of mottled dye extended to surface; by end of run dye observed on surface near wall.
20	2	PJMs + pump	15.5	--	2, 25°, 120 gpm	Slurry surface uniformly dyed after third PJM discharge cycle of recirculation pump. Dark particles observed where pump discharge line plumes struck tank wall and moved nearly vertically upward, as well as flow where slurry converged and turned down toward bottom, midway between where discharge plumes struck the tank wall.
21	1	PJMs only	14.0	--	--	Dye first noted near perimeter PJMs at lower rim and eventually 3 to 39 inches above lower rim. Dye noted on surface about 5 minutes before end of run in two small spots next to a pump discharge line and on nearest PJM; total coverage negligible.
21	2	PJMs+ pump	12[(a)]	--	2, 25°, 120 gpm	Soon after run started, dye patches along wall near two pump discharge lines broadened and extended upward as high as 30 and 42 inches above lower rim. Dye on surface observed in run 1 expanded to about 5% of slurry surface; a smaller spot appeared at another location between a PJM and the tank wall.
21	3	PJMs + pump	12[(a)]	--	2, 25°, 120 gpm	Dye upwelled to surface four PJM cycles after pump started in two locations consistent with positions where pump discharge line plumes struck wall. Surface completely dyed 12 minutes after starting recirculation pump. Tank wall completely dyed 20 minutes after pump started. Dark particles observed in slurry at two flow convergent points near lower rim about midway between where the pump discharge jets and discharge line plumes struck tank wall.

(a) Target velocity; actual velocity not calculated for this test.

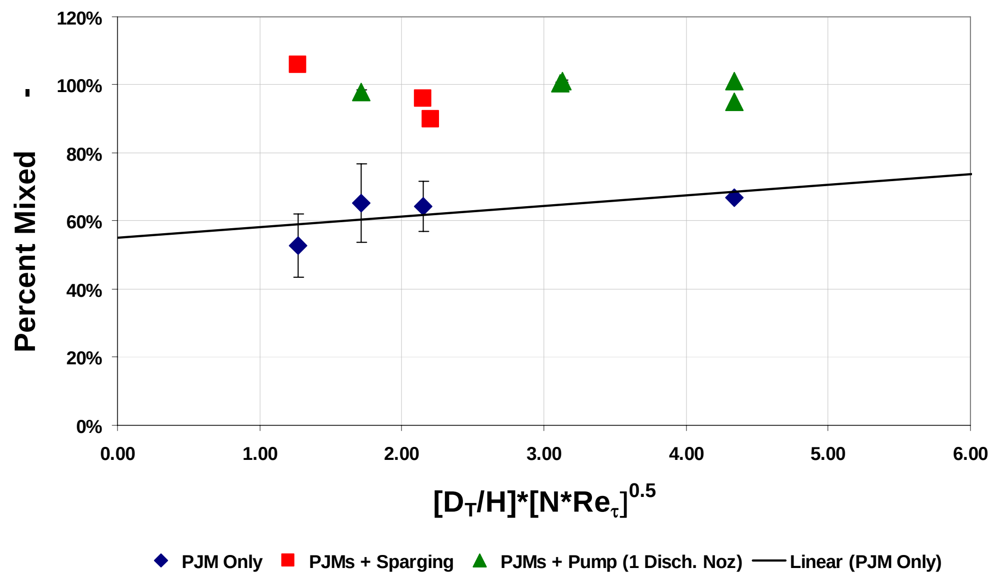

Figure 6.1. Percent Mixed Versus Yield Reynolds Number for UFP Scaled Test Stand During Operating Conditions

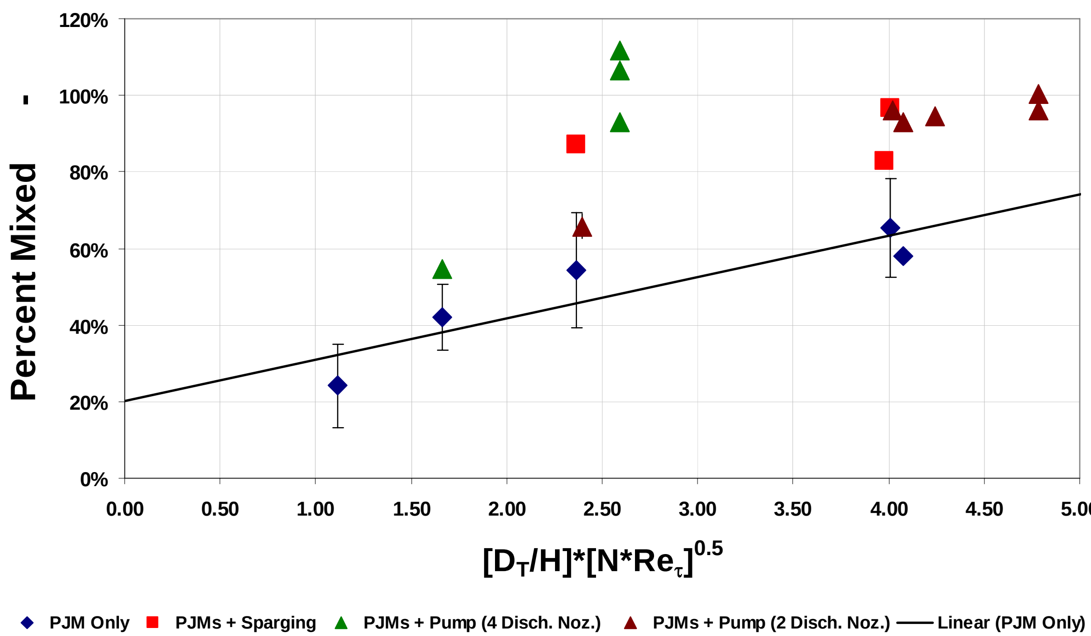

Figure 6.2. Percent Mixed Versus Yield Reynolds Number for LS Scaled Test Stand During Operating Conditions

The data in Figures 6.1 and 6.2 show that, with PJMs only, an increase in the yield Reynolds number results in an increase in the percent mixed. (The yield Reynolds number is the ratio of dynamic stress to slurry strength, which directly affects the size of the mixing cavern. It is considered a dominant nondimensional parameter in hybrid mixing scaling.) This is essentially because the PJM cavern increases with increasing PJM velocity or decreasing yield stress. It is also obvious that PJMs alone are not sufficient to completely mix the tank. The addition of sparging and/or recirculation generally results in complete mixing. When spargers are operating, modest changes in PJM velocity or rheology (yield Reynolds number) have a negligible effect on mixing. Similar observations can be made for the LS scaled test stand.

7.0 PJM/Hybrid System Final Test Configuration Results

This section describes the results obtained with the final test configurations of the UFP and LS scaled test stands. The features described do not necessarily reflect the final plant design configuration.[a] The descriptions of the final test configurations of the UFP and LS scaled test stands, found in Sections 7.1 and 7.2, respectively, are repeated from Section 2 for completeness and ease of duplication.

7.1 UFP Scaled Test Stand

7.1.1 Final Test Configuration

The final PJM test configuration for the UFP scaled test stand was the cluster (5+1) configuration with a Plexiglas shroud enclosing the PJMs, three spargers, and a recirculation system using a single discharge line and a suction line. This configuration was used in sequences 15 and 16; sequence 13 (see Section 6 for results) used a similar configuration with no shroud. The mixing vessel containing the configuration was a clear acrylic Plexiglas tube 34 ± 1 inches in diameter and 90½ ± ½ inches high with the bottom an approximately 2:1 elliptical dish of stainless steel. Top and plan views of the final PJM configuration in the UFP test stand are shown in Figures 7.1 and 7.2. The dimensions are considered approximate.

The cluster (5+1) configuration consisted of six PJMs, one in the center and five equally spaced around the center on a PCD of approximately 14¾ inches. The actual vessel will have six PJMs in a similar configuration. Each PJM consisted of a 6-inch-diameter schedule 40 stainless steel pipe with a cap on the top connected to an air line. A ¼–inch-diameter stainless steel tube was tapped through the end cap on the top (adjacent to the air-line fitting) to serve as a dye injection line; this line extended approximately ⅔ of the length of the pipe forming the PJM body. The lower end of the pipe was attached to a 60° tapered conical section truncated at the bottom and fitted with a 2-inch-diameter schedule 40 stainless steel pipe threaded section where the nozzle assembly was attached. The straight section of the PJM tube was approximately 37 inches long, as shown in Figure 7.2.

The center PJM nozzle assembly, shown in Figure 7.3, consisted of (in order of assembly) a 5½-inch-long, ¾-inch schedule 40 stainless steel pipe connected to a 1 × ¾-inch stainless steel bushing inserted into a 2 × 1-inch stainless steel reducer coupling. The pipe forming the nozzle tip extended 4 15/16 inches out of the bushing, as shown in the figure, and pointed straight down toward the bottom center of the tank. The dimensions shown for the center PJM nozzle in Figure 7.3 are based on direct measurements of the nozzle assembly used in sequence 13. The lowest point of the nozzle tip was raised approximately 1¼ inches off the bottom based on measurements made with a carpenter's rule.

The perimeter PJM nozzle assemblies, also shown in Figure 7.3, used standard schedule 40 stainless steel pipe and fittings consisting of (in order of assembly) a nominal 1½-inch-long, ¾-inch-diameter pipe, a 1 × ¾-inch-diameter bushing, a 1-inch-diameter 45° elbow, a 1-inch-diameter nipple, and a 2 × 1-inch-

(a) Differences between the test configurations and the proposed plant design include minor geometric differences due to the need to use commercially available pipe, the number and size of the sparge tubes, and the lag storage recirculation pump, which is not currently included in the plant design.

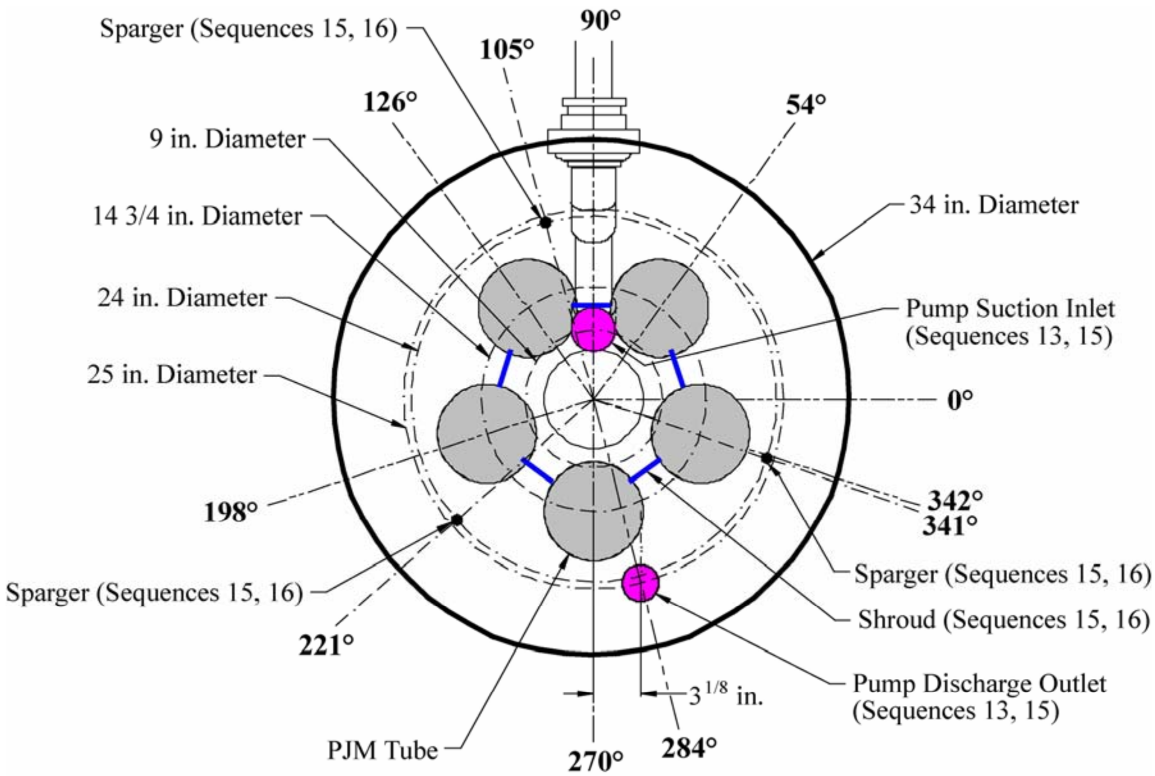

Figure 7.1. Top View of Cluster (5+1) Final Test Configuration in UFP Scaled Test Stand Showing Nominal Locations of PJMs, Spargers, Recirculation System Components

diameter threaded reducer coupling. The pipe forming the nozzle tip extended approximately 1 to 1⅛ inches out of the bushing, as shown, and pointed radially out from the tank centerline at a 45° angle (based on the 45° elbow fitting). The dimensions shown in the figure for the perimeter PJM nozzles are based on measurements of the five nozzle assemblies. The lowest point on the nozzle tip was raised 1¼ inches off the bottom, based on measurements made with a carpenter's rule.

The three spargers used in the final configuration were equally spaced around the tank centerline and approximately 12.5 inches from it, based on measurements of the distance between the center PJM nozzle and the sparger tubes. The approximate angular location of each sparger tube, shown in Figure 7.1, was determined by measuring its location with respect to the positions of three or more of the ¾-inch pipelines supplying air to the PJMs. The orientation was chosen to place one of the sparger tubes on the opposite side of the tank from the recirculation pump discharge line. The sparger tubes were made of ½-inch-OD stainless steel tubing (0.375-inch ID), and +the lower ends were raised 4 inches above the bottom of the tank as measured from the tank floor beneath. This was accomplished by placing the tube on the tank bottom and raising it 4 inches or by placing a tube that was marked 4 inches from its end next to the sparge tube and adjusting the sparge tube level to that mark.

The recirculation system used in the final configuration consisted of two centrifugal pumps placed in parallel and connected in series with a diaphragm pump that served to eliminate cavitation in the centrifugal pumps (see Figure 7.4). The centrifugal pumps fed a manifold that could supply flow to as many as four separate discharge lines. The recirculation pump system was configured to supply flow to a single discharge line in the final configuration and was operated at a target flow rate of 90 ±5 gpm.

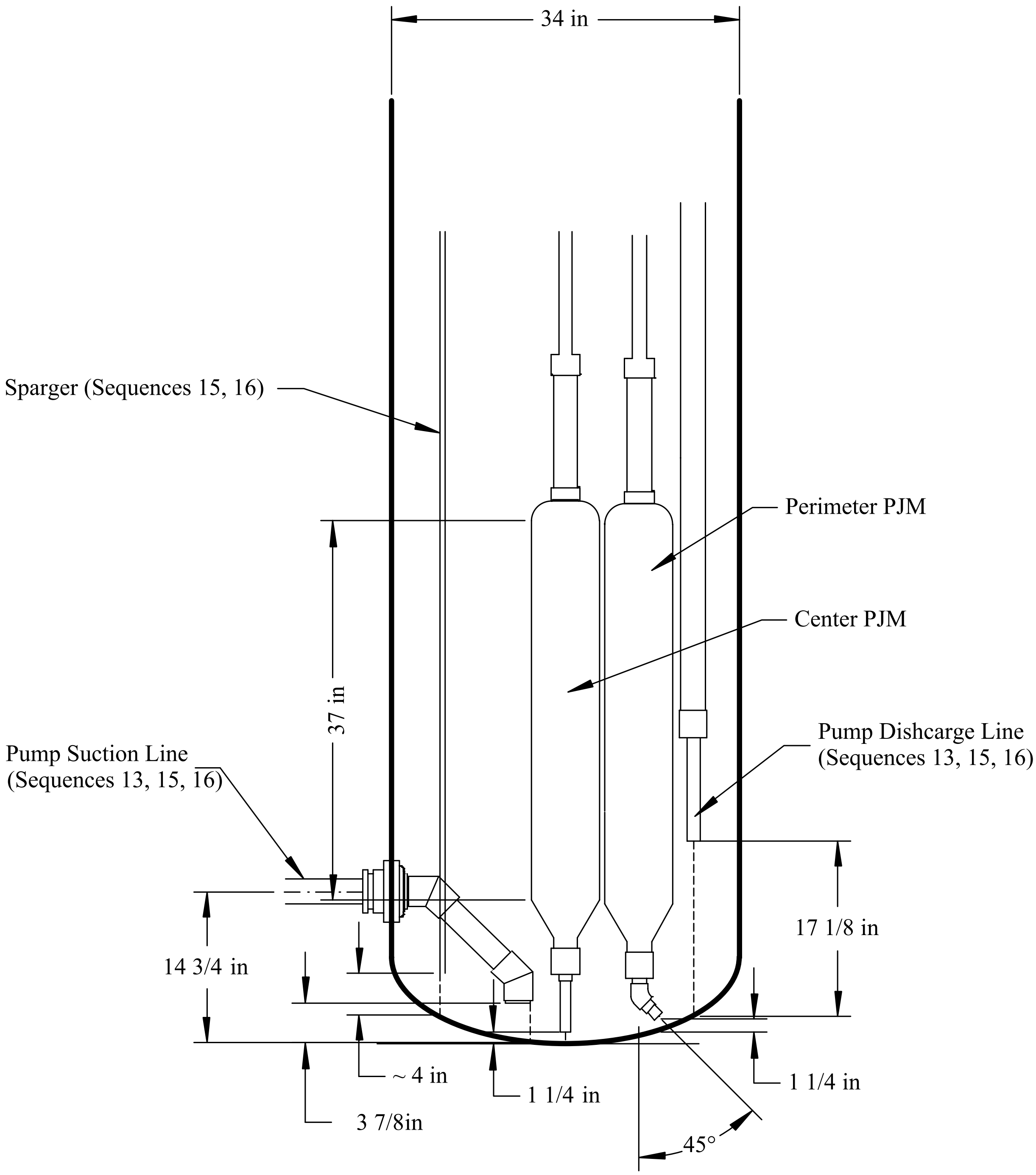

Figure 7.2. Plan View of Cluster Final Test Configuration in UFP Scaled Test Stand Showing Nominal Locations of PJMs, Spargers, and Recirculation System Components

The discharge line was a 2-inch-diameter schedule 40 stainless steel pipe connected to a nozzle assembly with the nozzle pointing straight down. The discharge line was approximately 12½ inches from the tank centerline and offset approximately 3⅛ inches from the PJM that was on the opposite side of the tank from the recirculation pump suction line, as shown in Figure 7.1. This placed it at an angular position of approximately 284°, as shown in the figure.

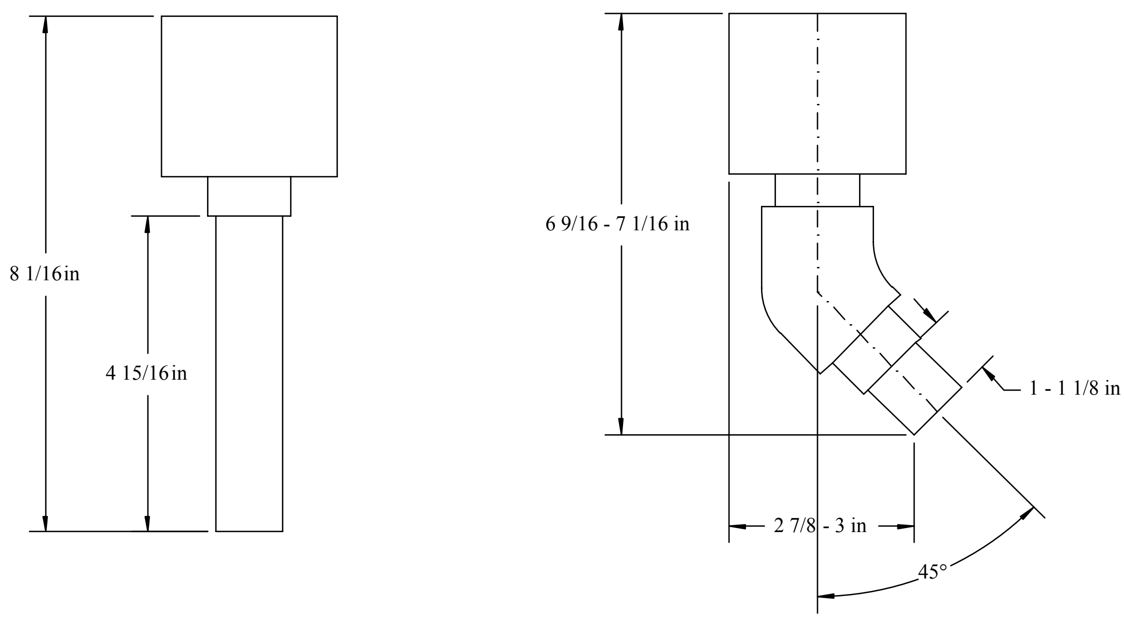

Figure 7.3. Schematic of Center (left) and Perimeter (right) Nozzle Assemblies Used in Final Test Configuration in UFP Scaled Test Stand Showing Range of Dimensions

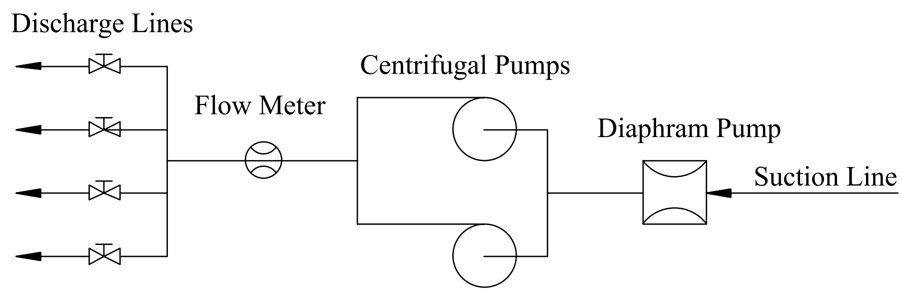

Figure 7.4. Final Test Configuration of Major Recirculation System Components

The nozzle assembly used in the final configuration and shown in Figure 7.5 consisted of a $10^{15}/_{16}$ inch-long, 1-inch-diameter schedule 40 stainless steel pipe bored to 1.107 inches ID and extending $10^{1}/_{16}$ inches out of a 2 × 1-inch-diameter stainless steel reducer coupling. The bottom of the nozzle assembly was raised approximately 17⅛ inches above the tank bottom immediately below the nozzle, as shown in Figure 7.2.

The centerline of the recirculation pump suction line inlet was approximately 4½ inches from the tank centerline at an elevation of approximately 3⅞ inches, as measured from the edge of the inlet closest to the tank centerline to the tank floor (see Figure 7.2). The suction line inlet was pointed down, but the suction line exited the tank through a side port approximately 14¾ inches above the bottom at the tank centerline.

A Plexiglas shroud was placed around the PJM assembly for sequences 15 and 16 to prevent slurry flow into the inner annulus formed between the perimeter and center PJMs. The sides of the shroud were located at the point of closest approach between adjacent perimeter PJMs, as shown in Figure 7.1. The bottom of the shroud was at the bottom of the coupling connecting the conical section to the cylindrical section of the PJM, as shown in Figure 7.6. The bottom of the shroud was a flat Plexiglas plate with holes

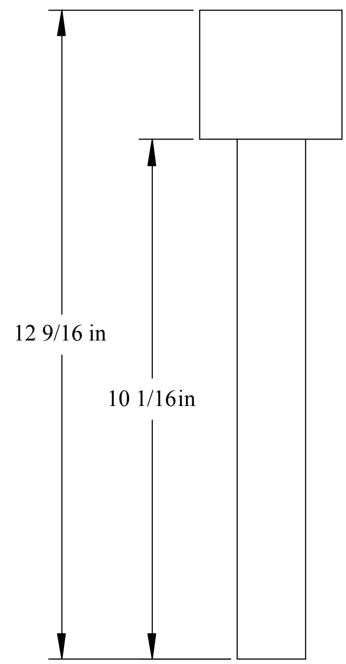

Figure 7.5. Side View of UFP Scaled Test Stand Final Configuration Recirculation Pump Discharge Line Nozzle

Figure 7.6. Side View of UFP Scaled Shroud (left) and Bottom (right)

for the PJM conical sections to pass through (Figure 7.6). The tops of the sides of the shroud extended up to the 2-inch couplings connecting the caps of the PJM to the 2-inch air line shown in Figure 7.7. The top of the shroud consisted of five connected wedge-shaped sections of Plexiglas plate forming a five-sided pyramid, with holes for the center PJM air line and sample lines to the perimeter PJMs. The Plexiglas top formed an angle of approximately 130° with the sides (approximately 40° above horizontal); the slope of the top gradually decreased to approximately 125° with the center PJM air line (approximately 25° below horizontal). The joints where the Plexiglas pieces met the PJM surfaces, piping, or another Plexiglas sections were caulked with silicon sealant. The interior of the shrouded PJM assembly was filled with a rigid polyurethane foam sealant, injected as expandable, polyurethane intermediate and cured over several days to provide rigid support to the shroud.

Figure 7.7. Top View of UFP Scaled Shroud Side (left) and Top (right)

7.1.2 Results with the UFP Scaled Test Stand

The mixing tests, percent mixed, and mixing ratio results for the UFP scaled test stand are summarized in Tables 7.1 and 7.2. All tests were performed with kaolin/bentonite clay simulant, whose yield stress was determined from thoroughly mixed samples (mixed by PJM overblow and sparging) collected before and after a sequence of runs. The yield stress of the kaolin/bentonite clay simulant is the average of results for these samples. H/D is the ratio of simulant height to tank diameter.

The nozzle velocities listed in Tables 7.1 and 7.2 were calculated based on the peak average velocity ($\bar{u}_{peak}$) defined in Eq. 2.2 and Bamberger et al. (2005). The peak average nozzle velocities are based on averages of all the PJMs (four or six for UFP and eight for LS) taken over 25 representative cycles of PJM operation during a run. Actual drive functions for UFP test sequences 15 and 16 are shown in Appendix B. The cycle times listed in Table 7.1 were based on scaling approximately equal to the inverse of the geometric scale factor of 4.94 for the UFP scaled test stand.

For tests using a recirculation pump, the pump flow rates were scaled approximately by the inverse square of the geometric scale factor ($4.94^2 = 24.4$) for the UFP scaled test stand. The recirculation flow rates listed in Tables 7.1 and 7.2 are based on the average flow rate measured over the duration of a run. In calculating recirculation pump averages, startup transients were ignored.

Table 7.1. Test Conditions and Fraction Mixed Results for Final Test Configuration of UFP Test Stand

Seq.	Run	Test Mode	H/D	Yield Stress (Pa)	Peak Avg. Noz. Vel. (m/s)	Cycle Time (sec)	Sparger Flow Rate (per sparge tube)	Pump Flow Rate (gpm)	Fraction Mixed	Mixing Ratio				Mixing Ratio Probability Score[a]	
										Dye	Error	Chloride	Error	Dye	Chloride
15	1	PJM Only	1.4	29	11.9	27	--	--	0.67	Inc	--	Inc	--	Inc	Inc
15	2	PJM + Pump + Spargers	1.4	29	11.6	27	0.08 acfm (2.3 L/m)	84	0.95	0.01	0.11	-0.1	0.26	67%	62%
16	1	PJM + Spargers	1.4	34	11.3	27	2.1 acfm	--	0.90	N/M	--	0.04	0.05	N/M	86%

(a) Inc = inconclusive results; N/M = not measured.

Table 7.2. Summary Dye Tracer Visual Observations for UFP Final Test Configuration

Seq. No.	Run	Test Mode	Peak avg. PJM nozzle velocity (m/s)	No. of spargers, target sparger flow rate per sparge tube (acfm)	No. pump discharge lines, nozzle angle, target flow rate (gpm)	Summary visual observations[(a)]
15	1	Cluster (5+1), PJM Only	11.9	--	--	Dye breakthrough on the surface occurred about 1 hour after dye injection nearly opposite pump suction line and between two adjacent PJMs and tank wall. About 10% of the surface dyed at the end of run. Dye observed on tank wall near perimeter PJM nozzles about 2 to 4 inches above lower rim after dye injection. A patch of dye extended 26 inches above the tank rim near where dye reaches the surface. A second patch extended about 13 inches above lower rim.
15	2	Cluster (5+1), PJM + Pump + Sparging	11.6	3 (perimeter), 0.08	1 vertical, 90	No obvious upwelling of slurry or dye on the surface occurred when the pump was first turned on. It appeared that the slurry surface moved away from the tank wall near the suction line and both directions toward the pump discharge line during PJM suction (about 2½ inches/PJM cycle. Three small splash zones about 1½ to 4 inches in diameter appeared when the spargers were turned on. Two of the splash zones were relatively close together even though the sparger tubes were not. Two of the spargers initially brought both dyed and undyed slurry to the surface. About 80 to 90% of the surface was dyed by the end of the run. The behavior of the dye along the tank wall indicated that flow from the discharge line was moving up the wall near the suction line as well as laterally both directions away from the suction line. The slurry on the surface was moving toward the pump discharge line and down the wall near the discharge line. The tank wall was uniformly dyed by the end of the run.
16	1	Cluster (5+1), PJM + Sparging	11.3	3 (perimeter)	--	Dye observed on tank wall localized near perimeter PJM nozzles about 3 in. above lower tank rim after injection. It took only two PJM cycles to completely cover the surface with dye after the spargers were turned on. Splash zones extended from shroud to tank wall and laterally about 12 to 16 inches, so about ⅓ of the slurry surface was covered by splash zones. Most of tank wall uniformly dyed by end of run, with the remaining wall having a marbled appearance.

(a) The lower rim is the lowest point on the tank wall visible from outside the tank, approximately 80 in. below the upper rim (approximately 10½ inches above the bottom).

For tests that involved sparging, the sparging system layout and air flow rates were determined using the zone of influence performance guidelines developed in Poloski et al. (2005). The sparger air flow rates shown in Tables 7.1 and 7.2 are actual flow rates (acfm) at the bottom of the sparge tube outlet. These values are based on the readout of the rotometers in-line with each sparger with corrections made for pressure, temperature, and pressure head due to simulant depth. Post-calibration of the flow meters indicated the sparger flow rates were accurate within ±15%. The relatively low air flow rate for sequence 15 run 2 represents the spargers in an "idle" mode, in which the air is supplied primarily to keep simulant out of the sparge tubes.

The "fraction mixed" and mixing ratio data presented in Table 7.1 are based on measurements obtained from the tracer chloride injected into the simulant before the start of a test sequence. The approach is discussed in Section 3.1. Isotherm errors using the Cl^- ion tracer are insignificant. Experimental variability due to sampling and analysis is still present.

Core samples were taken in several locations for UFP tests 15 and 16 after the mixing test was complete and all mixing equipment was turned off.[a] Because of the non-Newtonian nature of the simulant, these core samples represent a snapshot of the tracer concentration profile at the conclusion of the mixing test (i.e., the simulant stops moving when the mixers are turned off). Core samples were also taken at the beginning of the test before adding tracer[b] and after the final homogenization step.[c] Core sample locations are depicted schematically in Appendix C for the UFP scaled vessel.

The core samples were separated into 2-inch segments and analyzed for chloride concentration using ion chromatography (IC). Using initial and final tracer concentrations, mixing-ratio calculations and associated error were performed on each segment. The average concentrations of the initial and final core samples were used in the calculation. The average mixing ratio and the probability score for each core segment and associated error were calculated and are shown in Table 7.3. The mixing ratio and associated error for UFP-T15 creates a range of values that includes zero while this is not the case for UFP-T16. The probability scores for UFP-T15 and UFP-T16 are reasonably high, indicating good confidence that the tank contents were reasonably well mixed but not completely homogenous.

Table 7.3. Average Mixing Ratio Values and Probability Scores from Chloride IC Data for Core Samples Taken During Phase II Scaled Test Platform Tests

Test	Core 1	Core 2
UFP-T15	0.03 ± 0.06	-0.01 ± 0.06
UFP-T16	0.05 ± 0.02	0.06 ± 0.02
Probability Score		
UFP-T15	85%	88%
UFP-T16	99%	96%

(a) Core samples taken after mixing tests at locations 1 and 2 are labeled as "Core 1" and "Core 2," respectively.
(b) Core samples taken before adding tracer at locations 1 and 2 are labeled as "Core 1 Initial" and "Core 2 Initial," respectively.
(c) Core samples after final homogenization at locations 1 and 2 are labeled as "Core 1 Final" and "Core 2 Final," respectively.

To assess the tracer uniformity as a function of depth, the mixing-ratio depth profile for the core segments is shown in Figures 7.8 and 7.9. In general, the data indicate that the tracer concentrations fluctuate close to a mixing ratio of zero (fraction mixed of 1) for all core samples. This behavior is characteristic of a fully mobilized system that is in the process of complete homogenization. Because these tracer results do not indicate the presence of stagnant regions, the variation in the data indicates that there are regions of the tank where the mixing process occurs at a slower rate.

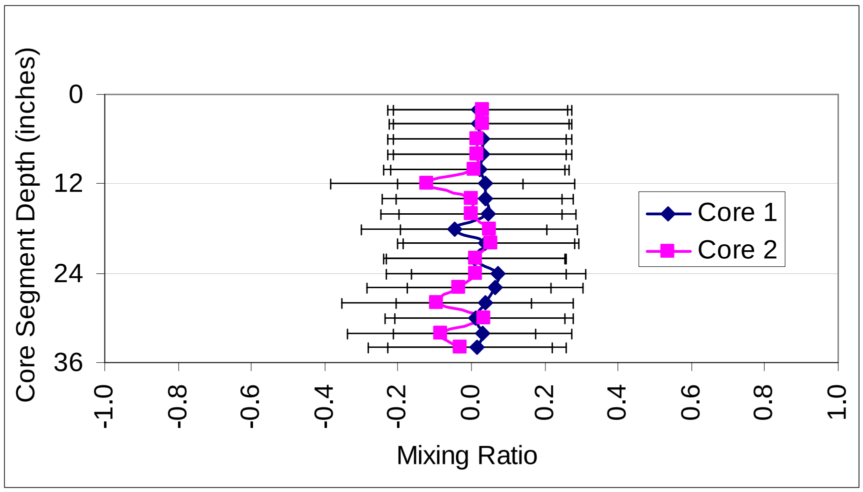

Figure 7.8. Mixing-Ratio Results from UFP Test Sequence 15 Core Samples Using Chloride Tracer

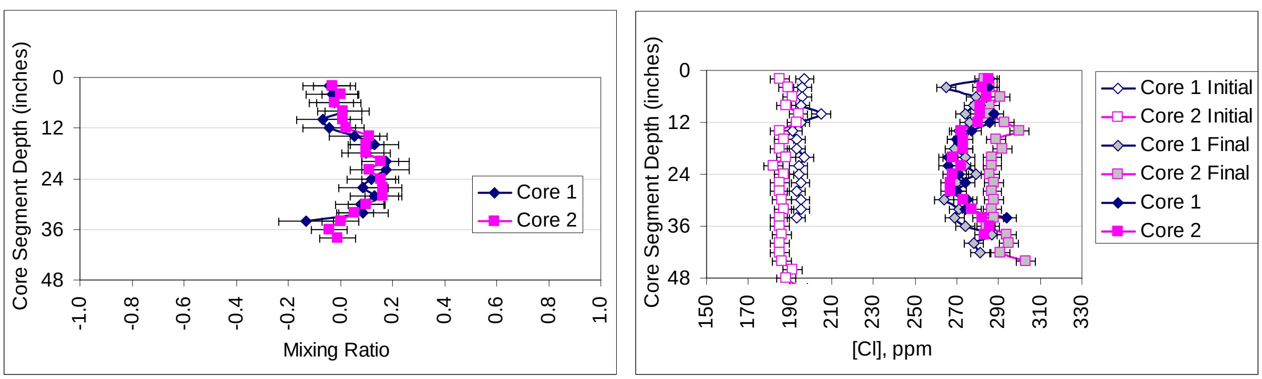

Figure 7.9. Mixing-Ratio Results from UFP Test Sequence 16 Core Samples Using Chloride Tracer (left) and Chloride Concentration as a Function of Depth (right)

Core samples from UFP test 16 show a pattern of slightly decreased tracer concentration in the midsection of each core. Increased tracer concentration is present at the top and bottom of each core. This test consists of PJMs operating with spargers and is consistent with a two-zone mixing model. This situation may occur if the sparging system is creating a relatively large circulation cell, where the tracer injected in the pulse tubes is brought to the surface by the sparger system and then forced back to the bottom along the tank walls. Because of the location of tracer injection, increased tracer concentration would be present along the top, sides, and bottom of the tank. A core sample taken from along the tank wall would have a profile consistent with that observed.

A plot showing the mixing ratio as a function of sampling event is shown in Figure 7.10 for sequence 16 (PJMs with full flow sparging). Samples were taken every 15 minutes after the start of the test. It appears that the tank was well mixed after the first 15 minutes although the tank was probably mixed in a lesser amount of time. Mixing times generally increase with the scale factor, so the time to mix in the full-scale vessel can be estimated as being less than 15 minutes multiplied by the geometric scale factor of 4.94. This provides an estimate of the time to mix in the full scale vessel of <75 minutes. A time to mix for operation with the PJMs and the recirculation pump (sequence 15) is not possible because run 1 (PJMs only) did not result in a mixed vessel and run 2 did not start with an unmixed simulant (refer to Figure A.15 in Appendix A).

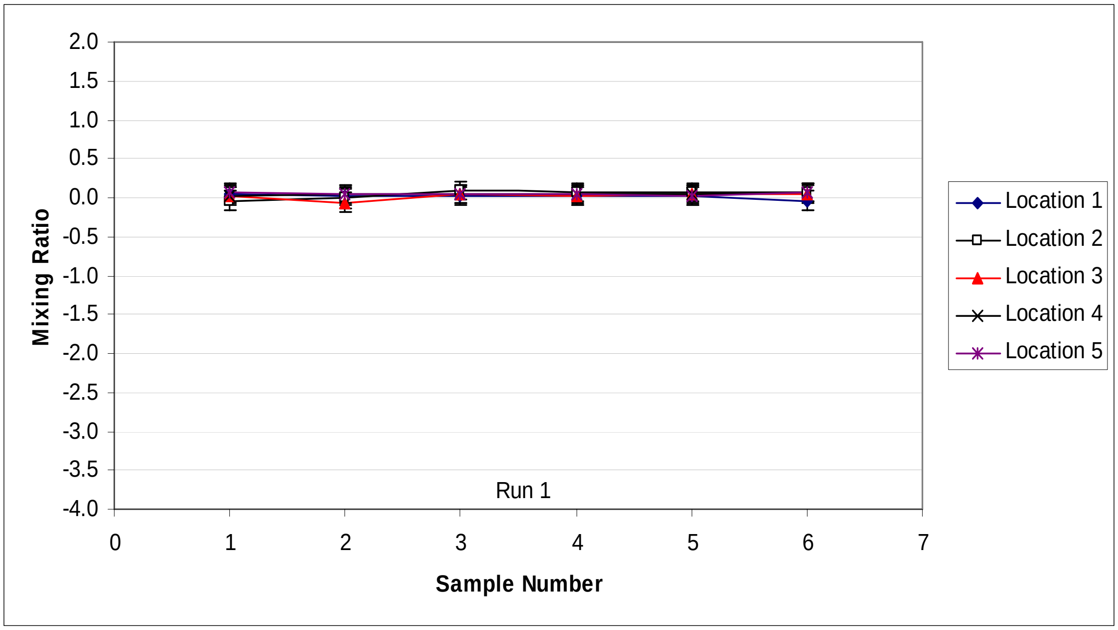

Figure 7.10. Mixing-Ratio Results from UFP Test Sequence 16 Using Chloride Tracer with IC

7.2 LS Scaled Test Stand

7.2.1 Final Test Configuration

The final test PJM configuration for the LS scaled test stand was the cluster (7+1) with a Plexiglas shroud enclosing the PJMs, eight spargers, and a recirculation system with two discharge lines and one suction line. This configuration was used in sequences 26, 27 and 28. Sequence 21 (see Section 6 for results) used a similar configuration with no shroud or spargers. The mixing vessel containing the configuration was a clear acrylic Plexiglas tube 70 ± 1 inches in diameter and 90½ ± ½ inches high with the bottom an approximately 100-6% stainless steel tank cap. Top and plan views of the final PJM configuration in the LS test stand are presented in Figures 7.11 and 7.12. The dimensions are considered approximate.

The cluster (7+1) configuration consisted of eight PJMs, one in the center and seven equally spaced around the center on a PCD of approximately 30 inches. The actual vessel will have eight PJMs in a similar configuration. Each PJM consisted of a 12-inch-diameter schedule 40 stainless steel pipe with a

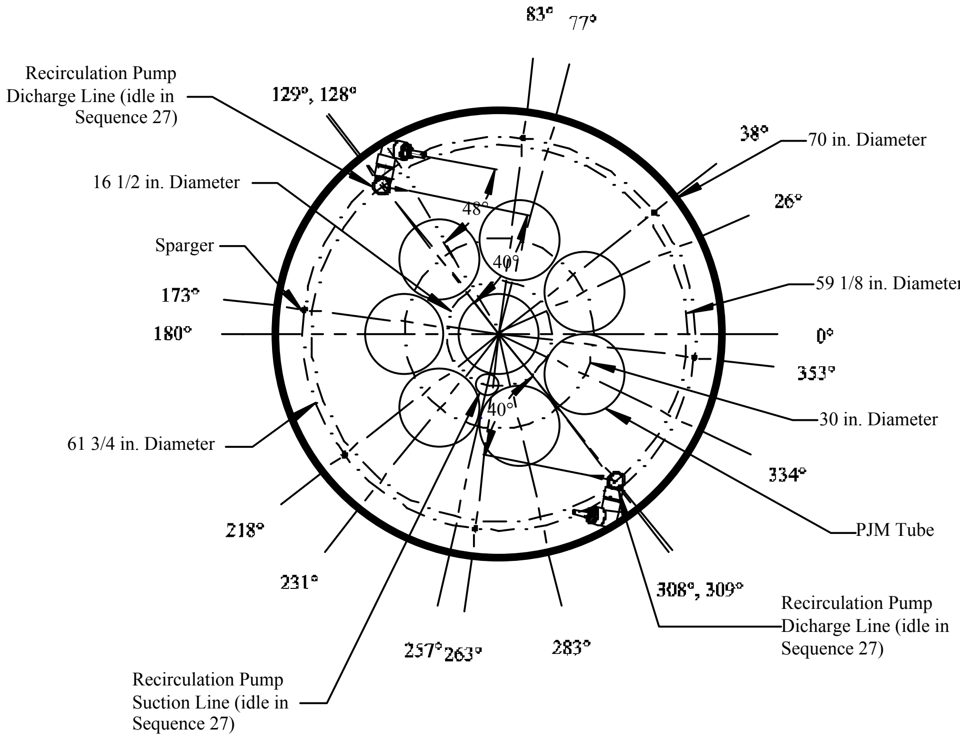

Figure 7.11. Top View of Expanded Cluster Final Test Configuration in LS Scaled Test Stand Showing Nominal Locations of PJMs, Spargers, Recirculation System Components

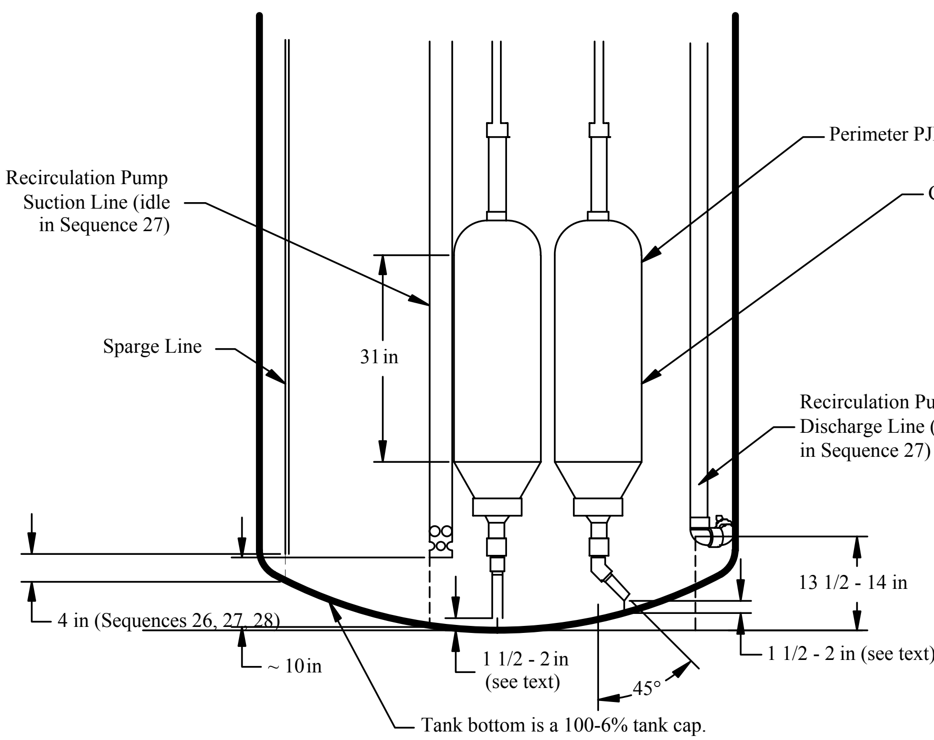

Figure 7.12. Plan View of Expanded Cluster Final Test Configuration in LS Scaled Test Stand Showing Nominal Elevations of PJMs, Spargers, and Recirculation System Components

cap on the top connected to an air line. (The straight section of the PJM tube was approximately 31 ± 1 inches long, as shown in Figure 7.12). A ¼-inch-diameter stainless steel tube was tapped through the end cap on the top (adjacent to the air-line fitting) to serve as a dye injection line; this line extended approximately ⅔ of the length of the pipe forming the PJM body. The bottom of the 12-inch-diameter pipe was welded to a 60° tapered conical section that was truncated at its lower end where it was welded to a 6-inch-diameter schedule 40 stainless steel coupling (7⅜-inch-OD). A second 60° tapered cone was welded to a 6-inch-diameter schedule 40 stainless steel pipe section that was threaded into the 6-inch-diameter coupling. This cone was also truncated at its lower end and welded to a threaded 2-inch-diameter section of schedule 40 stainless steel pipe. A nozzle assembly was threaded onto the bottom of this section.

The center PJM nozzle assembly for the final configuration shown in Figure 7.13 consisted of a 9¾-inch-long, 1-inch-diameter schedule 80 stainless steel pipe inserted into a 2 × 1-inch-diameter stainless steel reducer coupling and extending approximately 9½ inches out of it. The nozzle was pointed straight down toward the bottom center of the tank, as shown in Figure 7.13, and raised approximately 1½ inches above the bottom in sequences 21, 26, 27 and 28, based on direct measurements with a carpenter's rule.

The perimeter PJM nozzle assemblies for the final test configuration (Figure 7.13) consisted of, in order of assembly, a nominal 5-inch-long, 1-inch-diameter schedule 80 PVC pipe, a 1¼ × 1-inch-diameter bushing, a 45° PVC elbow, a 2 × 1¼-inch diameter PVC bushing, and a 2-inch-diameter PVC coupling. The nozzle tips extended 3⅞ to 4⅛ inches out of the bushings, as shown in the figure. Key measurements were made of the seven nozzle assemblies while they were attached to the PJMs. The nozzles were raised approximately 1½ inches above the tank floor, just below the lowest points of the nozzle assemblies, in sequences 21, 26, 27, and 28 based on direct measurements with a carpenter's rule.

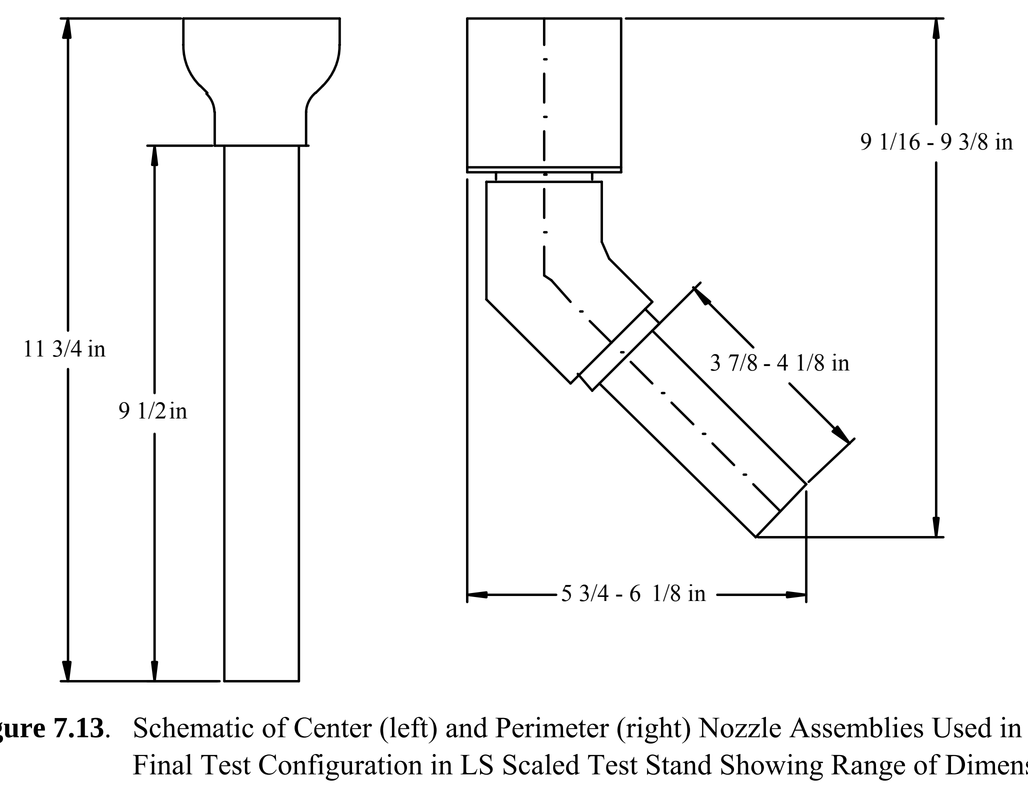

Figure 7.13. Schematic of Center (left) and Perimeter (right) Nozzle Assemblies Used in Final Test Configuration in LS Scaled Test Stand Showing Range of Dimensions

The eight spargers used in the final test configuration were equally distributed around the tank circumference at a PCD of approximately 61¾ inches and were offset clockwise about 7° from the quadrant angles (as shown in Figure 7.11). The sparger tubes were made from ½-inch OD (0.375-in. ID) stainless steel tubing. The lower ends of the sparger tubes were raised approximately 4 inches above the tank bottom in sequences 26, 27 and 28, as indicated in Figure 7.12.

The recirculation system used in the final test configuration of the UFP scaled test stand was also used in the LS scaled test stand. It consisted of two centrifugal pumps placed in parallel and connected in series with a diaphragm pump to eliminate cavitation (Figure 7.4). The centrifugal pumps fed a manifold that could supply flow to four discharge lines. The system was configured to supply flow to a two discharge lines in the final configuration for the LS scaled test stand and operated at a target flow rate of 120 ±5 gpm.

The pump discharge lines were 2-inch-diameter schedule 40 stainless steel pipes, each connected to a nozzle assembly. The discharge lines were at a PCD of approximately 59⅛ inches around the tank center-line and extended 7⅝ inches out of the 1 × ¾-inch-diameter reducer bushings. (Nozzle tips used angles of about 129° and 309°, as shown in Figure 7.11). Each pump discharge nozzle assembly (Figure 7.14) consisted of (in order of assembly) an 8-inch-long, ¾-inch-diameter schedule 40 stainless steel pipe, a nested assembly of 1 × ¾-inch-, 1½ × 1-inch-, and 2 × 1½-inch-diameter PVC bushings, a 2-inch-diameter, 90° PVC elbow, a 2-inch-diameter schedule 80 PVC nipple (with ¼-inch extension), and a second 90° elbow. The nozzle tips in sequence 20 were 4½ and 4 15/16 inches long, bored to 0.80 and 0.81 inches in diameter, and extended 3 13/16 and 4 inches out of the reducer bushings, as shown in the figure. The lateral arms of each nozzle assembly were oriented outward, forming an angle of approximately 40° with the tank centerline, as shown in Figure 7.11, so the nozzle tips were closer to the tank wall than the PJMs and the nozzle jets did not strike the PJM tube walls. The elevation arm of the assembly containing the nozzle tip formed an angle of approximately 48° with the centerline, as shown for one of the nozzles. The nozzle tips pointed approximately 25° above horizontal. The centerlines of the lateral arms of the nozzle assemblies were elevated approximately 13½ to 14 inches above the tank bottom measured at the tank centerline.

The suction line was in a space between the center and two adjacent perimeter PJMs and about 8¼ inches from the tank centerline, based on the calculated distance of the center point in the space from the tank centerline. This position was at an angle of approximately 257°, as shown in Figure 7.11. The suction line was raised approximately 10 inches above the tank bottom immediately below the suction line.

A Plexiglas shroud was placed around the PJM assembly for sequences 26, 27, and 28 to prevent slurry flow into the inner annulus between the perimeter and center PJMs. The bottom of the shroud was a flat Plexiglas plate with holes for the PJM conical sections and recirculation system pump suction line to pass through (Figure 7.15). It was glued to the PJM support frame used to position the bottom of the PJM assembly. The support frame was at the bottom of the coupling connecting the lower and upper conical sections of the PJM. The sides of the shroud were formed by placing insulated foam stripping in the space between adjacent perimeter PJMs (Figure 7.15) and covering it with silicon caulking. Plexiglas was inserted between the upper conical sections of adjacent PJMs and glued to the outside of the PJM support frame (Figure 7.16). The top of the sides of the shroud between perimeter PJMs extended up to the bottom of the 2-inch-diameter couplings connected to the caps of the PJMs with Plexiglas inserts (Figure 7.16).

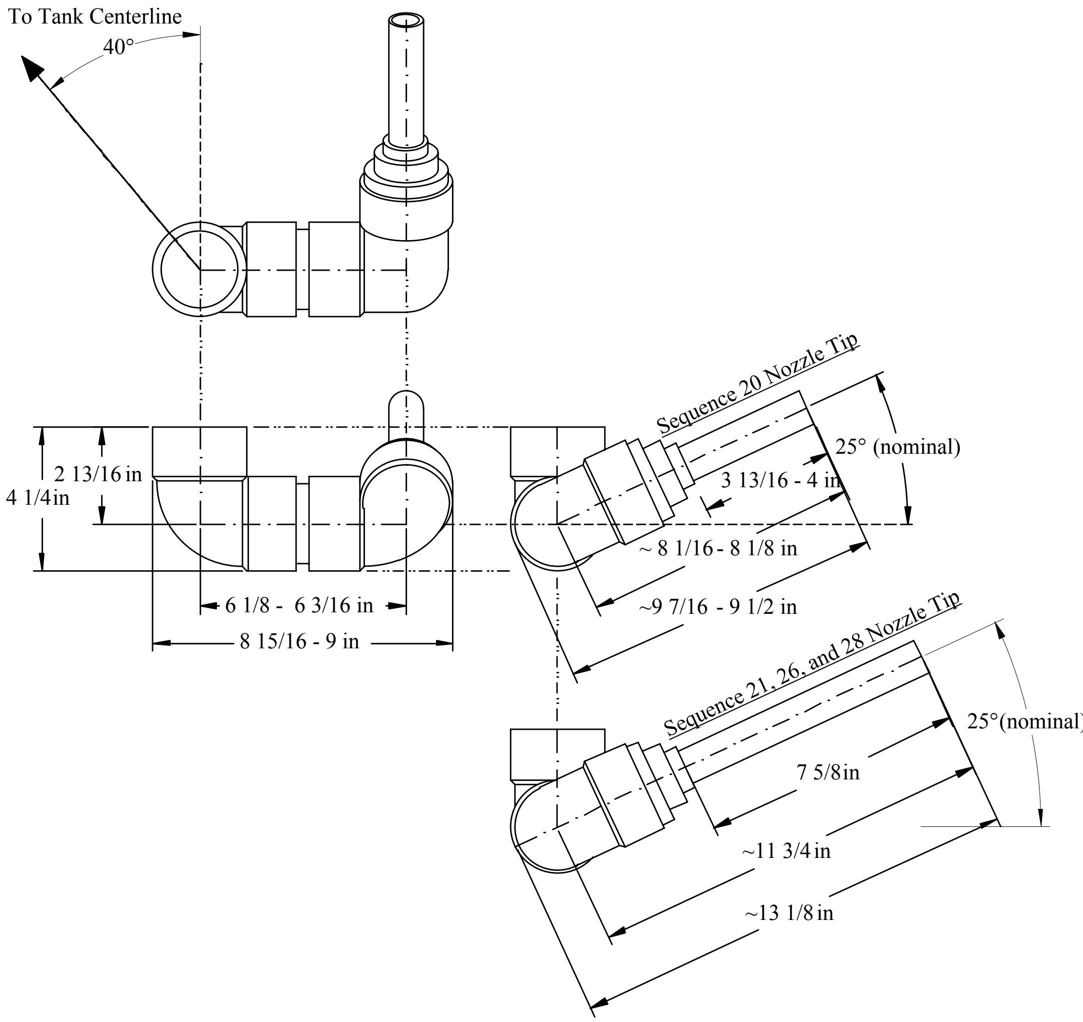

Figure 7.14. Side View of LS Scaled Test Stand Final Test Configuration Recirculation Pump Discharge Line Nozzle Used in Sequences 20 and 21, 26, and 28

The top of the shroud consisted of seven wedge-shaped sections of Plexiglas connected to form a seven-sided pyramid, with holes for the center PJM air line, recirculation system pump suction line, and sample lines to the perimeter PJMs. The Plexiglas top was angled so that its center was approximately 4 inches higher than the top of the perimeter where it met the Plexiglas side inserts. The joints where Plexiglas pieces met PJM surfaces, piping, or other Plexiglas sections were caulked with silicon sealant. The interior of the shrouded PJM assembly was filled with a rigid polyurethane foam sealant, injected as expandable foam polyurethane intermediate and cured for several days to provide rigid support to the shroud.

Figure 7.15. Close-up of LS Scaled Shroud Bottom Prior to Trimming and Caulking (left) and Foam Stripping Between Adjacent Perimeter PJMs (right)

Figure 7.16. Plexiglas Insert Between PJMs near LS Scaled Shroud Bottom (left) and Top View Showing Shroud Top and Plexiglas Insert Between PJMs Near Shroud Top (right)

7.2.2 Results for the LS Scaled Test Stand

The mixing tests, percent mixed, and mixing ratio results for the LS scaled test stand are summarized in Tables 7.4 and 7.5. All tests were performed with kaolin/bentonite clay simulant, whose yield stress was determined from thoroughly mixed samples (mixed by PJM overblow and sparging) collected before and after a sequence of runs. The yield stress of the kaolin/bentonite clay simulant is the average of results for these samples. H/D is the ratio of simulant height to tank diameter.

Nozzle velocities in Table 7.4 were calculated using the peak average velocity ($\bar{u}_{peak}$) defined in Eq. 2.2 and Bamberger et al (2005). Peak average nozzle velocities are averages of all eight PJMs taken over typically 25 representative cycles of PJM operation during a run. Actual drive functions for final LS configuration test sequences 26, 27, and 28 are shown in Appendix B. Cycle times listed in Tables 7.4 and 7.5 for the LS test stand were based on scaling approximately equal to the inverse of the geometric scale factor of 4.29.

For tests using a recirculation pump, the flow rates were scaled approximately by the inverse square of the geometric scale factor ($4.29^2 = 18.0$) for the LS scaled test stand. The recirculation flow rates listed in Tables 7.4 and 7.5 are based on the average flow rate measured over the duration of a run. In calculating recirculation pump averages, startup transients were ignored.

For tests with sparging, the sparging system layout and air flow rates were determined using the zone of influence sparging performance guidelines developed in Poloski et al. (2005). The sparger air flow rates in Tables 7.4 and 7.5 are actual flow rates (acfm) at the bottom of the sparge tube outlet. These values are based on the readout of the rotometers in-line with each sparger with corrections made for pressure, temperature and the pressure head due to the simulant depth. Post-calibration of flow meters indicated sparger flow rates were accurate within ±15%. The "fraction mixed" and the mixing ratio data in the tables are based on measurements obtained from the tracer chloride injected into the simulant before a test sequence started (discussed in Section 3.1 and Poloski et al. 2004b). Isotherm errors using the Cl^- ion tracer are insignificant. Experimental variability exists due to sampling and analysis.

Core samples were taken in several tank locations for LS tests 26, 27, and 28 after the mixing test was complete and all mixing equipment turned off. These core samples are a snapshot of the tracer concentration profile at the end of the mixing test. For LS test 26, core samples were also taken at the beginning of the test before adding tracer and after the final homogenization step. Core sample locations are depicted schematically in Appendix C for the LS vessel prototype.

The core samples were separated into 2-inch segments and analyzed for chloride concentration using IC. Using initial and final tracer concentrations, the mixing-ratio was calculated for each core sample segment. For LS Test 26, the average concentrations of the initial and final core samples were used to calculate the average mixing ratio and associated error. Results are shown in Table 7.6. With the exception of core 2 from LS Tests 27 and 28, every core sample mixing ratio with error creates a range of values containing zero mixing ratio. The average value of core 2 from LS tests 27 and 28 is relatively close to zero but of lower confidence, as indicted by the probability scores. These results indicate that the tank contents were reasonably well mixed but not completely homogenized.

Table 7.4. Test Conditions/Fraction Mixed/Mixing Ratio Results for Final LS Test Configuration

Seq.	Run	Test Mode	H/D	Yield stress (Pa)	Peak avg noz. vel. (m/s)	Cycle time (sec)	Sparger flow rate (per sparge tube)	Pump flow rate (gpm)	Fraction Mixed[(a)]	Mixing Ratio				Mixing Ratio Probability Score	
										Dye	Error	Chloride	Error	Dye	Chloride
26	1	PJMs only	0.74	32	12.2	45	--	--	0.58	-0.16	0.14	Inc	--	12%	Inc[(b)]
26	2	PJMs + pump + spargers	0.74	32	12.2	45	0.9 acfm	118	0.93	Inc	--	-0.07	0.22	Inc	59%
27	1	PJMs + spargers	0.74	33	12.3	45	2.2 acfm	--	0.83	Inc	--	-0.21	0.25	Inc	15%
28	1	PJMs + pump + spargers	0.74	34	12.3	45	0.16 acfm (4.5 L/m)	119	0.96	-0.01	0.28	-0.04	0.24	60%	62%

(a) Appendix A contains a detailed description of these test results.
(b) Inc = inconsistent results.

Table 7.5. Summary Dye Tracer Visual Observations for LS Final Test Configuration

Seq. No.	Run	Test Mode	Peak avg. PJM nozzle velocity (m/s)	No. of spargers, target sparger flow rate (acfm)	No. pump discharge lines, nozzle angle, target flow rate (gpm)	Summary visual observations
26	1	PJMs only	12.2	--	--	No dye observed on slurry surface during this run. Solid patches of dye seen near lower rim outboard of the perimeter PJMs that extended upward 2 to 4 inches Patches of dye that were not solid extended upward 4 to 18 inches except for a patch near a pump discharge line that extended 39 inches upward.
26	2	PJMs + Pump + Spargers	12.2	8, 0.9	2, 25°, 120	The surface was covered with dye within about 2 minutes of sparger startup. When the recirculation pump started, bubbles from a sparger tube near one of the discharge lines were swept to where the discharge line plume and adjacent sparger bubbles were reaching the surface when the PJMs discharged. This did not occur with a sparger near the other discharge line. Most of the tank wall was uniformly dyed in the run. Observations of black slurry particles showed flow patterns similar to those observed in sequence 21.
27	1	PJMs + Spargers	12.3	8, 2.2	--	Solid dye patches were observed outboard of the perimeter PJM following dye injection, extending 3 to 5 inches above the lower rim. The surface was covered with dye within about 2 minutes of starting the spargers. Splash zones extended from the tank wall to about 3 to 4 inches from the PJMs and laterally 12 to 16 inches parallel to the wall. Occasionally adjacent splash zones overlapped. The tank wall was uniformly dyed after about 1 hr of run time.
28	1	PJMs + Pump + Spargers	12.3	4, 0.16	2, 25°, 120	Solid dye patches observed outboard of perimeter PJM following dye injection, extending 3 to 5 inches above lower rim. When spargers started they brought dye to the surface. The splash zones were about 3 to 5 inches in diameter. The dye very slowly expanded over the surface from each sparger covering patches about 18 inches in diameter 4 minutes after starting the spargers. Breakthrough occurred within about 1 minute of starting the recirculation pump. It took four PJM cycles to completely dye the slurry surface after starting the pump. Bubbles from spargers near the pump discharge line broke up and were displaced by 2 to 3 ft discharge line plumes. Bubbles from the other two spargers did not break up and moved only a few inches. The tank wall was uniformly dyed about 75 minutes after starting the pump. Bubbles were observed at the wall in certain locations, suggesting that small bubbles may be formed by the pump discharge line plumes breaking up sparger bubbles.

Table 7.6. Mixing Ratio Values and Probability Scores from Chloride IC Data for Core Samples Taken During Phase II Scaled Test Platform Tests

Test	Core 1	Core 2	Core 3
LS-T26	-0.01 ± 0.05	-0.02 ± 0.05	nm[(a)]
LS-T27	-0.05 ± 0.05	-0.14 ± 0.06	-0.01 ± 0.05
LS-T28	0.00 ± 0.05	-0.08 ± 0.06	nm
Probability Scores			
LS-T26	94%	92%	nm
LS-T27	82%	26%	94%
LS-T28	94%	62%	nm
(a) nm = not measured			

To assess tracer uniformity as a function of depth, the mixing-ratio depth profile for each core segment is shown in Figures 7.17 and 7.18. In general, the data indicate the tracer concentrations fluctuating close to a fraction mixed value of unity for all core samples. This behavior is characteristic of a fully mobilized system in the process of complete homogenization. Because these results do not indicate any stagnant regions, the variation in data indicates that there are regions where mixing occurs at a slower rate.

Additional information on the mixing state of LS Test 27 can be inferred by comparing core sample results (Figures 7.17 and 7.18) with sampling tube results (Figure 7.19). Sampling tube results indicate that locations 1, 2, and 3 have a higher tracer concentration than locations 4 and 5. Locations 1, 2, and 3 are taken directly from the pulse tubes and 4 and 5 from low and high elevations near the sparge tubes. Core sample results are consistent with mixing ratio data from locations 4 and 5 and do not show increased tracer concentration near the bottom of the tank. This observation infers that increased tracer concentration should be present below the 36-inch depth of the core segments and represents the mixing cavern formed by PJM operation. The test consists of PJMs operating with spargers and is consistent with a two-zone mixing model where the bottom of the tank is mixed by PJMs and the upper portion by spargers. As material from the upper portion of the tank is mobilized and introduced into the PJM mixing region, the

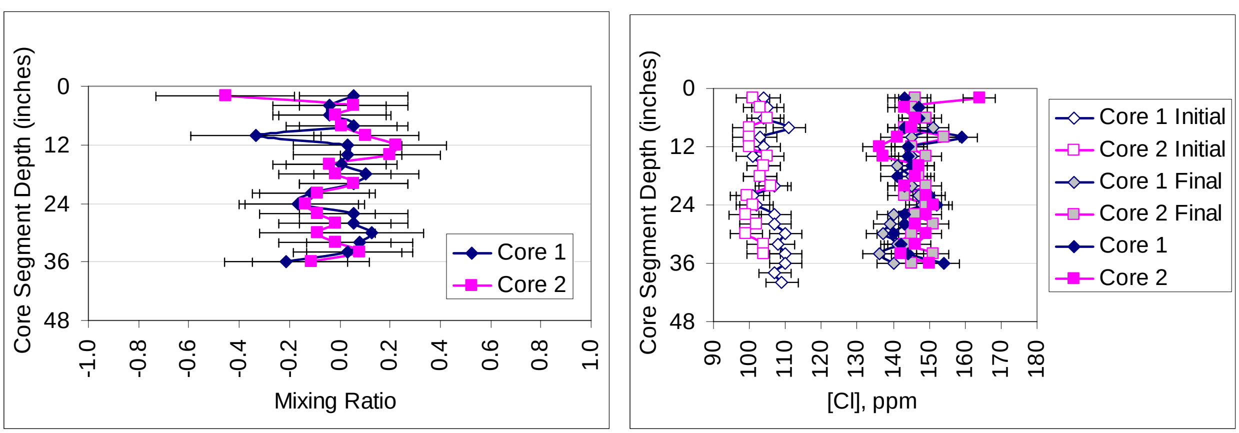

Figure 7.17. Mixing Ratio Results from LS Test Sequence 26 Core Samples with Chloride Tracer (left) and Chloride Concentration as a Function of Depth (right)

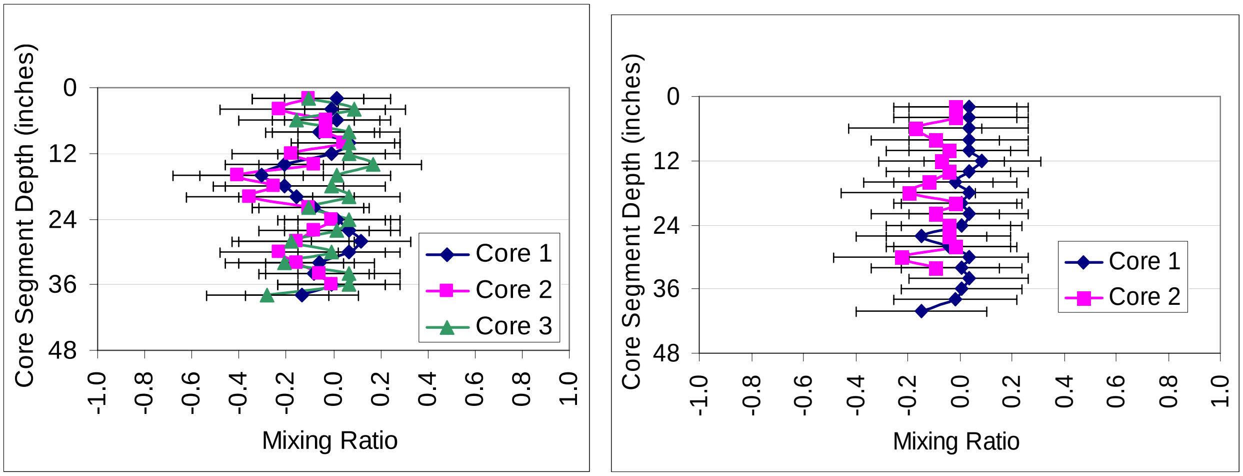

Figure 7.18. Mixing Ratio Results from Sequences 27 (L) and 28 (R) Core Samples with Chloride Tracer

entire tank contents become homogeneous. If the exchange rate between these two zones is small, the homogenization process will take longer to complete. LS Test 27 appears to follow this behavior; the entire tank contents are mobilized but total homogenization occurs at a slower rate than in the other tests.

Figure 7.20 shows the mixing ratio as a function of a sampling event for sequence 28 (PJMs plus the recirculation pump with idle flow sparging). Samples were taken every 15 minutes after the test started. It appears that the tank was well mixed after the first 30 minutes. Mixing times generally increase with the scale factor, so the time to mix in the full-scale vessel can be estimated as being 45 minutes multiplied by the geometric scale factor of 4.29. This provides an estimate of the time to mix in the full scale vessel of about 190 minutes. A time-to-mix estimate for operation with the PJMs and sparging (sequence 27) is not possible because the tracer concentrations were not homogeneous at the end of the run (see Figure 7.19). A time-to-mix estimate for sequence 26 is not possible because run 1 (PJMs only) did not result in a mixed vessel, and run 2 did not start with an unmixed simulant (see Figure A.11 in Appendix A)

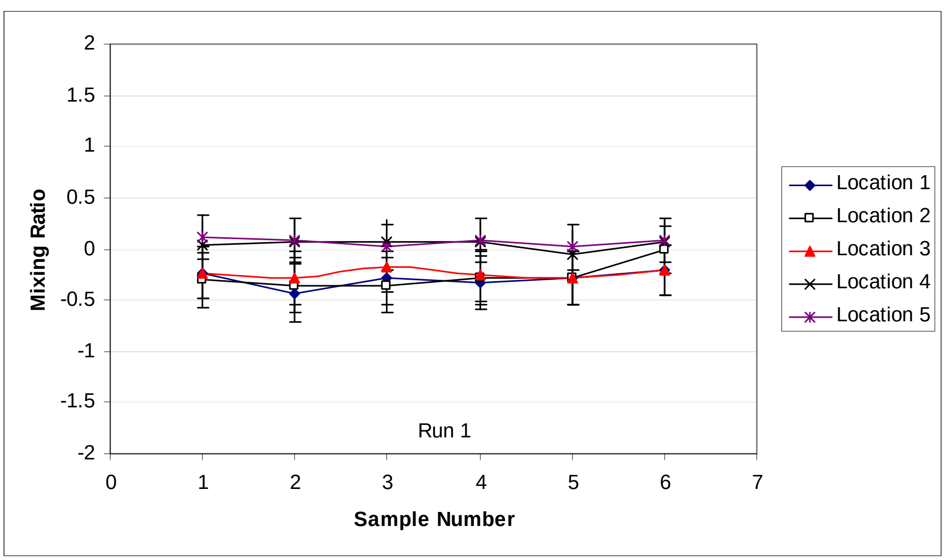

Figure 7.19. Mixing Ratio Results from LS Test Sequence 27 Core Using Chloride Tracer with IC

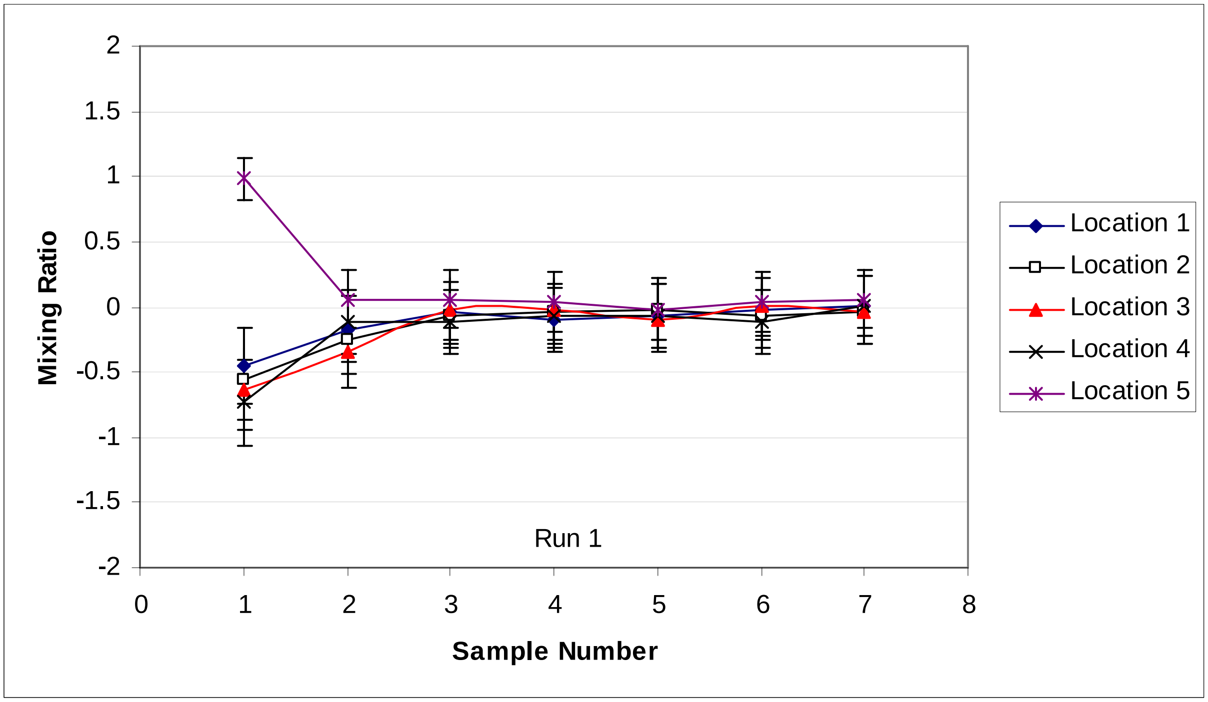

Figure 7.20. Mixing Ratio Results from LS Test Sequence 28 Using Chloride Tracer with IC

8.0 Conclusions

8.1 UFP

Mixing:

- The UFP with the final test configuration involved six (6) PJMs in a central cluster configuration (5+1) plus air sparging or a steady jet generated by a recirculation pump. Two mixing tests were completed with the final configuration; one involved the use of the recirculation pump plus idle-flow sparging and the other involved full-flow sparging without the pump. In both cases the clay simulant H/D was 1.4 and the PJM peak average nozzle velocity ranged from 11.3 to 11.9 m/s. Full mobilization of the simulant was demonstrated with the results of the tracer tests. Visual observation of the dye tracer and analysis of the tracer concentrations from samples indicate that the simulant was mobilized but not completely homogenized. Additional mixing time would have resulted in a homogeneous mixture.
- Based on tracer results for UFP sequence 16 conducted with PJMs and full flow sparging the time to mix was less than 15 minutes as defined by the first sampling event. Mixing times generally increase with the geometric scale factor so the time to mix in the full scale vessel can be estimated as being less than 75 minutes. Determination of a time to mix for operation with the PJMs and the recirculation pump (sequence 15) is not possible because run 1 (PJMs only) did not result in a fully mixed vessel and run 2 did not start with an unmixed simulant.
- The UFP with the final test configuration achieved mixing results approximately equivalent to the trifoil configuration but at a higher peak average drive velocity.

Solids Lift:

- Bead lift tests in the UFP test stand 5 + 1 cluster PJM array and 45° outer-PJM nozzle angle (closest to final test configuration) indicate that the minimum velocity required to lift the beads from the floor was between 6.4 and 7.1 m/s peak average nozzle velocity (solids liftoff tests performed with 4 mm glass beads in water).

Velocity Mapping:

- Velocity mapping in the final UFP configuration at a simulant H/D = 1.4 showed an average cavern height of 16.4 inches (H/D = 0.5) with only PJMs operating. With the PJMs and the recirculation pump operating the cavern height increased to an average of 18 inches (H/D = 0.53). Vertical velocities at the tank wall showed sharp delimitation with elevation, often changing tens of centimeters per second over a 1-inch elevation change. While the velocity mapping did not indicate a large increase in the cavern height, the recirculation pump provided full mobilization (as indicated by the tracer mixing tests) of the simulant, which was not achieved by using only the PJMs. In both tests, the cavern height obtained by velocity mapping underestimates the cavern size determined by tracer mixing tests because of the velocity cutoff of 80 mm/s used to determine the cavern boundary.

8.2 Lag Storage

Mixing:

- The LS final test configuration involved 8 PJMs in a central cluster configuration (7+1) and full-flow sparging (no recirculation pump). The simulant H/D was 0.74, and the peak average nozzle velocity was 12.3 m/s. Full mobilization of the simulant was demonstrated with the results of the tracer tests. Visual observation of the dye tracer and analysis of the tracer concentrations from samples indicate that the simulant was mobilized but not completely homogenized. Additional mixing time would have resulted in a homogenous mixture.
- It appears that there were two mixing regions: the PJM array mixed the bottom zone, and spargers mobilized the upper zone and introduced material from the PJM mixed zone to the air sparged upper zone.
- Based on the chloride tracer results for LS sequence 28 (PJMs plus the recirculation pump with idle flow sparging) the time to mix was 45 minutes. Mixing times generally increase with the scale factor so the time to mix in the full-scale vessel was estimated to be about 190 minutes. A time-to-mix estimate for operation with the PJMs and sparging (sequence 27) is not possible because the tracer concentrations were not homogeneous at the end of the run. A time-to-mix estimate for sequence 26 is not possible because run 1 (PJMs only) did not result in a mixed vessel and run 2 did not start with an unmixed simulant.

Solids Lift:

- For the LS 7+1 cluster PJM array with large-diameter center nozzle and 45° outer PJM nozzle angles (closest to final test configuration), the minimum velocity required to lift the beads from the floor was between 8.3 and 8.7 m/s (peak average nozzle velocity); the 7+1 expanded cluster with outer 23° nozzle angles required a minimum velocity between 9.5 and 10.4 m/s peak average nozzle velocity (solids liftoff tests performed with 4 mm glass beads in water).

Velocity Mapping:

- Velocity mapping in the final LS configuration at a simulant H/D = 1.4 showed an average cavern height of 23.4 inches (H/D = 0.33) with only PJMs operating. The cavern height obtained by velocity mapping underestimates the cavern size determined by tracer mixing tests because of the velocity cutoff of 80 mm/s used to determine the cavern boundary.
- Tank-bottom velocity measurements around the PJM array revealed maximum velocities that ranged from 600 mm/s to over 1250 mm/s.

9.0 References

Atiemo-Obeng VA, P Armenante, and WR Penney. 2003. "Solid Liquid Mixing." *Handbook of Industrial Mixing*, Ch. 10, pp. 543–582. EL Paul, SM Kresta, and VA Atiemo-Obeng (eds). Wiley and Sons, New York.

Bamberger JA, PA Meyer, JR Bontha, CW Enderlin, DA Wilson, AP Poloski, JA Fort, ST Yokuda, HD Smith, F Nigl, M Friedrich, DE Kurath, GL Smith, JM Bates, and MA Gerber. 2005. *Technical Basis for Testing Scaled Pulse Jet Mixing Systems for non-Newtonian Slurries.* WTP-RPT-113 Rev 0, Battelle – Pacific Northwest Division, Richland, Washington.

Bates JM, JW Brothers, JM Alzheimer, DE Wallace, and PA Meyer. 2004. T*est Results for Pulse Jet Mixers in Prototypic Ultrafiltration Feed Process and High-Level Waste Lag Storage Vessels*. WTP-RPT-110 Rev. 0, PNWD-3496. Battelle – Pacific Northwest Division, Richland, Washington.

Brown DAR, PN Jones, and JC Middleton. 2003. "Experimental Methods." *Handbook of Industrial Mixing*, Ch. 4, pp. 145–201. EL Paul, SM Kresta, and VA Atiemo-Obeng (eds.). Wiley and Sons, New York.

Poloski AP, PA Meyer, LK Jagoda, and PR Hrma. 2004a. *Non-Newtonian Slurry Simulant Development and Selection for Pulse Jet Mixer Testing.* WTP-RPT-111 Rev 0 (PNWD-3495), Battelle – Pacific Northwest Division, Richland, Washington.

Poloski AP, LA Snow, and ST Arm. 2004b. *Chemical Tracer Techniques for Assessing Mixing Performance in Non-Newtonian Slurries for WTP Pulsed Jet Mixer Systems.* WTP-RPT-121 Rev 0 (PNWD-3494), Battelle – Pacific Northwest Division, Richland, Washington.

Poloski AP, ST Arm, JA Bamberger, B Barnett, R Brown, BJ Cook, CW Enderlin, MS Fountain, M Friedrich, BG Fritz, RP Mueller, F Nigl, Y Onishi, LA Schienbein, LA Snow, S Tzemos, M White, and JA Vucelik. 2005. *Technical Basis for Scaling of Air Sparging Systems for Mixing in non-Newtonian Slurries*. WTP-RPT-129 Rev 0 (PNWD-3541), Battelle – Pacific Northwest Division, Richland, Washington.

Zwietering TN. 1958. "Suspending of Solid Particles in Liquids." *Chem. Eng. Sci.*, Vol. 8, p. 244.

Appendix A

Dye Method

Appendix A - Dye Method

The concentration of dye [in this case Food Dye Color No. 1, (Brilliant Blue FCF) (BB FCF)] in an aqueous sample was determined through the correlation shown in Figure A.1. This correlation follows Beer's law, which says that the dye concentration is proportional to the optical absorbance value of the dye at the mode wavelength. The mode wavelength for BB FCF is approximately 633 nm. The results are only accurate over a certain region of dye concentration. From visual inspection of Figure A.1, the linear region is present up to an absorbance value of 1.5 (approximately 9 ppm FCD1). When the dye concentration is above this level the sample must be diluted with water and remeasured. The original dye concentration can be calculated by knowing the quantity of water used for the dilution.

Absorption of dye onto the surface of the clay particles can be estimated through a linear approximation. This correlation is shown in Figure A.2, where the dye concentration in the liquid phase is plotted against the dye concentration in the solid phase. Due to batch to batch variations of the clay composition, small differences in the amount of dye absorbed were measured from sample to sample. The linear isotherm assumption allows for the use of Eq. A.1 to calculate percent mixed in a PJM test.

$$X_j = \frac{A_f - A_0}{A_j - A_0} \tag{A.1}$$

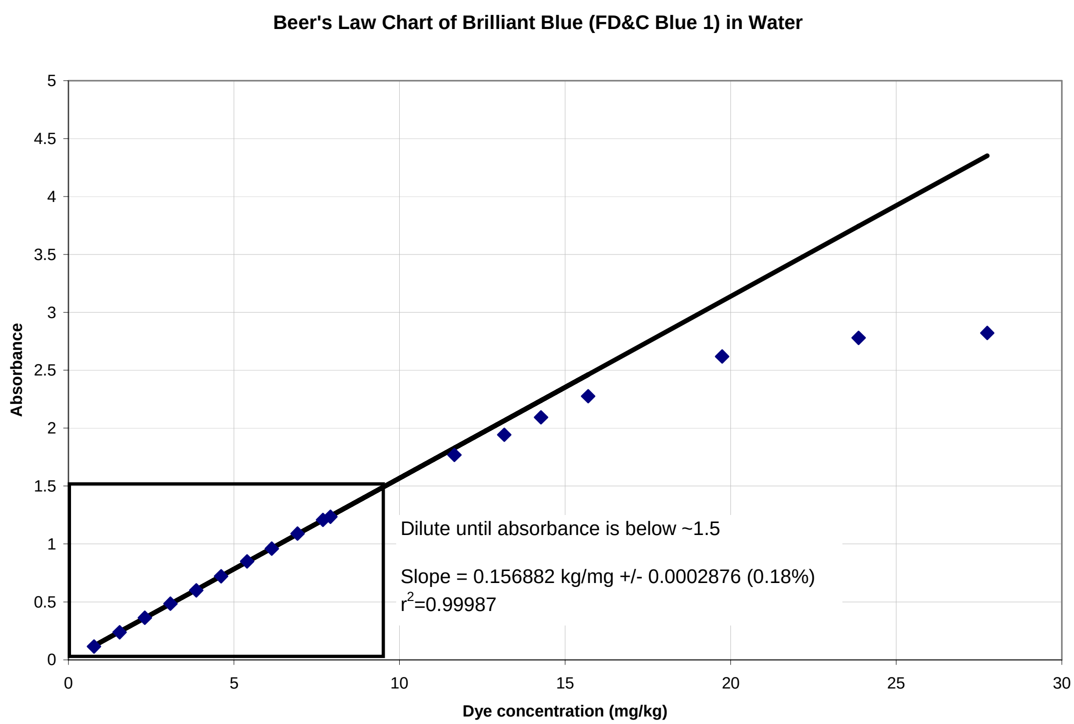

Figure A.1. Beer's Law Correlation of Optical Absorbance to BB FCF Dye Concentration in Water

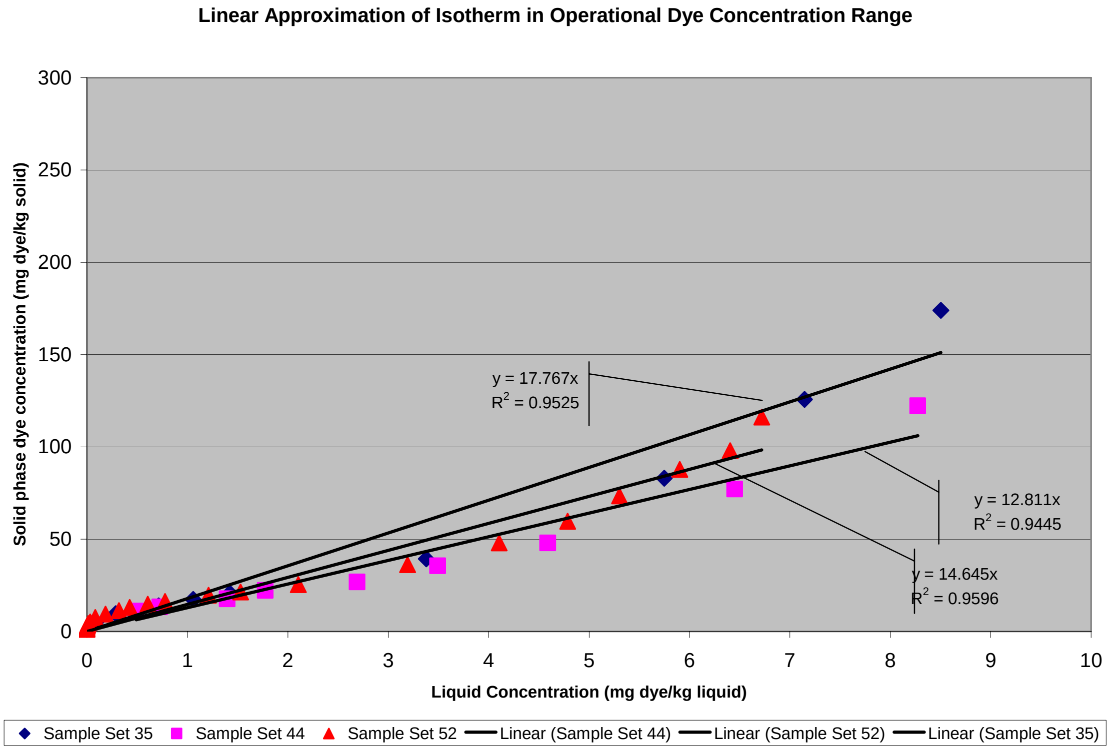

Figure A.2. Linear Fit of Isotherm Data over the Linear Beer's Law Region

where

X_j is the fraction mixed of the j-th tank sample
A_f is the optical absorbance of the final homogenized simulant
A_0 is the optical absorbance of the initial baseline simulant
A_j is the optical absorbance of the j-th tank sample

A polynomial fit to one of the isotherm data sets is shown in Figure A.3. This fit allows the error incurred through the assumption of a linear isotherm to be estimated by calculating the difference in the percent mixed between Eq. (A.1) and (A.2). To perform this calculation, the correlation shown in Figure A.3 is used to calculate the K_d values of each sample in the calculation. A conservative estimation of the solids loading in each sample is assumed at 30 wt% solids 70 wt% liquid.

$$X_j = \frac{Y_l\left(A_f - A_o\right) + Y_s\left(K_{df}A_f - K_{do}A_o\right)}{Y_l\left(A_j - A_o\right) + Y_s\left(K_{dj}A_j - K_{do}A_o\right)} \tag{A.2}$$

where

K_{df} is the distribution coefficient at the homogenized tank tracer concentration
K_{do} is the distribution coefficient at the initial baseline tracer concentration
K_{dj} is the distribution coefficient at the j-th tank sample tracer concentration

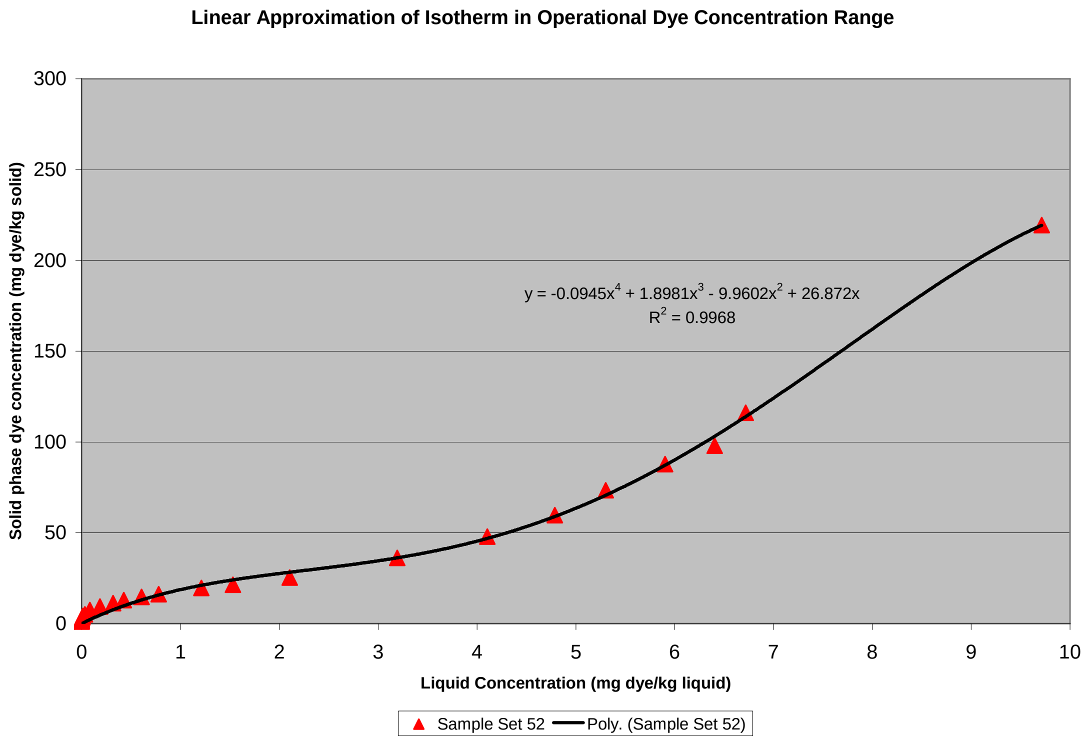

Figure A.3. Polynomial Fit of Isotherm Data over the Linear Beer's Law Region

During scaled stand testing, Eq. (A.1) was used to calculate a fraction mixed for each sample at each sample location. These samples were drawn from different locations in the testing vessel. Sample locations 1, 2, and 3 are from separate pulse tubes and represent the composition of the mixing cavern (see Section 1.4.6). Locations 4 and 5 were near the tank wall at low and high elevations, respectively. During the first run of a test sequence, samples from locations 1, 4, and 5 were taken approximately every 10 minutes after completion of dye injection. After 50 minutes of operation, samples were drawn from all sample locations and the next run experimental condition employed. During subsequent run conditions, samples from locations 1, 4, and 5 were taken every 15 minutes. After 45–90 minutes of operation, samples were drawn from all sample locations and the next run experimental condition employed. The fraction of the tank mixed as calculated from each sample is shown in Figures A.4 through A.7 for LS test sequences 4, 7, 11, and 20, respectively. Figures A.8 and A.9 show the fraction mixed results for UFP test sequences 2 and 3B.

The final fraction mixed value was determined as the minimum fraction mixed from locations 1, 2, and 3 of the last sample test run. This represents the fraction mixed value associated with highest dye concentration in the cavern after approximately 45–50 minutes of operation. As discussed above, the error associated with the linear isotherm approximation is estimated using Eq. (A.3). In the worst case, typical errors due to this assumption are less than approximately ± 0.15 fraction mixed; the error goes to zero as the fraction mixed approaches unity. The final fraction of the tank mixed calculated from each run is shown in Tables A.1 through A.4 for LS test sequences 4, 7, 11, and 20, respectively. Tables A.5 and A.6 show the fraction mixed results for UFP test sequences 2 and 3B.

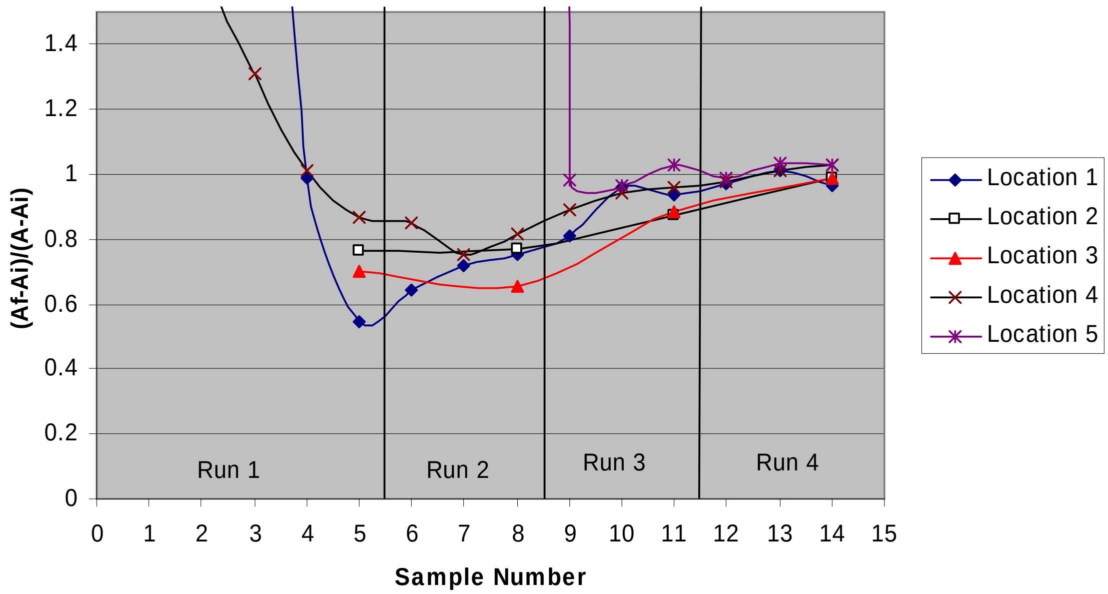

Figure A.4. Fraction Mixed Chart for LS Test Sequence 4

Table A.1. Final Fraction Mixed and Error Estimate Due to Linear Isotherm Assumption for LS Test Sequence 4

Run	Fraction Mixed	Linear Isotherm Estimated Error (±)[(a)]
1	0.54	0.15
2	0.65	0.13
3	0.87	0.052
4	0.97	0.014
(a) Estimated error due to assumption of linear isotherm for dye absorption. Experimental error not included.		

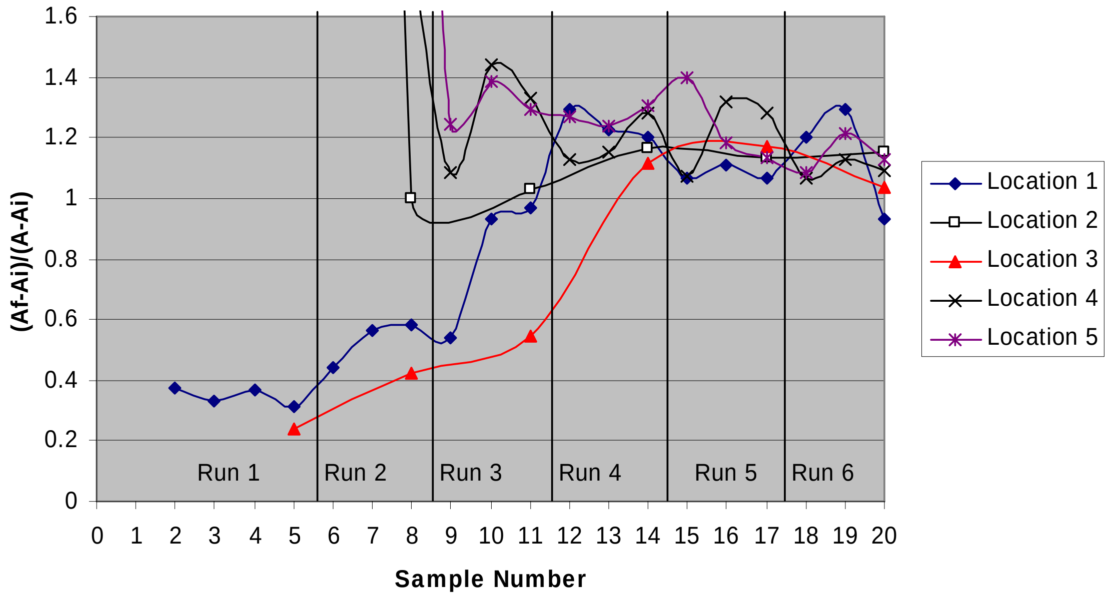

Figure A.5. Fraction Mixed Chart for LS Test Sequence 7

Table A.2. Final Fraction Mixed and Error Estimate Due to Linear Isotherm Assumption for LS Test Sequence 7

Run	Fraction Mixed	Linear Isotherm Estimated Error (±) [(a)]
1	0.24	0.11
2	0.42	0.085
3	0.55	0.060
4	1.1	0.010
5	1.1	0.0058
6	0.93	0.0067

(a) Estimated error due to assumption of linear isotherm for dye absorption. Experimental error not included.

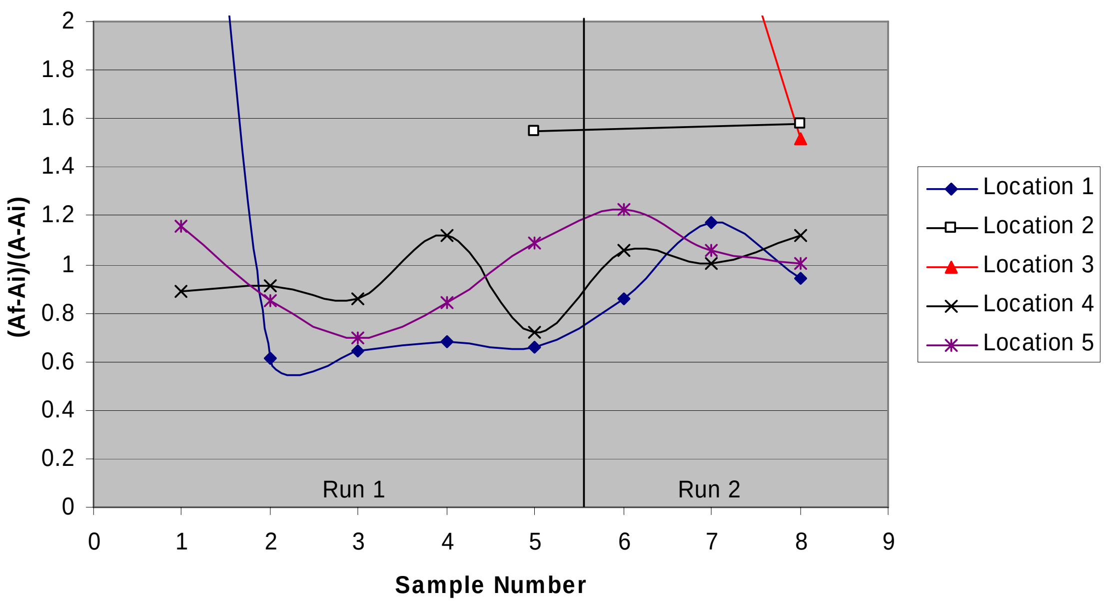

Figure A.6. Fraction Mixed Chart for LS Test Sequence 11

Table A.3. Final Fraction Mixed and Error Estimate Due to Linear Isotherm Assumption for LS Test Sequence 11

Run	Fraction Mixed	Linear Isotherm Estimated Error (±)[(a)]
1	0.66	0.033
2	0.95	0.0055
(a) Estimated error due to assumption of linear isotherm for dye absorption. Experimental error not included.		

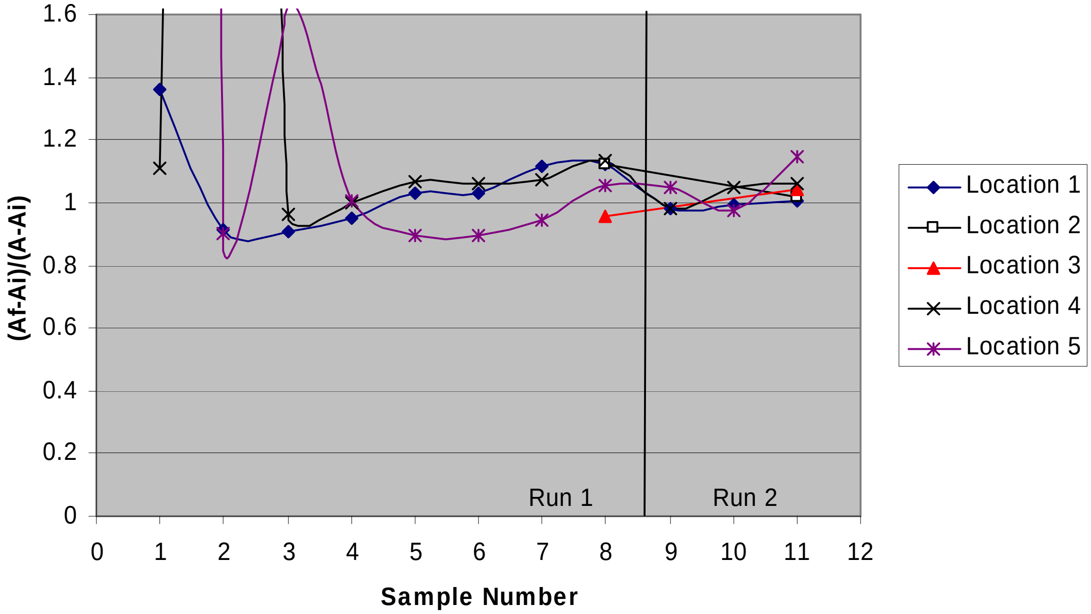

Figure A.7. Fraction Mixed Chart for LS Test Sequence 20

Table A.4. Final Fraction Mixed and Error Estimate Due to Linear Isotherm Assumption for LS Test Sequence 20

Run	Fraction Mixed	Linear Isotherm Estimated Error (±)[(a)]
1	0.96	0.0097
2	1.0	0.00069
(a) Estimated error due to assumption of linear isotherm for dye absorption. Experimental error not included.		

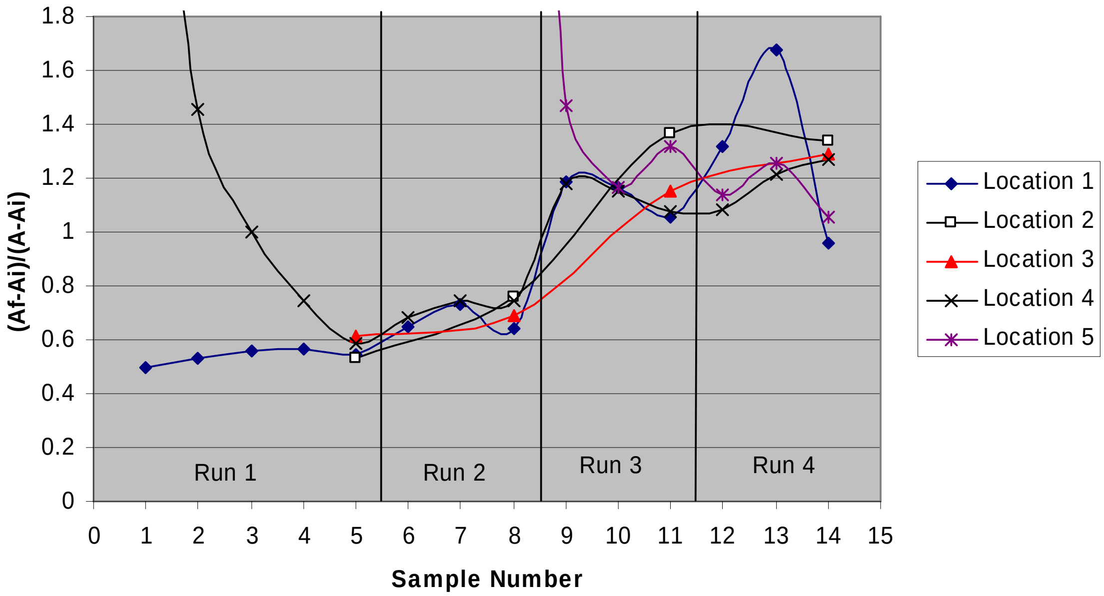

Figure A.8. Fraction Mixed Chart for UFP Test Sequence 2

Table A.5. Final Fraction Mixed and Error Estimate Due to Linear Isotherm Assumption for UFP Test Sequence 2

Run	Fraction Mixed	Linear Isotherm Estimated Error (±)(a)
1	0.53	0.093
2	0.64	0.074
3	1.1	0.013
4	0.96	0.0088
(a) Estimated error due to assumption of linear isotherm for dye absorption. Experimental error not included.		

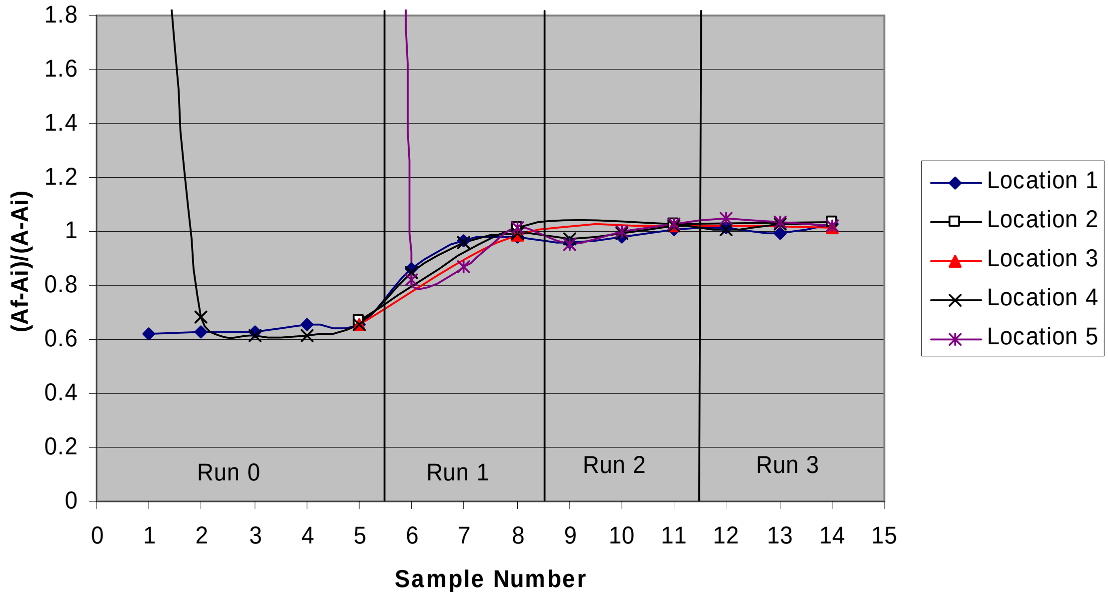

Figure A.9. Fraction Mixed Chart for UFP Test Sequence 3B

Table A.6. Final Fraction Mixed and Error Estimate Due to Linear Isotherm Assumption for UFP Test Sequence 3B

Run	Fraction Mixed	Linear Isotherm Estimated Error (±) [(a)]
1	0.65	0.12
2	0.98	0.0074
3	1.0	0.0019
4	1.0	0.0038

(a) Estimated error due to assumption of linear isotherm for dye absorption. Experimental error not included.

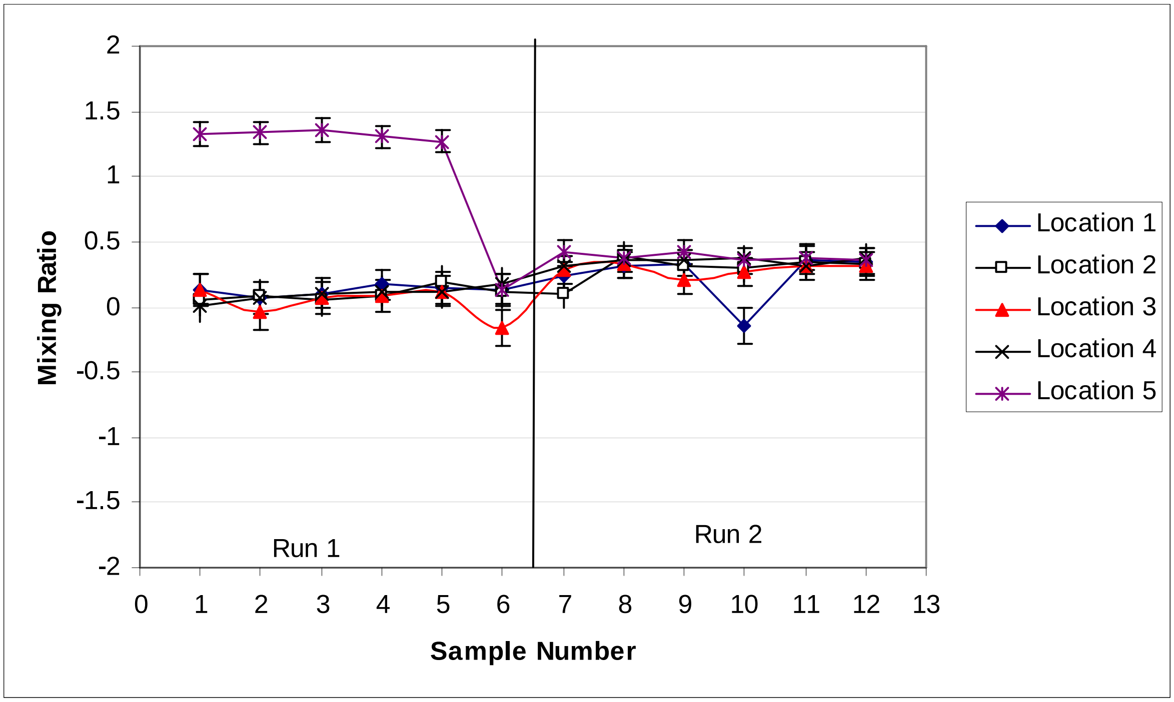

Figure A.10. Mixing Ratio Results from LS Test Sequence 26 Using BB Tracer

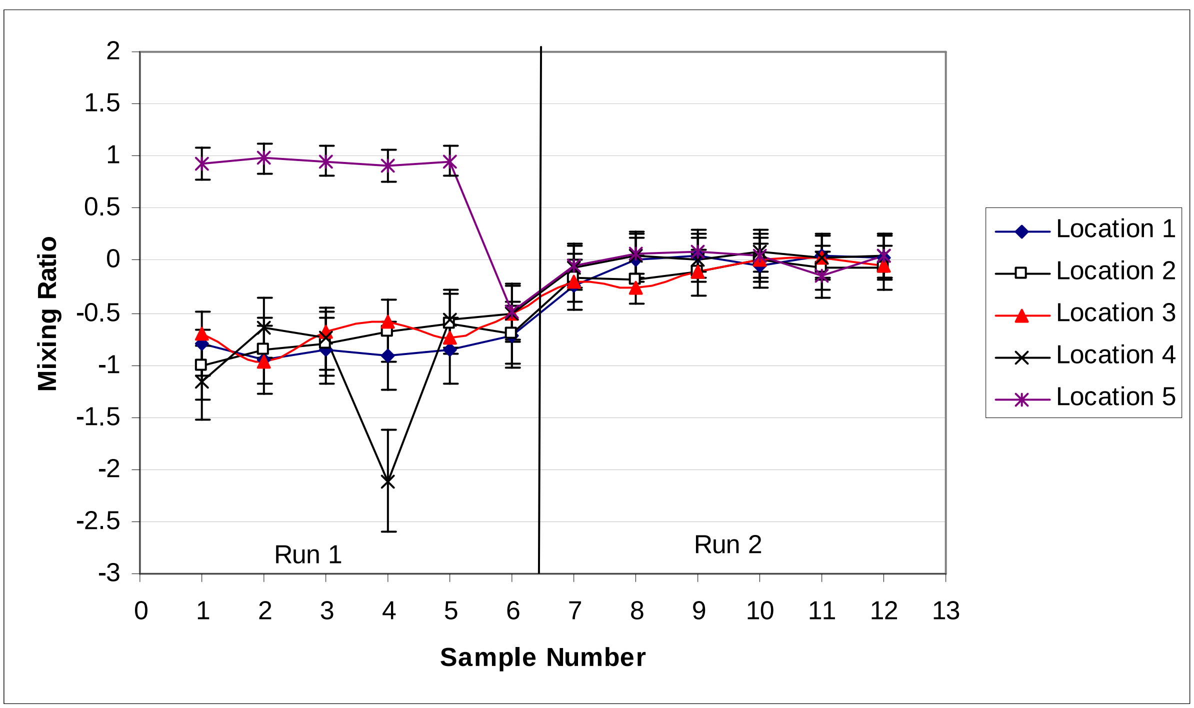

Figure A.11. Mixing Ratio Results from LS Test Sequence 26 Using Chloride Tracer with IC

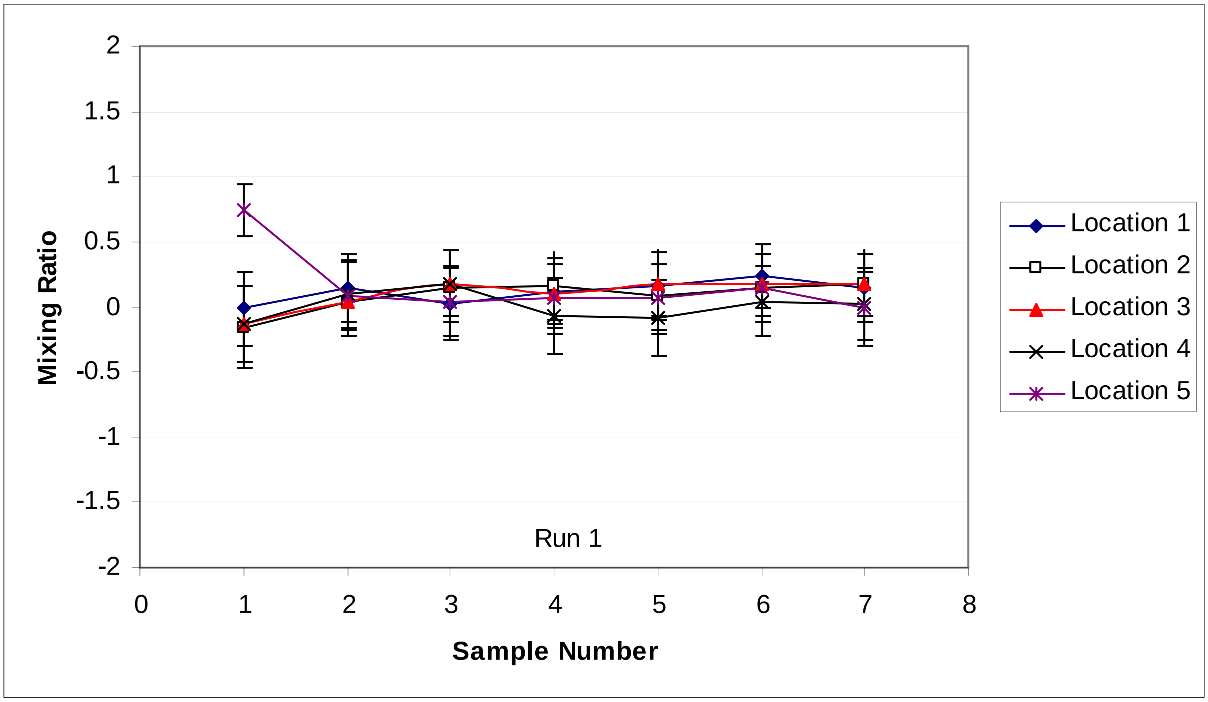

Figure A.12. Mixing Ratio Results from LS Test Sequence 28 Using BB Tracer

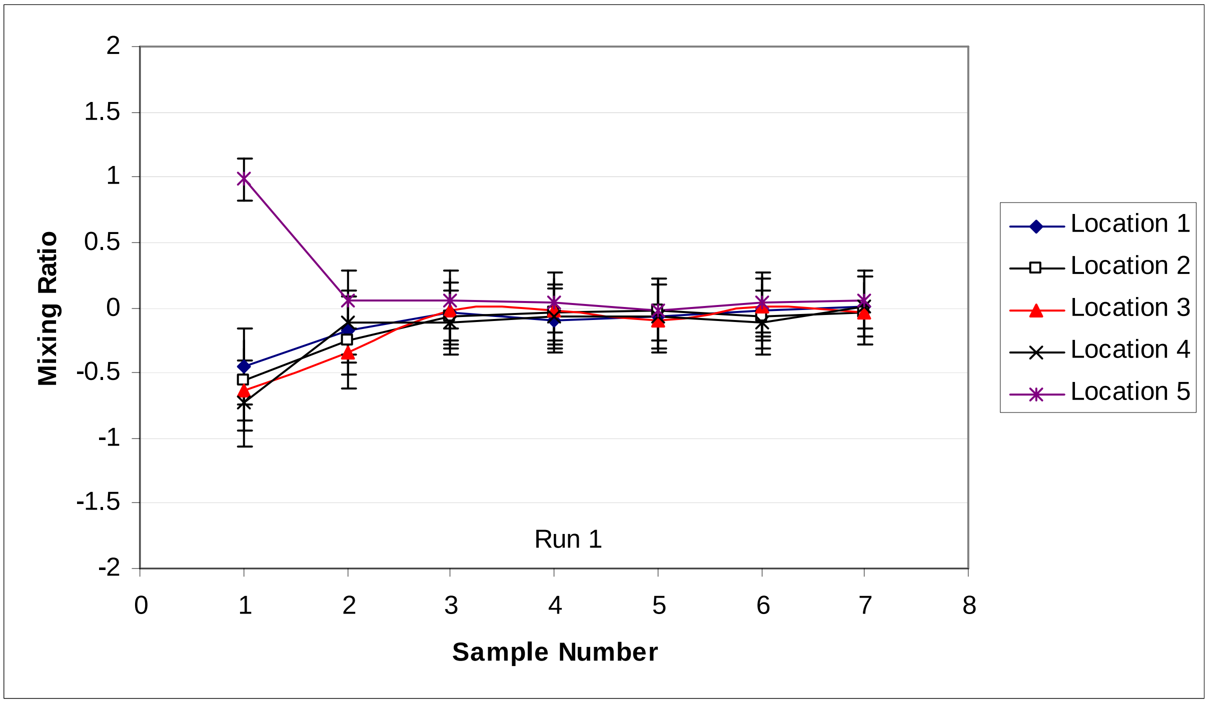

Figure A.13. Mixing Ratio Results from LS Test Sequence 28 Using Chloride Tracer with IC

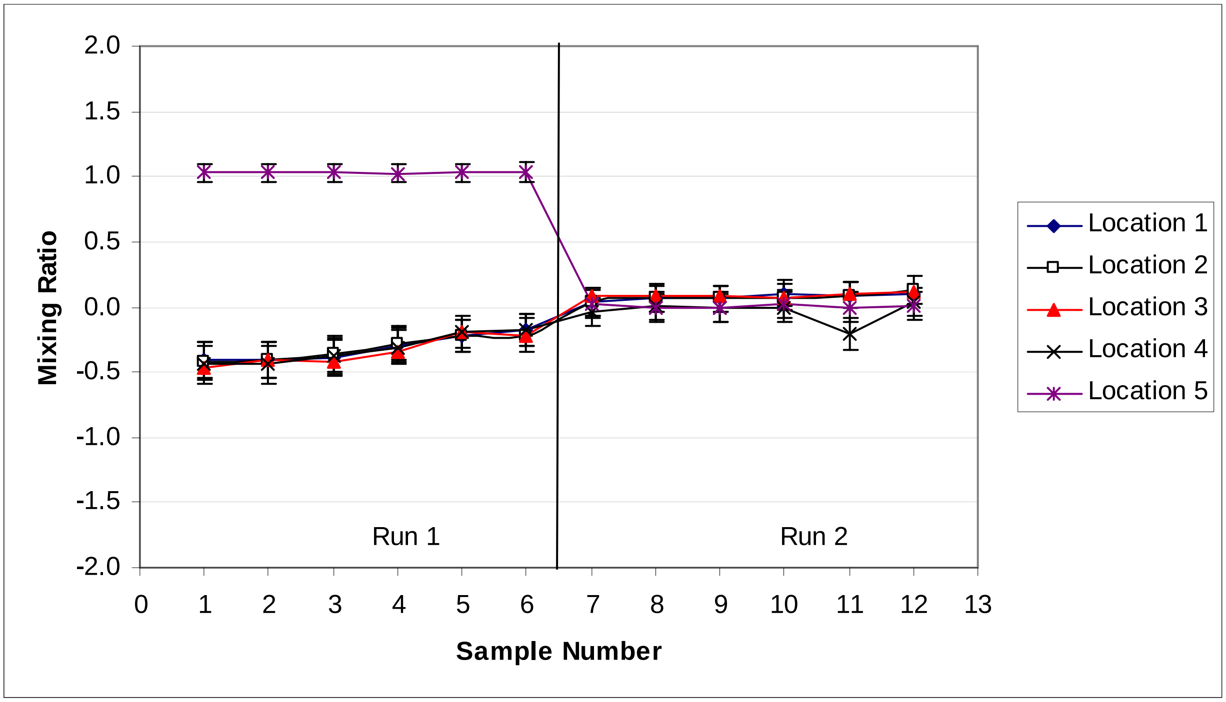

Figure A.14. Mixing Ratio Results from UFP Test Sequence 15 Using BB Tracer

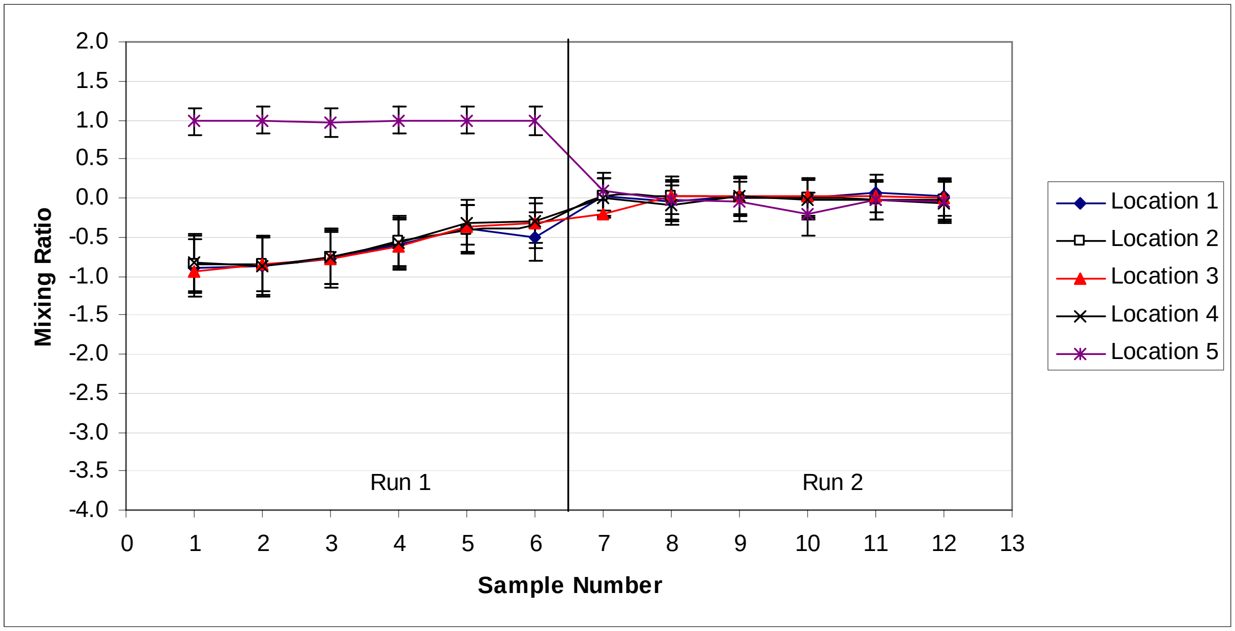

Figure A.15. Mixing Ratio Results from UFP Test Sequence 15 Using Chloride Tracer with IC

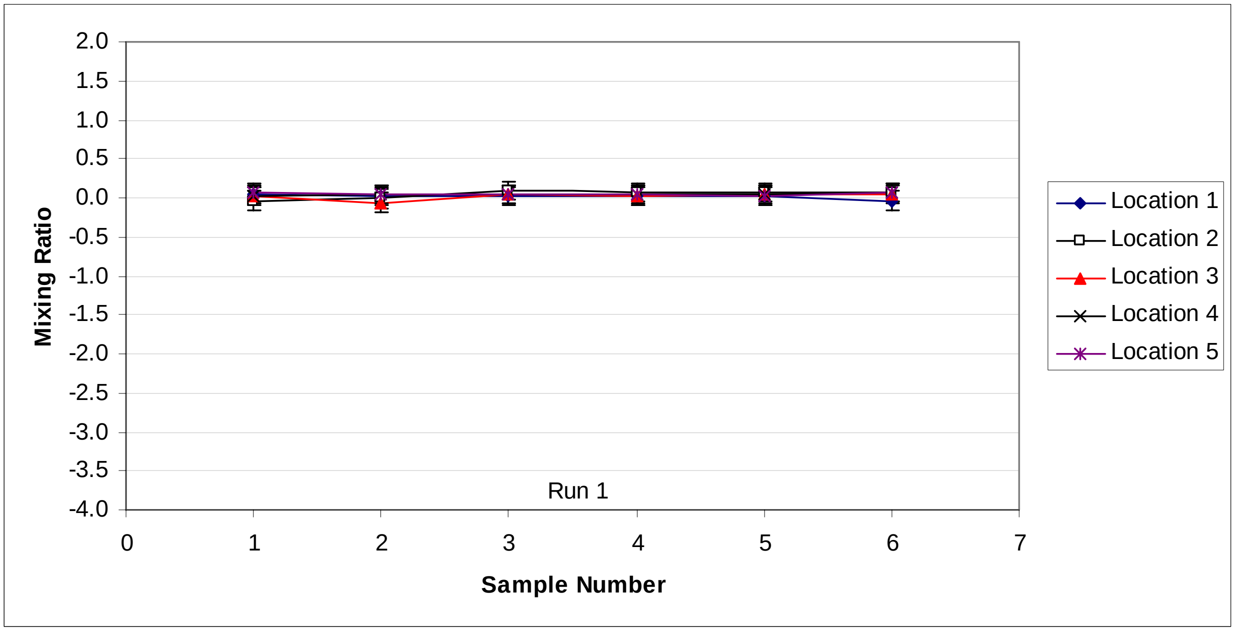

Figure A.15. Mixing Ratio Results from UFP Test Sequence 16 Using Chloride Tracer with IC

Appendix B

Drive Functions

Appendix B - Drive Functions

This appendix presents PJM velocity drive functions for the final mixing system configurations in the scaled LS and UFP Vessels. The drive functions shown in Figures B.1 through B.6 are the averages of the individual PJMs (eight for LS and six for UFP). These are then averaged over many cycles to create an overall average drive function. The instantaneous velocities are calculated from differential drive pressure (i.e., the difference of actual drive pressure and head at the PJM nozzle) and are estimated to be accurate within approximately plus or minus 5% of the maximum value.

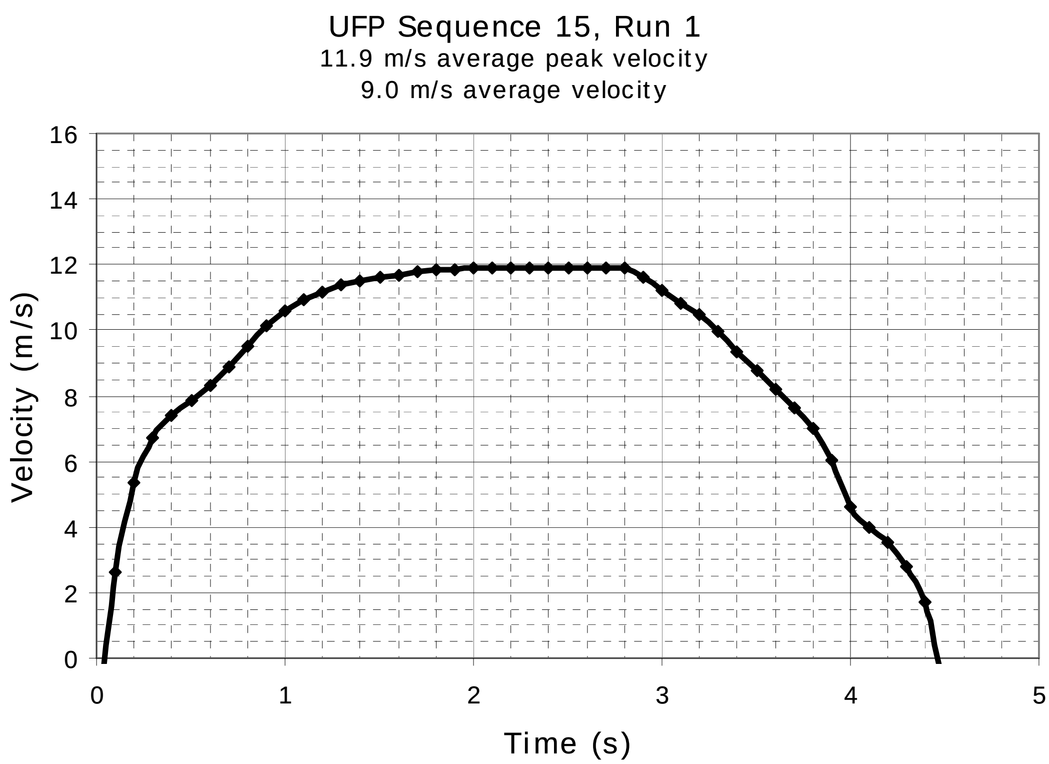

Figure B.1. PJM Drive Function for Scaled UFP Vessel; Sequence 15, Run 1

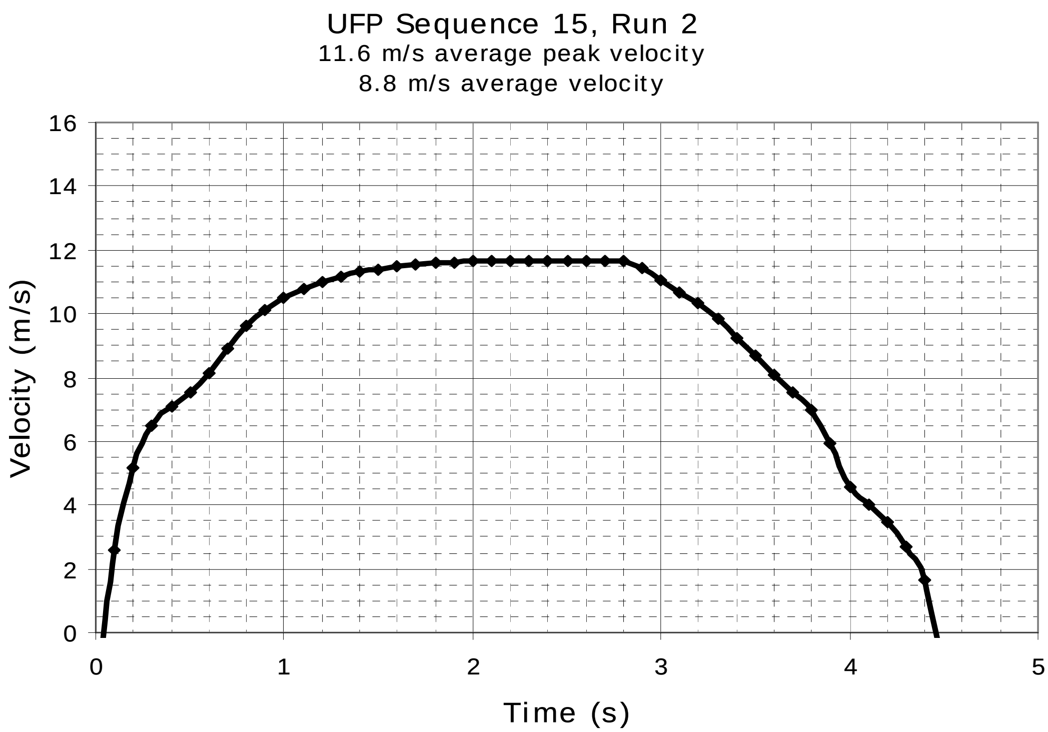

Figure B.2. PJM Drive Function for Scaled UFP Vessel; Sequence 15, Run 2

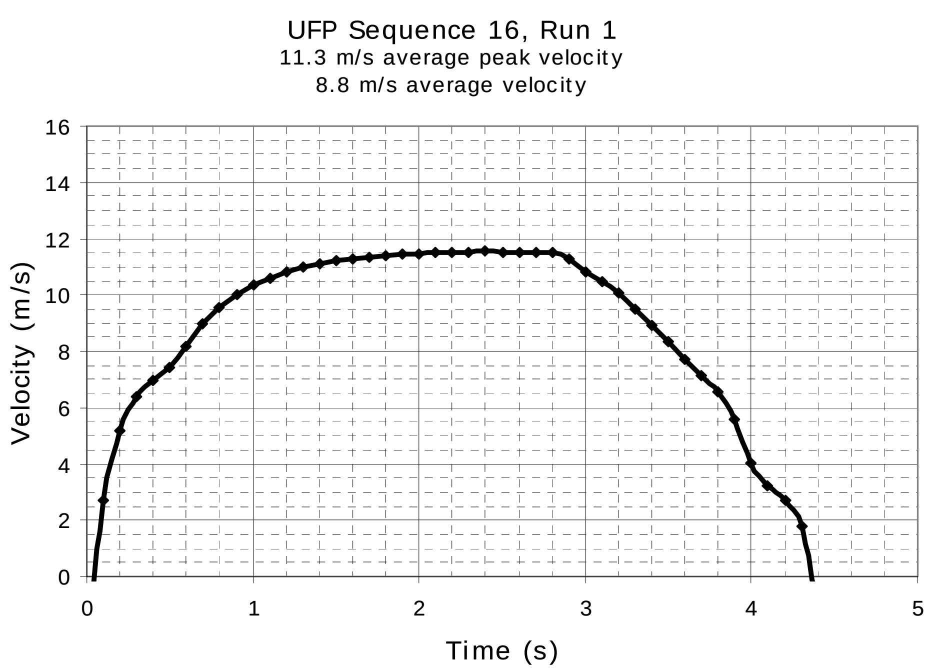

Figure B.3. PJM Drive Function for Scaled UFP Vessel; Sequence 16, Run 1

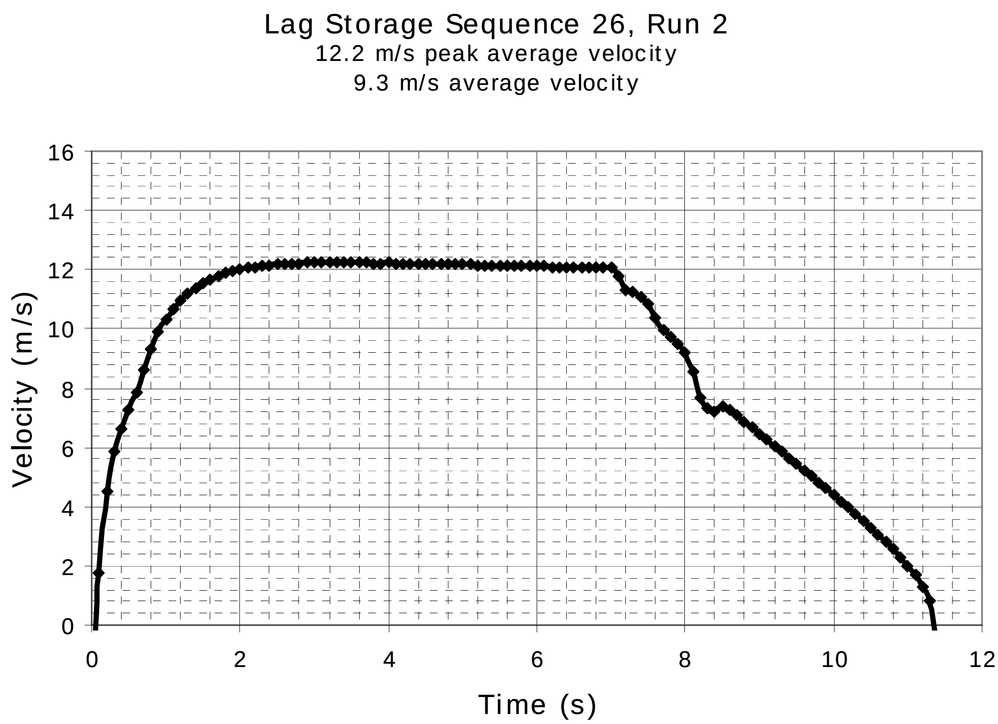

Figure B.4. PJM Drive Function for Scaled Lag Storage Vessel; Sequence 26, Run 2

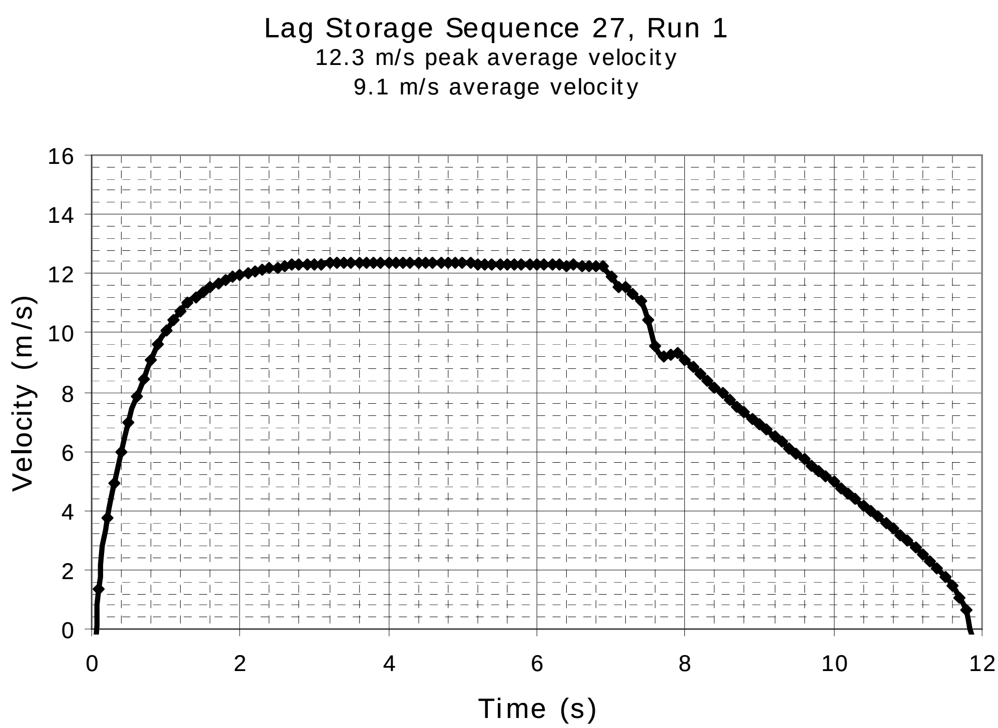

Figure B.5. PJM Drive Function for Scaled Lag Storage Vessel; Sequence 27, Run 1

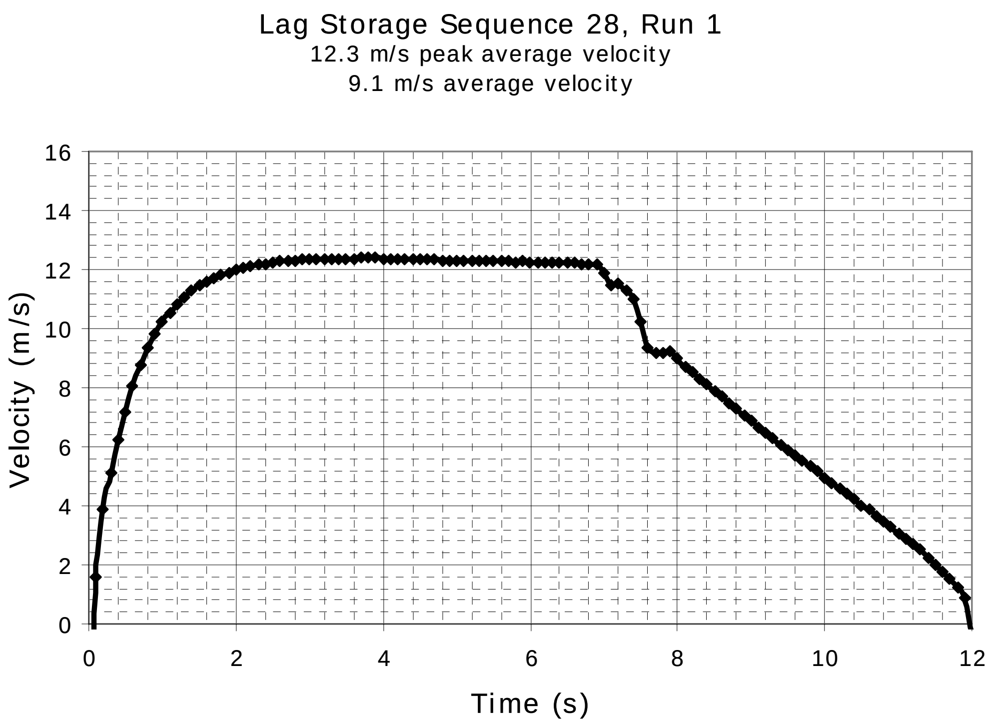

Figure B.6. PJM Drive Function for Scaled Lag Storage Vessel; Sequence 28, Run 1

Appendix C

Core Sampling Locations

Appendix C - Core Sampling Locations

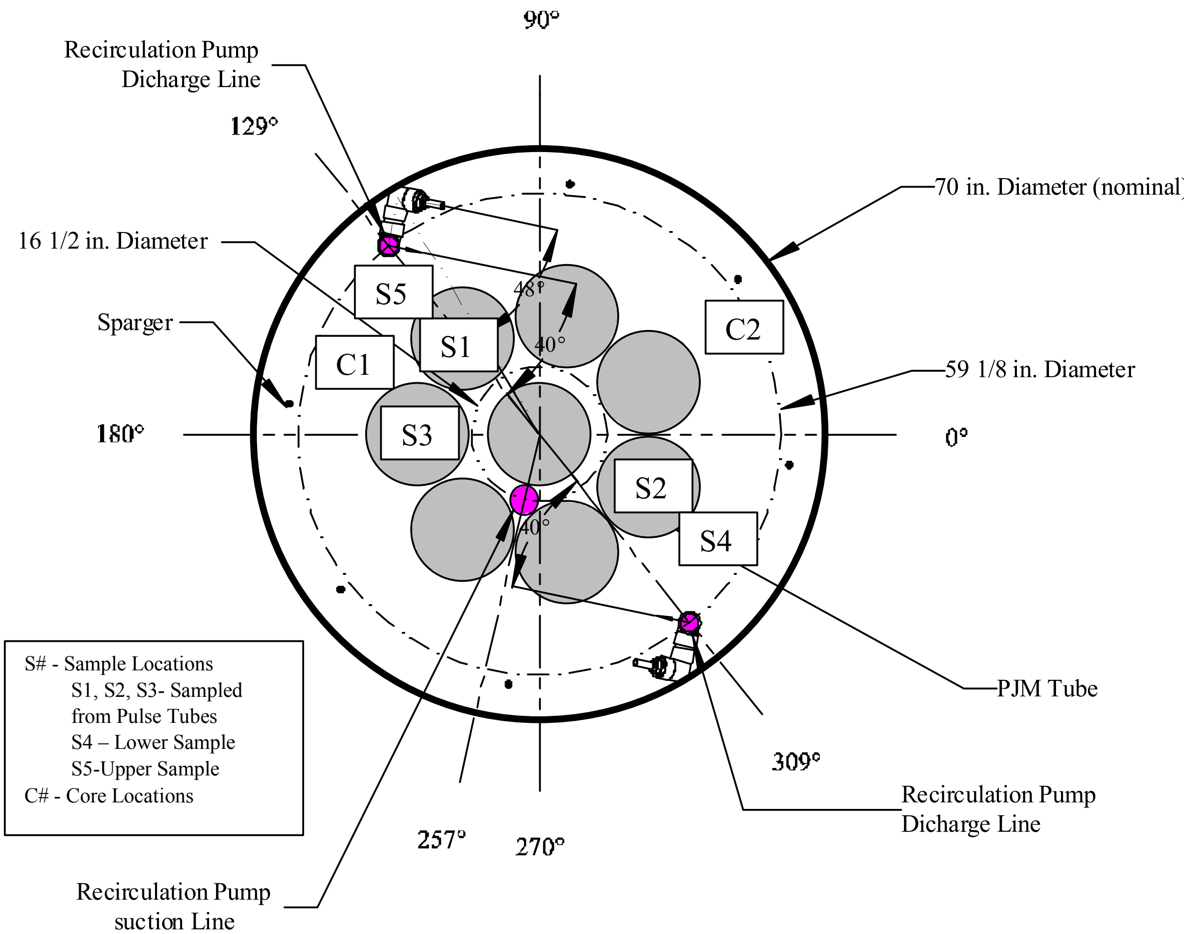

Figure C.1. Schematic of Lag Storage Vessel Tracer Sampling Locations During Phase II Scaled Test Platform Tests (Test Sequence 26)

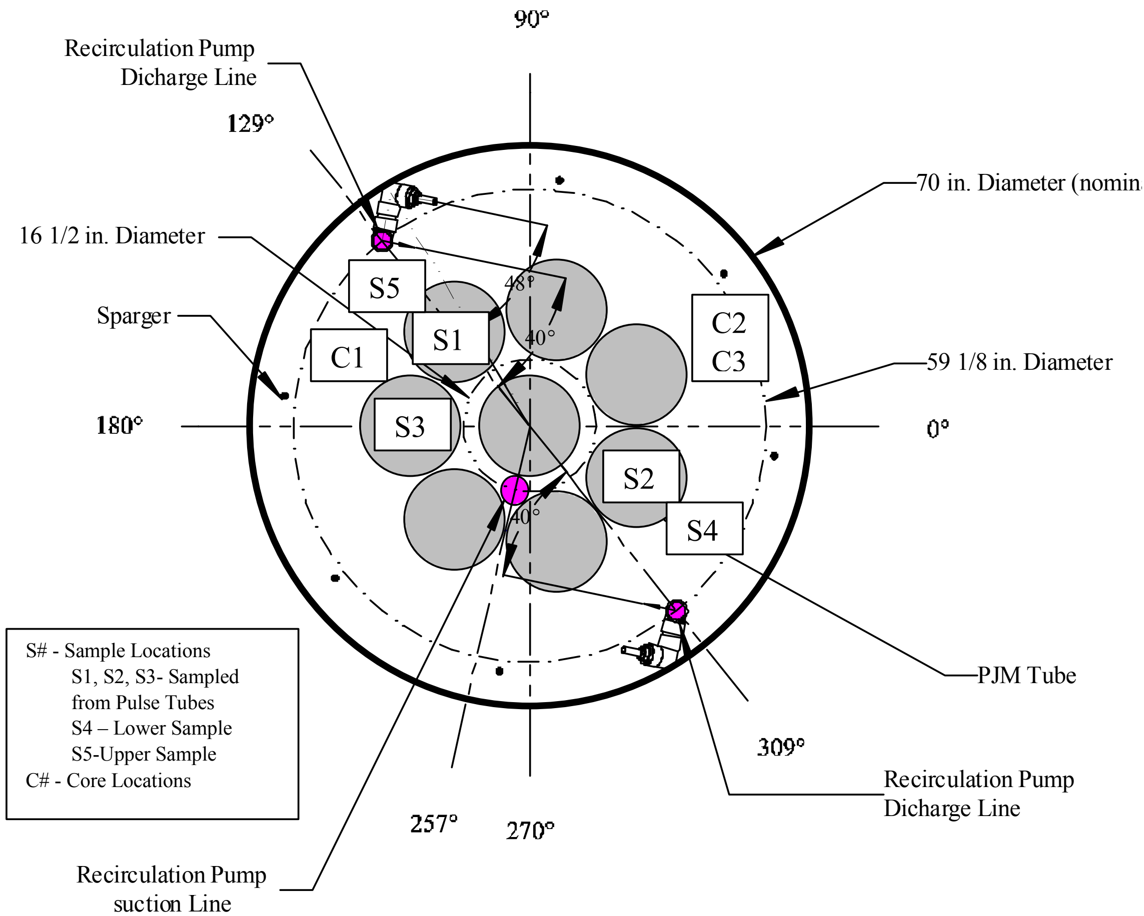

Figure C.2. Schematic of Lag Storage Vessel Tracer Sampling Locations During Phase II Scaled Test Platform Tests (Test Sequence 27)

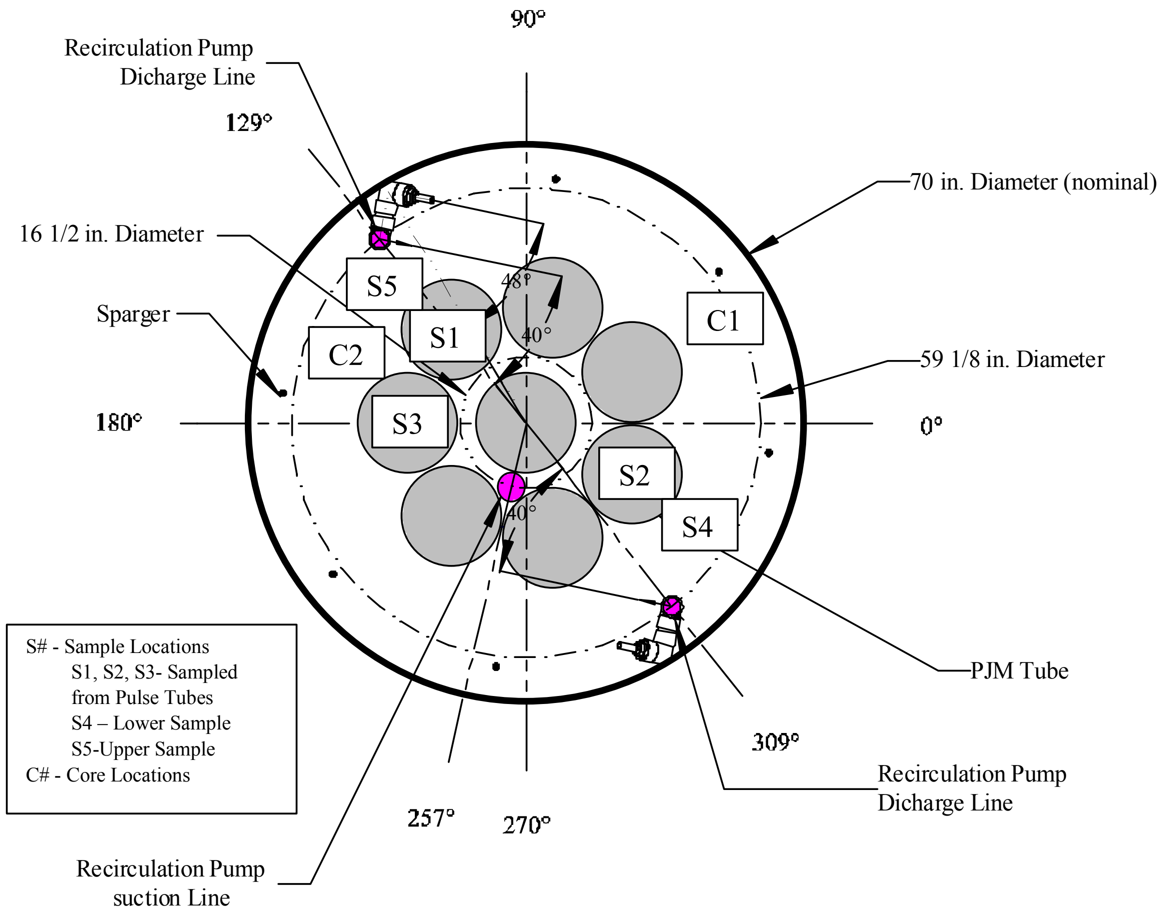

Figure C.3. Schematic of Lag Storage Vessel Tracer Sampling Locations During Phase II Scaled Test Platform Tests (Test Sequence 28)

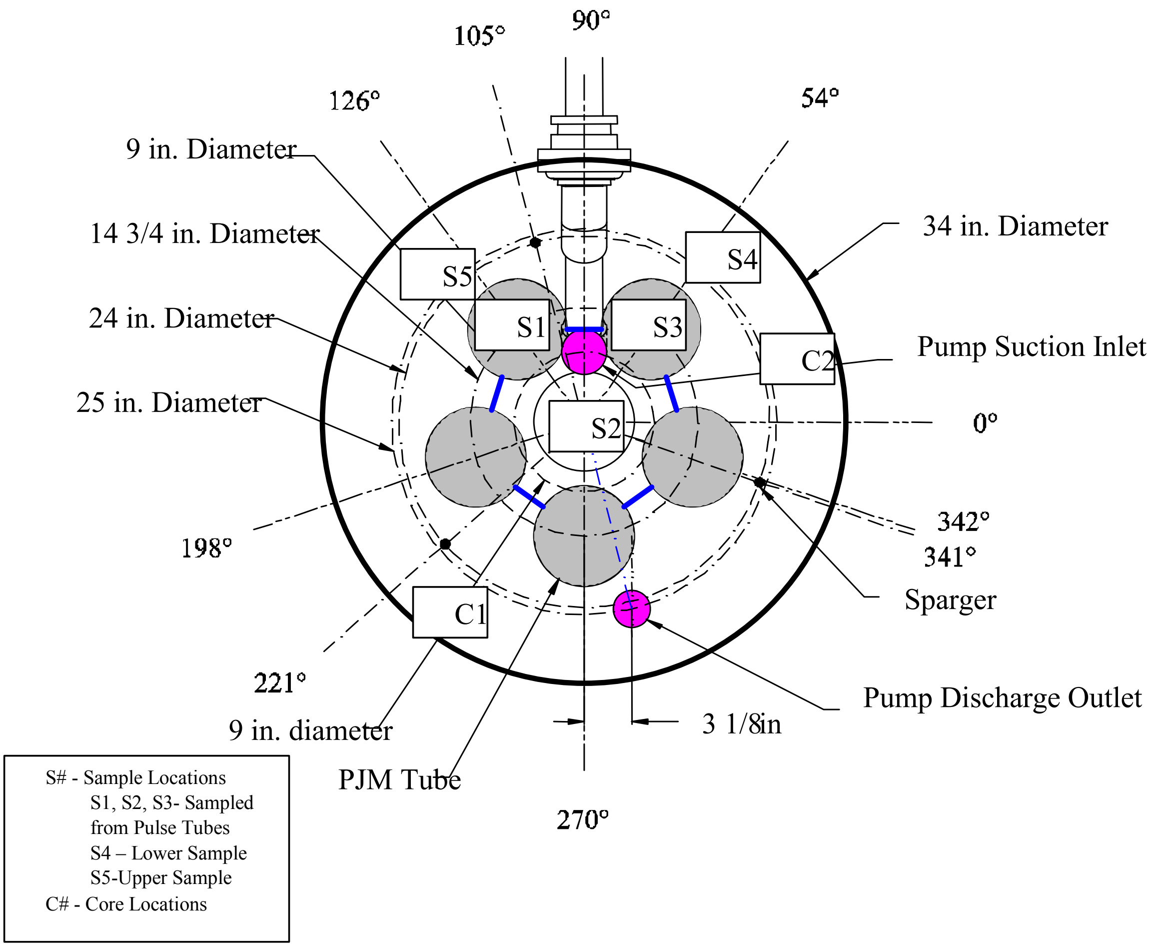

Figure C.4. Schematic of UFP Vessel Tracer Sampling Locations During Phase II Scaled Test Platform Tests (Test Sequence 15)

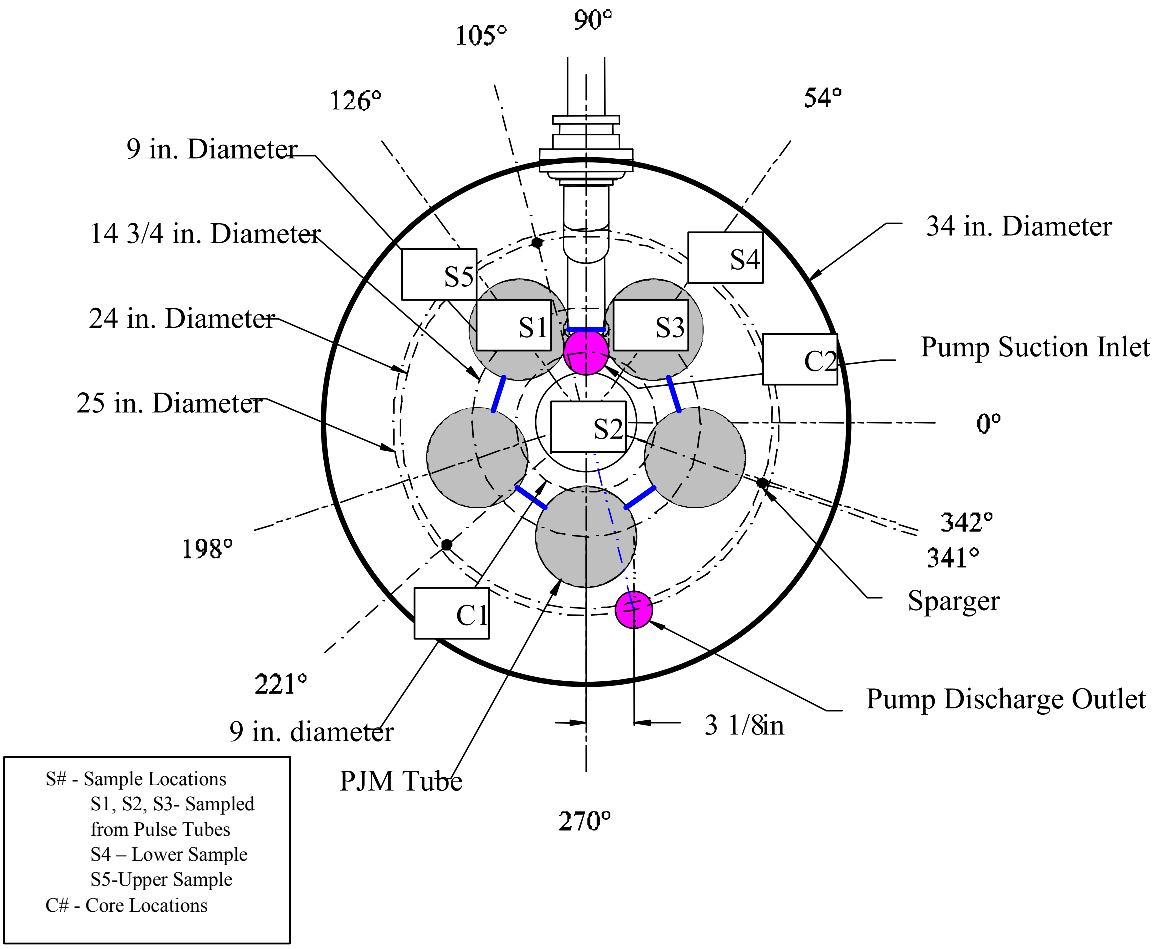

Figure C.5. Schematic of UFP Vessel Tracer Sampling Locations During Phase II Scaled Test Platform Tests (Test Sequence 16)

Distribution

No. of Copies

OFFSITE

1 Savannah River National Laboratory
Richard Edwards
Savannah River National Laboratory
Westinghouse SA
Aiken, SC 29808-0001

1 DuPont Engineering Technology
Art Etchells
Nemours Building 6410
1007 Market Street
Wilmington, DE 19898

No. of Copies

ONSITE

14 Battelle – Pacific Northwest Division

J. R. Bontha	K6-24
P. A. Meyer	K7-15
C. W. Enderlin	K7-15
M. A. Gerber	K2-12
R. T. Hallen	K2-12
M. D. Johnson	K6-96
D. E. Kurath	P7-28
A. P. Poloski	P7-25
S. K. Sundaram	K6-24
D. E. Wallace	K6-28
Project File (2)	P7-28
Information Release Office (2)	K1-06

6 Bechtel National, Inc.

H. A. Abodishish	H4-02
S. M. Barnes	H4-02
J. C. Deckers (2)	H4-02
D. E. Larson	H4-02
J. M. Perez	H4-02